

FINAL REPORT

**ACCELERATED TESTING OF SEPARATION LAYERS
FOR OPEN-GRADED DRAINAGE LAYERS**

Project IB-H1, 1994

Report No. ITRC FR 94-2

Prepared by

J.M. Signore and B.J. Dempsey
Department of Civil Engineering
University of Illinois at Urbana-Champaign

May 1998

Illinois Transportation Research Center
Illinois Department of Transportation



ACKNOWLEDGMENTS

The con
and acc
reflect t
report d

This final report on the examination of separation layers for open-graded layers was prepared by the Department of Civil Engineering, University of Illinois at Urbana-Champaign. This report is based upon research sponsored by the Illinois Transportation Research Center, ITRC C960014. Mr. Steven J. Hanna is the administrator for the center.

Special thanks are due to Ms. Christine Reed, Mr. Jeff South, and Mr. Riyad Wahab of the Illinois Department of Transportation for their consultation during this research. The advice of Mr. James Hall of Norgren Chicago on pneumatic design and the contribution of geotextiles by Mr. David Andrews of Synthetic Industries were greatly appreciated.

ABSTRACT

An accelerated testing procedure was developed to evaluate performance of separation layers used between open-graded bases and lime stabilized subgrades. Significantly of concern was assessing separation layer performance in regard to the degree of pumping into the open-graded base and the magnitude of deformations occurring during testing. A pneumatically driven, electronically controlled, repeated loading laboratory apparatus was designed and constructed to perform the testing of these materials. A low plasticity clay and a silty clay till soil were tested in this research. The separation layers investigated included non-woven geotextiles and a dense-graded base aggregate blend. Specimens were housed in a stiff wall plexiglas cylinder during testing. Tests were conducted at various loading levels and durations in order to develop the accelerated testing procedure. Comparisons of specimen deflection and pumping relative to non-separated test cases were made to determine the relative performance of the separation layers and the effect of different loading conditions. Ultimately, loading at levels upwards of 5 times expected in the field, for short durations (20,000 cycles or less) was performed to evaluate separation layer performance. Separation layer performance under these conditions can be compared to typical loading level performance provided relative measurements are used and it is understood the failure mechanisms may be different. Geotextiles consistently provided separation between the soils and open-graded aggregates though pumping of fines occurred. The dense-graded separation layer showed a marked drop-off in performance upon wetting of the material. Though the dense-graded layer often prevented the soil layer from intruding into the open-graded layer, the dense-graded layer itself intermixed into the open layer. A distinct breakpoint in performance occurred at a soil strength of CBR 4 under accelerated testing. Soils below CBR 4 showed considerable pumping and deformation while soils above that strength yielded minimal pumping and deformation regardless of separation layer type. Based upon performance comparisons with non-separated test cases, the use of a separation layer between lime stabilized subgrades and open-graded aggregate bases is imperative.

PERSISTENCE

"Nothing in the world can take the place of persistence. Talent will not; nothing is more common than unsuccessful men with talent. Genius will not; unrewarded genius is almost a proverb. Education will not; the world is full of educated derelicts. Persistence and determination alone are omnipotent. The slogan 'Press On' has solved and always will solve the problems of the human race."

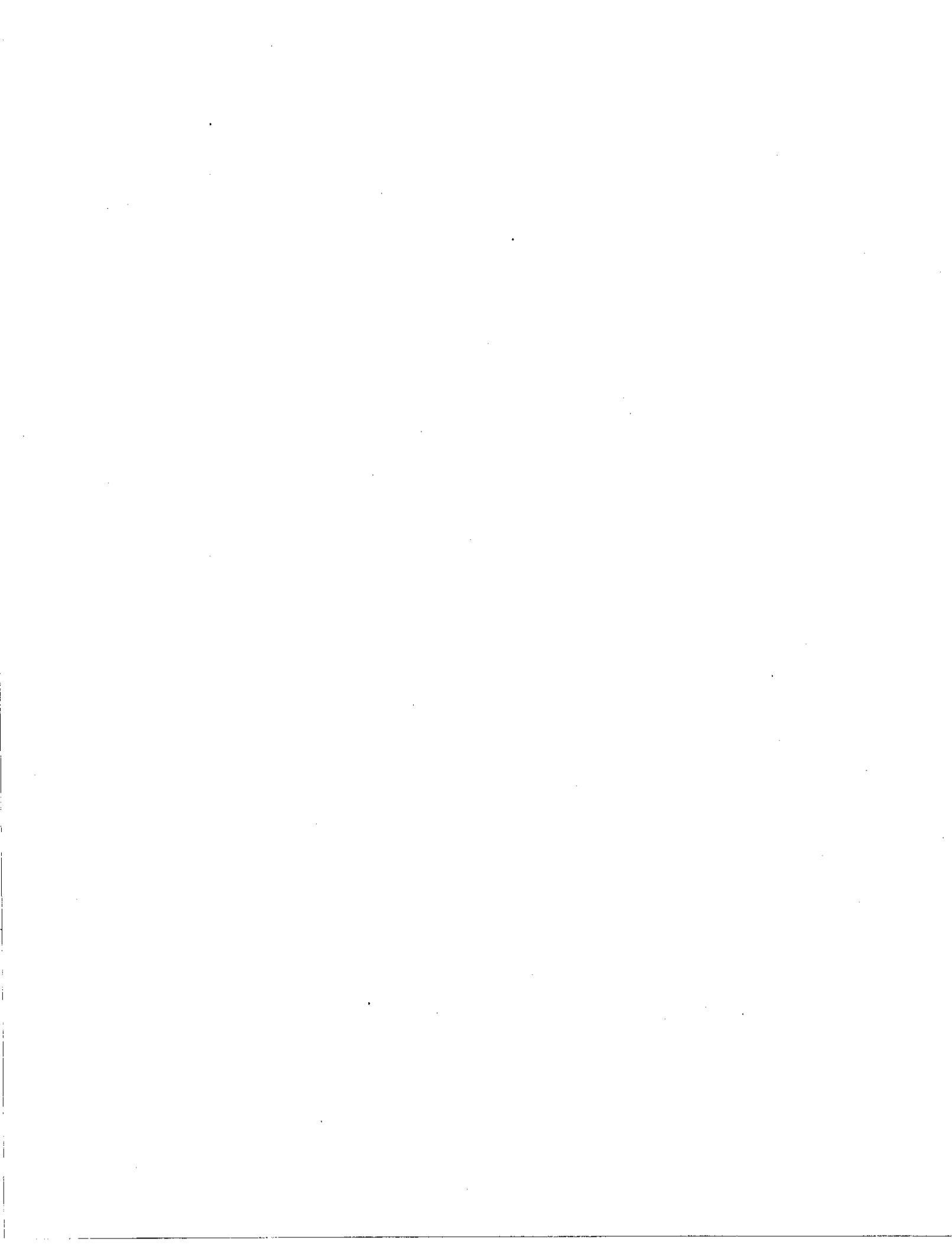
*Calvin Coolidge
(Amherst 1894)*

TABLE OF CONTENTS

LIST OF TABLES	x
LIST OF FIGURES	xi
LIST OF ACRONYMS, SYMBOLS, AND ABBREVIATIONS	xvi
1. INTRODUCTION.....	1
1.1 Background.....	1
1.2 Research Objectives	2
1.3 Problem Statement	2
1.4 Research Approach	3
1.5 Thesis Overview.....	3
2. LITERATURE REVIEW	4
2.1 General.....	4
2.2 Separation Layer Testing Research	5
2.3 Durability of Stabilized and Modified Materials.....	14
2.4 Pore Pressure Effects on Granular Materials in Pavements.....	15
2.5 Open-Graded Base Courses	17
2.6 Geotextiles as Filters/Separation Layers.....	21
2.7 Research Relevance	23
2.8 Summary of Applied Information.....	24
3. MATERIALS UNDER INVESTIGATION	27
3.1 Introduction.....	27
3.2 Subgrade Materials	27
3.2.1 Mexico Clay	27
3.2.2 Wisconsinan Silty Clay Till.....	28
3.2.3 Lime	29

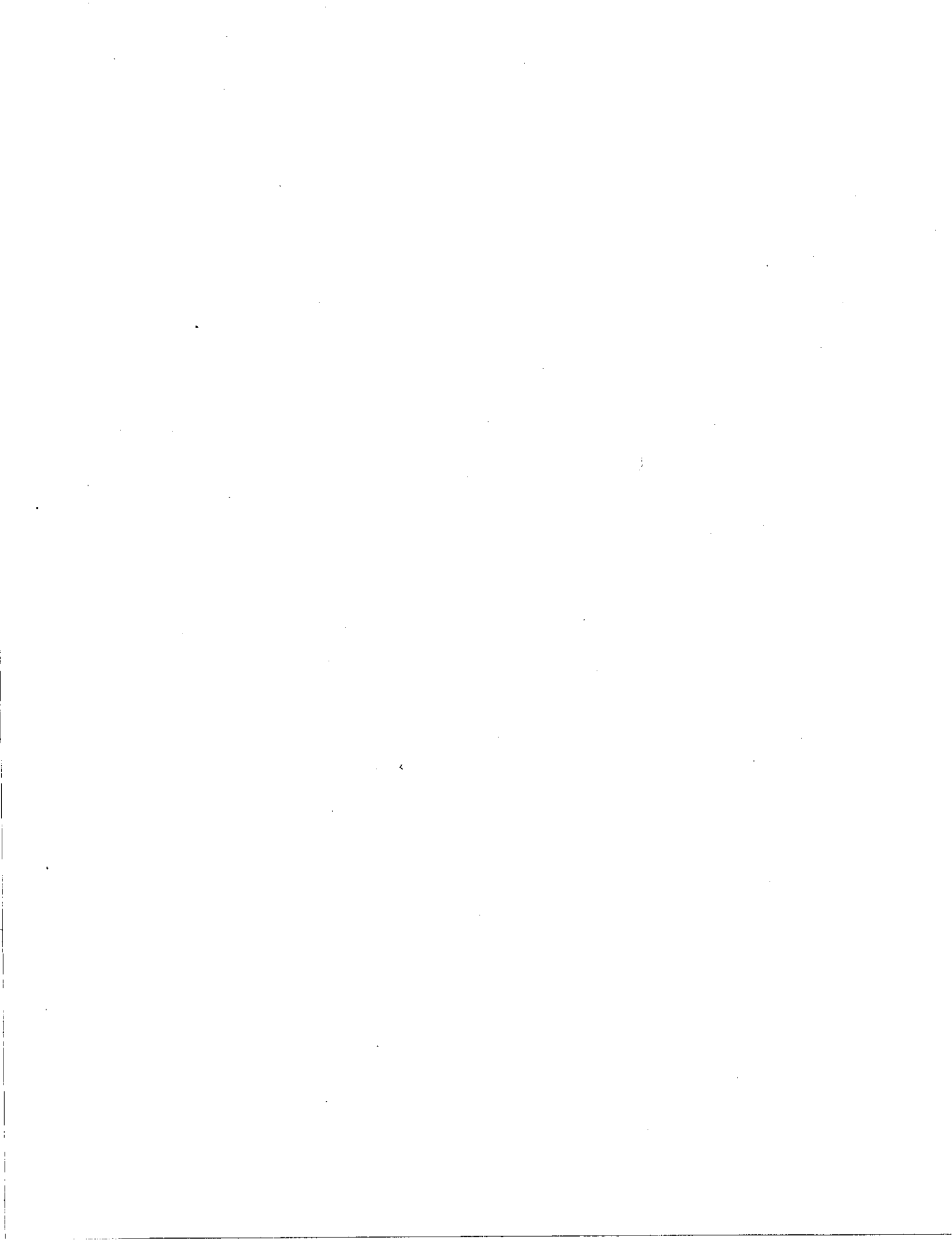
3.3 Aggregate	30
3.3.1 <i>IDOT CA 7 Base Layer</i>	30
3.3.2 <i>IDOT CA 6 Dense-Graded Aggregate Separation Layer</i>	30
3.4 Geotextile Selection and Characterization	30
4. EQUIPMENT DESIGN AND DEVELOPMENT	38
4.1 Equipment Overview	38
4.2 Pneumatic System Design	38
4.2.1 <i>System Loading Requirements</i>	39
4.2.2 <i>System Design Configuration</i>	39
4.3 Electronic Control and Data Acquisition	41
4.4 Test Cylinder and Load Head	43
4.5 Load Frame	44
5. TEST PROCEDURE	57
5.1 Procedure Development and Experimental Design	57
5.1.1 <i>Overview and First Testing Phase</i>	57
5.1.2 <i>Testing Phases Two and Three</i>	58
5.2 Testing Setup and Operation	59
5.2.1 <i>Soil Specimen Mix Design</i>	59
5.2.2 <i>Soil Specimen Preparation</i>	60
5.2.3 <i>Test Cylinder Preparation</i>	63
5.2.4 <i>Setting Up and Running Test Equipment</i>	64
5.2.5 <i>Post Testing Procedure</i>	65
5.3 Performance Evaluation	66
5.3.1 <i>Deflection as a Measure of Performance</i>	67
5.3.2 <i>Pumping as a Measure of Performance</i>	67
6. SEPARATION LAYER TESTING AND RESULTS	91
6.1 General	91
6.2 Open-Graded Aggregate Performance	92

6.3 Stabilized Mexico Clay Soil and Separation Layer Performance.....	92
6.3.1 <i>No Separation.....</i>	93
6.3.2 <i>Geotextile Separation.....</i>	95
6.3.3 <i>Dense-Graded Separation.....</i>	97
6.4 Wisconsinan Silty Clay Till and Separation Layer Performance.....	98
6.4.1 <i>No Separation.....</i>	98
6.4.2 <i>Geotextile Separation.....</i>	98
6.4.3 <i>Dense-Graded Separation.....</i>	100
6.5 Separation Layer Comparison with Respect to Both Soils.....	100
6.5.1 <i>No Separation.....</i>	101
6.5.2 <i>Geotextile Separation.....</i>	101
6.5.3 <i>Dense-Graded Separation.....</i>	102
6.6 Performance Index Based Comparison.....	102
6.6.1 <i>Separation Performance Index for Mexico Clay.....</i>	103
6.6.2 <i>Separation Performance Index for Wisconsinan Silty Clay Till.....</i>	104
6.7 Separation Layer Performance Comparison.....	105
6.7.1 <i>Separation Layer Performance with Mexico Clay.....</i>	105
6.7.2 <i>Separation Layer Performance with Wisconsinan Silty Clay Till.....</i>	106
6.8 Applicability of Test Results to Field Performance and Use of Index Test.....	107
6.8.1 <i>Test Overview.....</i>	107
6.8.2 <i>Test Procedure.....</i>	108
7. SUMMARY AND SIGNIFICANT FINDINGS.....	174
7.1 Summary.....	174
7.2 Significant Findings.....	174
7.3 Suggestions for Further Research.....	178
APPENDIX.....	179
REFERENCES.....	226



LIST OF TABLES

Table 3.1: IDOT CA 7 Mix Design.....	32
Table 3.2: IDOT CA 6 Mix Design.....	32
Table 3.3: Synthetic Industries Geotex 1101	32
Table 5.1: Testing Variables	70
Table 5.2: Mexico Clay Mix Design.....	71
Table 5.3: Wisconsin Silty Clay Mix Design	71
Table 5.4: Soil Specimen - Batch Mixes.....	72
Table 5.5: Mexico Clay Specimen Saturation Data.....	73
Table 5.6: Wisconsin Silty Clay Till Specimen Saturation Data.....	76
Table 6.1: Performance Evaluation Parameters	109



LIST OF FIGURES

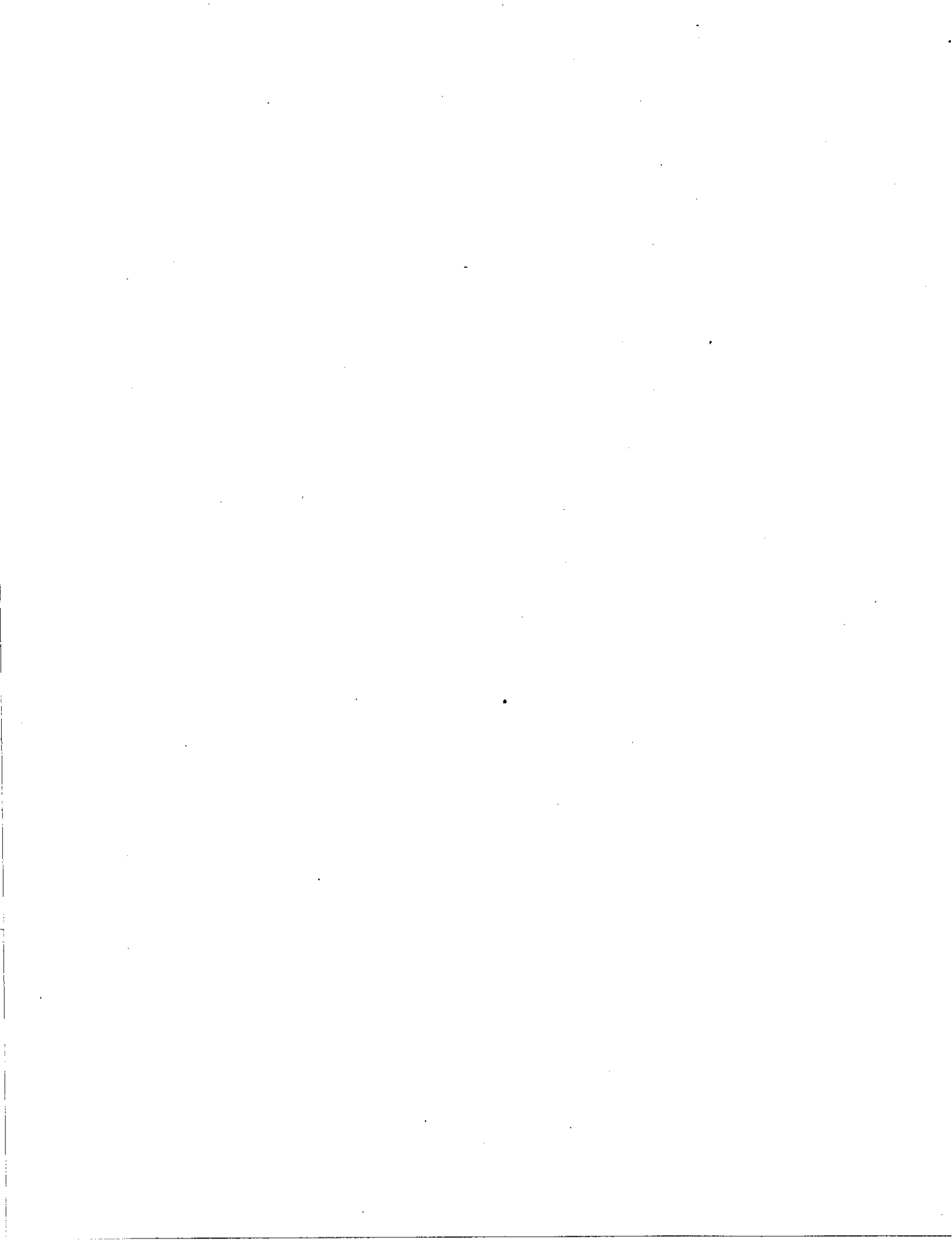
Figure 3.1: Mexico Clay Particle Gradation	33
Figure 3.2: Lime Stabilized Soil Moisture-Density Relations.....	34
Figure 3.3: Mexico Clay Unconfined Compressive Strength Testing	35
Figure 3.4: Wisconsinan Silty Clay Till Particle Gradation	36
Figure 3.5: Wisconsinan Silty Clay Till Unconfined Compressive Strength Testing	37
Figure 4.1: Loading Frame and Cylinders	46
Figure 4.2: Block Diagram of System Control	47
Figure 4.3: Overall System	48
Figure 4.4: Equipment in Test Configuration	49
Figure 4.5: Pneumatic System Design.....	50
Figure 4.6: Air Cylinder and Test Chamber.....	51
Figure 4.7: Block Diagram of Electronic Control Circuitry	52
Figure 4.8: Electronic Control Circuitry.....	53
Figure 4.9: Test Cylinder Design	54
Figure 4.10: Load Head Design.....	55
Figure 4.11: Load Head in Operational Position	56
Figure 5.1: Experimental Design for Accelerated Test Development.....	77
Figure 5.2: Accelerated Testing - Load / Strength Combinations.....	78
Figure 5.3: Accelerated Testing - Separation Layer Combinations	79
Figure 5.4: Mexico Clay/Separation Testing Combinations	80
Figure 5.5: Wisconsinan Silty Clay Till/Separation Testing Combinations	81
Figure 5.6: Vacuum Saturation Apparatus.....	82
Figure 5.7: Mexico Clay, Cone Index vs. Specimen Dry Density.....	83

Figure 5.8: Mexico Clay, Cone Index vs. Specimen Saturated Density	84
Figure 5.9: Mexico Clay, Cone Index vs. Specimen Saturated Moisture Content.....	85
Figure 5.10: Wisconsinan Silty Clay Till, Cone Index vs. Specimen Dry Density	86
Figure 5.11: Wisconsinan Silty Clay Till, Cone Index vs. Specimen Saturated Density	87
Figure 5.12: Wisconsinan Silty Clay Till, Cone Index vs. Specimen Saturated Moisture Content	88
Figure 5.13: Geotextile Installation with Retaining Ring	89
Figure 5.14: Test Evaluation.....	90
Figure 6.1: CA 7 Aggregate, Permanent Deformation vs. Load Cycle.....	110
Figure 6.2: Mexico Clay/No Separation/CA 7, Intruded Soil vs. Cone Index.....	111
Figure 6.3: Mexico Clay/No Separation/CA 7,Permanent Deformation vs. Intruded Soil...	112
Figure 6.4: Mexico Clay/No Separation/CA 7, Intruded Soil vs. Elastic Deflection	113
Figure 6.5: Mexico Clay/No Separation/CA 7, Permanent Deformation vs. Cone Index....	114
Figure 6.6: Mexico Clay/1101 Geotextile/CA 7, Pumped Soil vs. Cone Index.....	115
Figure 6.7: Mexico Clay/1101 Geotextile/CA 7, Pumped Soil vs. Cone Index, Long Term	116
Figure 6.8: Mexico Clay/1101 Geotextile/CA 7, Geotextile Soil Retention.....	117
Figure 6.9: Mexico Clay/1101 Geotextile/CA 7, Permanent Deformation vs. Pumped Soil	118
Figure 6.10: Mexico Clay/1101 Geotextile/CA 7, Pumped Soil vs. Elastic Deflection	119
Figure 6.11: Mexico Clay/1101 Geotextile/CA 7, Permanent Deformation vs. Cone Index	120
Figure 6.12: 1101 Geotextile with Pumped Mexico Clay - Post Test.....	121
Figure 6.13: Mexico Clay Specimen Surface Underlying 1101 Geotextile - Post Test.....	121
Figure 6.14: Mexico Clay Pumped into 1101 Geotextile and CA 7 - Post Test.....	122
Figure 6.15: Mexico Clay Slurry Coating 1101 Geotextile and CA 7 - Post Test.....	122
Figure 6.16: Mexico Clay/CA 6/CA 7, Material Transfer vs. Cone Index	123
Figure 6.17: Mexico Clay/CA 6/CA 7, Permanent Deformation vs. Material Transfer	124

Figure 6.18: Mexico Clay/CA 6/CA 7, Material Transfer vs. Elastic Deflection.....	125
Figure 6.19: Mexico Clay/CA 6/CA 7, Permanent Deflection vs. Cone Index.....	126
Figure 6.20: Wisconsinan Silty Clay Till/No Separation/CA 7, Intruded Soil vs. Cone Index.....	127
Figure 6.21: Wisconsinan Silty Clay Till/No Separation/CA 7, Permanent Deformation vs. Intruded Soil	128
Figure 6.22: Wisconsinan Silty Clay Till/No Separation/CA 7, Intruded Soil vs. Elastic Deflection.....	129
Figure 6.23: Wisconsinan Silty Clay Till/No Separation/CA 7, Permanent Deformation vs. Cone Index.....	130
Figure 6.24: Wisconsinan Silty Clay Till/1101 Geotextile/CA 7, Pumped Soil vs. Cone Index.....	131
Figure 6.25: Wisconsinan Silty Clay Till/1101 Geotextile/CA 7, Geotextile Soil Retention vs. Cone Index.....	132
Figure 6.26: Wisconsinan Silty Clay Till/1101 Geotextile/CA 7, Permanent Deformation vs. Pumped Soil	133
Figure 6.27: Wisconsinan Silty Clay Till/1101 Geotextile/CA 7, Pumped Soil vs. Elastic Deflection.....	134
Figure 6.28: Wisconsinan Silty Clay Till/1101 Geotextile/CA 7, Permanent Deformation vs. Cone Index	135
Figure 6.29: Wisconsinan Silty Clay Till Slurry Coating 1101 Geotextile - Post Test.....	136
Figure 6.30: Wisconsinan Silty Clay Till Pumped into 1101 Geotextile and CA 7 - Post Test	136
Figure 6.31: Wisconsinan Silty Clay Till Specimen Surface Underlying 1101 Geotextile - Post Test.....	137
Figure 6.32: 1101 Geotextile and CA 7 with Pumped Wisconsinan Silty Clay Till - Post Test.....	137
Figure 6.33: Wisconsinan Silty Clay Till/CA 6/CA 7, Material Transfer vs. Cone Index	138
Figure 6.34: Wisconsinan Silty Clay Till/CA 6/CA 7, Permanent Deformation vs. Material Transfer.....	139

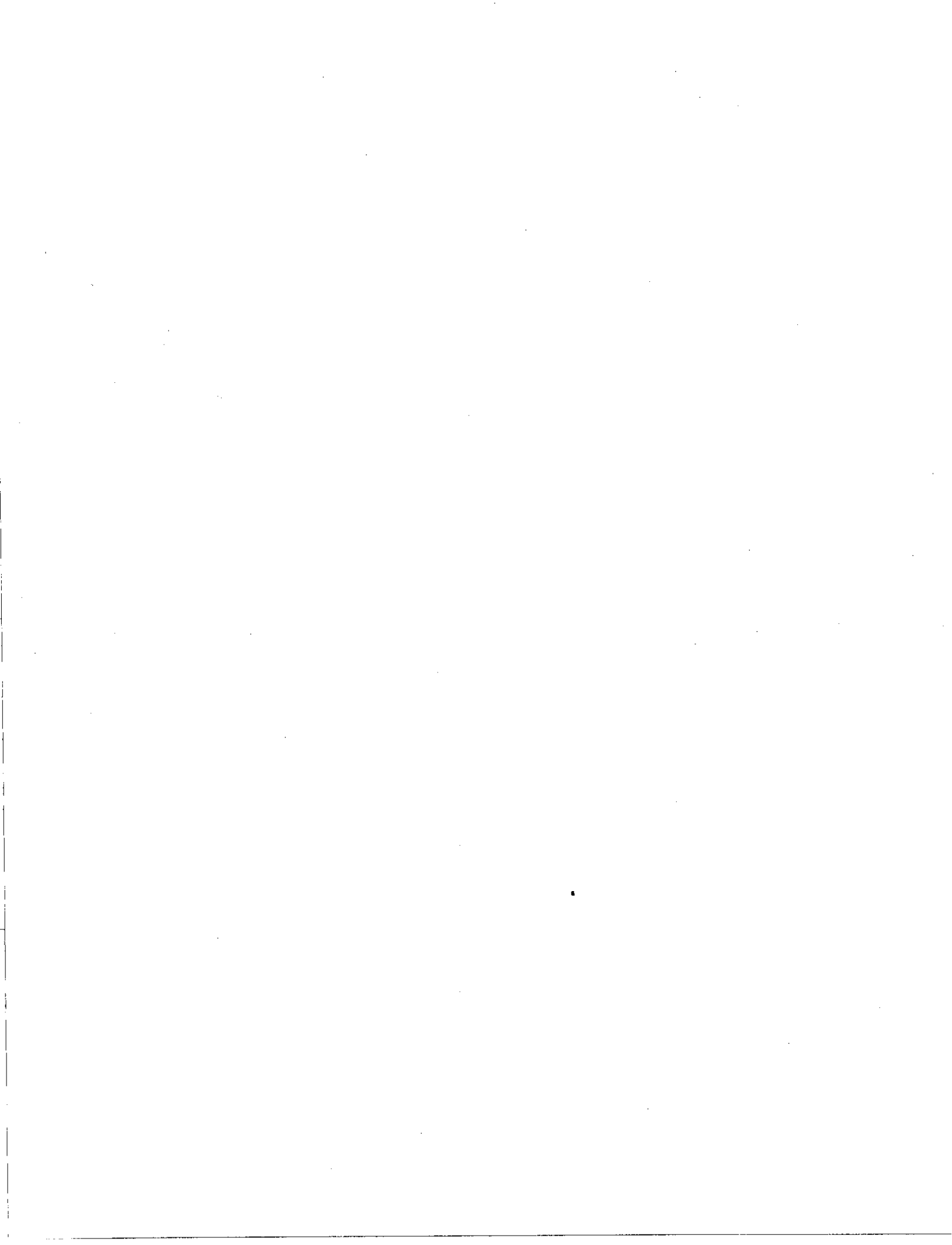
Figure 6.35: Wisconsin Silty Clay Till/CA 6/CA 7, Material Transfer vs. Elastic Deflection.....	140
Figure 6.36: Wisconsin Silty Clay Till/CA 6/CA 7, Permanent Deformation vs. Cone Index.....	141
Figure 6.37: Soil/No Separation/CA 7, Intruded Soil vs. Cone Index.....	142
Figure 6.38: Soil/No Separation/CA 7, Permanent Deformation vs. Intruded Soil	143
Figure 6.39: Soil/No Separation/CA 7, Intruded Soil vs. Elastic Deflection.....	144
Figure 6.40: Soil/No Separation/CA 7, Permanent Deformation vs. Cone Index.....	145
Figure 6.41: Soil/1101 Geotextile/CA 7, Pumped Soil vs. Cone Index	146
Figure 6.42: Soil/1101 Geotextile/CA 7, Permanent Deformation vs. Pumped Soil	147
Figure 6.43: Soil/1101 Geotextile/CA 7, Pumped Soil vs. Elastic Deflection.....	148
Figure 6.44: Soil/1101 Geotextile/CA 7, Permanent Deformation vs. Cone Index	149
Figure 6.45: Soil/CA 6/CA 7, Material Transfer vs. Cone Index.....	150
Figure 6.46: Soil/CA 6/CA 7, Permanent Deformation vs. Material Transfer.....	151
Figure 6.47: Soil/CA 6/CA 7, Material Transfer vs. Elastic Deflection	152
Figure 6.48: Soil/CA 6/CA 7, Permanent Deformation vs. Cone Index.....	153
Figure 6.49: Mexico Clay/No Separation/CA 7, Separation Performance Index vs. Cone Index.....	154
Figure 6.50: Mexico Clay/1101 Geotextile/CA 7, Separation Performance Index vs. Cone Index.....	155
Figure 6.51: Mexico Clay/CA 6/CA 7, Separation Performance Index vs. Cone Index	156
Figure 6.52: Mexico Clay/Separation/CA 7, Separation Performance Index vs. Cone Index.....	157
Figure 6.53: Wisconsin Silty Clay Till/No Separation/CA 7, Separation Performance Index vs. Cone Index.....	158
Figure 6.54: Wisconsin Silty Clay Till/1101 Geotextile/CA 7, Separation Performance Index vs. Cone Index.....	159

Figure 6.55: Wisconsinan Silty Clay Till/CA 6/CA 7, Separation Performance Index vs. Cone Index.....	160
Figure 6.56: Wisconsinan Silty Clay Till/Separation/CA 7, Separation Performance Index vs. Cone Index.....	161
Figure 6.57: Mexico Clay/Separation/CA 7, Pumped/Intruded Material vs. Cone Index	162
Figure 6.58: Mexico Clay/Separation/CA 7, Pumped/Intruded Material/Material Transfer vs. Cone Index.....	163
Figure 6.59: Mexico Clay/Separation/CA 7, Permanent Deformation vs. Pumped/Intruded Material.....	164
Figure 6.60: Mexico Clay/Separation/CA 7, Permanent Deformation vs. Pumped/Intruded Material/Material Transfer	165
Figure 6.61: Mexico Clay/Separation/CA 7, Pumped/Intruded Material/Material Transfer vs. Elastic Deflection	166
Figure 6.62: Mexico Clay/Separation/CA 7, Permanent Deformation vs. Cone Index.....	167
Figure 6.63: Wisconsinan Silty Clay Till/Separation/CA 7, Pumped/Intruded Material vs. Cone Index.....	168
Figure 6.64: Wisconsinan Silty Clay Till/Separation/CA 7, Permanent Deformation vs. Pumped/Intruded Material	169
Figure 6.65: Wisconsinan Silty Clay Till/Separation/CA 7, Permanent Deformation vs. Pumped/Intruded Material/Material Transfer	170
Figure 6.66: Wisconsinan Silty Clay Till/Separation/CA 7, Pumped/Intruded Material/Material Transfer vs. Elastic Deflection.....	171
Figure 6.67: Wisconsinan Silty Clay Till/Separation/CA 7, Permanent Deformation vs. Cone Index.....	172
Figure 6.68: Proposed Index Test Flow Chart.....	173



LIST OF ACRONYMS, SYMBOLS, AND ABBREVIATIONS

AASHO	American Association of State Highway Officials
AASHTO	American Association of State Highway Transportation Officials
AOS	Apparent Opening Size
ASTM	American Society of Testing and Materials
CA 6	IDOT Dense-Graded Aggregate
CA 7	IDOT Open-Graded Aggregate
CBR	California Bearing Ratio
CI	Cone Index
DC	Direct Current
D ₈₅	85 th Percentile Aggregate Passing Size
e	Void Ratio of Clean Geotextile
e*	Void Ratio of Clogged Geotextile
EOS	Effective Opening Size
ESAL	Equivalent Single Axle Load
γ_d	Maximum Dry Density
IDOT	Illinois Department of Transportation
LL	Liquid Limit
LVDT	Linear Variable Differential Transformer
O ₉₅	95 th Percentile Geotextile Opening Size
PI	Plasticity Index
PL	Plastic Limit
PSI	Pavement Serviceability Index
q _u	Unconfined Compressive Strength
SCV	Soil Contamination Value
SPI	Separation Performance Index
tex	Weight in grams of 1000 m of fiber
ω_{opt}	Optimum Moisture Content



1. INTRODUCTION

1.1 Background

Adequate pavement drainage is one of the most important requirements for long pavement life. For years, solutions have been sought to efficiently and economically remove infiltrated water from pavements. The ancient Romans built their roads above the level of the surrounding terrain because they knew of the damaging effects of water.¹ However, road building became a lost art with the fall of the Roman empire. Minimal improvements occurred until Tresaguet in France and McAdam in England developed improved construction methods in 18th Century.² McAdam was quoted in 1820 as saying “. . . *it is the native soil which really supports the weight of traffic; that whilst it is preserved in a dry state it will carry any weight without sinking. . . . that if water pass through a road and fill the native soil, the road whatever may be its thickness loses support and goes to pieces.*”³ It is well known by researchers today that open-graded drainage layers can provide the drainage capability required to produce longer pavement life. Until recently, these layers were not well accepted by state highway agencies since the construction techniques required to produce adequate pavements with open-graded layers were not available. Recent advances in highway construction capabilities and an acceptance of open-graded aggregate materials as drainage layers by state agencies have led to a renewed interest in these base types. There are however, problems associated with pavements having open-graded drainage layers. These layers are subject to clogging due to pumping of fines from subgrades, aggregate intruding into the subgrade, and crushing of the open-graded layers themselves. Pioneering road builders such as John L. McAdam knew of this phenomenon and placed a thin layer of dry stone screenings between the crushed stone and the soil subgrade to prevent soil from working into the base course.⁴ Due to the inevitable infiltration of fines, considerable deformations in pavement layers can occur under repeated loading. Separation layers are required to minimize the potential for infiltration.

1.2 Research Objectives

This research is an outgrowth of problems encountered in the State of Illinois with open-graded drainage layers underlying continuously reinforced concrete pavements.^{5,6} The main objective of this research was to characterize the behavior and performance of separation layers placed between stabilized bases and open-graded aggregate drainage layers through newly developed testing methods. The specific goals of this research are as follows:

- 1) Evaluate the infiltration or plugging of open-graded aggregate layers by pumping of fine materials under repeated loading for:
 - a) Open-graded layers placed directly on an untreated subgrade.
 - b) Open-graded layers placed directly upon a lime stabilized subgrade.
 - c) Geotextiles as separation layers between the lime stabilized subgrade and the open-graded layer.
 - d) Dense-graded layers as separation layers between the lime stabilized subgrade and the open-graded layer.
- 2) Develop an index test for evaluating separation layer requirements to minimize infiltration of subgrade materials into open-graded layers.
- 3) Design and construct the testing equipment for the index test.
- 4) Based upon results of 1 and 2, develop subgrade separation criteria required for adequate field pavement performance when using open-graded base courses with a lime stabilized subgrade.

1.3 Problem Statement

The subgrade soil, open-graded aggregate base, and separation layer comprise an interrelated system beneath the pavement surface. The goal of this research was to develop a

rapid index test to establish strength standards for stabilized subgrade soils and to select appropriate separation layers based upon performance results from laboratory testing. Stabilized subgrade soils and appropriate filtering layers that satisfy the requirements of this test can ideally be placed directly beneath open-graded drainage layers with minimal potential for loss of support and subsequent plugging of the open-graded layer.

1.4 Research Approach

Based upon the objectives of this research and from ideas obtained from previous researchers, this work commenced with two major phases. The first phase of this research was to design and construct an accelerated loading test facility. The second phase consisted of using this equipment with an experimental design that would lend itself to identifying suitable separation layers for use with open-graded drainage layers and lime stabilized subgrades.

1.5 Thesis Overview

The balance of this thesis describes the nature of the investigation into separation layer performance and assessment. Chapter 2 summarizes literature regarding separation layers, stabilized soils, open-graded aggregates, and geotextile filters/separators. Chapter 3 follows with an evaluation of the materials used in this research. Chapter 4 gives a description of the design and construction of the testing equipment. The testing procedure that evolved during this research is presented in Chapter 5. Chapter 6 interprets the test results and assesses the applicability of this test to field conditions. A proposed index test is described. A summary and listing of significant findings is presented in Chapter 7.

2. LITERATURE REVIEW

2.1 General

This chapter presents an overview of background information required for conducting this research. Applicable literature is reviewed. Particular points not present in the knowledge base relevant to this research are outlined. A summary of how information obtained from the literature was used in this research is presented.

This research involves the use of stabilized soils, separation layers such as geotextiles and dense-graded aggregates, and open-graded drainage aggregates. The traditional way to perform this research was with a test system that can simulate high levels of traffic loading and perform large numbers of loading repetitions in a short time. This has typically been done housing the test materials in triaxial cells or rigid containers and using hydraulics or pneumatics to drive a loading head.

Since the purpose of this research was to develop a rapid index test procedure to evaluate separation layer performance with stabilized soils and open-graded aggregates, a search of the literature was conducted to determine what knowledge existed on the subject to date. Several researchers world wide have performed separation layer studies with varying objectives. Pertinent and applicable literature is summarized in Section 2.2.

The durability and strength requirements for stabilized and modified materials to mitigate subgrade intrusion was a prime focus of this research. Accelerated loading tests soil durability, erosion potential, and strength. Literature dealing with these topics is explained in Section 2.3.

The development of pore pressure within pavement granular layers under repeated loading was worth investigating due to its relationship to this study. Much research exists on the development of pore pressures within granular materials. Pumping occurs when pore-water pressure buildup induced by heavy wheel loads is high enough to cause ejection of material and water through the cracks and joints in a pavement slab.⁷ All failures in the rigid pavement sections at the AASHO road test were preceded by pumping of material from

beneath the concrete slab.⁸ Several relevant papers on this subject are summarized in Section 2.4.

Pavements utilizing open-graded bases offer the potential for long life due to their ability to easily remove excess water from the pavement system. However, impediments to satisfactory performance of these pavements include plugging of the open-graded layers by fine materials, which markedly decrease drainage layer permeability. Large deformations are also a problem due to breakdown of the individual aggregate particles and subgrade intrusion into the base course aggregate. Literature dealing with open-graded aggregate drainage potential and performance under repeated loading is discussed in Section 2.5

Geosynthetics, specifically non-woven geotextiles, have shown good potential as filters for fine soils in numerous applications ranging from highway strip drains to earth dams. In the case of an earth dam, the geotextile is subjected to flow from one direction under a constant head condition. For the geotextile to adequately function as a filter in pavement applications however, it must be able to filter under multi-directional water flow. The repeated loading of the pavement results in variable hydraulic head and flow through and within the plane of the geotextile. Section 2.6 summarizes literature dealing with the use of geotextiles as filters and separators within pavement systems.

2.2 Separation Layer Testing Research

Work closely related to this research has been performed on railway ballast and its separation from the underlying subgrade. Railroad ballast behaved similarly under repeated loading to open-graded aggregates used in highway applications. McMorrow⁹ looked into the performance capabilities of non-woven geotextiles when placed between cohesive subgrades and ballast in railway structural sections. McMorrow believed geotextiles did not perform as well as correctly designed sand filters when used as separation layers. To test this belief, a device called the "pulsator" was used to apply repeated loads to specimens contained within an 8 in. (20 cm) diameter cylinder. This device consisted of a 4 in. (10 cm) diameter loading head surrounded by an 8 in. (20 cm) outer diameter, by 4 in. (10 cm) inner diameter annular ring acting as a seating load. Deflections of both the inner and outer ring were measured.

Soil specimens 1 in. (25 mm) thick were cut from actual railroad subgrades for his research. For testing, the specimens were placed upon the bottom of the chamber and the geotextile placed above the soil. Uniformly graded gravel was placed above the geotextile followed by the loading apparatus. To prevent soil migration around the edge of the sample, beeswax was used to seal the perimeter of the chamber. Loading stresses of 40 psi (275 kPa) at 184 cycles per minute with repetitions up to 1,000,000 cycles were performed. This stress level was significantly higher than expected by British Rail during actual operations. McMorrow used two methods to define separation performance. The first was the deflection of the loading platen and the second the weight of clay eroded during the test. Good correlations between the deflection, weight, and \sqrt{N} (N load repetitions) were found for various geotextiles. Staple fiber, needle punched, geotextiles provided the lowest erosion and the lowest rate of deflection increase per load cycle. Continuous fiber, needle punched, non-woven geotextiles performed comparably with cumulative deflections of 400 mils (10 mm) at 1,000,000 repetitions. It should be noted with a sand filter alone, no significant clay movement occurred with up to 11,000,000 cycles of loading and there was only 75 mils (1.9 mm) of deflection at 1,000,000 repetitions. Based upon these results the sand filter performed better than the geotextile filters.

Hoare¹⁰ repeatedly loaded natural clays 3.15 in. (80 mm) thick and an aggregate layer separated by a heavy needle-punched geotextile in a 10 in. (25 cm) diameter cylindrical chamber. The loading platen covered the full surface area of the chamber. The geotextile was cut slightly larger than the chamber diameter to allow it to rise somewhat up the side of the chamber and contain the aggregate above it. Three types of aggregate layers were used; a single-sized $\frac{3}{4}$ in. (20mm) crushed rock, a dense-graded limestone, and $\frac{5}{8}$ in. (17mm) uniform spherical glass balls. A non-woven 4 oz/yd² (140 g/m²) melt bonded geotextile and 2 non-woven needle punched geotextiles of varying weights were used. Dynamic loads were applied at 2.9 psi (20 kPa) and 7.3 psi (50 kPa) at varying frequencies up to 10 Hz for duration of between 13,500 and 216,000 cycles. Hydraulic head was maintained during the test by pouring 17 oz. (0.5 liters) of water over the aggregate. Pressure transducers measured the time it took pore pressures to dissipate. The time to pore pressure dissipation depended on the separation layer and aggregate layer type. The increase in weights in the geotextile and

aggregate represented the amount of material passing into and through the geotextile from the soil below. The soil contamination value (SCV) was determined by comparing pre and post test weights of the geotextile and aggregate. The SCV was computed by dividing the weight increases by the surface area of the materials and presenting the data as a weight/unit area. The researchers found considerable variation in the data for this test when used as a measure of the geotextile's ability to control pumping. Loading frequency rates also did not have any significant effect on SCV. It was found thicker geotextiles (EOS 4 mils, 0.10 mm) showed lower SCV but even the "thick needle-punched geotextile was not capable of restraining soil migration under the conditions of the test."¹⁰ Soil migration through the geotextiles still continued after high repetitions, indicating stabilizing effects such as development of internal filtering was not present. Soil tended to migrate through the geotextile "at points where the subbase particles had been in contact with the geotextile."⁸ With the glass balls, SCV values were much more consistent due to their constant footprint on the geotextile. Soil squeezing through the geotextile at the points of aggregate contact increased the effective pore size locally which further diminished the geotextile's resistance to soil migration. This punching into the subgrade appeared to be the major cause of soil migration through the geotextile. "Reducing the stresses at the points of contact should reduce the punching effect and hence reduce the SCV."¹⁰ The use of finer subbase materials increased the number of contact points and lowered contact stresses and therefore reduced the SCV. To further validate that soil had moved through the fabric at aggregate contact points, moisture content profiles were measured across the specimen surfaces. Directly beneath the contact points, moisture contents approached the soil liquid limit and were significantly higher than the equilibrium moisture away from the contact points. Local shearing occurred as particles punched into the soil and this shearing resulted in local increases in soil moisture content beneath the aggregate contact points. This lower shear strength material more easily penetrated through the fabric openings.

Further research into geotextiles protecting soft subgrades from pumping into coarse aggregate layers was performed by Bell et al.¹¹ Field testing showed a non-woven geotextile was "relatively ineffective in preventing clay fines contamination, but was more successful in preventing penetration of the granular sub-base into the softened subgrade."⁹ The granular

filter layer seemed to perform well, with no evidence of clay fines migration. Due to the ease of installation and low cost of geotextiles, further laboratory studies were undertaken. Dynamic testing with both geotextiles and sand filters were performed at loads from 3 psi (20 kPa) to 10 psi (70 kPa) for 432,000 cycles (24 hr. at 5 Hz). The subgrade soil tested was a stiff silty clay with 20% by weight smaller than 2 microns. Two of the granular filters were primarily one sized sand in the 8 mil (0.2 mm) range with the third varying from 8 mil (0.02 mm) to 400 mil (10 mm). The aggregate layer was a uniform 3/4 in. (20mm) sized material. The testing mold was 14 in. (355 mm) in diameter. The soil was statically compacted in 4 lifts within the test chamber. As in Hoare's¹⁰ work, soil contamination values (SCV) were determined. It was apparent AOS values of the geotextile were a major factor in controlling clay fines migration. Additionally, initial subgrade moisture determined to a great degree the amount of contamination occurring during testing. Bell believed it was unlikely to "completely prevent fines contamination... and thus the object in using a filter beneath subbases must be to limit fines migration to an acceptable level."¹¹ Additionally, Bell believed the thick and incompressible granular filter layers maintain consistent filtering properties during loading. These granular layers also have a definite load spreading capability that the geotextile will not have if the geotextile's strength was not mobilized. No evidence of softening or slurry formation at the surface of the subgrade was found beneath the sand filter. With the geotextile filter, slurry was found clinging to the aggregate particles.

Friedli¹² tested woven polypropylene split film geotextiles as separation layers between fine subgrades and railway base course materials. Triaxial cells were used to test silty subgrades with sand or geotextile filters underlying a coarse granular base material. The silt was compacted within the split mold and the overlying layers compacted upon them. Each test sample was consolidated (with a phreatic head maintained) overnight to allow complete consolidation of the silt. Each test consisted of 5000 repetitive loads of a 7 psi sine wave corresponding to "the passage of an axle load of approximately 20,000 lb. (90 kN) at a depth of 20 in. (50 cm) below a concrete tie."¹² Both plastic creep and elastic rebound was measured during each loading cycle. Resilient modulus, defined as the ratio of the deviator stress divided by the recoverable axial strain was determined from these deformation measurements. The resilient modulus "generally decreased with load cycles and for any given

number of load applications a consistently higher (10% to 50%) resilient modulus occurred when the geotextile was used.”¹² The plastic strains were also smaller when a geotextile was used as well. Friedli expressed concern that ballast pockets formed in the subgrade beneath geotextiles. Water tended to accumulate in these pockets and reduced the subgrade strength.

LaFleur¹³ et al. investigated fines migration through non-woven geotextiles separating fine soils and coarse aggregates under dynamic consolidation of 5000 load cycles. Loading rates of 1, 5, and 10 Hz were used with stresses of 2 psi (12 kPa) and 7psi (48 kPa). A 2 part “consolidator” (LaFleur’s name for the device) chamber with a 4 in. (100 mm) inner diameter contained the subgrade and subbase material. The top half of the chamber held the aggregate subbase and received the load. The chamber was water-tight on the bottom so any water movement was upward. Soft subgrades were formed by compacting a material of slurry consistency to a height of 2.6 in. (66 mm). It was felt this soft subgrade was more representative of that found in the field. Image analysis was performed from cut geotextile specimens and examined under a microscope to get the spatial distribution of trapped particles. It was found that particles were concentrated at the gravel contact points and the clogging was very low between those points. Weight per unit area and consolidation/displacement was determined as was done by other researchers¹⁰⁻¹⁴. A linear relationship was determined between settlement and clogging for the coarse subbase. For the silty subgrades, settlement had stabilized at 5000 repetitions. However with the clayey subgrade settlement was still on the increase. This difference had been attributed to the incomplete dissipation of pore water pressures within the clay samples. Additionally, the larger aggregates induced a greater settlement rate and faster consolidation of the soil. Constant head permeability tests were conducted both prior to and after testing. Overall, the “pumping of subgrade particles was related to the piping ratio O_{95}/D_{85} of the combinations” and “the rate of clogging was directly related to the size of the aggregate and the uneven compression induced by open-graded aggregate.”¹³

Faure and Amir¹⁴ examined geotextile performance overlying soft clays. They concluded “the design of the separator geotextile cannot be done only using grain size distribution. The main parameter, significant of soil behavior and easy to determine, is the undrained cohesion C_u .”¹⁴ Their test cell was 6 in. (15 cm) in diameter and had two pistons

compressing symmetrically from above and below the samples. Faure and Amir felt this would avoid differential displacements that were too large between the center and sample sides. Clay layers 4 in. (0.1m) thick, underlying 4 in. (0.1 m) thick glass bead layers were loaded at 14.5 psi (100 kPa) at 1Hz for up to 40,000 repetitions. In this research, "the separation function was characterized not only by the passing soil but also by the ability of the structure to consolidate the fine soil and to drain it."¹² Comparisons were made between the mass of extruded water to the mass of extruded soil. It was found larger AOS non-woven and wide strip/slit film woven geotextiles were more efficient than other geotextiles during the initial 10,000 cycles.

The performance of geotextiles as separating layers with glacial till subgrades was researched by Glynn and Cochrane.¹⁵ It was noted "with repeated traffic loading plastic flow of softened clay can occur (i.e. squeezing upwards of failed subgrade into the stone layer interstices above). This leads to loss of useful depth of sub-base."¹⁵ The three soils were tested ranging from a heavy clay to silty/sandy material. Single sized ¾ in. (20 mm) aggregate was used above the geosynthetic. The soil samples were statically compacted at 72.5 psi (500 kPa) in 2 layers of 1.5 in. (40mm) each within a 10 in. (250 mm) diameter steel mold. To simulate severe construction traffic, static loading was performed and the average sub-base penetration into the subgrade was measured. The test also examined how well the geosynthetic reduced stone penetration into the subgrade during construction. A measurement of surface "unevenness" was made by taking 30 depth readings on the post test surface, 15 peaks and 15 indentations. Dynamic testing was performed at 7.3 psi ± 3.6 psi (25 to 75 kPa) for 108,000 cycles. The results showed "all fabrics successfully reduced stone point penetration, however, the thicker compressible membranes (geotextiles) performed markedly better at higher soil moisture contents than the two thinner incompressible membranes (geotextiles). It is also apparent from the low values recorded for average amplitude of penetration, plastic flow of softened clay into the stone interstices above was virtually eliminated by the presence of a geotextile. This was partially attributed to a local restraining effect being imposed on the subgrade due to the development of tensile forces in the geotextile between individual aggregate particles."¹⁵ The test results "clearly indicate the major importance of both loading levels and soil moisture content on clay contamination."¹⁵

For 50kPa at 18% moisture the SCV was 500 g/m² (value often considered an acceptable limit) while at 25% moisture contamination worsened considerably to 3 times that value. At moisture contents greater than 25%, the SCV became progressively worse. Additionally, the thickness of the non-woven fabric was attributed to good in-plane permeability and porewater pressure relief as well as a cushioning effect on the subgrade. A unique aspect of this research was the use of a "sandmat" filter. This filter was created by the inclusion of a fine sand within the non-woven geotextile fabric pore structure. This filter was very rigid and had a high resistance to local deformation, however "larger stress levels caused sand particles to penetrate through the fabric and become embedded in the subgrade surface."¹⁵ This behavior demonstrated the importance of matching the density of the fiber mat to the particle size grading of the granular material. The advantage of "this type of filter over conventional filters was its mechanical and hydraulic properties did not change significantly under test conditions. For instance, sand is a highly incompressible material and will remain permeable under load. By incorporating sand into the voids of a fabric, the fabric was prevented from collapse when stressed and serves to maintain the filtration characteristics of the composite. The fabric can complement this by providing the sand layer with a tensile resistance to movement. Under cyclic loading the sub-base particles may tend to punch into and through the sand, however, any displacement of the granular material is impeded by the fabric."¹⁵

Soil intrusion into the overlying aggregate also has detrimental effects beyond diminishing layer drainability. Bell, McCullough, and Gregory¹⁶ noted soil "material acts as a lubricant which also significantly reduces the shear strength of the stone sub-base aggregates".¹⁶

In a field study on geotextiles in railway track, Hillig and Lieberenz¹⁷ examined test sites lined with PVC/PET non-woven 14 oz./yd² (450 g/m²) geotextiles covered with 10 in. (25 cm) of gravel. The bearing capacity was measured at regular intervals and the presence of the geotextile sufficiently increased the bearing capacity of the soil to prevent intermixing of the soil and gravel. It was found non-woven geotextiles clearly separated the exposed loess loam and red marls from the gravel. The geotextiles were penetrated by fine grains of soil and the "tangle" network of the geotextiles were filled up with the soil silt fraction, increasing the weight from 14 oz. (450 g/m²) to 110 oz (3132 g/m²) with a decrease in permeability of a

factor of 4. It was noted by Hillig and Lieberenz "in earth stored samples, fiber movement was hindered by incorporating fine grains. The phases of fiber orientation, cross-point shifting and fiber stretching were thus scarcely possible or even impossible, so single fiber was essentially earlier exposed to stress, therefore absorbing forces at considerably lower elongations...these non-wovens prevent detrimental grain displacements, thus maintaining the gravel's strength properties for a long time."¹⁷

Raymond and Bathurst¹⁸ in another study of railway track geotextiles, examined the performance of in-service geotextiles. The results of their study led to a set of basic functional requirements for geotextiles placed below clean ballast:

1. To drain water away from the track roadbed on a long-term basis, both laterally and by gravity along the plane of the geotextile without buildup of excessive hydrostatic pressures.
2. To withstand the abrasive forces of moving aggregate caused by the tamping compacting process generated during initial construction and during subsequent cyclic maintenance, and by the passage of trains on a frequent basis.
3. To filter or to hold back soil particles while allowing the passage of water.
4. To separate two types of soil of different sizes and gradings that would readily mix under the influence of repeated loading and water migration.
5. To have the ability to elongate around protruding large gravel-size particles without rupture or puncture.

In-plane permeability of non-woven needle punched geotextiles is comparable to clean (no fines) sand. Virtually any clean non-woven needle punched geotextile should have a coefficient of in-plane permeability of at least 25 times the problem subgrade it is used to separate. The American Railroad Engineering Association suggests the d_{15} of the subballast be greater than 5 times the d_{15} of the subgrade since permeability of a uniform soil is approximately proportional to the square of its d_{15} value (k proportional to d_{15}^2). For the filtration opening size (FOS), the d_{85} subgrade $> 1/5 d_{15}$ subballast (typical subballast will have maximum void space sizes about $1/5$ of d_{15} and thus retain all particles of the subgrade soil). Thus the 95% retained value of EOS, which is a direct measure of the maximum size of the geotextile voids, should be less than the d_{85} of the subgrade soil in order to prevent fouling of

the geotextile. Raymond and Bathurst also suggest non-woven fabrics with at least 80 needle penetrations per square centimeter perform best in track rehabilitation. These geotextiles combine high in-plane permeabilities with low EOS values. They are generally made from fibers having a mass per unit length of less than 0.67g/1000m (0.67 tex) of fiber. These geotextiles when placed in front of bright light will show no penetration of light through even the minutest holes. Additionally, resin bonding outperformed unbonded geotextiles. The bonding agent should be a minimum of 5% by dry weight resin with no more than 20 % low modulus acrylic resin. For greater abrasion resistance, geotextiles with more fibers per unit area are recommended, though fibers as low as 0.3 tex would likely be damaged during needle punching. A tex of 0.67 is most common today.

A laboratory examination of geotextile separation performance under severe conditions was performed by Tsai and Holtz¹⁹. Geotextiles were assessed for their in-service survivability (rutting), the ability to retard fines migration, and their influence on subgrade pore pressure dissipation. A 110 gallon (0.416 m³), 40 in. (100 cm) diameter steel drum contained the soil and aggregate under test. A 4 in. (10 cm) diameter plate loaded the soil. This small load head ensured the container boundary did not interfere with the potential soil failure zone. Two different aggregate thicknesses 1.5 in. and 4 in. (40 mm and 110 mm) were tested. Loads of 90 psi (620 kPa) for up to 40,000 repetitions were performed. Rutting in the 1.5 in. (40 mm) aggregate base was about 0.75 in. to 1.5 in. (20 to 40 mm) greater than the rutting in the 4 in. (110 mm) aggregate base. Also, the geotextiles increased the bearing capacity of subgrades if the geotextiles survived construction and repeated loading. Additionally, it was found "tests with geotextiles over soft subgrades resulted in similar or smaller ruts than the test on a much stronger subgrade. Hence even non-woven geotextiles appeared to provide some reinforcing effect. However the results show no significant difference in ruts among the tests with different geotextiles."¹⁹ Tests with the thinner aggregate layer and geotextile when compared to the thicker aggregate layer alone show about the same or smaller ruts. "This implies that, if the geotextiles survive placement and dynamic loading, geotextiles may replace up to a 70 mm aggregate layer at the laboratory model scale, which corresponds to 190 mm in full scale."¹⁹

2.3 Durability of Stabilized and Modified Materials

In one of several studies on lime stabilized soils, Dempsey and Thompson²⁰ analyzed the effects of cyclic freezing and thawing (F-T) on the compressive strength and durability of lime treated soils. An accelerated testing apparatus was used to facilitate the research. The samples were subjected to temperatures and moistures calculated from a soil heat transfer model developed by the authors. In each case, the first 5 F-T cycles resulted in the greatest strength loss. The unconfined compressive strength for 4 of the fine grained soils tested dropped from 250-350 psi (1725 kPa-2400 kPa) to 20-150 psi (140 kPa-1725 kPa), resulting in an average strength loss of 50%. Subsequent F-T cycles resulted in negligible strength loss. This further confirmed previous work by Thompson²¹ where post F-T strength was determined or predicted from initial strength. Additionally, Thompson²² provides guidelines for lime-soil mixture design upon which subsequent work was based. The principles of mixture design developed by Thompson were utilized in this research.

A major study on the durability of stabilized subbase materials and their relationship to rigid pavement design was performed by Van Wijk²³ at Purdue University. In Van Wijk's research the erosion potential of Portland cement stabilized (1% to 7%) materials was investigated. Weight loss of small soil samples was measured during and after testing to determine erosion potential and rates. The samples were tested by both a brush test and a rotational shear device. Tests based upon 4 different compaction-gradation combinations for each of 4 different U.S. climatic zones were performed. It was found higher Portland cement contents resulted in lower erosion rates. Also "asphalt material with a large percentage of fines and a low compaction is likely to erode in any of the four climatic regions."²¹ For dense stabilized materials, surface erosion was the more important failure mechanism and not pore pressure buildup, since free water did not readily penetrate the stabilized materials ($k \sim 0.003$ ft/day (10E-8 m/s)). This surface erosion was increased by severe environmental conditions such as freezing and thawing cycles. With additional curing time, these effects were diminished. There was also the factor of stripping of asphalt modified soils. Van Wijk frequently discussed the practical situation of stabilized layer construction. During the

construction process it was inevitable the surface will be damaged to some degree, resulting in loose material that can easily erode away.

Kawamura and Diamond²⁴ studied the erosion characteristics of Portland cement and hydrated lime stabilized soils through the impact of simulated rainstorms. Their work was aimed at studying the erosion loss of soil on construction sites and how to best alleviate the erosion potential. Three stabilizers were tested, an analytical reagent grade hydrated lime, a poor commercial grade lime, and Type I Portland cement concrete. For the Crosby soil tested, a B-horizon type soil containing montmorillonite and other clays, 1% lime adequately stabilized this soil, leading to a decrease in erosion by a factor of 3 after 1 week curing when compared to untreated soil. Increasing the lime level to 2.5% resulted in considerable improvement. After 21 days, erosion was down by a factor of 30 from the untreated soil. Kawamura and Diamond noted however, while erosion potential was down, the material was not a solid "pavement" and the material was still porous and lacking in strength.

Eades and Grim²⁵ developed a test method to determine sufficient lime content for stabilizing soils. Soil-lime-water slurries were added to soils until a pH of 12.4 was reached. Thompson and Eades²⁶ further evaluated this procedure through unconfined compressive strength tests of the materials from Eades and Grim.²⁵ They concluded "the test conservatively indicates the lime required to produce effective stabilization in terms of the development of mechanical strength."²⁶

Litton and Lohnes²⁷ conducted similar testing on soil cement samples composed of loess-derived alluvium and sand mixtures and found much lower erosion rates (as measured by weight loss) as cement content increased from 5% to 9%. Additionally, the velocity of water flowing over the samples was directly related to the amount of erosion. The rate of weight loss also diminished rapidly during the first hour suggesting a logarithmic relationship between weight loss and test time.

2.4 Pore Pressure Effects on Granular Materials in Pavements

Dempsey,²⁸ evaluated channeling and pumping of pavement base courses by using 2 dense-graded base course materials (IDOT CA 6 and CA 9) and an open-graded base course

material (IDOT CA 7). The magnitude of pore-water pressure was an important factor affecting degradation, channeling, and pumping in granular base course materials. No pumping or degradation was observed in the CA 7 base course, in which the pore-water pressures never exceeded 0.3 psi (2.1kPa). However the CA 6 and CA 9 did pump and degrade. In the CA 7 no major gradation changes resulted from repeated loading due to the extremely rapid dissipation of excessive pore pressures. After testing, the percentage of base course material less than 0.4 in. (10 mm) had decreased substantially for the CA 6 and CA 9 due to pumping. Large accumulations of fines were found on the surface of concrete slab and shoulders at conclusion of testing. Considerable deformation of the open-graded CA 7 base course did occur. Inspection showed substantial amounts of A-6 (AASHTO) subgrade material had intruded into the lower portion of the base course. This was not a problem with CA 6 or CA 9. Additionally, for the open-graded base CA 7, excess pore pressure was affected very little by varying the loading durations from 0.1s to 1s. Dempsey concluded "subgrade intrusion must be considered when open-graded materials are used as subbases" and "a separation layer must be used between open-graded bases and fine subgrade soils".²⁸

In an extensive study on material breakdown and pumping, Hansen et al.,²⁹ measured pressure differences between approach and receiving slabs, and water velocities at slab joints as vehicles traveled over the joints. Field tests indicated vehicle traffic produced high pressures beneath the receiving slab and suction pressures beneath the approach slab, which induced water velocities in the opposite direction of vehicle motion. Water pressures beneath thermally upward curled slabs as a three axle truck passes at 24 mph (40 kph) ranged up to ± 2 psi (14 kPa). These values increased to ± 2.3 psi (16 kPa) as speed of the vehicle increased to 43 mph (72 kph.) The values ranged from 0.7 psi (5 kPa) to 4.5 psi (30 kPa) overall depending upon the type and speed of the vehicle. An evaluation of the ejected water showed no large (sand sized) grains, but sediment composed of extremely fine, clay-like particles. These fine particles were carried out by the water. To test subbase erosion based upon ejected water, water droplets were allowed to fall tangentially on the curved surface of dry cylindrical samples to simulate an impulsive shear stress. After 10,000 water drops at droplet velocities of 19 ft/s (6 m/s), erosion of only 0.007 oz. (0.2 ml) was measured. Thermal expansion of pavement slabs was also investigated as a possible mechanism for production of

finer. Hansen conducted tests in which slabs were slid back and forth 125 mil (3.2 mm) for 1095 cycles, simulating three years of thermal cycling. Afterwards, the slabs were lifted and loose materials were collected by the use of a fine bristle brush. Based upon the material collected, with appropriate volume computations, an estimated 19 mil (0.48 mm) of faulting per year was estimated. Hansen also theorized one other means of breakdown of the subbase material. A passing truck in afternoon sun can cause a curled down pavement slab to dig into and erode the subbase, possibly faster than axial or in-plane thermal expansion and contraction.

Dempsey, Carpenter, and Darter³⁰ performed large scale tests on rigid pavement sections. Their study indicated dynamic pore-water pressure could develop in the granular subbase when the pavement was subjected to repeated loads. The pavement sections were soaked and loaded at the rate of 15 times per minute. An increase of pore pressure was observed with an increase in the number of load applications. Water and soil directly beneath the slab seemed to pump up along the sides of the slab and throughout the joint between the slab and shoulder. Similar tests performed on open-graded bases showed no evidence of pumping or pore pressure values in excess of 0.3 psi (2 kPa).

According to Raad,³¹ current design and evaluation techniques of subsurface drainage systems rely on the ability of these systems to drain pavement moisture under gravitational flow conditions. Compatible permeabilities of the structural and drainage materials were the essential factors influencing water drainage in these pavements. Repeated stress pulses could result in residual pore water pressure buildup causing progressive loss of shear strength and stiffness in the underlying soil. Liquefaction of granular materials under the rigid slab occurred when the residual pore-water pressure became equal to the initial effective overburden pressure. Additional load repetitions could then result in the ejection of fine granular materials through cracks and joints in the pavement.

2.5 Open-Graded Base Courses

Crovetti³² discussed the feasibility of designing a drainage layer that will never become saturated. While this drainage layer may never become saturated, that does not mean the

underlying subgrade will not become saturated at some point. He suggested the concept of coefficient of transmissibility of the drainage layer (product of the thickness and permeability) as the controlling factor in water transmission. According to Jackson,³³ the drainage layer should be designed to transmit all infiltrated water during rain under partially or fully saturated flow conditions, and to limit the time during which the drainage layer is fully saturated to a short duration of a few hours or less after the rain stops. Tests on open-graded layers for IDOT using a constant head permeability device in which water flow was perpendicular to the direction of loading (closer to field conditions) showed saturated permeability's of IDOT CA 7 ranging from 26,000 ft/day (0.09 m/s) for a coarse gradation (< 1% passing #200) to 1250 ft/day (0.004 m/s) for a fine gradation (8% passing #200). Midrange gradation permeability was close to the fine gradation, 5000 ft/day (0.016 m/s). Corresponding drainage times to 85% saturation were 0.5 hr. and 0.03 hr. for the fine and coarse gradations respectively. This showed the extreme variation in drainage capabilities based on fine material content (<#200), even for open-graded layers.

A field evaluation of cement stabilized (cement content 200 and 300 lb/yd³ (120 kg/m³ and 180 kg/m³)), asphalt cement stabilized (1.8% AC content), and unstabilized open-graded base layers was conducted by Kazmierowski et al.³⁴ The open-graded layers tested were easily able to accept an inflow rate of 5.8 gal/min (22 liters/minute) through core holes without flooding and produced an outflow rate of 2.3 gal/min (9 liters/minute) through the outlet drains. While the outflow rate was below 50% of the inflow, Kazmierowski cites numbers from comparable tests on different base courses were not available. The aggregate used consisted of 100% face crushed aggregate. FWD deflection measurements (18 in. (450 mm) plate and 9000 lb. (40 kN) dynamic load) on the open-graded bases ranged from 13 mil (0.53 mm) for the cement treated base to 19 mil (0.74 mm) for the untreated base. With the addition of the concrete slab, deflections decreased to 3 mil (0.07 mm) for each base type, thereby showing no structural benefit of one type of modified base over another.

Barenberg and Tayabji³⁵ performed a full scale test on open-graded bituminous aggregate mixtures (OGBAM) utilizing the University of Illinois Test Track. Four inch thick OGBAM (CA 7 and CA 14) drainage layers with various base/subbase/geotextile combinations were tested. Early in the research it was found permeability was inversely

proportional to the compaction effort used to prepare the specimen. "Excessively high compaction efforts lead to particle breakdown and subsequent changes in particle gradation, as well as a reduction in the volume of voids in the specimen."³⁵ It was also found coarser CA 7 was much more strongly affected by the subgrade fines than the CA 14, resulting in a higher degree of plugging in the CA 7. This was determined by continually measuring outflow rates versus load applications during the research. Subgrade intrusion depths of up to 0.5 in. (13 mm) were seen in the OGBAM layers. Barenberg and Tayabji found for structural drainage sections subjected to heavy wheel loadings and high inflow, excessive rutting occurred in the test section using a filter cloth separation layer. Barenberg and Tayabji state this could be due to a detrimental effect of the filter cloth in soil fines washed out immediately as loads were applied. However, the subgrade soil in Barenberg and Tayabji's study was unstabilized. For the test sections without filter cloth, the aggregate layers were clogged with soil up to 3 in. (75 mm) into the layer. Barenberg and Tayabji point out the addition of a small amount of lime "restricted quite efficiently the washing out of subgrade fines."³⁵ Good success was found however with sand filter layers used as separation layers. Barenberg and Tajabji pointed out on several occasions, the severity of the load imparted by the test track system. This severe loading, which does hasten testing, may also cause problems not normally seen in the field. High deformations seen in the OGBAM and subgrade layers resulted in fatigue type failures, which would have been considerably reduced had the loading levels been comparable to those expected in the field.

To address the stability or deformation resistance of open-graded layers, Bathurst and Raymond³⁶ tested thin (4 in. (100 mm)) open-graded layers under dynamic plate loading. Guidance for their testing was obtained from similar testing for ballast aggregates in railway tracks. Bathurst and Raymond investigated how fracture resistance, abrasion resistance, and gradation affected the stability of the material under repetitive loading. For comparison purposes the aggregates were characterized by the "aggregate index number", I_a . This value was obtained by running both Mill Abrasion and LA abrasion tests on the aggregate in question. The Mill Abrasion (MA) test indicated more about the aggregate's resistance to abrasion (hardness), while the LA abrasion test was more indicative of the aggregate's resistance to fracture (toughness). Raymond cites studies by the CP Railroad have shown

“aggregates that were tough with respect to fracture resistance were not necessarily highly abrasion resistant”, hence the need for the combined aggregate index number I_a .³⁷ For this study, and the CP Railroad: $I_a = 5*MA + LA$. Bathurst and Raymond performed the tests with the open-graded layer resting upon a closed-cell gum-rubber mat (CBR ~ 40) to simulate a flexible support condition. Unstabilized aggregates were tested since it was felt over time, asphalt treated aggregates would strip and the resulting strength would be the strength of the unbound aggregates themselves. The results of their study showed “displacement versus number of loads was highly nonlinear, with most of the deformation occurring early in the loading program.” Permanent deformation in the aggregate layer ranged from 0.2 in. (5 mm) for trap rock to 0.6 in. (15 mm) for limestone. Bathurst and Raymond were quick to point out permanent deformation after a given number of cycles was sensitive to the initial seating of the plate upon the open-graded layer. Bathurst and Raymond also found for unbound aggregate, the ability to resist permanent deformation was directly related to the quality of the aggregate as measured by the aggregate index number. Additionally, this permanent deformation increased as the underlying support decreased, i.e. with weak subbase/subgrade.

The capability of open-graded aggregate layers to sustain construction traffic during paving is an important practical concern. Hall³⁸ tested cement treated open-graded layers with varying cement contents under traffic loading to determine acceptable cement contents for both drainage capability and stability. Field responses such as rutting and raveling were examined. Additionally, field compression and split tensile tests and laboratory compression and flexural tests were performed. Recommendations for cement content of 150 lb/yd³ (90 kg / m³) for low trucking volumes to 250 lb/yd³ (150 kg/m³) for high trucking volumes and/or low support were made.

Hoffman³⁹ compared five types of subbases ranging from very impermeable to highly permeable and found an open-graded base layer provided adequate support for construction equipment and could be placed at a competitive cost. After 15 months of service, the Pavement Serviceability Index (PSI) of the open-graded sections were equal to or exceeded the PSI of standard dense-graded subbase typically specified by PennDot. For these open-graded layers to function properly, minimal material must pass the 80 mil (2.00 mm, #10) sieve. It was suggested a minimum amount (less than ~2%) of 80 mil (2.00 mm) sieve size

material be present in the matrix since it was found not to add to the material stability. As much as 5% of this fine material migrating through the matrix could substantially lower the layer permeability and clog the base drain system.

2.6 Geotextiles as Filters/Separation Layers

In an application such as addressed in this research, the geotextile was placed between the stabilized layer and the base course. It was felt properly selected geotextiles (see following section) could act as filtering devices to eliminate or at least minimize the plugging of open-graded bases with fines from the underlying stabilized subbases.

Copeland,⁴⁰ studied subdrain filtration and permeability and discovered there was an interaction between the soil and filter geotextile. "A complex bridging or arching occurs in the soil next to the geotextile that permits particles much smaller than the openings in the geotextile to be retained"⁴⁰

In research into the behavior of geotextile filters for use in pavement subdrains, Janssen⁴¹ found the geotextile was able to clean itself and not plug up. Janssen surmised this was probably due to the nature of the loading. "If the total hydraulic gradient in the sample had been constant, plugging of the soil-geotextile system and loss of permeability would probably have been irreversible. However the hydraulic gradient was pulsed. The accelerating water velocity caused by the changing hydraulic gradient transfers momentum to the soil particles and dislodges them from their existing structure. Each gradient pulse, although short in duration is able to move the soil particles a bit."⁴¹ The direction of this particle movement being from the soil into the geotextile. Janssen found several problems with geotextiles such as high hydraulic gradients in conjunction with the stretching of the geotextile and enlargement of the geotextile pores can lead to piping of fines through the geotextile.

Proper geotextiles must be selected and evaluated in this research if success in mitigating fine movement is desired. A detailed evaluation of geotextile filter criteria was produced by Carroll⁴² and several points relevant to this research were made. Accepted criteria for permeability and clogging resistance of geotextiles must assure geotextile permeability greater than the permeability of the protected soil throughout the life of the

drain. It was suggested the permeability (k) of the geotextile be 10 times the permeability (k) of the soil. It was not a problem for geotextiles to meet this standard when compared with the stabilized subbase material. However this standard was not easily met for geotextiles with respect to open-graded aggregates; 120 ft/day ($4E-4$ m/s) and 15,000 ft/day (0.05 m/s) respectively. In a sense, the geotextile acted as a barrier to water when compared to the open-graded aggregate. Carroll suggested EOS (geotextile)/ D_{85} (soil) be less than 2 to 3 for proper filtration. Additionally, the clogging behavior of a geotextile should be evaluated in a test simulating in-place conditions as closely as possible and with the appropriate compressive forces expected in the field. Compressive forces were shown to reduce the k value of compressible needle-punched geotextiles by a factor of up to 8. Test conditions had a significant influence on geotextile performance and appropriate hydraulic gradients and soil types need to be used when evaluating geotextiles.

Weimar,⁴³ studied the performance of geotextiles for erosion control and postulated the concept of the geotextile as a "permeable constraint" and not as a filter. A true filter removed suspended particles from a fluid and by this action must plug. Therefore, a geotextile must be designed to retain large particles and allow suspended particles from the pore water to pass.

Lawson,⁴⁴ studied in detail the filter requirements for low hydraulic uni-dimensional flow conditions and discussed the mechanism of stabilization of the soil / geotextile interaction with time. He cites the need for the piping of fines to stop shortly after installation and for the soil conditions to stabilize over a 4 to 5 month period following geotextile installation. He found a "bridging network" of fine free soil material formed against the geotextile. Next to this fine free layer was the soil filter (dense-graded) followed by undisturbed soil.

Seitz and Kany⁴⁵ performed dynamic loading of aggregate/geotextile/soil specimens under flow conditions. In analyzing their results, Seitz and Kany calculated void ratios of contaminated geotextiles based upon the amount of soil retained within a given geotextile. Evaluations were made by comparing the post test void ratio (e^*) to the void ratio of the clean geotextile (e). For a fine sand as the soil under test, post test e^*/e values for mechanically stabilized (needle punched) non woven geotextiles averaged 76%, while for chemically stabilized geotextiles it averaged 85%. The cumulative deformations for this soil ranged from

1% to 4% over 14,400 cycles. During 8 hours of loading with clay/silt soils, measurable passing soil was only observed for the thin geotextile (5 oz., 170 g/m²).

The behavior of geotextiles as separators in roads was simulated in a different way by Floss et al.⁴⁶ in a 0.7 m x 0.7 m chamber. Loading was accomplished by 3 hydraulically controlled 150 mm diameter pistons spaced evenly within the chamber. These pistons applied loads to the soil/geotextile system alternately to simulate a rolling and mixing action of truck tires. Comparisons between 10 oz./yd² and 4 oz./yd² (351 g/m² and 140 g/m²) mechanically bonded non-woven geotextiles showed the heavier geotextile allowed only half the amount of particles through it compared to the lighter geotextile. "Here the buffer effect of the higher mass per unit area and thickness has a favorable effect."⁴⁶ The heavier geotextile pores had not "saturated" with fine soil particles even though particles had passed through it. Tests with thermally bonded non-woven geotextiles showed with their greater stiffness, deformations and stress on the silt were reduced hence lower fine particle movement. Floss also surmised with thermally bonded geotextiles, if particles were too large to pass through voids then they will be blocked until the force was sufficient to break the bond, however in mechanically bonded geotextiles, the individual filaments may be moved as necessary for the particles to pass through. Therefore, thermally bonded non-woven geotextiles were preferred over mechanically bonded geotextiles.

2.7 Research Relevance

The failures of continually reinforced concrete pavements with open-graded bases overlying lime treated soils in Illinois have spawned this research. A thorough review of the existing literature has shown that a detailed and wide knowledge base exists in relation to this subject. However, several points of interest to this research were not covered in the literature and made this research pertinent. These points are outlined below.

1. Many types of soils ranging from in-situ to remolded soils have been tested under repeated loading conditions. Lime stabilized or modified soils, frequently used as pavement subgrades/subbases in Illinois, have not been examined in the fashion of this research. The

use of accelerated curing and vacuum saturation techniques to rapidly produce saturated specimens has not been used before in this same context.

2. The concept of soil strength as a determinant of performance has not been addressed. Frequently separation performance was examined for various soils and separation methods without reference to any quickly measurable parameter such as soil strength. The use of the cone penetrometer to measure strength in this context has not been attempted.

3. Direct comparisons between accelerated loading (high stress levels and low repetitions) and typical field loading (low stress levels and high repetitions) have not been sufficiently investigated. Any attempt to correlate performance between the two types of loading conditions has not been made. The importance of developing a correlation between the two types of loading can foster much more rapid evaluation of separation layer performance.

4. An aggregate layer consisting of an actual in use open-graded aggregate gradation has not been tested in this context. Single sized aggregate, typically 0.5 in. (13 mm) to 0.75 in. (19 mm), or more commonly a denser aggregate blend has been used. An actual gradation imposes differing contact stresses on the soil surface and can lead to more variation in the results, but is more realistic of field conditions.

2.8 Summary of Applied Information

There were many concepts and testing techniques gleaned from the literature that were applied to this research. A number of the more important ideas obtained and how they were adapted for this research are highlighted below.

1. In much of the literature, needle-punched, non-woven geotextiles were shown to perform better than other types of geotextiles at minimizing soil pumping into the aggregate layer. A single appropriately selected geotextile was used whenever geotextile separation was sought. The goal of this research was not to determine which geotextile performed best, but to establish whether soil strength standards with respect to accelerated loading can be used to determine long term performance.

2. Several different variations of stiff walled testing chambers were commonly used instead of triaxial cells. A stiff walled testing chamber was used in this research. The cylinder was made from Plexiglas™ so that the pumping and intrusion processes could be visualized in real time. The chamber was made to readily assemble and disassemble to facilitate testing of large numbers of specimens. The loading head was constructed to cover the entire soil surface so as to minimize any bearing capacity type failures seen with accelerated load testing.

3. The concept of determining soil movement by measuring and comparing pre and post test material weights was common among virtually all researchers. New techniques to determine material movement for tests without separation and for dense-graded separation layers were developed in much the same way for this research.

4. Applying realistic field loading levels for large numbers of repetitions was frequently cited in the literature. The use of over-loading levels for smaller numbers of repetitions was also cited. This research performed both types of loading and correlated the performance between the two types of loading scenarios. An accelerated loading methodology minimizing the need for extremely time consuming low loading level tests was developed.

5. The literature frequently mentioned measuring both permanent and elastic deformations. A technique to measure deformations through the loading head itself by linear variable differential transformers (LVDTs) was used in this research.

6. Pre and post test aggregate gradation comparisons were made. This procedure was initially performed in this research but was abandoned after minimal differences were found.

7. A phreatic head applied above the soil and within the aggregate was used in this research as did all the previous researchers. The water used for this study was dyed so that the movement of the water could be viewed through the plexiglas test cylinder.

8. Relating deformations with material movement was cited in the literature. In this research, deformations were related to material movement and were also related to soil strength.

9. Costly, computer controlled servo-hydraulic test systems were commonly used in previous research. For this research, an computer controlled pneumatic test system was

designed and constructed since the Illinois Department of Transportation did not possess such a device and it was more cost effective.

3. MATERIALS UNDER INVESTIGATION

3.1 Introduction

Three groups of materials were tested in this research. The first group consisted of lime stabilized soils. The second group consisted of two separation layers: non-woven geotextiles and dense-graded aggregates. Open-graded aggregates for the base course were the third group of materials tested. Details pertaining to the soils, geotextiles, and aggregates used in this research are presented in this section. Applicable literature is cited followed by the laboratory material characterization of each material.

3.2 Subgrade Materials

3.2.1 *Mexico Clay*

The first soil used in this study was Mexico Clay. This brick clay from Mexico, Missouri had 99% by weight passing the # 200 sieve and was classified as an AASHTO A-6 soil. The soil gradation is shown in Figure 3.1. The gradation of the clay was determined by hydrometer analysis performed according to AASHTO T 88-93 (ASTM 422). This material was ideal for initial testing since it was not highly lime reactive, yet was very uniform in composition. Atterberg limit testing according to AASHTO T 89-93 and T 90-92 (ASTM D4318) gave a PL of 18%, a LL of 33%, and a PI of 15%. Moisture-density relations were developed by compacting specimens according to AASHTO T 99 (ASTM D698-A) Proctor specifications. Tests were conducted with no lime and 3% lime for various water contents to determine the optimum moisture and maximum dry density for the clay-lime mixes. Samples prepared with 5% lime did not improve the soil physical properties over the 3% lime soil mix. The moisture density relations are shown in Figure 3.2.

Strength tests were also performed in conjunction with the moisture-density tests to establish the optimum lime content. Figure 3.3 shows the results of strength testing with identically prepared 2 in. (50 mm) diameter by 4 in. (100 mm) long cylindrical samples loaded

at 0.05 in/min (0.2 m/s) according to AASHTO T 208-92. Twenty samples were oven cured at 120° F (50° C) for 48 hours. This curing level has been shown to simulate 30 days curing in the field at 68° F.^{18,46} Ten of these samples were then vacuum saturated with a 2 hour soaking period. A dramatic strength drop from 148 psi to 19 psi was seen. Samples prepared at 5% lime had comparable strengths to those produced with 3% lime. For practical purposes, the maximum strength occurred at 3% lime with further increases in lime content providing little if any strength gain. Note the significant decrease in strength with specimen saturation shown in Figure 3.3. This was an important factor in this research since pumping rates increased markedly with decreasing soil strength as described in Chapter 6. Based upon moisture-density and strength testing, mixes with 3% lime were chosen. The resulting mixes had an optimum moisture content of 17.5% and a maximum dry density of 106 pcf.

In Chapter 6, analysis of the tests performed in this research is presented. Specimen strength was measured using a hand held cone penetrometer resulting in a cone index reading (CI). The hand held cone penetrometer consisted of a 20 in. (500 mm) long by a 0.5 in. (12 mm) diameter steel shaft with a 0.5 in² (320 mm²) conical tip, 1.5 in. (40 mm) long, affixed to a proving ring/dial gage. The cone was pushed into the soil specimen at approximately 1.5 in./sec (38 mm/sec). The gage read strength values from 0 to 300. From this testing a rough correlation between CI and unconfined compressive strength q_u was found. CI values of 300 were equivalent to a q_u of approximately 150 psi. CI values of 150 corresponded to q_u values of approximately 50. Samples with CI values of 80 or less were estimated to have q_u values of 20 or less.

3.2.2 *Wisconsinan Silty Clay Till*

It is commonly known silty materials are more prone to pumping behavior than clayey materials due to their small size and minimal cohesive properties. A low PI silty material was the second choice of material to evaluate in this study. The gradation analysis for this Wisconsinan Silty Clay Till is shown in Figure 3.4. This soil was obtained at a local construction development in Urbana, Illinois. Prior to testing, the soil was broken into small pieces, dried, and then ground into fine particles passing the #40 sieve. Moisture density

relations are shown in Figure 3.2. This soil, had 85 percent by weight passing the #200 sieve with 25% finer than 0.08 mil (2 μm) according to AASHTO T 88-93 (ASTM D2487). Atterberg limit tests according to AASHTO T 89-93 and T90-92 (ASTM D4318) gave a PL of 18%, a LL of 44%, and a PI of 26%. The material was classified as an AASHTO A-7-6 due to the soil's plasticity though it was considerably coarser than the Mexico Clay. The moisture density properties of this till were determined in the same manner as for the Mexico Clay. This was accomplished by compacting specimens according to ASTM D698-A (AASHTO T-99) Proctor specifications on soil-lime-water mixes. Tests with 0% and 3% lime were conducted for various water contents to determine the optimum moisture and maximum dry density for the clay-lime mixes.

Strength tests were also performed in conjunction with the moisture-density tests to establish the optimum lime content. Figure 3.5 shows the results of strength testing with 2 in. (50 mm) diameter x 4 in. (100 mm) long cylindrical samples loaded at 0.05 in/min (0.2 mm/s). As with the Mexico Clay, these values were the average of several test specimens. These samples were oven cured at 120° F (50 C) for 48 hours. This curing level has been shown to simulate 30 days curing in the field at 68° F.^{18,46} For practical purposes, the maximum unconfined compressive strength occurred at 3% lime with further increases in lime content providing little if any strength gain. For this reason, 3% lime was selected as the design lime content. Specimens compacted and cured with 3% lime showed unconfined compressive strength gains over 100 psi more than those prepared without lime. The saturated strength of this lime stabilized soil was considerably lower than the strength at optimum moisture as shown in Figure 3.5. The resulting mixes have an optimum moisture content of 19.5% and a maximum dry density of 101.5 pcf.

3.2.3 Lime

The lime used in the stabilization of the soils in this research was a high calcium hydrated lime from the Mississippi Lime Company in Alton, Illinois. This lime contained from 96.0% to 97.2% $\text{Ca}(\text{OH})_2$ with a CaO equivalent of 72.6% to 73.6%. Gradation analysis of the lime yielded 100% passing the #100 sieve, 98.5% passing the #200 sieve, and 92% passing

the # 325 sieve. The specific gravity of the lime was approximately 2.4. The bulk density of the lime ranged from 20 lb/ft³ to 32 lb/ft³ (320 kg/m³ to 515 kg/m³) depending upon the degree of compaction.

3.3 Aggregate

3.3.1 *IDOT CA 7 Base Layer*

The open-graded aggregate selected for use in this research study was a mid-band IDOT CA 7 gradation. The only exception made to the gradation was the elimination of minus #200 material. This was done to ensure fines measured within the aggregate and geotextile after testing came from pumping of the subgrade soil and not the aggregate. Individual aggregate batches were blended based upon the CA 7 mix design from pre-sieved aggregate piles to maximize uniformity and repeatability of results. The aggregate gradation used in each test is presented in Table 3.1.

3.3.2 *IDOT CA 6 Dense-Graded Aggregate Separation Layer*

The dense-graded aggregate evaluated in this research was a mid-band gradation IDOT CA 6. This gradation was commonly used as a separation/filter layer by IDOT. This aggregate had an optimum moisture content of 6.5% and maximum dry density of 130 pcf. A 2 in. (50 mm) layer at maximum dry density when placed above the stabilized soil within the testing chamber contained 7.5 lb. (3400 g) of dry mix. The mix design is presented in Table 3.2.

3.4 Geotextile Selection and Characterization

The goal of this research was not to establish which geotextile performed the separation function best, but to determine whether geotextiles in general were likely to be successful as separation layers between stabilized soils and open-graded aggregates. Previously cited researchers established ample criteria for geotextile filter and separator selection. A non-woven geotextile (Synthetic Industries GEOTEX 1101), typical of those

used for separation purposes was selected for testing. This geotextile met the specifications required for particle size, retention, and flow capability for the soils tested in this research. As stated in the previous section, Carroll's criteria was $O_{95}(\text{geotextile}) < (2 \text{ or } 3) d_{85}(\text{soil})$. As shown in Figures 3.1 and 3.4, the d_{85} values for the Mexico Clay and Wisconsinan Silt were 2 mil (0.05 mm) and 8 mil (0.2 mm) respectively. The geotextile's AOS of 100 or O_{95} of 6 mil (0.150 mm) met this criteria for the clay and was conservative for the silt. Additionally, a thick geotextile was desired since it would impart a "cushioning" effect on the soil from the open-graded aggregate footprint. This geotextile had a weight/area of 10.3 oz/m² (350 g/m²). The geotextiles' grab tensile strength of 300 lb. (1.34 kN) and puncture resistance of 170 lb. (0.75 kN) were sufficient to prevent aggregate punch through and stretching of the fabric. The concern over stretching was warranted based upon previous researchers'⁷⁻¹¹ findings that soil tended to pump at the points of aggregate contact. The fabric was also sufficiently pliable to conform to aggregate imprints which has been shown to aid in soil filter formation at the fabric interface.⁷ The properties of the geotextile tested in this research are presented in Table 3.3.

Table 3.1: IDOT CA7 Mix Design

Sieve Size	Weight	% Passing
1 in.	352 g	94
½ in.	2996 g	42
#4	2412 g	0
Total	5760g	

Table 3.2: IDOT CA6 Mix Design

Sieve Size	Weight	% Passing
½ in.	714 g	79
#4	1054 g	48
#16	714 g	27
# 200	612 g	9
Pan	306 g	0
Total	3400 g	

Table 3.3: Synthetic Industries GEOTEX 1101

Non-woven, Needle punched Polypropylene, Staple fiber 10.3 oz/y ² (345 g/m ²) AOS 100 (0.150 mm) Permeability 0.30 cm/sec Permittivity 1.20 sec ⁻¹

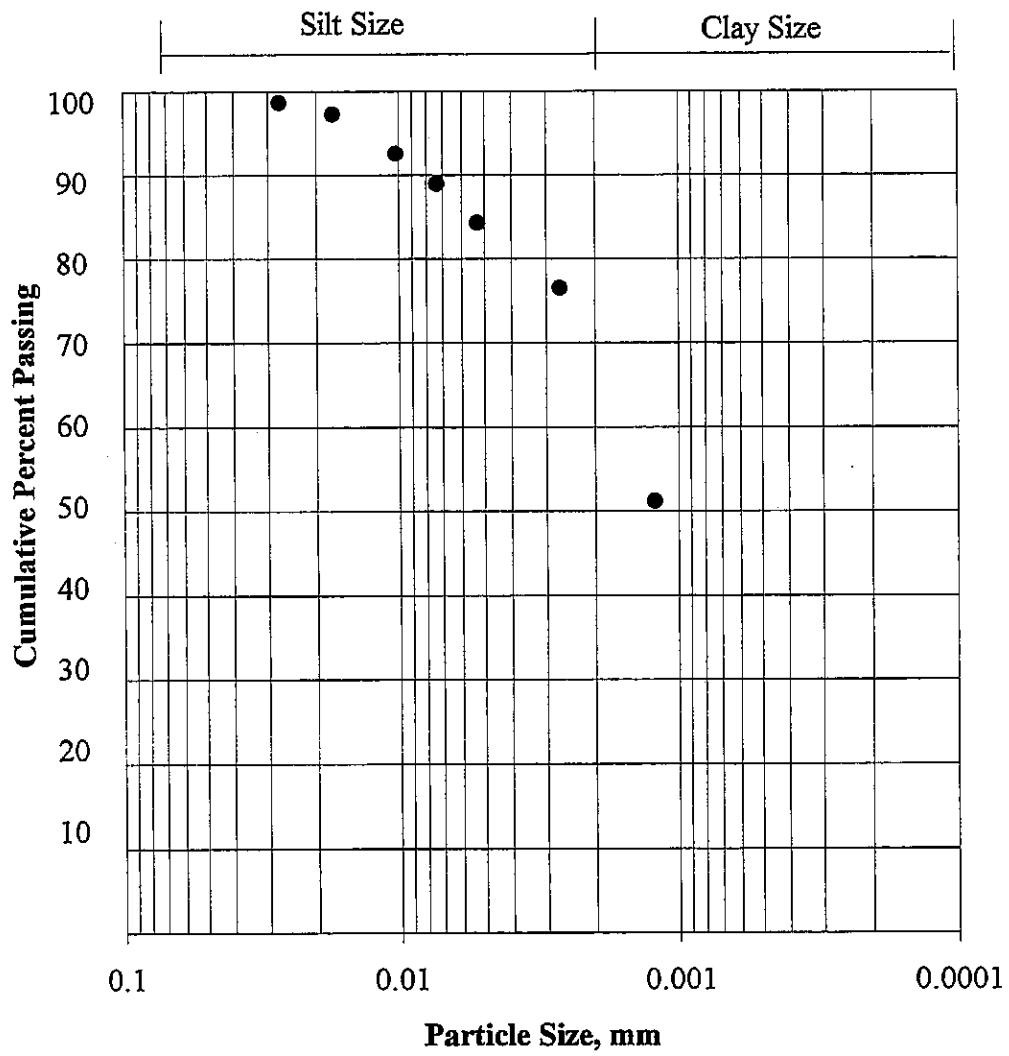


Figure 3.1: Mexico Clay Particle Gradation

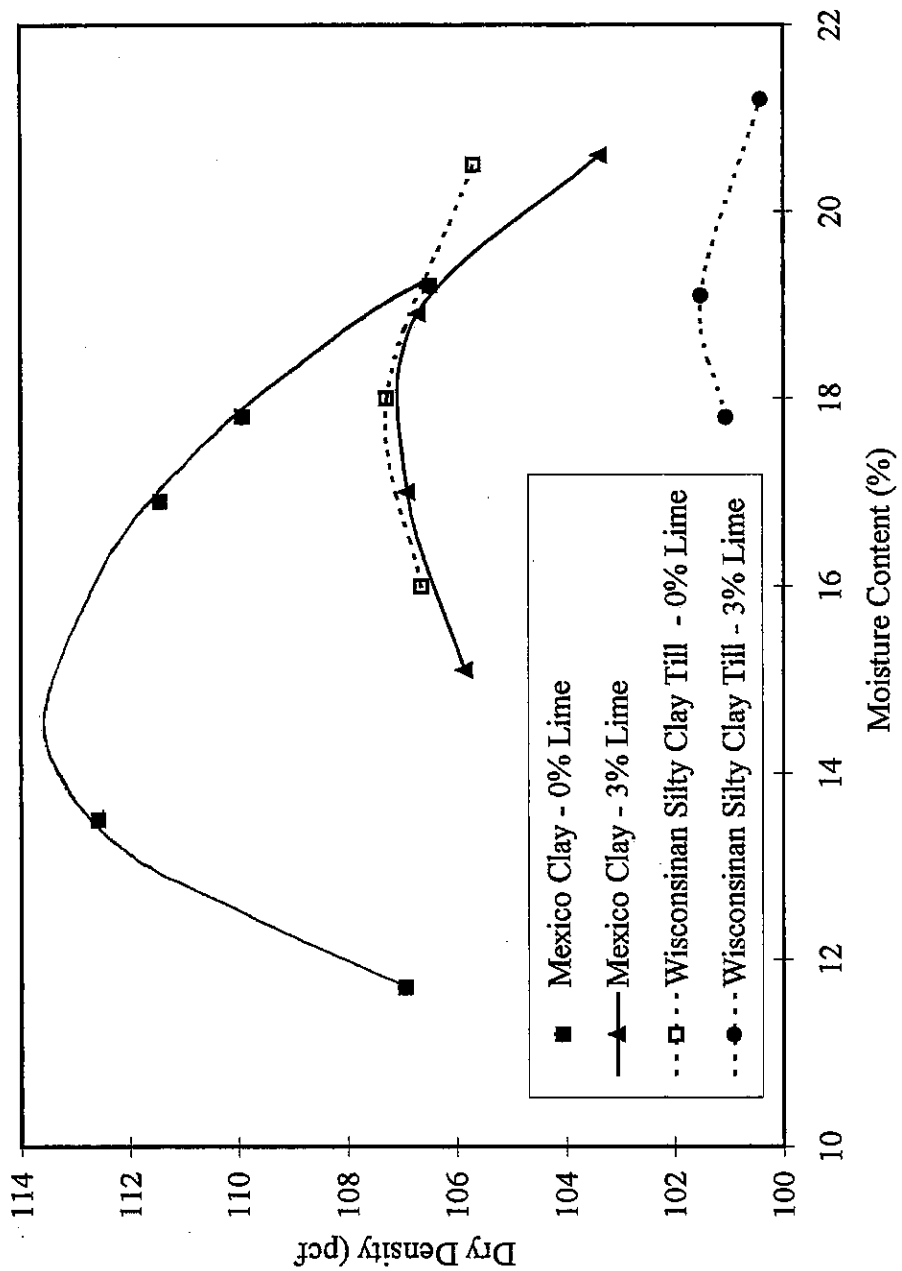


Figure 3.2: Lime Stabilized Soil - Moisture Density Relations

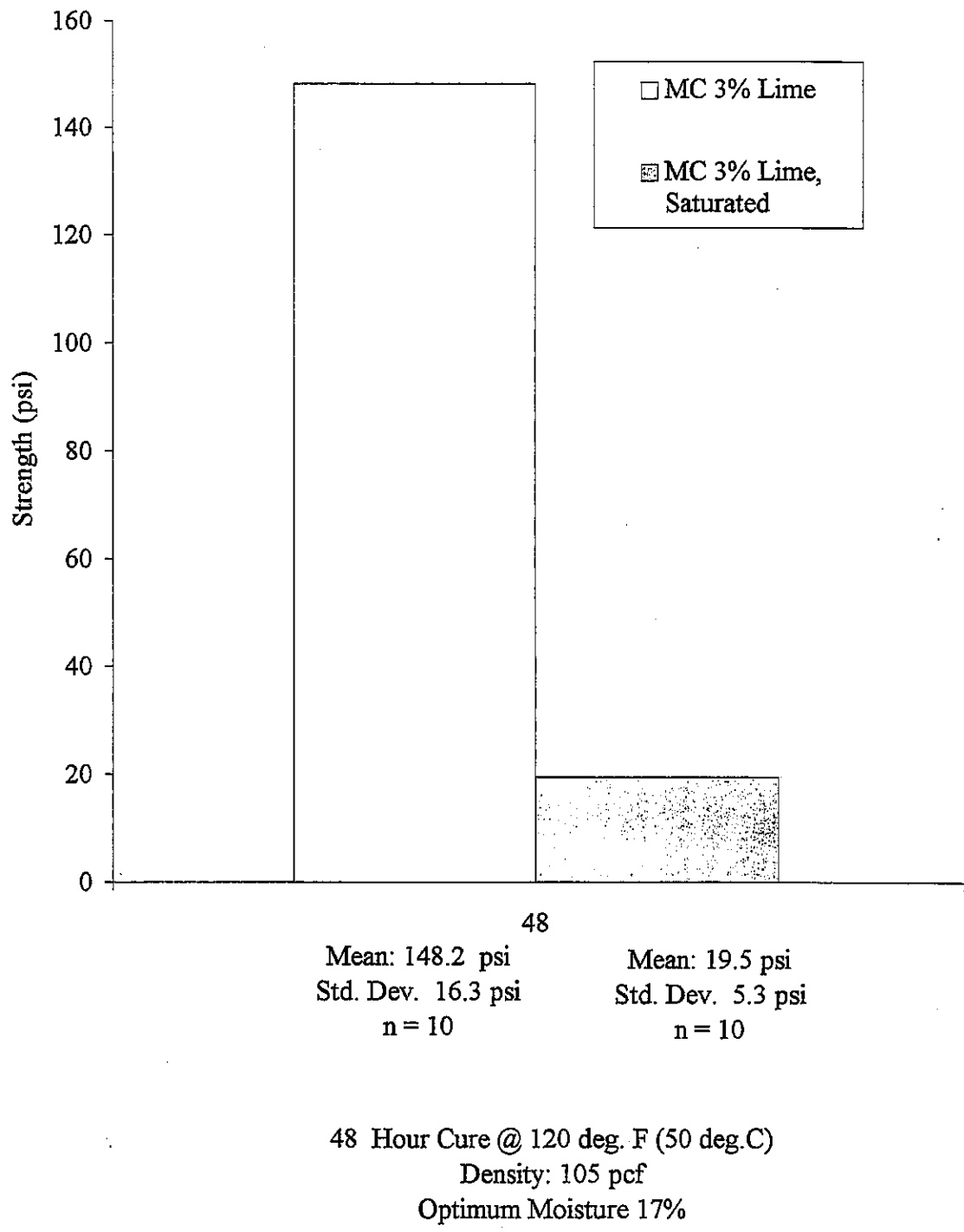


Figure 3.3: Mexico Clay Unconfined Compressive Strength Testing

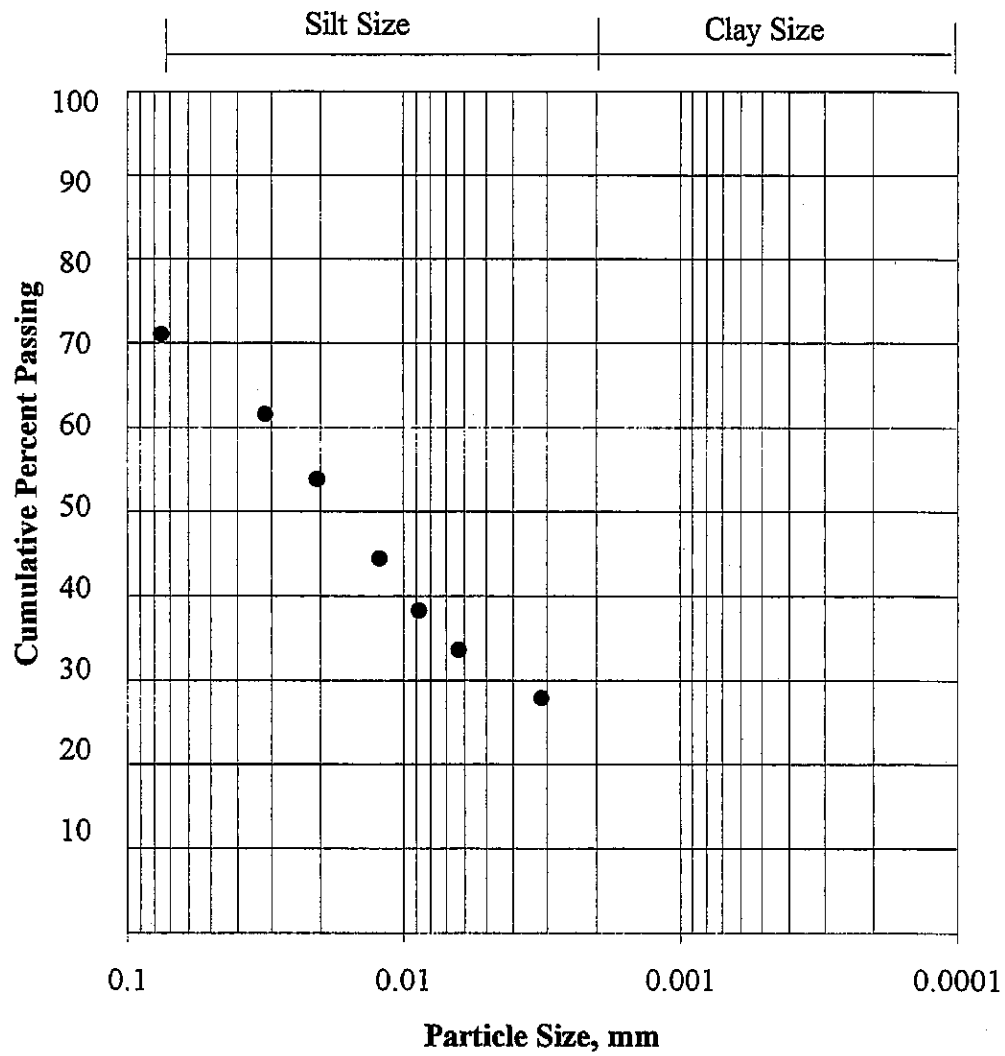


Figure 3.4: Wisconsin Silty Clay Till Particle Gradation

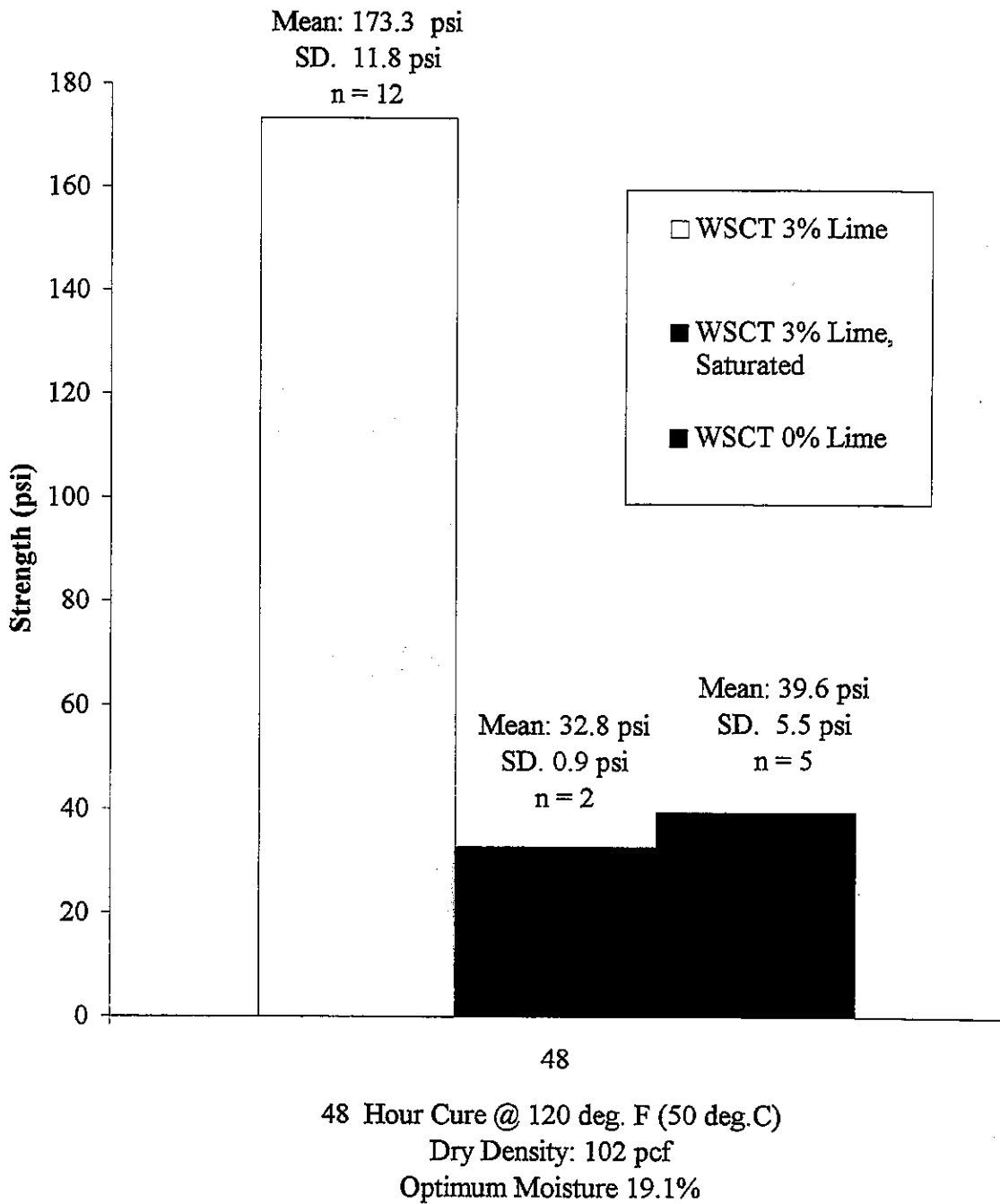


Figure 3.5: Wisconsin Silty Clay Till - Unconfined Compressive Strength Testing

4. EQUIPMENT DESIGN AND DEVELOPMENT

4.1 Equipment Overview

To accomplish this research study, new repeated loading test equipment was designed and constructed. The Illinois Department of Transportation did not possess the proper equipment for this study. Repeated loading apparatus was not available for use in this research and it was more cost effective to design and construct a new pneumatic system than to purchase an expensive servo-hydraulic system. The resulting system consisted of a loading frame containing two pneumatic loading heads, each with electronic control and computer data acquisition. The samples were tested in newly designed stiff wall plexiglas test cylinders. These cylinders eliminated the need for labor intensive and time consuming triaxial cells. Details of the design and construction of each part of the equipment follow.

The goal of this research was to develop a quick and straightforward test procedure to evaluate separation layer performance. Therefore, the equipment should be easy to operate in the laboratory. Additionally, the equipment should be inexpensive to design and build. All of the researchers previously cited in this report utilized very costly servo-hydraulic systems. To minimize costs in this research a pneumatic system rather than a hydraulic system was constructed. Tradeoffs had to be made and accepted in performance however since load control by large quantities of air was not as precise as servo-hydraulic control. Also, customized electronic controls were designed and built. Figures 4.1, 4.2, and 4.3 show the overall system.

4.2 Pneumatic System Design

To develop an inexpensive dynamic repeated loading test system, pneumatic actuation was chosen since it was more cost effective. The loading requirements were selected based upon previous researcher's work and layered elastic analysis of material properties. After the loading requirements were known, the system components were selected appropriately. The main components of each loading station were an air cylinder, a two-way valve, an air

reservoir, and a pressure regulator/filter. Figure 4.4 shows the two loading cylinders and a test chamber in operational position.

4.2.1 *System Loading Requirements*

Elastic layer analysis was performed on a typical concrete pavement with an open-graded aggregate base and stabilized subgrade. The stresses computed at the top of the subgrade were approximately 5 psi (35 kPa). In order to provide accelerated testing, it was felt new loading equipment provide an overloading factor of at least 10, or 50 psi (350 kPa). While this high level of loading may never be used, the capabilities were built in so other types of high load level testing may be accomplished if desired.

The test cylinder and loading head were nominally 8 in. (20 cm) in diameter with an area of 50 in² (0.0325 m²). For a loading pressure of 50 psi (350 kPa), a force of 2,500 lb. (11,000 N) must be produced by each loading head. This force should also be continuously adjustable to lower levels if desired. The air pressure available within the laboratory was regulated to 150 psi (1,000 kPa). Pressure regulation devices were built into the pneumatic equipment to maintain usable pressures in the 5 psi (35 kPa) to 80 psi (550 kPa) range.

4.2.2 *System Design Configuration*

The design of the pneumatic system required 5 main steps: sizing of the air cylinders, sizing of the air reservoirs, selecting valves, sizing piping and connections, and designing the piping layout. Figure 4.5 illustrates the overall pneumatic system design for one loading station. The second station is of identical design.

To produce a maximum force of 2500 lb. (11,000 N) from a pneumatic air cylinder (also known as an air diaphragm) at an input pressure of 80 psi (550 kPa), a piston area of $2500/80 = 30$ in² (0.0195 m²) was required. Six inch diameter air cylinders have a piston area of 28.3 in² (0.0182 m²), which made them a good choice for this research. The cylinders used in this design had a stroke (piston movement) of 3 in. (75 mm). The maximum displacement expected during this research was 0.5 in. (13 mm). The extra travel enabled easy specimen placement and removal from the test system. Figure 4.6 shows the air cylinder and peripheral

equipment in operational position. Note the airline filters in the background and the Linear Voltage Differential Transformers (LVDTs) positioned near the load head. In order to properly size the remaining components as well as the fittings, the air flow required during dynamic loading was calculated. Air flow was determined from an equation from the Norgren pneumatic design guide. The flow equation used was:⁴⁷

$$\underline{Q}(scfm) \equiv 0.273 \cdot \frac{D^2}{t} \cdot L \cdot \frac{p_2 + 14.7}{14.7}$$

where D was the cylinder diameter (6 in., 150 mm), L was the stroke (0.5 in., 13 mm), t was the stroke time (0.3 sec.), and p₂ was the outlet pressure. Conventionally, p₂ is taken as 53% of 14.7 psi for this calculation. This equation results in a flow value of 2.5 standard cubic feet per minute (SCFM). This value was very conservative since most stroke movements were well below 0.5 in. (13 mm). An air reservoir with a 10 gallon (1.2 ft³, 0.11 m³) capacity was installed in-line to give 30 seconds (1.2/2.5 min.) of backup in case of momentary air compressor failure.

According to the manufacturer's (Norgren) design charts⁴⁷, 0.5 in. (13 mm) valves and fittings were adequate for the design flow rates used in this research. The main valve, air diaphragms/cylinders, and filters were designed with 0.5 in. (13 mm) National Pipe Thread (NPT) connections. The pilot valve attached to the main valve required a 0.25 in. (6 mm) NPT connection. A pilot valve regulator maintained the pressure to the pilot valve at 80 psi (550 kPa). This pilot valve allowed for variable and independent flow rates through the main 2 way valve into the air cylinders. The 10 gallon air reservoirs were manufactured with 1 in. (25 mm) NPT female threads and were stepped down through black bushings down to 0.5 in. (13 mm) NPT for overall system compatibility. Similarly, the refrigerated air dryer was manufactured with 0.375 in. (9.5 mm) NPT female connections and were stepped up to 0.5 in. (13 mm) connections. This 0.375 in. (9.5 mm) constriction in the overall air flow did not hamper the system's air flow capabilities in this research and confirmed the initial design as being conservative. All non steel pipe connections were made through brass fittings and flexible high pressure (250 psi, 1700 kPa) hose.

The desired loading pulse was a pure haversine waveform. Due to equipment performance and the nature of air loading and relieving, a “pseudo-haversine” waveform was produced. The resulting air pulse produced by this pneumatic equipment was 0.25 seconds in duration from load initiation to full load release. Time from load initiation to load peak was 0.15 seconds. The load curve produced by the downward or force stroke of the piston resembled an increasing sine wave as air compressed into the cylinders. During the upward or release stroke of the piston, the load curve resembled a decaying exponential as air was released from the cylinder through the relief valving.

The overall system design consisted of two pneumatic air cylinders driven by the valving previously discussed. The compressed air supply delivered to the main outlet was split by a “T” into 2 separate lines. On each of these lines following the split were 3-way ball valves permitting independent operation of either cylinder. These valves allowed for flow directly through the valves into the cylinders during normal operation and for back flow to bleed the compressed air from the air reservoirs should adjustments or repair be required.

During normal operation the compressed air supply valve was opened and air entered into the system. The air dryer was turned on and all the filters were bled of condensed water as required. Both the pre-filter and coalescing filter had automatic drains activated at 10 psi (70 kPa). The main filter/regulator was then set to the desired pressure and the pneumatic system was ready for use.

4.3 Electronic Control and Data Acquisition

The measurable parameters of interest in this research were specimen permanent and elastic deformation and applied load force. Deformations were measured by LVDTs and load was measured by full wheatstone bridge load cells. Custom control circuitry was designed and built for this research to specifically interface with these instruments as well as the computer data acquisition program LABVIEW® by National Instruments Inc. The entire circuitry was housed in a 6 in. x 18 in. x 24 in. (15 cm x 46 cm x 61 cm) steel junction pull box. Sensor and control wiring were fed through circular punchouts in the box walls.

The electronics consisted of 3 main parts. The first part was relay control for on/off valve switching. The second part was power and signal reception to and from the LVDTs and

load cells. The third part was the interface of these signals to the computer. Each of these parts is described in greater detail in the following paragraphs. Figure 4.7 shows a schematic block diagram of the control circuitry. Figure 4.8 shows a photo of the control circuitry.

National Instruments data acquisition program LABVIEW® controlled the overall system operation and acquired measurement information in real time as the tests progressed. There were 2 LVDTs and 1 load cell per station for a total of 4 LVDTs and 2 load cells to provide signal data. A 6 channel data logger within LABVIEW® recorded data at fixed increments. Typically a reading of the 6 channels was made at every 50 to 100 loading cycles depending upon the number of load applications in a given test. At each reading, the input data was sampled at rates up to several thousand points per second. Due to electrical noise in the laboratory, an averaging technique was used which sampled 50 consecutive points, averaged them, and output them as one value. The procedure continued for each succeeding group of 50 points until the cycle was completed. This allowed each curve to be described by a minimum of 40 points which was adequate for the purposes of this study.

Deformation measurements were made by DC (direct current) LVDTs with a ± 1 in. (25 mm) stroke limit. For each test, 2 LVDTs were used to measure deformation and the deformation value used in analysis was the average of the 2 values. During use, the core of the LVDTs rested on a steel plate lying atop the aggregate layer, but beneath the load head. Core movement was represented by varying output voltages directly proportional to the amount of movement of the core within the LVDTs. To ensure accuracy of measurement, each LVDT used in this research was calibrated with a micrometer to give a relationship of core movement versus output signal voltage. These LVDTs were powered by a 24 volt DC power supply but the LVDTs reached full scale deflections at ± 19.8 V. This corresponded to a 50.7 mil/V conversion factor for core movement. Each LVDT varied slightly from this average and this variation was noted in the conversion program in the computer.

Load was measured through a full wheatstone bridge load cell attached to the loading head. A 10 V excitation powered the load cell. The load cell had a loading range up to 5,000 lb. (22,000 N) with an output signal of 30 mV corresponding to full scale. The loading expected in this research was typically below 2,000 lb. (8,900 N) indicating a load cell output voltage of less than 12 mV. Laboratory noise prevented reading signal levels this low

accurately, therefore amplification was required. An amplifier/signal conditioner card with adjustable gain took the output signal of the load cell, amplified it and removed spurious noise from the signal. For this research the gain was set to 333 resulting in a 10 V signal for a 5,000 lb. (22,000 N) load, or a conversion factor of 500 lb./V (22,000 N/V).

Control of the pneumatic valve was performed by on/off voltage signals into the 2-way main valve leading into the air cylinder. The LABVIEW program was written to produce a +5V signal to the output board at frequencies up to 1 Hz for the number of cycles selected upon running of the program. This control signal was fed from the computer to a set of solid state relays, one for each valve. The 24 volt power for the valve was switched through these relays in response to the control signal.

4.4 Test Cylinder and Load Head

To facilitate testing for this research a new chamber allowing faster turnaround time than conventional triaxial cells was developed. Figure 4.9 shows the cylinder design. Several of the previous researchers¹⁰⁻¹⁸ had used stiff walled though not clear chambers with much success. The plexiglas™ test chamber had 0.5 in. (13 mm) thick walls, an 8 in. (200 mm) inner diameter and a 12 in. (300 mm) height. The 12 in. (300 mm) height was chosen in order to accommodate a 4 in. (100 mm) stabilized soil “specimen”, a 4 in. (100 mm) open-graded aggregate layer, a 2 in. (50 mm) dense-graded separation layer, and a 1 in. (2.5 cm) thick load head. The 8 in. (20 cm) inner diameter was required to minimize aggregate size effects from 1.25 (31 mm) to 1.5 in. (38 mm) top size aggregate. Plexiglas™ was selected so the pumping and intrusion mechanism would be visible in real time as the testing progressed. The stiff walled cylinder also produced confining pressures on the test materials that varied with the applied vertical load, as in a real pavement system.

The cylinder split vertically into two semicircular pieces and fit into a recessed aluminum base plate. The walls were affixed to the base plate by machine screws through the plate. The two plexiglas™ side walls were held together at the top and at 3 in. (75 mm) above the base plate by removable circular aluminum clamps. The chamber was water tight through the use of O-rings.

The load heads making contact with the testing specimens were 7.75 in. (197 mm) diameter by 1 in. (25 mm) thick circular plates. Figures 4.10 and 4.11 show the load head design and the load head in operational position. The load head plates were welded to a 4 in. (100 mm) diameter by 2 in. (50 mm) tall extension which bolted directly to the 5,000 lb. (22,000 N) capacity load cell. The top of the load cell attached to a 2 in. (50 mm) diameter fitting which screwed onto the air cylinder piston.

Two 1 in. (25 mm) diameter holes were drilled through the face of the load heads on opposite sides of the center post. A 0.125 in. (3 mm) thick steel plate placed below the load head during testing made contact with the aggregate. The 1 in. (25 mm) holes were for the LVDT cores so they would rest upon the cover plate. These holes and cover plate were essential since the load head lifted off the specimen during unloading of specimens experiencing large permanent deformation. The plate movement therefore directly matched the test material movement and was used for elastic and permanent deformation measurements. Flat magnets were attached to the end of the cores of the LVDTs to ensure continual contact with the cover plate.

4.5 Load Frame

The loading frame for this research was constructed with two criteria in mind. First, the frame had to be large enough to accommodate at least 2 pneumatic loading stations. Second, the frame had to be rigid enough to be useful for additional research requiring significantly higher loading than this study. The frame is shown with the installed loading equipment in Figure 4.3.

The overall frame size was 80 in. tall x 56 in. wide x 24 in. deep. The base was 24 in. deep x 48 in. wide. The upper horizontal cross beams were adjustable to heights from 30 in. to 62 in. above the base plate. The base consisted of 4 - 40 in. long C10 x 30 channel beams at 6 in. spacings, welded to and supporting a $\frac{3}{4}$ in. thick steel plate. Two 24 in. long C10 x 30 channel beams ran perpendicular to the ends of the 40 in. long channel beams beneath the base plate for attachment to the vertical support members. The 2 vertical columns were MC10 x 41.1 channels. The webs of both the columns and 24 in. base end channels were bolted together. The adjustable horizontal cross beams were MC12 x 50 channels. These

two beams were bolted through their web to the flange of the two vertical channel columns. Moveable $\frac{3}{4}$ in. x 14 in. x 18 in. steel plates bridged the span between the two upper beams. The pneumatic loading diaphragms were bolted to the underside of these plates.

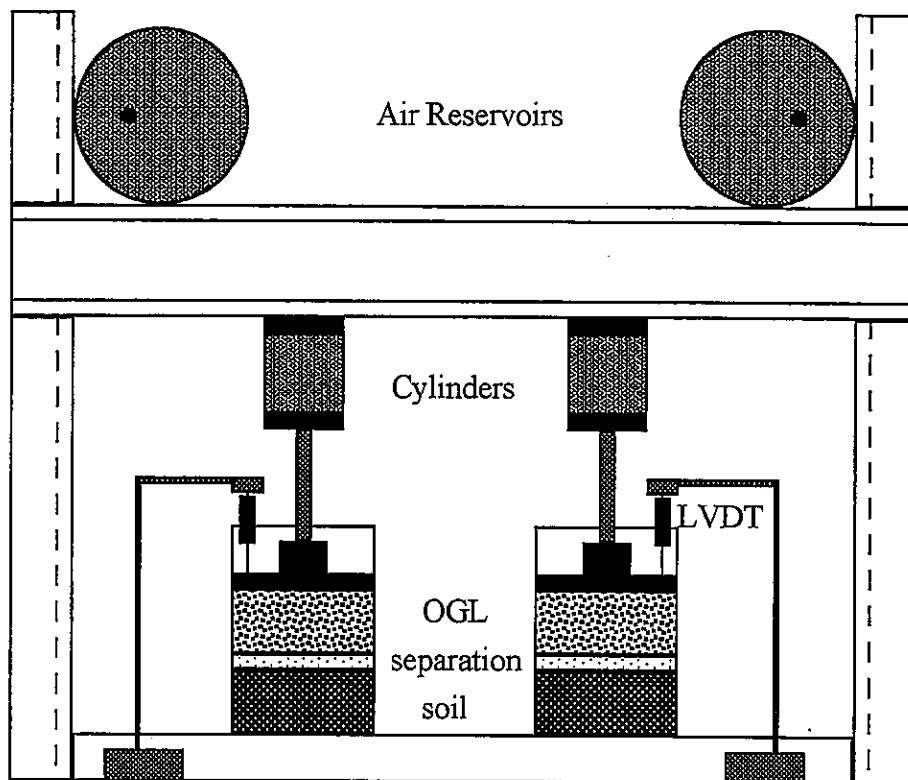


Figure 4.1: Loading Frame and Cylinders

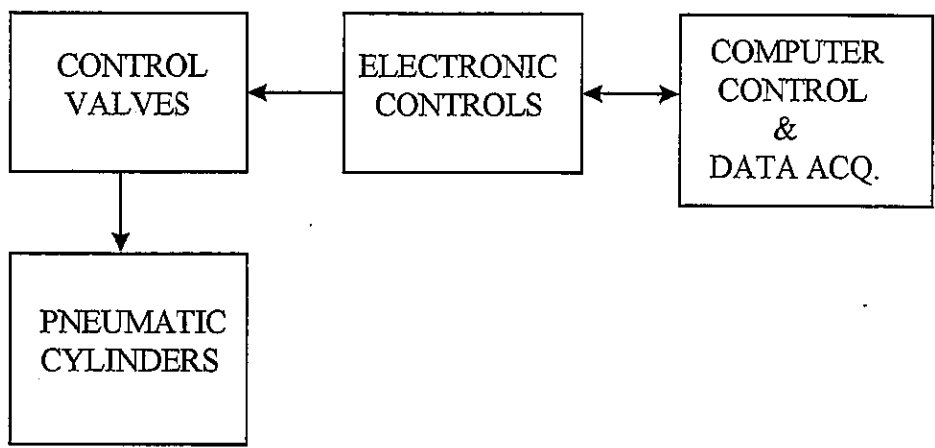


Figure 4.2: Block Diagram of System Control

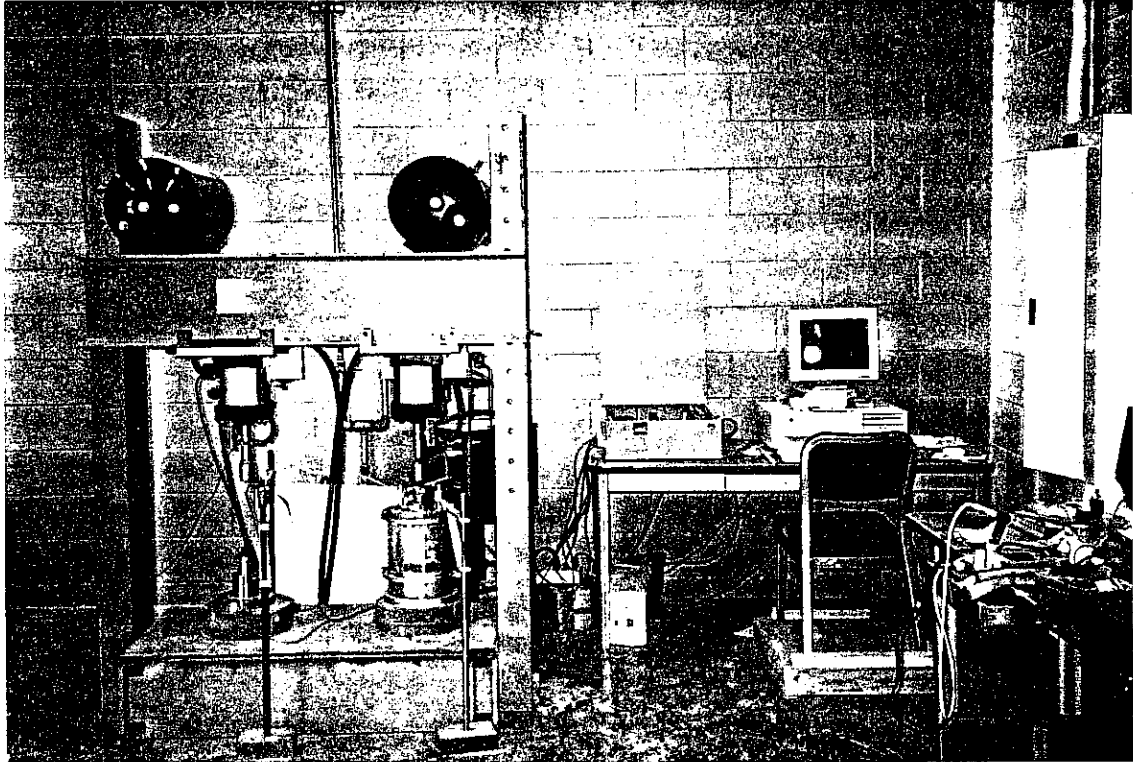


Figure 4.3: Overall System

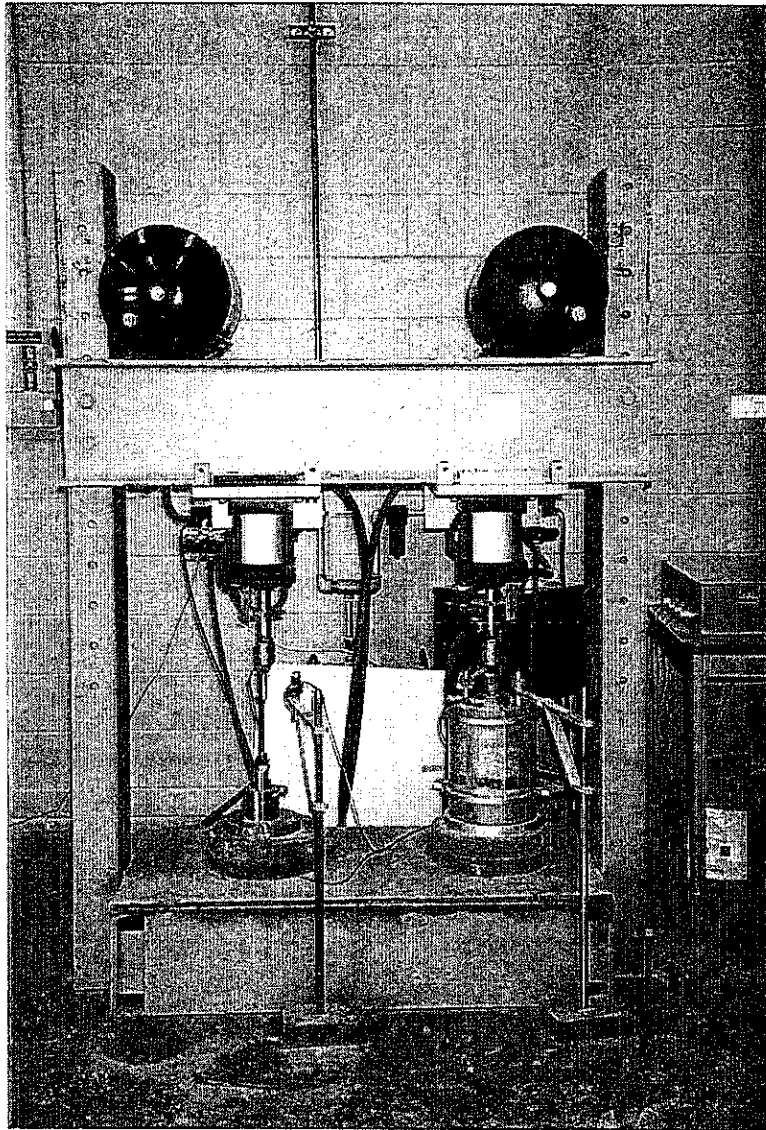


Figure 4.4: Equipment in Test Configuration

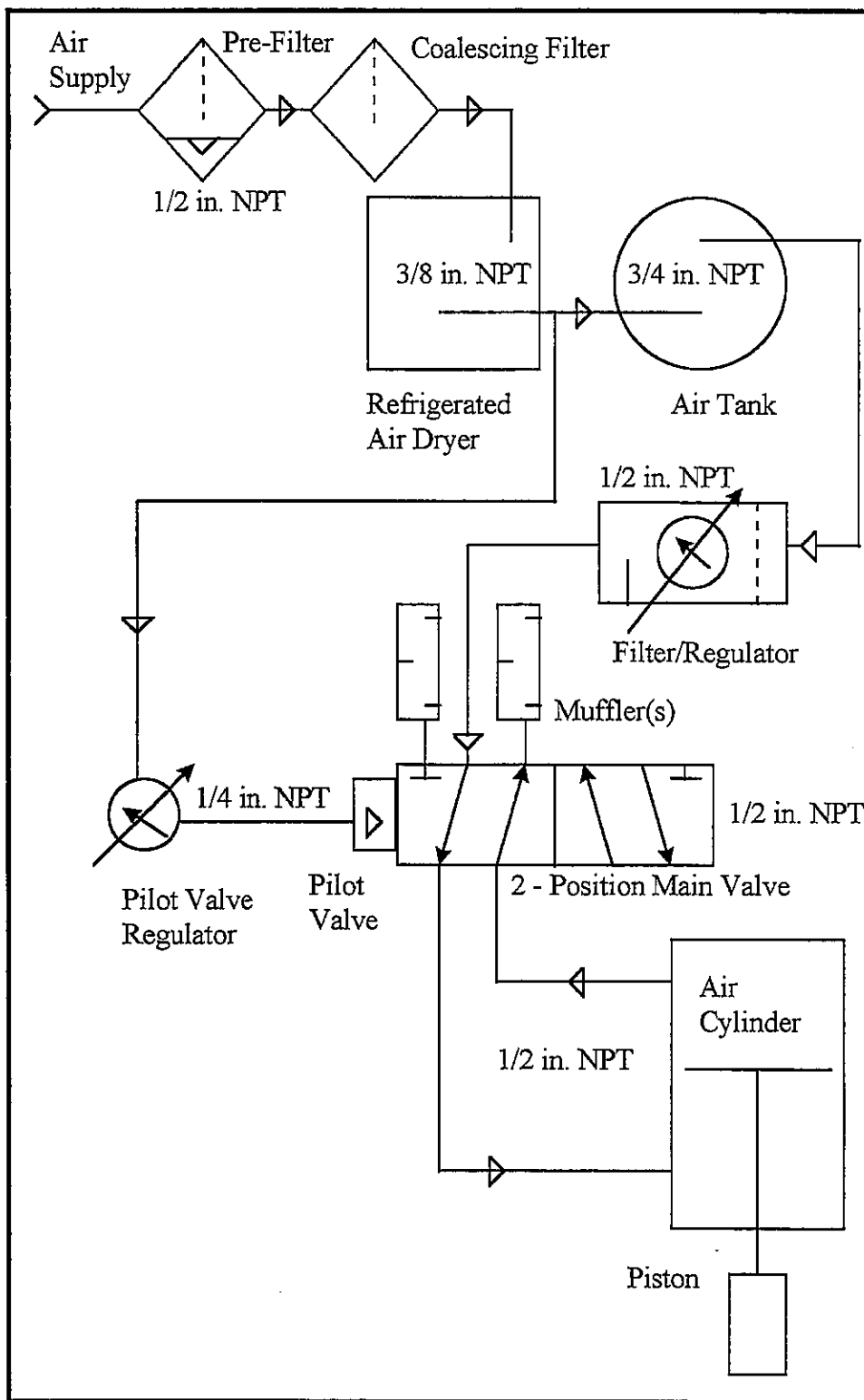


Figure 4.5: Pneumatic System Design (One of Two Halves)

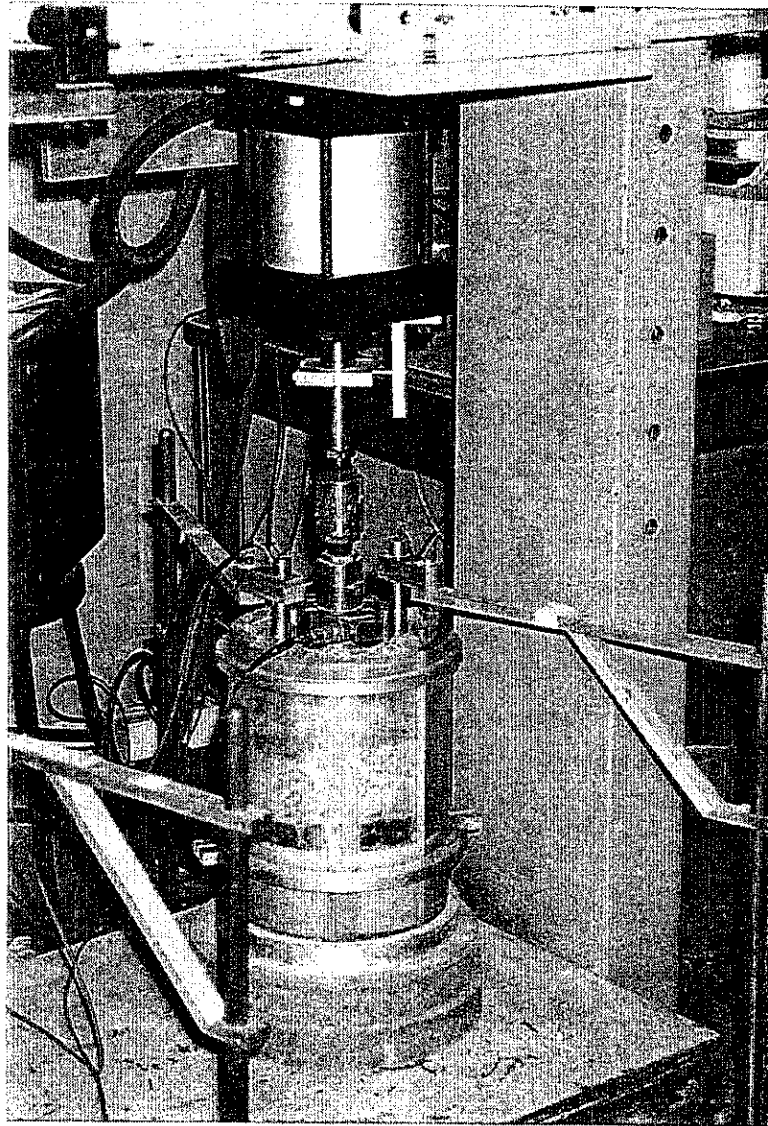


Figure 4.6: Air Cylinder and Test Chamber

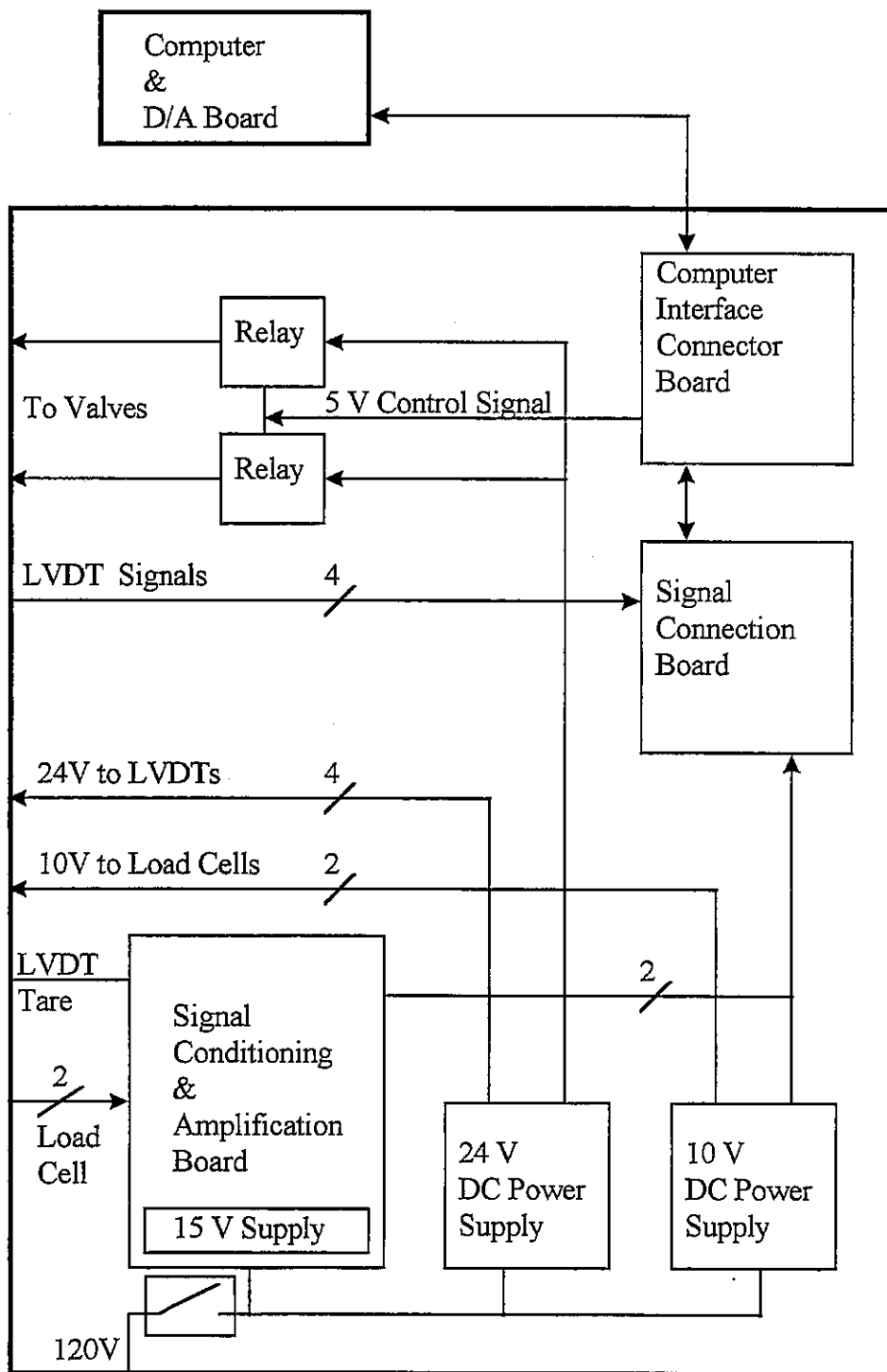


Figure 4.7: Block Diagram of Electronic Control Circuitry

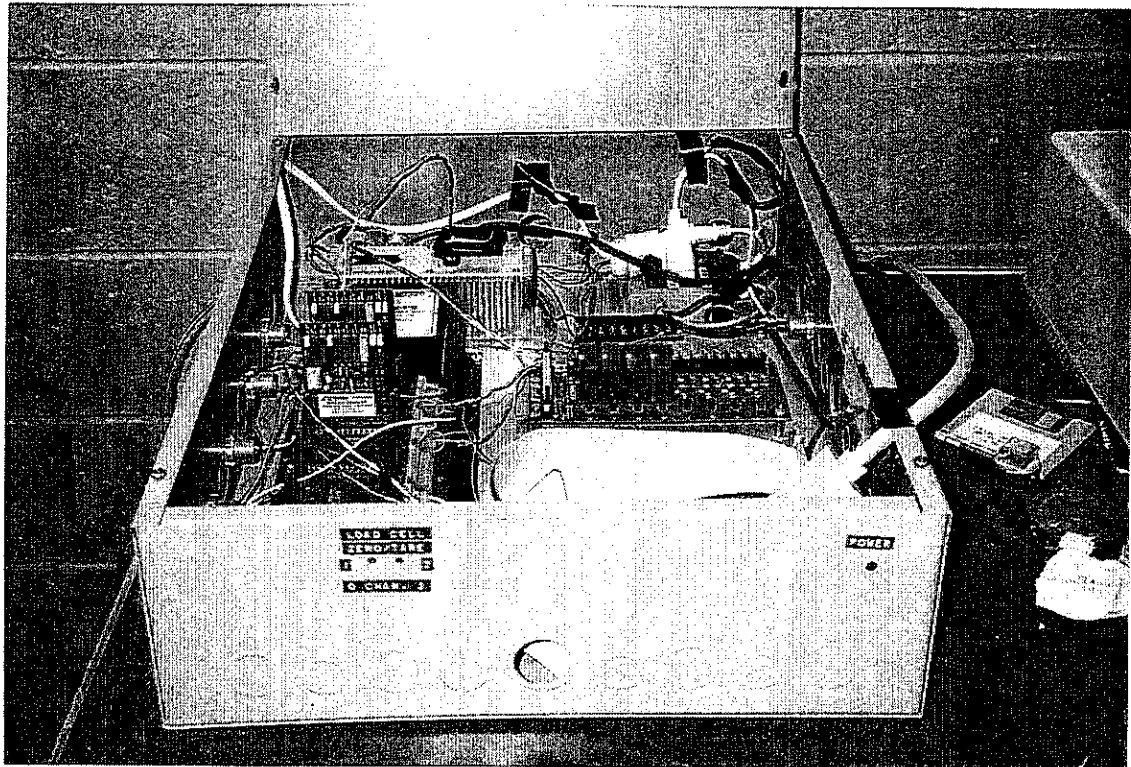


Figure 4.8: Electronic Control Circuitry

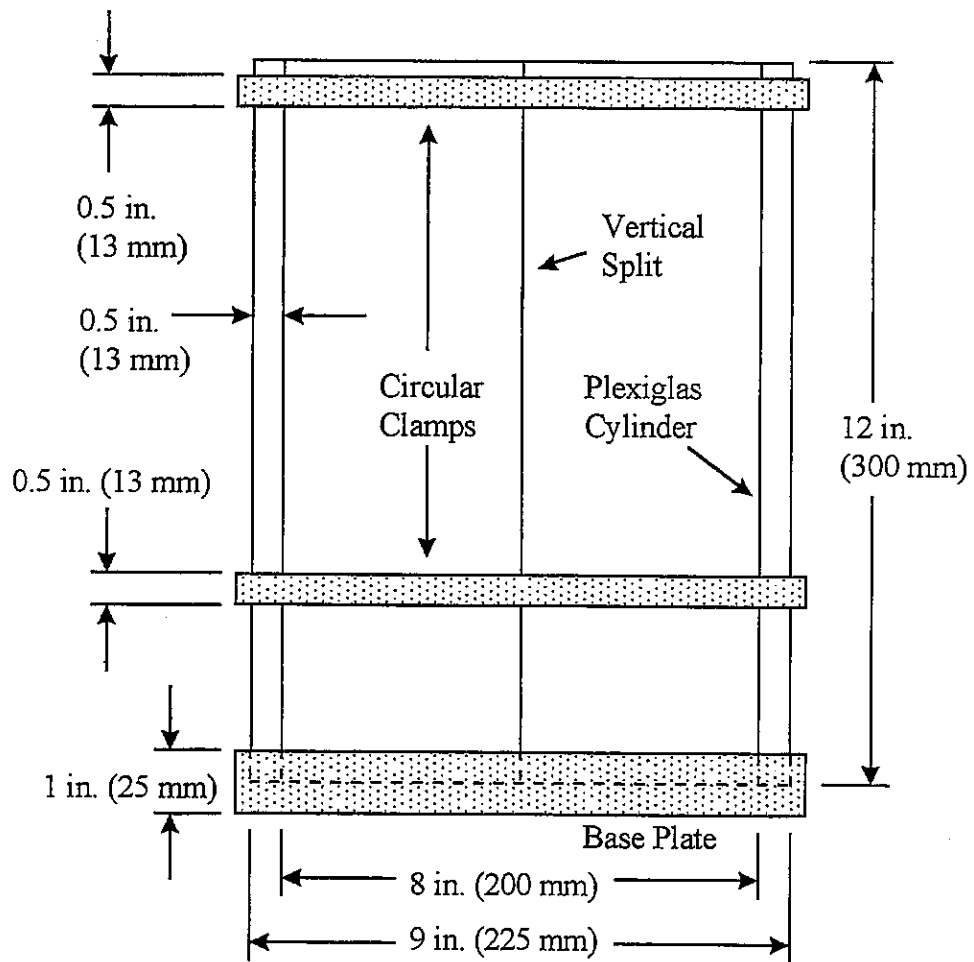


Figure 4.9: Test Cylinder Design

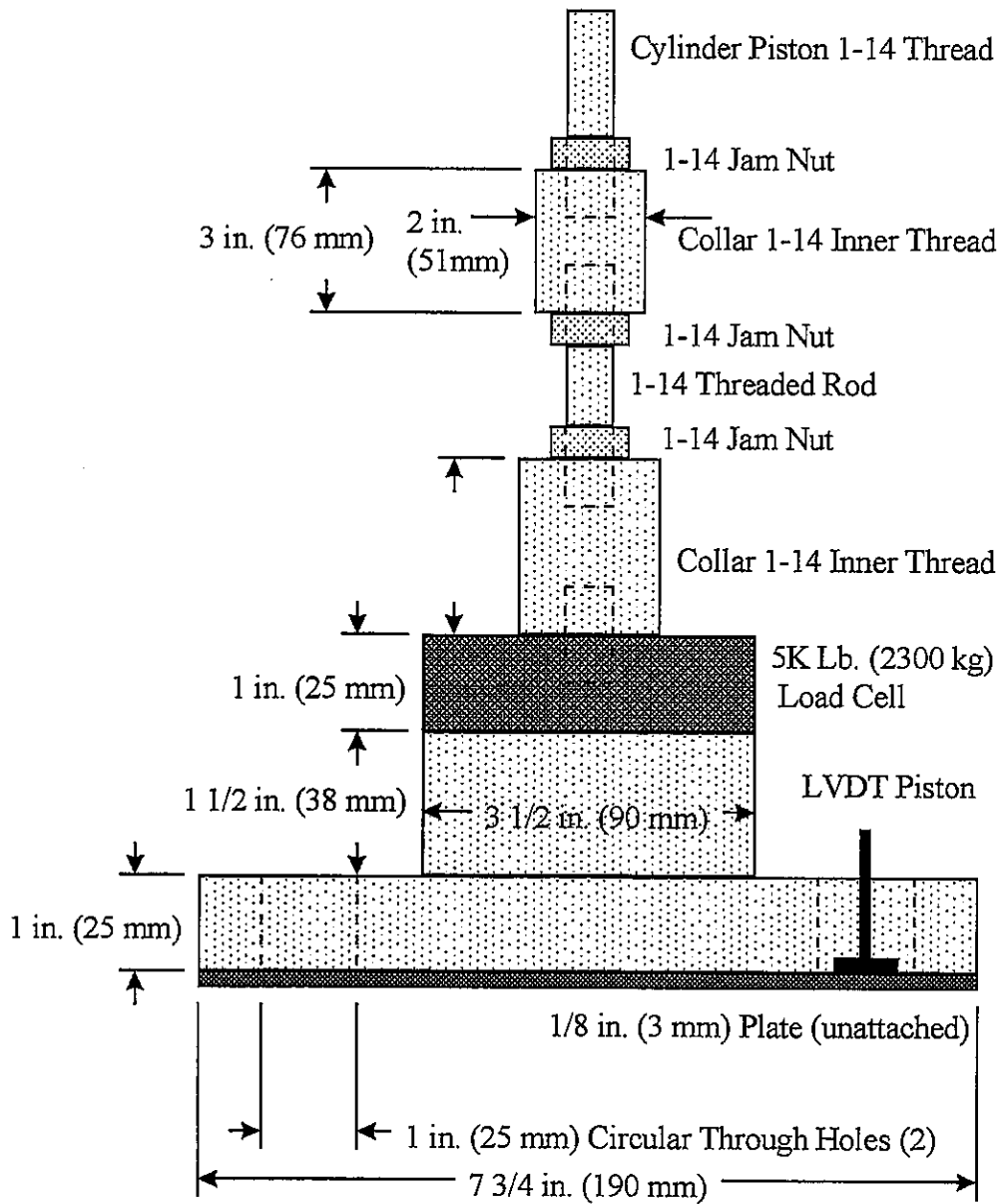


Figure 4.10: Load Head Design

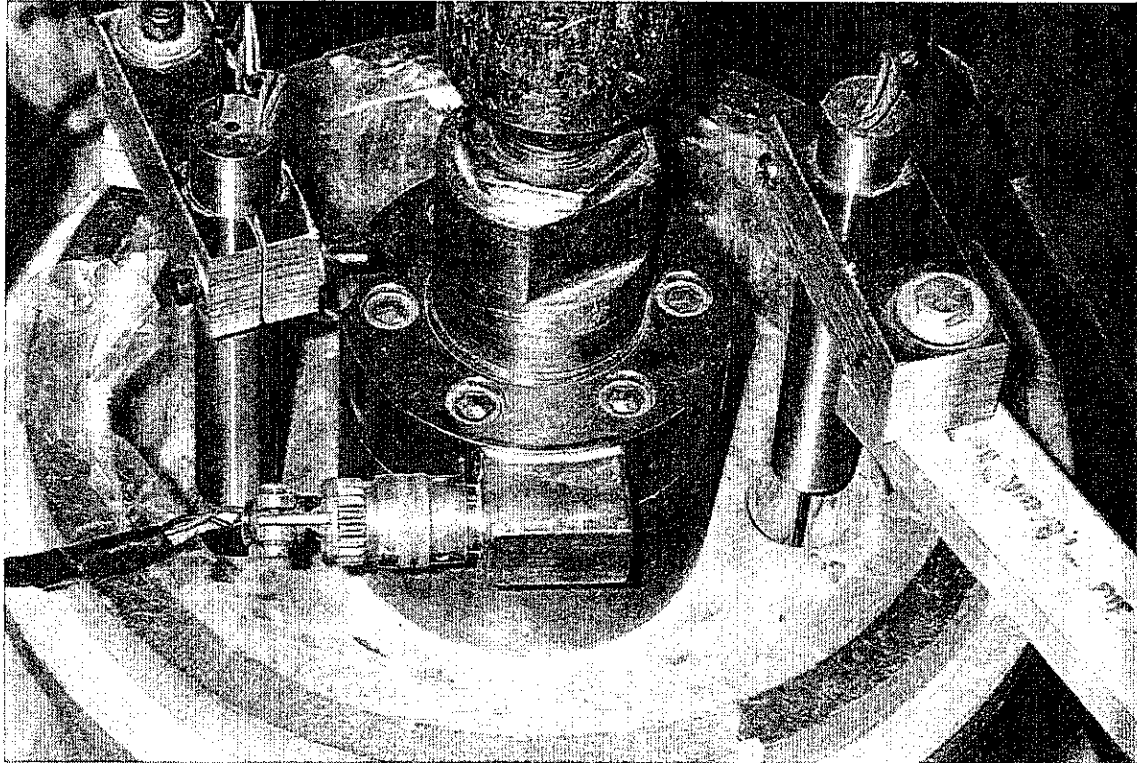


Figure 4.11: Load Head in Operational Position

5. TEST PROCEDURE

5.1 Procedure Development and Experimental Design

5.1.1 *Overview and First Testing Phase*

The main goal of this research was the development of a quick index test for separation layer evaluation. Testing of the materials used in this research required a proper experimental design to ensure all material combinations were evaluated. Of primary concern was the relationship between soil strength, soil type, separation layer type, and the magnitude and number of loading applications as indicators of separation layer performance. The materials and testing properties investigated in this research are summarized in Table 5.1.

There were three phases of testing within this research. The first phase consisted of a preliminary evaluation of material performance with the newly developed test equipment. Knowledge about material performance under these testing conditions had to be obtained before any further testing decisions were made. Troubleshooting of the newly developed test equipment took place here. The second phase was testing with respect to an experimental design. In this phase, many different testing combinations of loading levels, repetitions, and soil strengths were conducted. From these results, correlations were made and an accelerated loading condition was selected. The third phase was testing these materials under accelerated conditions and evaluating performance.

The development of the experimental design in the first testing phase was an iterative process. There were three primary variables controllable for each test; soil strength, load level, and load repetitions. Loading levels and corresponding number of repetitions that yielded sufficient "failure" were unknown. These tests were conducted with varying loading levels and repetitions until enough knowledge of material behavior was gained. At that point, the experimental design was created. It was realized early on that testing high load levels at high load repetitions was not practical or realistic. The energy imparted to the test specimens was far too severe. These tests were not conducted in subsequent phases of testing.

5.1.2 Testing Phases Two and Three

The experimental design used in the second testing phase to develop the accelerated testing procedure is shown in Figure 5.1. A 3^3 full factorial design was used in which each of the three variables were described as "low", "medium", and "high" or -, 0, + respectively. These levels were determined based upon the first testing phase results. This 3^3 design yielded a total of 27 possible testing combinations for each soil. For practical purposes, each factor (-, 0, +) was assigned a range of values. The determination of these ranges is described below. These values are tabulated in the lower portions of Figures 5.1 and 5.2. Figure 5.2 shows the reduced experimental design after the elimination of testing conditions deemed too severe.

To determine appropriate loading levels for the second phase of testing, an elastic layer analysis was run on a PCC pavement (8 in.) with an open-graded base (4 in.) over a lime stabilized subgrade (12 in.). The goal of the analysis was to determine subgrade stresses appropriate for a concrete pavement experiencing realistic field loading. It has been shown that for a fatigue life greater than 1,000,000 ESALS, a stress ratio of no greater than 0.6 (σ/M_r) is required. M_r is the slab modulus of rupture and σ is the repeated vertical stress. A typical slab with a M_r of 600 psi (4300 kPa) therefore experiences slab bending stresses of 360 psi (2500 kPa) for a stress ratio of 0.6. A vertical subgrade stress of 3 psi at mid-slab locations (plan view) corresponded to this slab bending stress of 360 psi. For worst case edge loading, where much material movement occurs, this stress doubled to 6 psi (42 kPa). Load levels on the open-graded aggregate within the test cylinder of 8 psi were therefore selected for low level long term loading. These low load level tests were needed to establish a standard against which to compare accelerated loading. The effective pressure limit of the test equipment was approximately 40 psi (275 kPa) plate load. At a level of 28 psi to 30 psi (190 kPa to 210 kPa), the equipment ran efficiently and was easily controllable and resulted in an overload factor of up to 5 times field loading. Load levels of 28 psi to 30 psi were chosen for high level loading. Load levels of 16 psi to 20 psi were chosen for medium level loading.

Loading repetition levels were selected based upon testing duration constraints and early performance evaluation. Low repetition levels were selected at 20,000 cycles, at which permanent deflection often had leveled off and significant pumping had occurred for high level

loading. A medium repetition level of 20,000 to 80,000 cycles was chosen. For high level repetitions more than 80,000 loading cycles were conducted. Typically, 400,000 to 500,000 cycles were performed.

As for soil strength levels, saturated specimens with cone indices (CI) of up to 300 (see Section 3.2.1) were produced. For the experimental design, it was straightforward to divide this strength range into $CI < 100$, $100 < CI < 200$, and $CI > 200$.

Tests corresponding to Figure 5.2 were run and trends emerged. It was seen early on that performance, as indicated by deformations and pumping at high level loading and low repetitions was in many aspects comparable to low level loading and high repetitions. Chapter 6 presents the results of this testing and further details may be obtained there. Based upon these results, low repetitions at high load levels was selected for the accelerated testing condition, the third testing phase. Figure 5.3 shows these accelerated testing combinations selected for separation layer testing. Note for each testing combination, three different separation layer types were tested; non-woven geotextile, dense graded aggregate, and no separation. The particular tests performed on Mexico Clay and Wisconsinan Silty Clay Till for validation of the accelerated loading condition are shown in Figures 5.4 and 5.5.

5.2 Testing Setup and Operation

Testing of each specimen was a multi-step procedure. Individual soil specimen preparation was followed by separation layer installation and aggregate compaction. The completed specimens were placed within the testing apparatus and measurement devices (load cells and LVDTs) were installed. Each step is described in detail below.

5.2.1 Soil Specimen Mix Design

As previously described in Chapter 4, the testing chamber had a nominal inner diameter of 8 in. (200 mm). The compaction mold for preparing specimens and the test cylinder actually were slightly smaller than nominal and yielded finished specimens 7.85 in. to 7.90 in. (~200 mm) in diameter. Based upon the moisture density relations presented in Chapter 3, the individual material weights composing the test specimens are shown in Tables

5.2 and 5.3. The actual material weights for specimen production, in batches of 2 are presented in Table 5.4. These batches were large enough to yield 2 test specimens plus soil for moisture measurements and 4 - 2 in. (50 mm) diameter x 4 in. (100 mm) tall strength cylinders. To produce the 8 in. (200 mm) diameter by 4 in. (100 mm) tall specimens within the compaction mold, a total of 0.112 ft³ (0.0032 m³) of compacted material was required. For the Mexico Clay, the 2 specimens were made from 2 lifts of 6.88 lb. (3120 g) each from a total mix weight of 34.17 lb. (15500 g). For the Wisconsin Silty Clay Till, the 2 specimens were made from 2 lifts of 6.12 lb. (2775 g) each from a prepared mix of 26.46 lb. (12,000 g).

For the Wisconsin Silty Clay Till, compaction to 95% Proctor density yielded very strong durable samples even after saturation. This clay till, though predominantly silt sized was very lime reactive due to its unweathered nature and high cation exchange capacity. Initial tests with this material found it nearly unpumpable, even with the loading and cycle levels used in this research. When compacted at AASHTO T 99 (ASTM D698A) or slightly higher, CBR levels of 10 and above were typical even after saturation. Due to this high strength, subsequent samples were then prepared and tested at 85% to 90% of T 99. The samples produced had low CBRs, in the range of 1 to 5 after vacuum saturation. These lower CBR levels were felt to be more indicative of saturated field conditions. The values presented in Table 5.3 reflect this density reduction.

5.2.2 *Soil Specimen Preparation*

Soil specimen preparation started with mixing the soil, lime, and water to the desired moisture content. Typically, specimens at optimum moisture content and maximum dry density were sought, but often weaker or stronger specimens were produced for comparison. Each mix was then mellowed in an air tight environment for one hour to facilitate hydration of the mix. The air tight environment was used to maintain moisture control in the laboratory rather than to be representative of field practices.

The first step in specimen preparation was to separate out 2 batches equal to one-half the total specimen weight. The 4 in. (100 mm) high specimens were then compacted in 2 lifts of 2 in. (50 mm) high each. Between the first and second lift, the top surface of the specimens were scarified to a depth of 0.5 (13 mm) to 0.75 in. (20 mm) to promote bonding between

layers. The specimens were then extruded from the compaction mold by a screw driven load testing machine. After the specimens were extruded from the mold, they were labeled and weighed. The specimens were then wrapped in damp paper towels and placed in air-tight plastic bags to cure at 50C for a set number of hours depending upon the level of strength desired.

When accelerated curing was completed the samples were vacuum saturated to at least 95% saturation. Without specimen saturation, pumping of both soils was not achieved. Saturation also represents long term field conditions. Specimen saturation was a two step procedure in which the 2 specimens were pulled into vacuum for between 1.5 and 2 hours and then soaked in water for an additional 1 to 2 hours. Figure 5.6 shows the vacuum saturation apparatus. The saturated weight was recorded and the degree of saturation determined based upon volumetric calculations. Tables 5.5 and 5.6 present the moisture characteristics for each specimen tested.

The curing time, vacuum time, and soaking time used for a given specimen were based upon the saturated strength desired for a given specimen. These time versus strength relationships were determined empirically in a trial and error procedure through the construction of many soil specimens. Typically, curing times ranged from 2 hours to 48 hours. There was not a great degree of control in the outcome however, hence a high variability of saturated specimen strength could result from “identical” preparation methods. Specimen initial dry density was an important factor in the ultimate saturated strength. Figure 5.6 presents soil strength versus dry density for stabilized Mexico Clay specimens. Significant variability in strength existed, with differences of up to 80 psi (cone reading) not uncommon from similarly prepared, equal density, specimens. The coefficient of variation of strength for these specimens ranged from 11% to 40% for long cured and short cured specimens respectively. It was readily apparent during specimen production that curing time (120 °F (50 °C)) played a major role in the development of soil-lime specimen strength. Though strength does increase with increasing density, the strength increase is only approximately 15% from lowest to highest density along the trendline. Figure 5.8 shows soil strength for these same specimens versus saturated density. The same trends are seen here with minimal strength gains with increased density. Note that strength variability decreased with increased density.

Figure 5.9 shows soil strength versus saturated moisture content for the three curing ranges. As expected strength decreased with increased moisture content. Increased saturation moisture content implied lower densities, and as shown above, led to decreased strength. Increased curing time resulted in the production of additional cementing agents thereby diminishing the potential for water absorption into the specimen regardless of density. Figure 5.10 presents soil strength versus dry density for Wisconsin Silty Clay Till specimens. Significant variability in strength existed here as well. The coefficient of variation of strength for these specimens ranged from 11% to 38% for long cured and short cured specimens respectively. In both soils the variation in strength increased markedly with decreasing average specimen strength. Strength increased with increasing density to a greater degree than the Mexico Clay. For the long cured specimens there is actually a decrease in strength with increased density, though data is limited. Figure 5.11 shows soil strength for these same specimens versus saturated density. The same trends are seen here with minimal strength gains with increased density. Figure 5.12 shows soil strength versus saturated moisture content for the three curing ranges. As expected strength typically decreased with increased moisture content. Again, with increased saturation moisture content lower dry densities were implied. Longer curing times led to diminished potential for water absorption into the specimens. This process takes place regardless of density.

The strength of the lime stabilized soil specimens tested in this research depended upon several factors. These factors included specimen dry density, moisture content during preparation, curing time, post saturation moisture content, and degree of saturation. Strength was a good parameter to characterize specimens in this research since the cone penetrometer gave a quick indication of strength. It must be noted strength can be derived in many ways and samples possessing the same strength may not necessarily perform to the same level in this research. Though target densities and moisture contents were sought, preparation variability often led to specimens of differing performance characteristics. A specimen prepared at a slightly higher density and with a short curing time may develop its strength through this higher density and through cation exchange and flocculation and agglomeration. Another specimen of equal strength with a somewhat lower density curing longer may develop its strength through cation exchange, flocculation and agglomeration, and the formation of

cementing products. Therefore, while the strength of these two specimens was comparable, their durability and erodability performance in this research might have been significantly different.

5.2.3 *Test Cylinder Preparation*

With the test chamber assembled, the soil specimen was pushed down into the bottom of the chamber so it rested tightly upon the bottom plate. After the specimen was in place, circular clamps were put around the outside of the cylinder. These clamps held the specimen tight to the inner wall of the chamber and aided in maintaining the water level above the specimen during testing. A cone penetrometer test was conducted on both specimens and the strength reading recorded as the pre-test strength. This cone indentation did not appear to affect specimen performance. Previously tested “un-coned” specimens tended to exhibit comparable behavior when under test.

If a non-woven geotextile was used as the separation layer in a given test, the geotextile was first cut to 2 in. greater diameter (10 in., (250 mm)) than the cylinder diameter. The geotextile was then placed calendered side up into the mold directly on the surface of the soil. Figure 5.13 illustrates the ring in pre-testing position. Stainless steel rings acting as circular expansion springs were snapped in place to hold the extra geotextile “skirt” (1 in., (25.0 mm) excess) tight to the chamber wall to negate any pumping of material around the edge of the geotextile and along the cylinder wall.

If a dense-graded aggregate separation layer was tested, it was compacted directly above the soil specimen. This dense-graded aggregate, when initially compacted at optimum moisture and maximum dry density, produced a “rock like” hardness with very low permeability. The phreatic head applied when testing did not permeate this layer initially and only minimally during testing. It was well known dense-graded aggregate loses significant strength when saturated. Therefore, for all subsequent tests (those reported here), the aggregate was compacted at near saturated moisture contents (7⁺%) and allowed to “rest” while the added testing water permeated through the layer prior to load testing. Difficulties were encountered however, when compacting at this higher moisture content such as piping

of fines around the perimeter of the load head, and material sticking to the load head and not getting compacted properly.

The pre-weighed open-graded aggregate was shaken in a metal can for one minute to blend fully and was poured directly on top of the separation layer. The aggregate was then gently compacted with a pneumatic vibratory hammer for approximately one minute until optimum density at a height of approximately 4 in. (100 mm) was reached. The weight of the aggregate, 12.70 lb. (5760 g) was calculated based upon a 4 in. (100 mm) lift compacted to 100 pcf (1600 kg/m³) within the cylinder. This unbound density was consistent with IDOT's published densities of 110 pcf (1760 kg/m³) for cement stabilized open-graded layers since 9.3 pcf (250 lb./yd³ (150 kg/m³) of this 110 pcf (1760 kg/m³) is cement. As in previously cited research, the aggregate used here was unbound since it would provide the most stringent testing conditions.

The top surface of the aggregate was carefully checked to ensure it was level so there would be complete contact with the loading head. To make the test more realistic of field conditions, 14 oz. (400 mL) of water was poured into each test chamber producing a head of 1 to 1.5 in. (25 to 38 mm) on top of the soil specimen. A 0.125 in. (3 mm) thick circular steel plate was then laid on top of the aggregate. Both the loading head and LVDTs rested on this plate during testing.

5.2.4 Setting Up and Running Test Equipment

The assembled test cells were placed upon the base plate of the loading frame, each one directly beneath a loading head. The loading heads were placed atop the plate on the open-graded aggregate and were then screwed on to the air cylinders shafts. The LABVIEW® computer program was started and the load cells were zeroed out with the external tare adjustment screws built into the electronic controls.

Prior to running the test, the load heads were tightened to a level of 3 psi (20 kPa). This seating load minimized any "pounding" during the initial phase of the tests. The LVDTs were then put into place and adjusted to read approximately 2 volts. The control board input voltage limit was 10 volts. Two volts at pre-testing allowed for ample increases in LVDT voltage before the input signal went above the acquisition board input voltage limit. Air

pressure was adjusted to achieve a 15 psi (100 kPa) load on the specimen and 1,000 conditioning cycles were conducted. This conditioning phase helped to seat the aggregate and reduce any excess permanent deformation prior to full scale loading. It also ensured all measurements were being made as desired and the pneumatic equipment was running properly. After conditioning, the LVDTs were removed, the load heads re-tightened to 3 psi (20 kPa), the LVDTs re-installed, and the air pressure adjusted to the desired load.

After the measuring devices were installed, the LABVIEW program was re-started. The number of load cycles was then entered along with the data collection rate. The output files were named appropriately and the program was executed.

5.2.5 *Post Testing Procedure*

Following the completion of repeated loading, the test chamber was taken apart and contents examined as follows. Figure 5.14 depicts material movement following testing. Additionally, raw data from the load cells and LVDTs was transferred to computer spreadsheets for analysis. Details regarding the use of the measured values obtained here are described in Chapter 6.

- 1) The LVDTs were carefully removed from their positions atop the test specimens and set aside.
- 2) The load heads were loosened and separated from the load cylinder and removed from the test chamber.
- 3a) **No Separation:** The cylinder was inverted and all the loose open-graded aggregate and any accompanying water/slurry was dumped into a pre-weighed pan. The remaining aggregate embedded in the soil was carefully removed to the level of its deepest penetration and placed in a pre-weighed pan. The post-test soil specimen strength was measured with a hand held cone penetrometer while still confined in the cylinder. The depth of aggregate penetration into the bottom surface of the soil was measured. The aggregate was then oven dried at

150°C for 24 hours.

- 3b) **Geotextile Separation:** All the open-graded aggregate and any accompanying water/slurry were dumped into a pre-weighed pan. The geotextile was removed from the chamber and placed in the pan with the aggregate. The post-test soil specimen strength was measured with a hand held cone penetrometer while still confined in the cylinder. The aggregate and geotextile were oven dried at 150°C for 24 hours.
- 3c) **Dense-Graded Separation:** The cylinder was inverted and the *loose* open-graded aggregate and any accompanying water/slurry was dumped into a pre-weighed pan. The remaining open-graded and dense-graded aggregate were carefully removed from the chamber so as to obtain all the dense material with minimum soil disturbance. These materials were placed into a pre-weighed pan. The aggregate was then oven dried at 150 °C for 24 hours. More details regarding this procedure are given in section 5.3.2
- 4) If soil moisture contents were of interest, small samples were removed from the soil specimens and weighed (approximately 100 g) and then oven dried at 105 +/-5°C for 24 hours.
- 5) After 24 hours, the oven dried contents were weighed, weights recorded, and photographed if desired.
- 6) The cylinder was taken apart, cleaned, and reassembled. The tested soil specimen was discarded. The geotextile if used was saved for future examination.

5.3 Performance Evaluation

There were three principal variables controllable during this testing procedure; number of load cycles, load pressure, and soil strength. Resulting from this test were three performance parameters evaluated against these controlling variables; weight of pumped or transferred material, and magnitude of permanent deformation and elastic deformation. During the development of this testing procedure, the experimental design was used to

evaluate the performance parameters against the controllable variables to determine which factors were important.

5.3.1 *Deflection as a Measure of Performance*

Deflection measurements of the combined soil/separation layer/aggregate system were performed during each test. Early test results indicated permanent and elastic deformation values were related to soil strengths. The deflection measurements were however, also highly sensitive to both the strength of the soil sample and the level of compaction of the aggregate. Variations in compaction levels of 5 to 10 percent were not uncommon due to potential intermixing of aggregates, separation layers, and soil during sample preparation. The conditioning loading prior to actual test loading helped to minimize much of this variability.

5.3.2 *Pumping as a Measure of Performance*

The weight of fine material pumped through the separation layers was shown early on in this research to correspond directly to material strength and to be unrelated to aggregate compaction variations. The amount of pumped material was a good parameter to use to evaluate separation layer performance.

The degree of pumping was assessed in three ways depending upon the type of separation. The specific techniques are described as follows:

1) No Separation: The total weight of the oven dried loose aggregate and the oven-dried embedded aggregate with its "attached" soil was first determined. The original aggregate weight was subtracted from this value to determine the amount of soil intruded or pumped into the aggregate layer. To express this result, the weight in kilograms divided by the cross-sectional area of the cylinder in square meters gave an intrusion index in kg/m^2 . The depth of penetration was also noted.

2) Geotextile Separation: The difference in the sum of weights of the geotextile and open-graded aggregate before and after the test indicated the amount of material pumped into and through the geotextile. Additionally, the weight gained by the geotextile was determined

as well. To express the results, the total weight of material in kilograms was divided by the cross-sectional area of the chamber to give a “pumping index” in kg/m^2 .

3) Dense-Graded Separation: Evaluating dense-graded layer separation capabilities was a bit more involved since there was intermixing at 2 interfaces; the soil/dense-graded and the dense-graded/open-graded.

After testing it was difficult to accurately separate out the dense-graded aggregate intruded into the open-graded aggregate. Both materials were produced from the same aggregate stockpile and there was significant intermixing of the two materials during testing. In each test there was a point within the open-graded aggregate layer *above* which it still remained “loose” and unmixed. The intermixing occurred below this depth.

There was similar behavior at the soil/dense-graded interface. At this interface there was a depth into the clay *below* which dense-graded aggregate did not penetrate or mix. Above that depth there was significant mixing of the two materials. These materials were more easily discernible due to a color difference, but they still could not be practically separated out in the mixed region. Also, fine soil would pump through the dense-graded layer and into the open-graded layer.

A two step procedure was then developed to determine the amount of material “transferred” during the test. After testing, the loose open-graded aggregate (and included dense aggregate) that freely fell out of the chamber was dried and weighed. The weight of this material was subtracted from the original open-graded weight. The original dense-graded weight was then subtracted from the remaining dense-graded and open-graded material removed from the chamber. The absolute value of the sum of these two differences was then determined. The “Material Transfer Index”, MTI was determined by dividing the total weight by the cross-sectional area of the test sample and expressing the value in kg/m^2 . A MTI of zero indicates no material transferred during the test. Typical maximum MTI values seen in this research were up to 80 kg/m^2 . An example follows:

Original Open-Graded Weight: 5750 Grams

Original Dense-Graded Weight: 3400 Grams

Post-Test Open-Graded Weight (includes some dense-graded) : 4800 Grams

Post-Test Dense-Graded Weight (may include open-graded) : 3800 Grams

Cylinder cross sectional area: 50 in^2 (0.03m^2)

$$\left((5750 - 4800) + (3800 - 3400) \right) \text{g} / 0.03\text{m}^2 \equiv 45.0 \text{kg} / \text{m}^2$$

In a severe testing case in which open-graded aggregate was severely infiltrated with dense-graded aggregate, the post-test open-graded weight could be as low as 2000 grams and the post-test dense-graded weight as high as 7450 grams. Under these conditions a MTI of 230 kg/m^2 would result.

Both parts of this equation were required since some open-graded aggregate intruded down into the dense-graded layer while some dense material pumped up into the open-graded layer. As previously mentioned, it was not possible to identify the dense-graded aggregate from the open-graded aggregate by direct observation following a test.

It must be noted MTI includes the weight of the aggregate as well as the weight of the soil. The previous intrusion indices include only soil movement and not aggregate movement. Due to this difference, direct comparisons between the previous indices and the MTI may not be appropriate. However, relative performance between “dry” and “wet” dense-graded separation layers may be evaluated by comparing the respective MTI values. The evaluation presented in Chapter 6 will compare the three indices to each other.

Table 5.1: Testing Variables

VARIABLE	PROPERTIES / VALUES
Soil	<ul style="list-style-type: none"> • Mexico Clay - Unstabilized, High moisture • Mexico Clay - 3% Lime, Varying Cure, Saturated • Wisconsinan Silty Clay Till - Unstabilized, High Moisture • Wisconsinan Silty Clay Till - 3% Lime, Varying Cure, Saturated
Separation Layers	<ul style="list-style-type: none"> • None • Geotextile (non-woven, polypropylene, AOS 100) • Dense-Graded CA6 (mid range gradation)
Open-Graded Aggregate	<ul style="list-style-type: none"> • CA7 (mid range gradation, no fines)
Loading Level	<ul style="list-style-type: none"> • 28 psi. (200 kPa) +/- 5% for accelerated tests • 5 (35 kPa) to 15 psi. (105 kPa) for long term tests
Loading Repetitions	<ul style="list-style-type: none"> • 20,000 for accelerated tests • As needed for long term tests, up to 500,000

Table 5.2: Mexico Clay Mix Design

Specimen Dry Density:	$104.5 \text{ pcf} \cdot 0.975 = 101.9 \text{ pcf}$
Specimen Volume:	$104.5 ((7.85^2 \cdot \pi)/4 \cdot 4) / 12^3 = 0.112 \text{ ft}^3$
Specimen Solids Weight:	$101.9 \cdot 0.112 \cdot 453.6 = 5170 \text{ g}$
Hygroscopic Moisture 3.3%	$5170 \cdot 0.033 = 170 \text{ g}$
Mexico Clay Weight	$5170 / (1 - 0.033) = 5350 \text{ g}$
Lime Weight	$5170 \cdot 0.03 = 155 \text{ g}$
Water Weight	$(5170 \cdot 0.175) - 170 = 735 \text{ g}$
Sample Weight	$5346 + 155 + 735 = 6240 \text{ g/sample}$

Table 5.3: Wisconsinan Silty Clay Till Mix Design

Specimen Dry Density:	$101.5 \text{ pcf} \cdot 0.95 = 96.4 \text{ pcf}$
Specimen Volume:	$((7.85^2 \cdot \pi)/4 \cdot 4) / 12^3 = 0.112 \text{ ft}^3$
Specimen Solids Weight:	$96.4 \cdot 0.112 \cdot 453.6 = 4898 \text{ g}$
	<i>Density Reduction to 92.5%</i>
Hygroscopic Moisture 5.5%	$0.925 \cdot 4898 \cdot 0.055 = 250 \text{ g}$
Mexico Clay Weight	$0.925 \cdot 4898 / (1 - 0.055) = 4530 \text{ g}$
Lime Weight	$0.925 \cdot 4898 \cdot 0.03 = 135 \text{ g}$
Water Weight	$(0.925 \cdot 4898 \cdot 0.195) - 270 = 635 \text{ g}$
Sample Weight	$4530 + 135 + 635 = 5550 \text{ g/sample}$

Table 5.4: Soil Specimen - Batch Mixes

	Mexico Clay Mix	Wisconsinan Silty Clay Mix
Soil	13,200 g	11,000 g
Lime	400 g	313 g
Water	1,900 g	1,670 g
Total Mix	15,500 g	12,983 g
Weight/Lift	3120 g	2775 g
Total Specimen Weight	6240 g	5550 g

Table 5.5: Mexico Clay Specimen Saturation Data

Sample Name	Pre-Sat Weight	Pre-Sat Moist.	Post-Sat Weight	Post-Sat Moist.	Deg. of Sat.
C0221C	6225	16.7	6555	22.4	98.0
C0221D	6230	16.7	6616	23.4	96.5
C0227A	6222	15.9	6585	22.2	95.6
C0227B	6216	15.9	6537	21.4	95.1
C0301A	6236	16.4	6570	22.1	94.9
C0301B	6232	16.4	6565	22.1	97.9
C0307A	6230	16.7	6566	22.5	95.6
C0307B	6230	16.7	6567	22.5	95.7
C0310A	6231	17.3	6568	23.1	94.1
C0310B	6235	17.3	6569	23.1	94.0
C0312A	6225	16.8	6570	22.8	99.5
C0312B	6228	16.8	6571	22.7	96.3
C0317A	6229	18.3	6488	22.7	96.1
C0317B	6233	18.3	6479	22.4	95.2
C0324A	6225	17.8	6560	23.6	94.8
C0324B	6224	17.8	6555	23.5	94.5
C0326A	6226	16.8	6559	22.5	98.6
C0326B	6227	16.8	6560	22.5	95.5
C0331A	6235	16.7	6590	22.8	94.3
C0331B	6228	16.7	6540	22.0	93.6
C0331C	6230	17.7	6488	22.0	94.7
C0331D	6226	17.7	6597	24.2	97.4
C0404A	6290	16.9	6665	23.3	98.2
C0404B	6390	16.9	6714	22.3	94.7
C0405A	6229	16.7	6546	22.1	91.1
C0405B	6228	16.7	6572	22.6	99.3
C0407A	6231	16.7	6540	22.0	90.6
C0407B	6229	16.7	6573	22.6	93.2
C0410A	6226	17.4	6563	23.2	99.0
C0410B	6220	17.4	6572	23.5	95.1
C0421A	6229	16.8	6485	21.1	86.7
C0421B	6228	16.8	6396	19.4	85.1
C0427A	6232	16.5	6611	23.1	95.6
C0427B	6235	16.5	6592	22.7	94.0
C0429A	6216	16.8	6620	23.9	97.6
C0429B	6215	16.8	6590	23.3	95.3

Table 5.5: Mexico Clay Specimen Saturation Data (continued)

Sample Name	Pre-Sat Weight	Pre-Sat Moist.	Post-Sat Weight	Post-Sat Moist.	Deg. of Sat.
C0512A	6228	17.0	6510	21.8	94.9
C0512B	6226	17.0	6528	22.2	90.6
C0602A	6228	16.9	6594	23.2	96.8
C0602B	6232	16.9	6571	23.1	96.5
C0602C	6224	18.1	6561	23.9	98.7
C0602D	6229	18.1	6544	23.5	97.1
C0605A	6219	17.4	6555	23.2	98.7
C0605B	6227	17.4	6600	23.9	98.8
C0605C	6222	17.0	6543	22.5	94.9
C0605D	6229	17.0	6562	22.7	96.1
C0610A	6228	16.8	6585	23.0	99.4
C0610B	6230	16.8	6661	24.4	99.1
C0618A	6229	16.9	6591	23.2	98.2
C0618B	6235	16.9	6578	22.8	96.9
C0621B	6223	16.6	6662	24.3	99.0
C0621B	6222	16.6	6600	23.2	98.5
C0730A	6231	16.4	6610	23.0	95.4
C0730B	6225	16.4	6618	23.2	96.3
C0802A	6225	17.9	6620	24.8	99.7
C0802B	6229	17.9	6655	25.4	99.2
C0805A	6227	17.1	6550	22.6	95.5
C0805B	6230	17.1	6587	23.3	98.3
C0808A	6241	16.2	6632	23.0	96.3
C0808B	6235	16.2	6534	21.3	94.7
C0814A	6233	17.4	6570	23.2	97.5
C0814B	6235	17.4	6593	23.6	99.2
C0816A	6222	17.5	6552	23.2	96.7
C0816B	6228	17.5	6556	23.1	96.8
C0820A	6233	18.0	6590	24.2	99.1
C0820B	6230	18.0	6593	24.3	97.7
C0822B	6232	18.1	6422	21.2	93.3
C0908A	6225	18.3	6532	23.6	99.9
C0908B	6233	18.3	6529	23.4	99.3
C0916A	6227	16.9	6604	23.5	96.3
C0916B	6225	16.9	6617	23.7	97.3

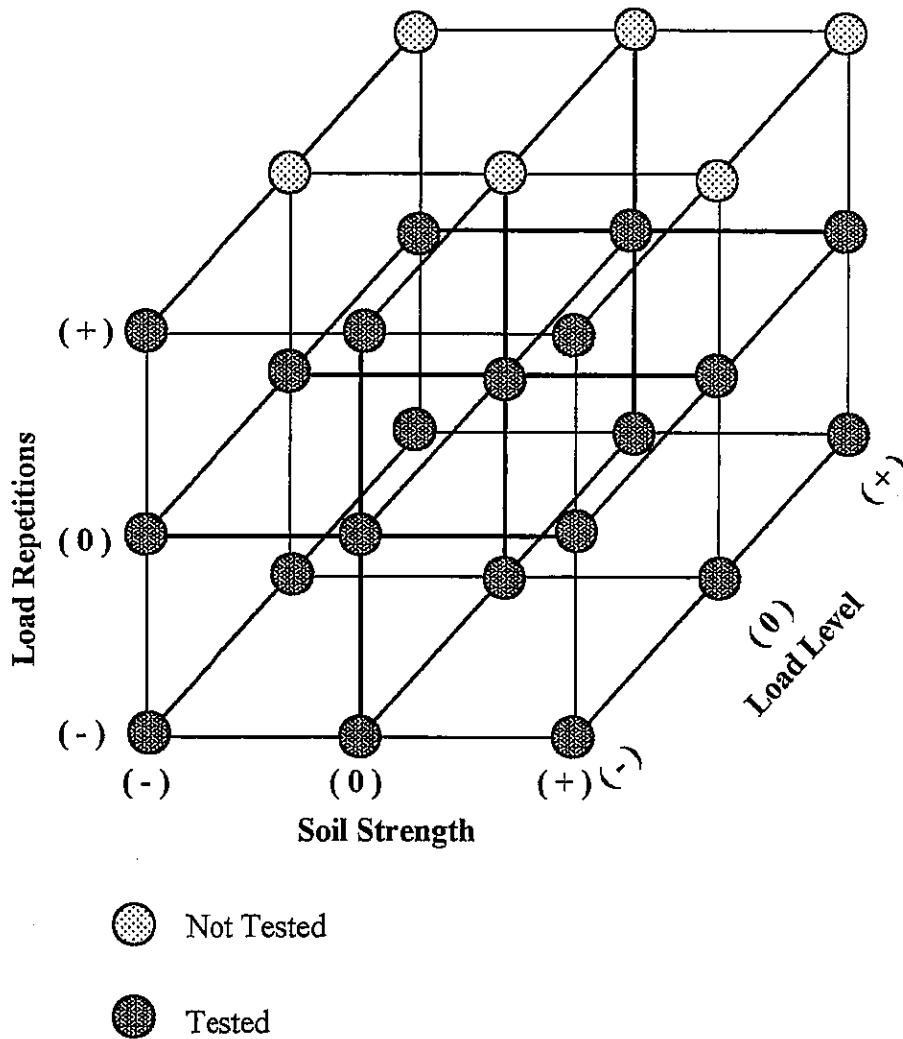
Table 5.5: Mexico Clay Specimen Saturation Data (continued)

Sample Name	Pre-Sat Weight	Pre-Sat Moist.	Post-Sat Weight	Post-Sat Moist.	Deg. of Sat.
C0922A	6227	18.0	6755	27.4	98.0
C0922B	6231	18.0	6726	26.8	98.6
C1001A	6215	17.1	6640	24.6	99.8
C1001B	6228	17.1	6654	24.6	99.1
C1017A	6230	16.7	6632	23.7	99.7
C1017B	6234	16.7	6555	22.2	97.7
C1027A	6227	17.0	6665	24.7	99.3
C1027B	6232	17.0	6639	24.1	99.6
C1029A	6223	17.5	6568	23.5	99.2
C1029B	6226	17.5	6557	23.2	98.2
C1104A	6226	16.0	6580	22.1	98.5
C1104B	6226	16.0	6571	21.9	97.7
C1116A	6235	16.6	6613	23.2	99.6
C1116B	6221	17.7	6563	23.6	98.1
C1117A	6224	16.2	6545	21.7	92.0
C1117B	6230	16.2	6439	19.6	90.1
C1120A	6235	16.2	6658	23.6	98.5
C1120B	6233	16.2	6633	23.2	96.7
C1204A	6218	17.6	6686	25.9	99.5
C1204B	6232	17.6	6739	26.6	99.9

Table 5.6: Wisconsinan Silty Clay Till Specimen Saturation Data

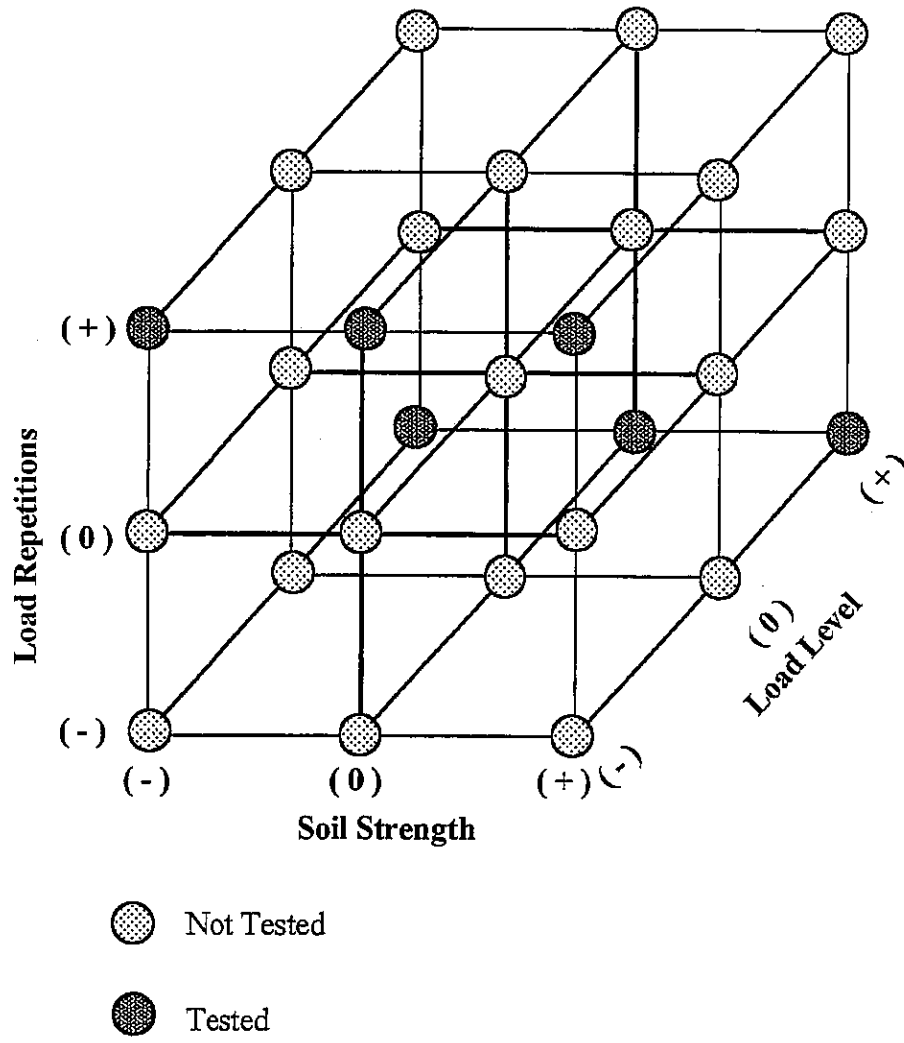
Sample Name	Pre-Sat Weight	Pre-Sat Moist.	Post-Sat Weight	Post Sat Moist.	Deg. of Sat.
S0707A	6299	19.2	6600	24.3	99.7
S0707B	6299	19.2	6568	23.7	98.4
S0707C	6305	19.2	6572	23.7	95.5
S0707D	6308	19.2	6562	23.4	97.6
S0708A	6299	19.3	6572	23.9	97.8
S0708B	6298	19.3	6562	23.7	98.2
S0709A	6140	19.3	6501	25.7	97.7
S0709B	6140	19.3	6477	25.3	95.9
S0709C	6126	19.3	6490	25.8	99.7
S0709D	6145	19.3	6520	26.0	98.3
S0710A	6073	19.4	6414	25.8	96.7
S0710B	6066	19.4	6400	25.7	95.9
S0715A	5776	21.3	6188	29.3	97.8
S0715B	5762	21.3	6100	27.8	97.6
S0722A	5536	21.5	5975	30.5	97.5
S0722B	5537	21.5	6038	31.8	96.5
S0723A	5540	21.0	5811	26.3	78.4
S0723B	5543	21.0	5841	26.9	82.4
S0723C	5534	20.8	5894	28.0	96.1
S0723D	5540	20.8	5883	27.6	95.0

Sample Name	Pre-Sat Weight	Pre-Sat Moist.	Post-Sat Weight	Post-Sat Moist.	Deg. of Sat.
S0725A	5540	21.5	6010	31.1	92.2
S0725B	5540	21.5	6070	32.4	96.0
S0728A	5536	21.4	5866	28.0	82.8
S0728B	5541	21.4	5889	28.4	88.7
S0729A	5530	23.7	6045	34.5	95.6
S0729B	5537	23.7	6043	34.2	95.3
S0804A	5537	21.6	6001	31.1	96.8
S0804B	5541	21.6	6107	33.3	98.5
S0806A	5536	21.8	6020	31.8	98.4
S0806B	5540	21.8	6043	32.2	97.2
S0811A	5537	22.7	5942	31.0	94.5
S0811B	5538	22.7	5964	31.4	98.6
S0813A	6185	23.6	6357	26.3	95.9
S0813B	6191	23.6	6363	26.3	96.1
S0815A	6191	22.0	6472	26.9	98.2
S0815B	6193	22.0	6460	26.6	97.3
S0819A	5543	21.4	6031	31.4	98.3
S0819B	5543	21.4	6054	31.9	94.7
S0821A	5538	20.6	6087	31.9	98.3
S0821B	5540	20.6	6039	30.8	97.6



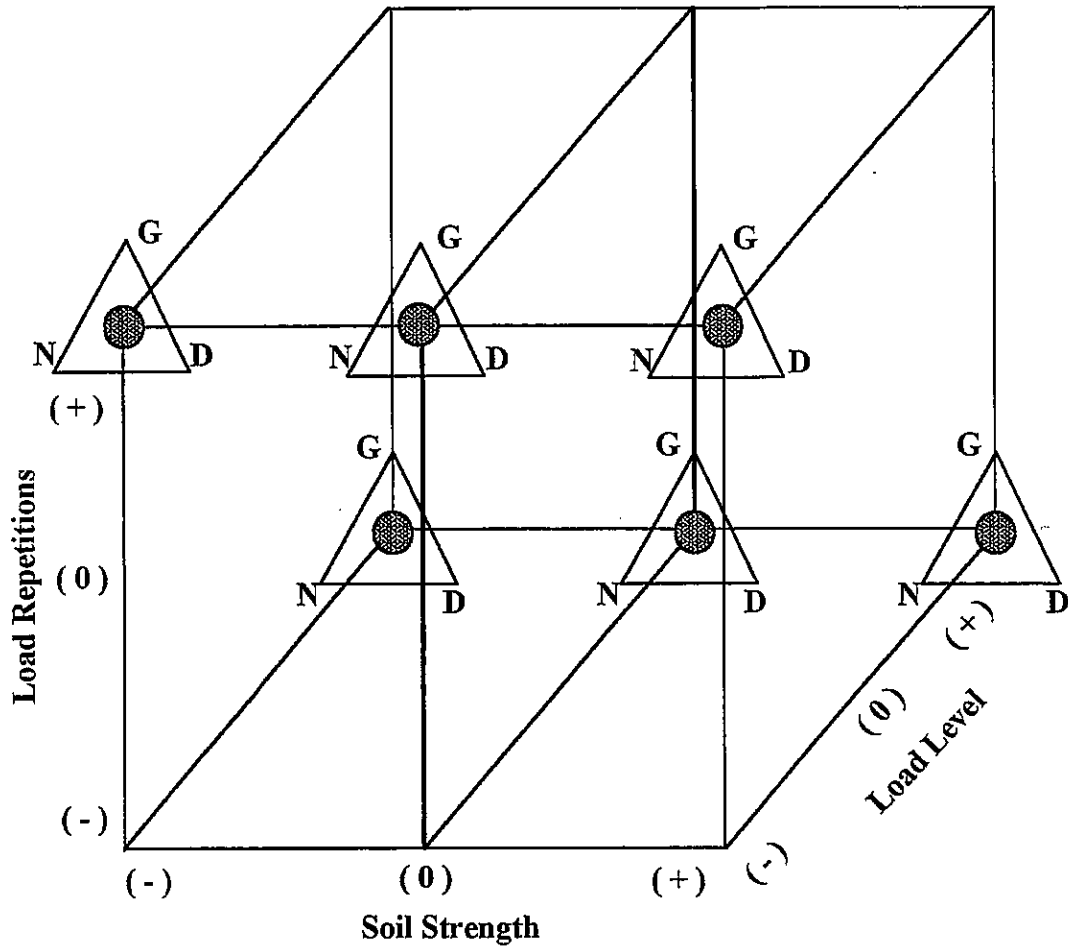
	(-)	(0)	(+)
Soil Strength	CI < 100	100 < CI < 200	CI > 200
Load Level	LL < 10 psi	10 psi < LL < 28 psi	LL > 28 psi
Load Repetitions	LR < 20000	20000 < LR < 80000	LR > 80000

Figure 5.1: Experimental Design for Accelerated Test Development



	(-)	(0)	(+)
Soil Strength	CI < 100	100 < CI < 200	CI > 200
Load Level	LL < 10 psi	10 psi < LL < 28 psi	LL > 28 psi
Load Repetitions	LR < 20000	20000 < LR < 80000	LR > 80000

Figure 5.2: Accelerated Testing - Load /Strength Combinations



Separation Types

G Geotextile

D Dense Graded

N No Separation

Figure 5.3: Accelerated Testing - Separation Layer Combinations

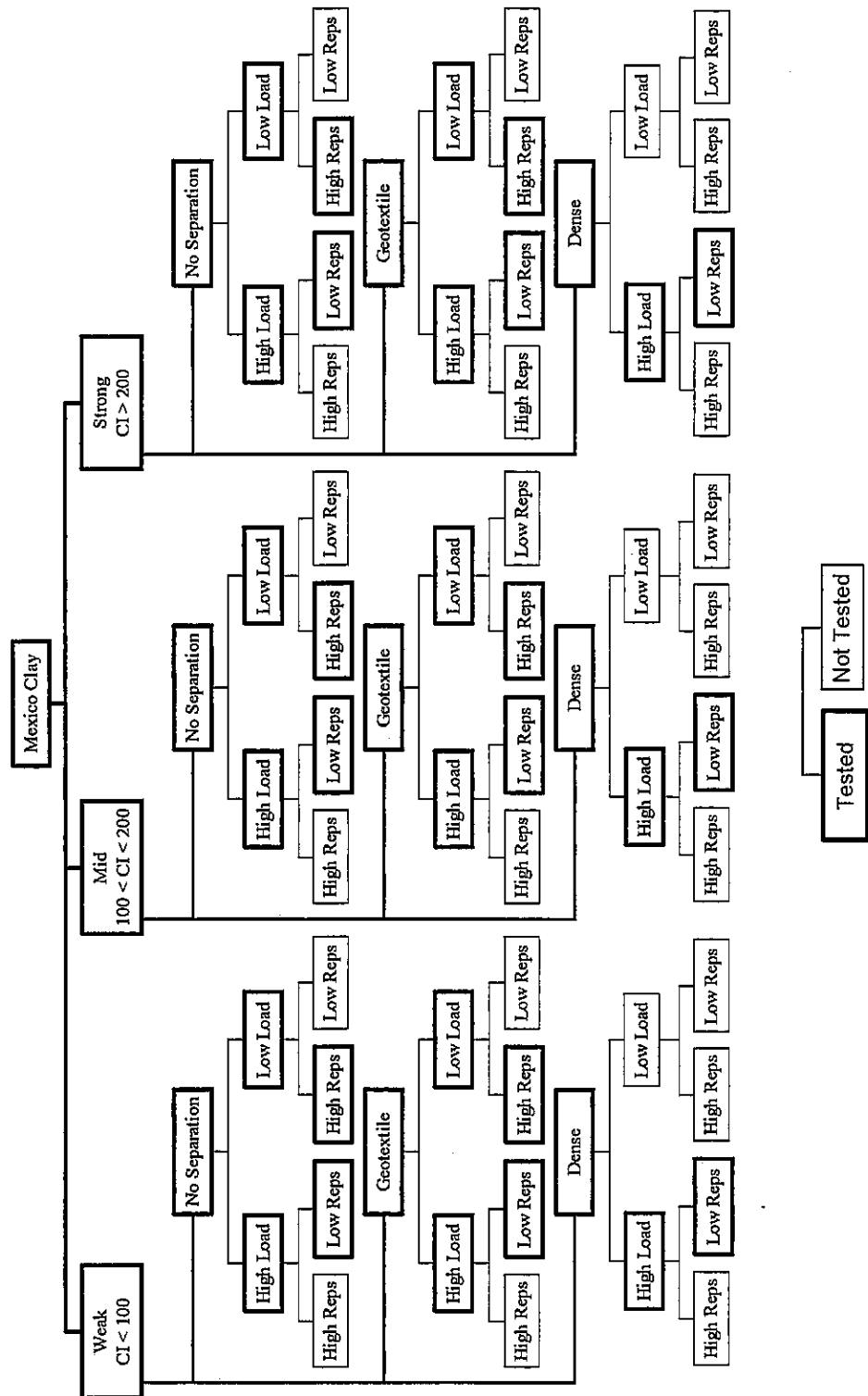


Figure 5.4: Mexico Clay/Separation Testing Combinations

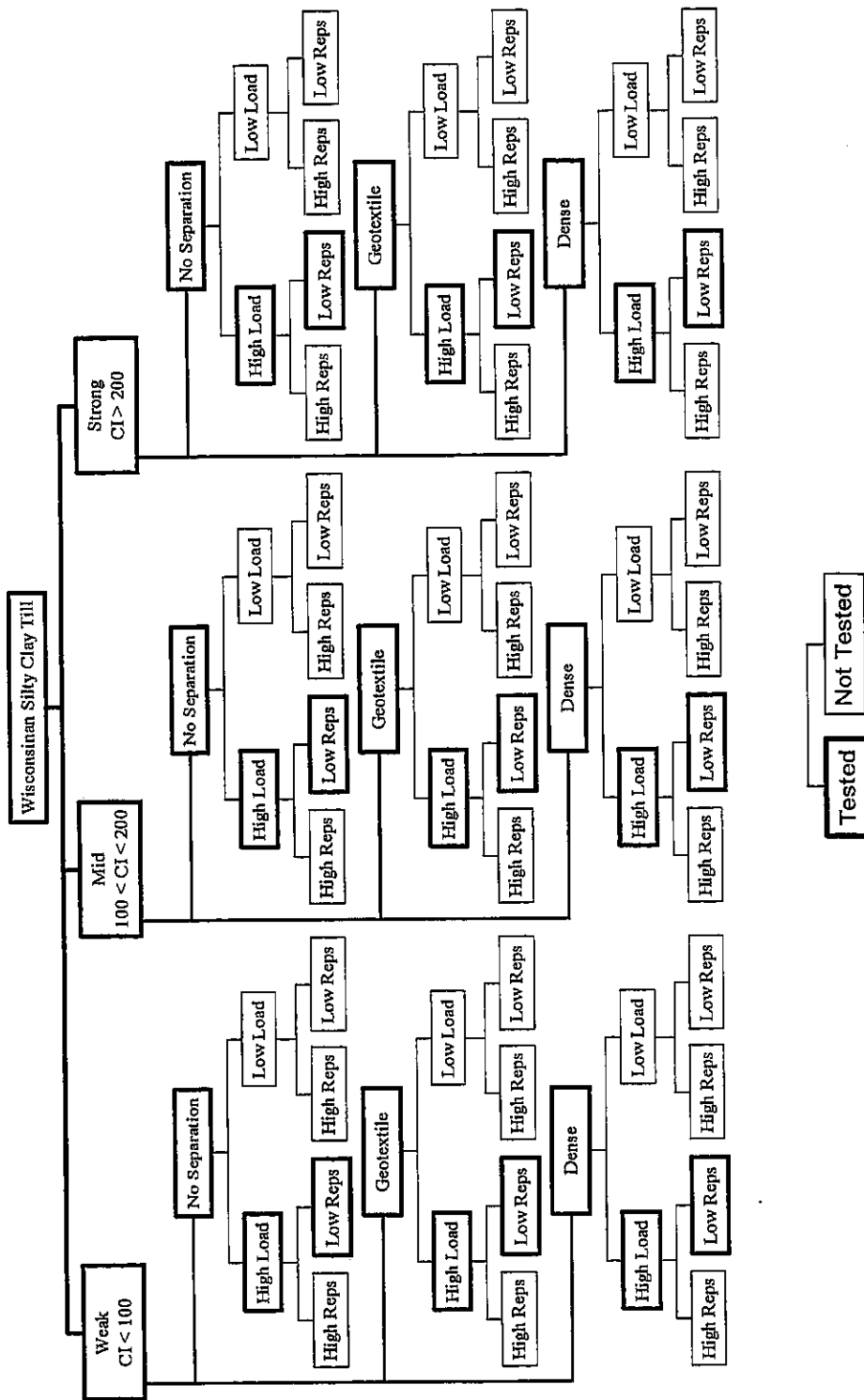


Figure 5.5: Wisconsin Silty Clay Till/Separation Testing Combinations

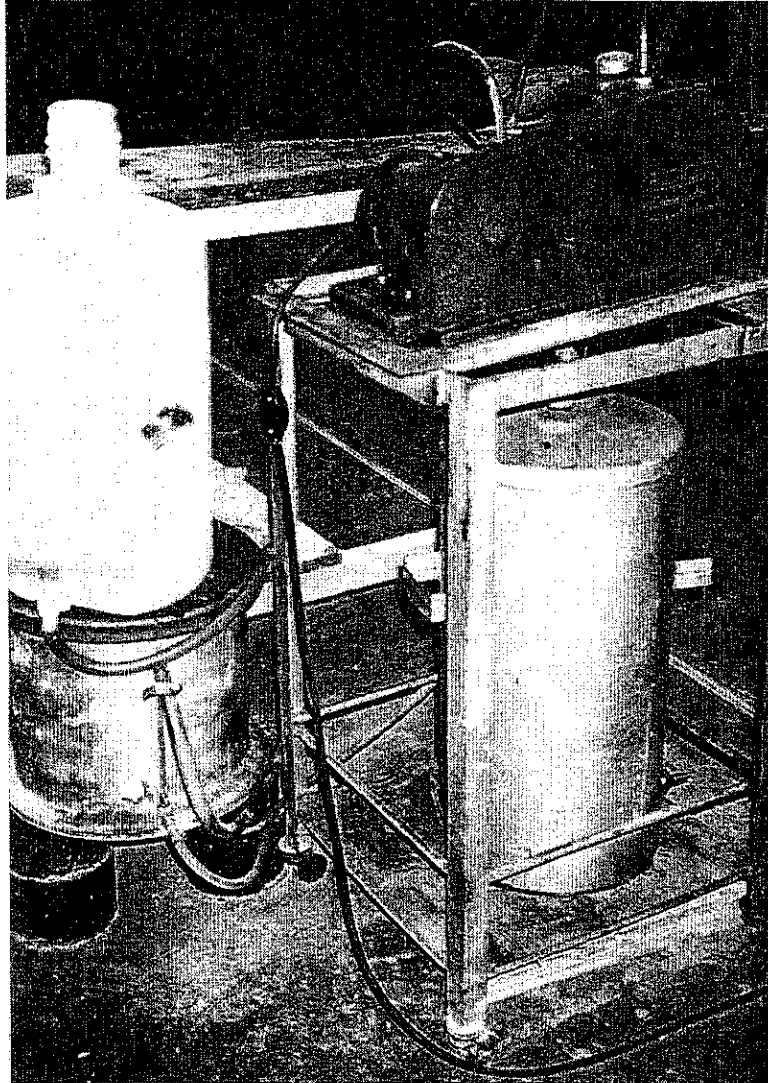


Figure 5.6: Vacuum Saturation Apparatus

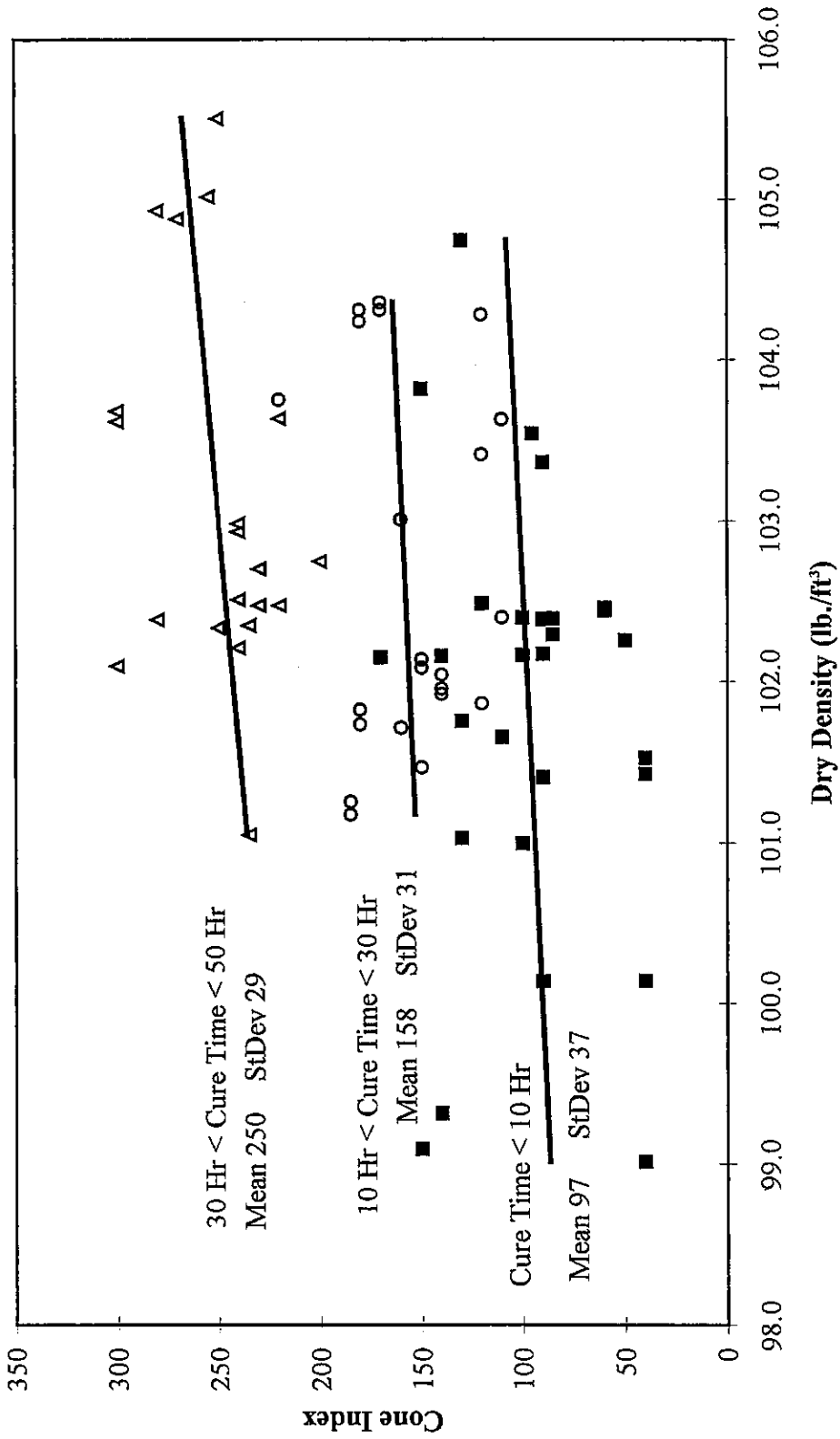


Figure 5.7: Mexico Clay, Cone Index vs. Specimen Dry Density

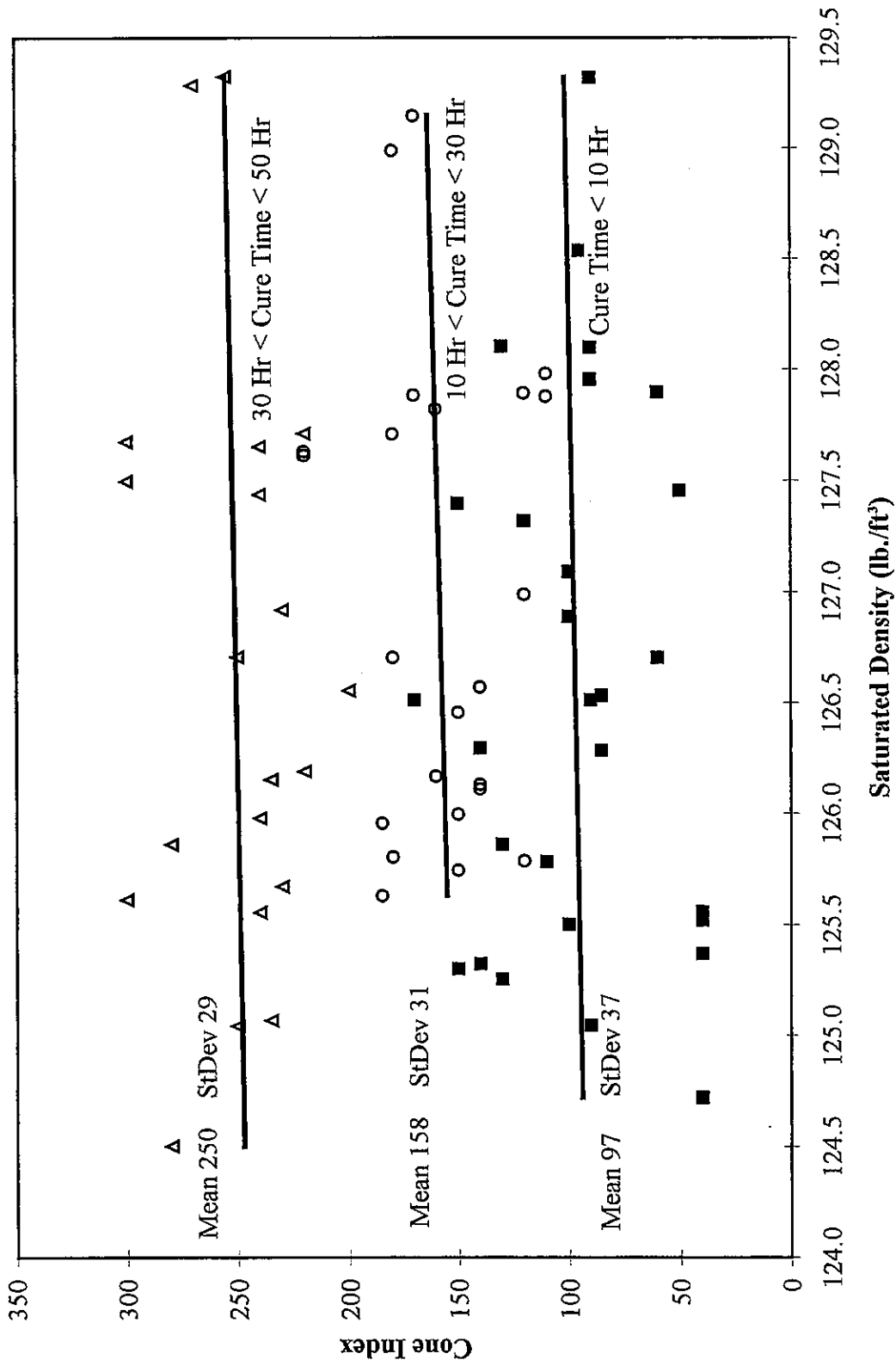


Figure 5.8: Mexico Clay, Cone Index vs. Specimen Saturated Density

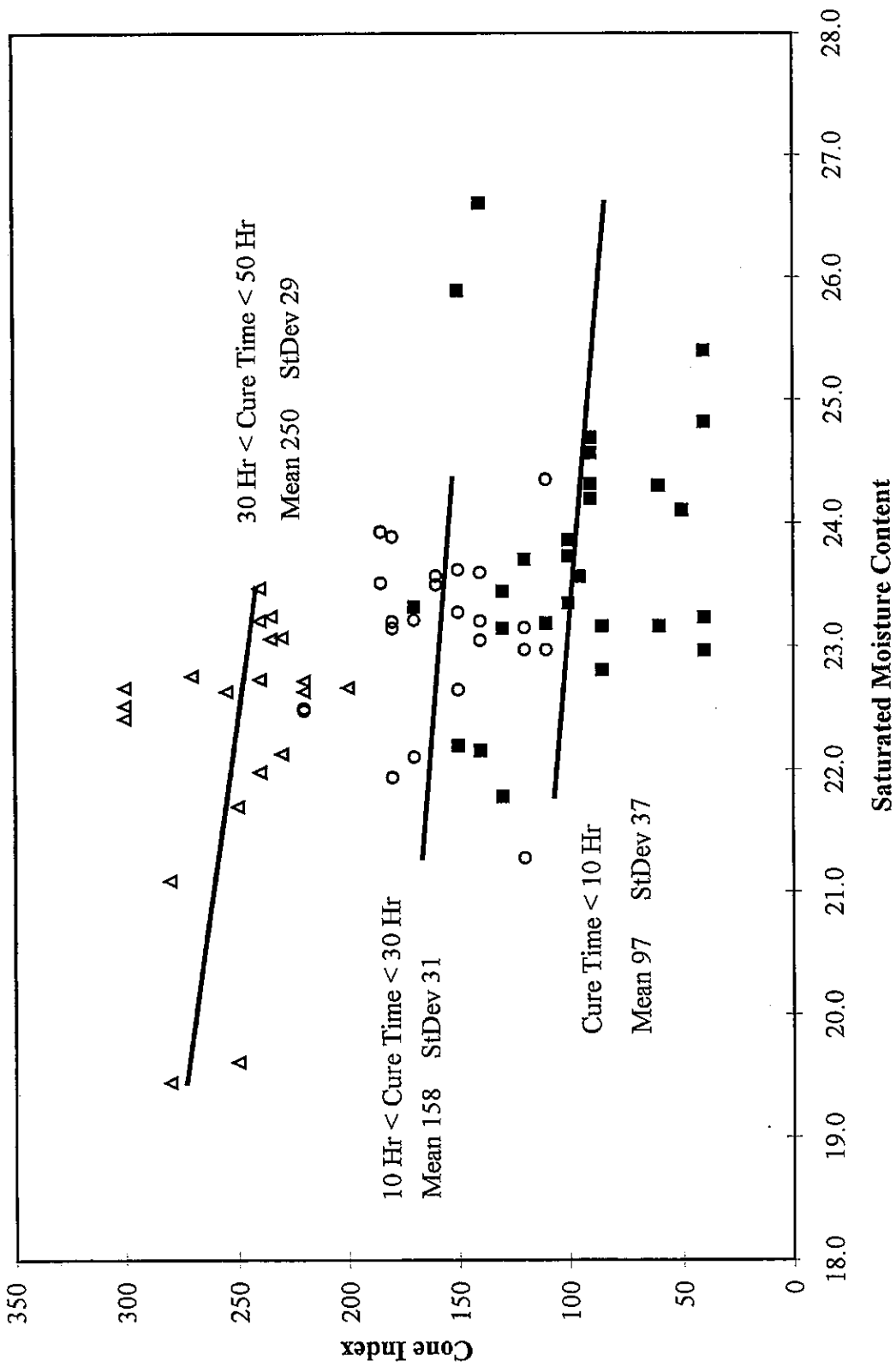


Figure 5.9: Mexico Clay, Cone Index vs. Specimen Saturated Moisture Content

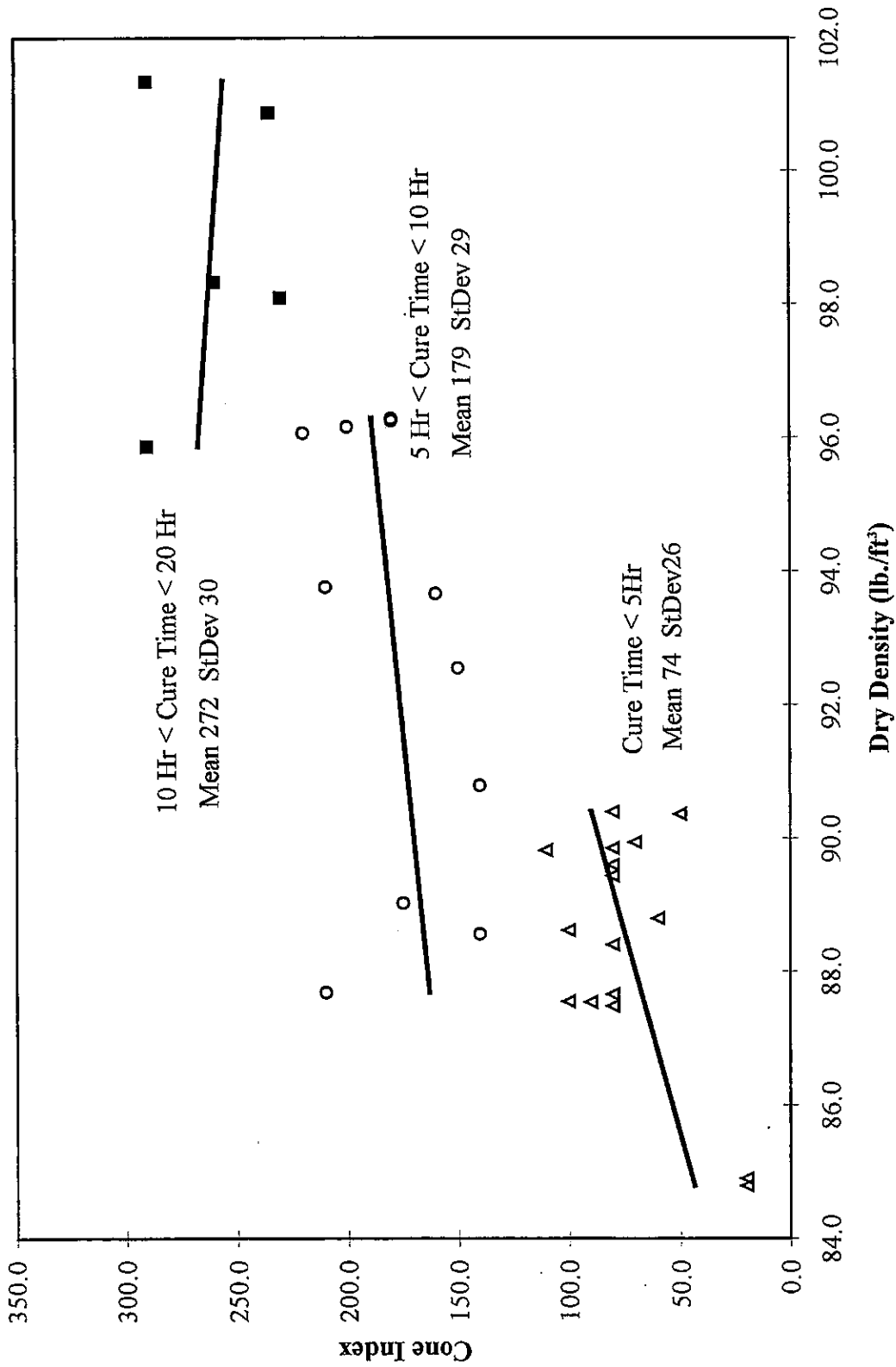


Figure 5.10: Wisconsin Silty Clay Till, Cone Index vs. Specimen Dry Density

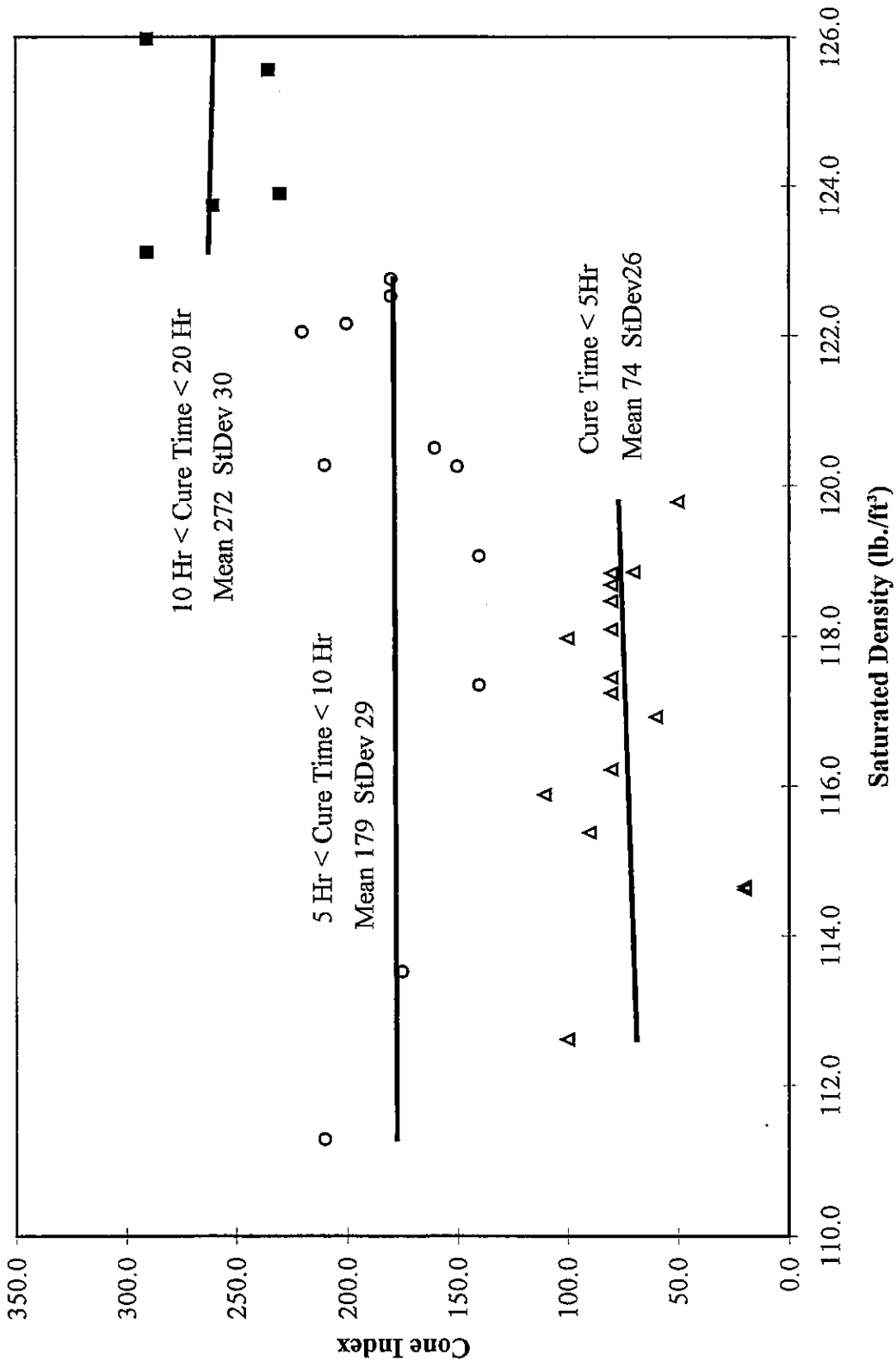


Figure 5.11: Wisconsin Silty Clay Till, Cone Index vs. Specimen Saturated Density

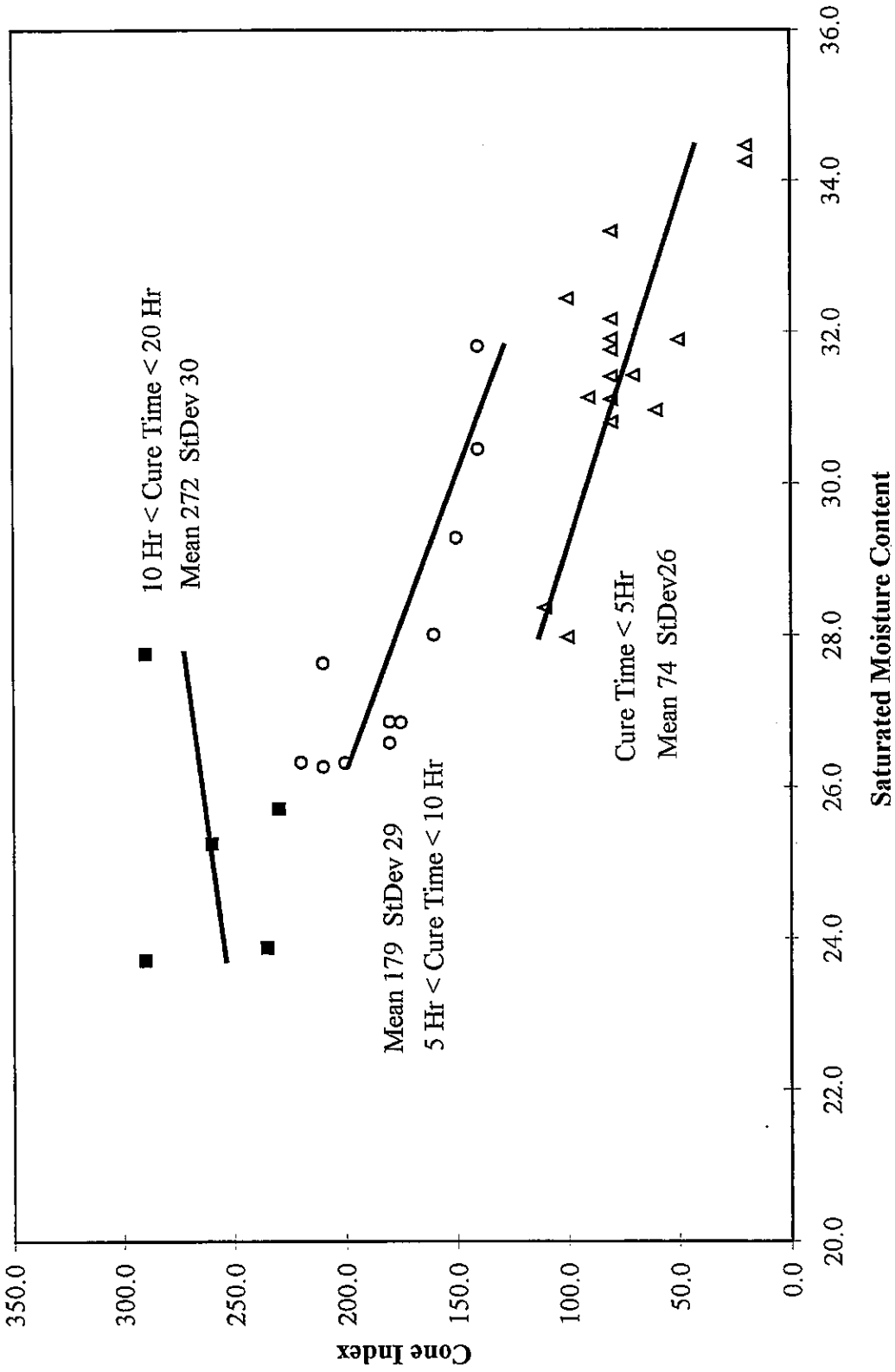


Figure 5.12: Wisconsin Silty Clay Till, Cone Index vs. Specimen Saturated Moisture Content

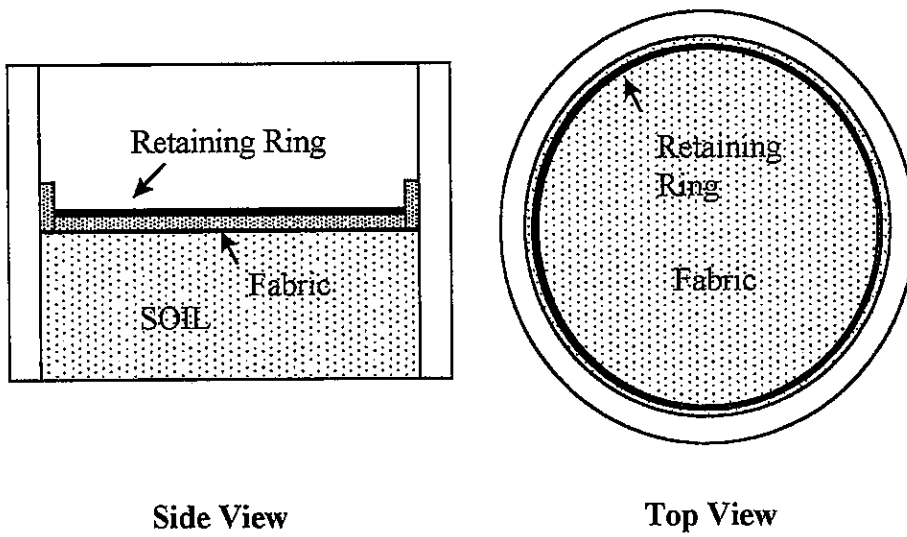
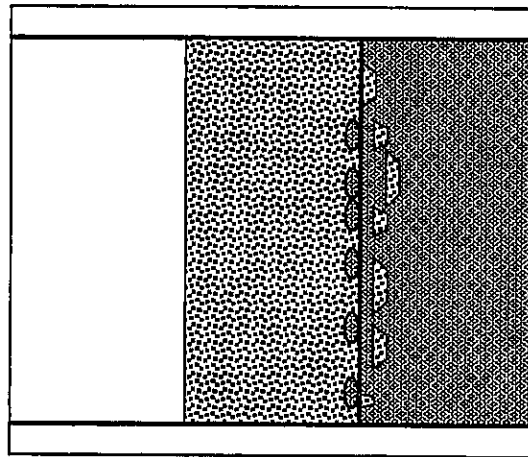
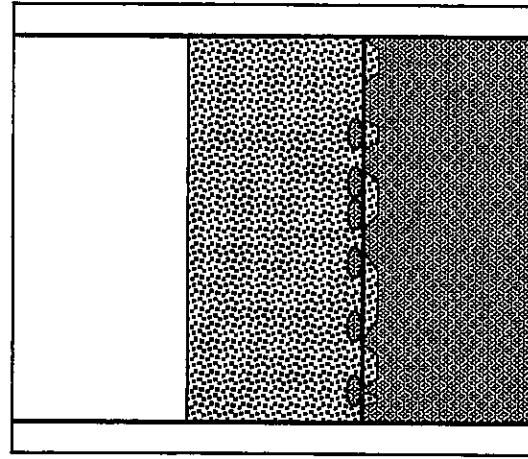


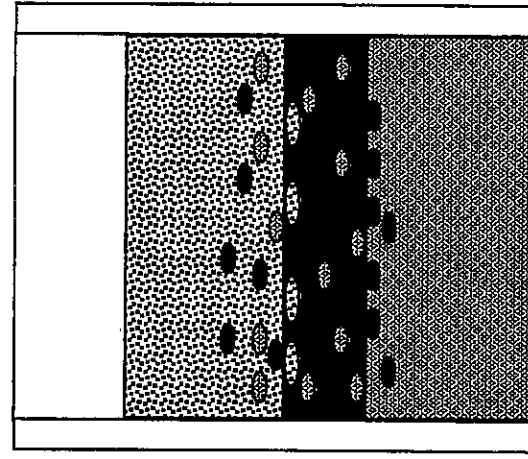
Figure 5.13: Geotextile Installation with Retaining Ring



No Separation: Aggregate intrudes into Soil. Soil Pumps into Aggregate.



Fabric Separation: Aggregate deforms soil through fabric but does not penetrate into soil. Minimal soil pumps through fabric into aggregate.



Dense Separation: Aggregate intrudes into dense-graded. Dense-graded pumps into aggregate. Soil pumps into dense-graded and aggregate.

Figure 5.14: Test Evaluation

6. SEPARATION LAYER TESTING AND RESULTS

6.1 General

This chapter presents an analysis of the performance of the separation layers evaluated in this research. This analysis is broken up into 5 sections. The first section discusses general aggregate performance under the testing conditions imposed in this research. The second section discusses the performance of the 2 individual soils with respect to the three types of separation layers tested. The third section compares the 3 different separation layers with each other for both soils. The fourth section looks at separation performance with regard to a newly created “separation performance index” (SPI). The fifth and most important section examines the performance of the 3 separation layers with respect to the 2 soils tested individually.

As discussed in Chapter 5, there were 3 principal variables controlled during this testing procedure; number of load cycles, load pressure, and soil strength. There were also 3 performance parameters for test evaluation. These parameters were weight of pumped or intruded soil, magnitude of permanent deformation, and magnitude of elastic deformation.

For each separation layer type, 4 different methods were developed to relate these principal variables to the performance parameters. The first method compared the degree of pumping or intrusion to the subgrade strength as measured with a hand held cone penetrometer. The penetrometer scale read strength directly in psi and this strength has also been shown to correlate directly to CBR as $CBR=CI/50$. The second method compared permanent deformation with the weight of pumped or intruded soil. The third method compared the weight of pumped or intruded soil to elastic deformation, while the fourth method related permanent deformation to soil strength. An additional analysis method comparing the amount of pumped soil to the “energy of subgrade reaction” was performed with minimal correlation found. Table 6.1 summarizes these methods of comparison.

Regression lines are commonly drawn in Figures 6.2 through 6.67. These best fit lines are used to illustrate general trends. In many cases the correlation is low. In all cases, these lines and corresponding equations should be interpreted with caution. Refer to the text associated with each figure for elaboration.

6.2 Open-Graded Aggregate Performance

The deflection testing results obtained in this research were from total system deformations; soil / separation layer / aggregate. To quantify the degree of both elastic and permanent deformation CA 7 aggregate experienced by itself, CA 7 aggregate was loaded repeatedly, directly on the base of the testing cylinder. The amount of deformation measured in this research was dependent upon both the initial compaction of the aggregate and the seating of the loading plate. Several accelerated loading tests of 20,000 load repetitions at 28 psi (200 kPa) were conducted to obtain an expected range of values for aggregate deformation. Figure 6.1 shows a deflection versus load cycle plot for aggregate batches G and H. The results obtained were typical of granular behavior showing the vast majority of permanent deformation occurring in the first 2000 load cycles and leveling off thereafter. These 2 samples were of identical gradation and were compacted to near equal densities. Even with this nearly identical preparation procedure, permanent deformations vary by as much as 300%, 5 mils to 15 mils. Overall, the magnitude of the peak permanent deformations varied from between 5 mils (0.12 mm) and 50 mils (1.2 mm) for all the aggregate samples tested. Elastic deformations within the aggregate ranged from 5 to 9 mils (0.12 mm to 0.23 mm) for the same loading level of 28 psi (200 kPa).

The original intent of measuring aggregate deformations was to separate out the aggregate deformations from the total system deformations when conducting accelerated loading tests. This would have enabled a direct examination of soil/separation deformations. However, with the high degree of variability in these test results, analysis of separation layer performance was therefore restricted to measuring total system deformations.

6.3 Stabilized Mexico Clay Soil and Separation Layer Performance

The first soil investigated in this research was Mexico Clay. The performance of separation layers used in conjunction with this soil is presented in this section with respect to the 4 evaluation methods described previously. The deformation versus number of load cycle plots are presented in the Appendix. The results presented are primarily testing at low and high loading levels and repetitions. Testing at mid-level loading is shown when applicable.

6.3.1 No Separation

Initial testing was performed without a separation layer between the stabilized clay and CA 7 aggregate to establish a separation layer performance baseline. Soil specimens with strengths ranging from cone index (CI) values of 80 to 300 were prepared and tested. Graphs depicting the 4 methods of performance analysis are shown in Figures 6.2 through 6.5. Figure 6.2 shows the trend of decreasing intruded soil with increasing soil strength. For a standard accelerated test of 20,000 cycles at 28 psi, the amount of intrusion ranged from a high of 13 kg/m² for soils with CBR < 2 to a low of 1 kg/m² for high strength soils with CBR > 6 to 8. Keep in mind a value of 1 kg/m² represents 1.2 oz (35 g) or 13 cm³ (0.8 in³) of soil intruding into the CA 7 aggregate within the 8 in. (200 mm) diameter test cylinder.

The variation in intrusion between samples was larger for softer soils than for stiffer soils. The contact stresses on the stiffer soils did not degrade the soil surface as much as the softer soils. Since the aggregate was primarily a blend of #4 and ½ in. aggregate, higher contact stresses were imparted for tests having a greater degree of ½ in. aggregate contacting the soil. For softer soils, a greater proportion of ½ in. aggregate contacting the soil surface imparted a significantly harsher contact stress than did the #4 aggregate when it contacted the soil surface. For stiffer soils, this stress difference was “resisted” by the soils and minimal performance differences were seen. Adequate mixing of the aggregate took place prior to testing, but no control was available over which aggregates actually resided on the soil surface during a given test. An actual in-use IDOT aggregate gradation was desired in this research otherwise a uniform + ½ in. aggregate could have been used to help minimize this variation in contact stresses. Figure 6.2 shows pumping versus soil strength, but for typical field loading conditions. Specimens were loaded for 500,000 cycles at 8 psi. Similar performance trends occurred with high stress and low repetitions and low stress and high repetitions. The actual magnitude of pumping for both the accelerated loading case and the typical field loading cases were comparable indicating a similar level of load-repetition effort. This indicated accelerated testing could give results similar to conditions experienced in the field after long term loading.

As indicated previously a major Interstate in Illinois suffered severe permanent deformation due to significant intrusion in the underlying open-graded/soil interface. With this in mind, permanent deformation is shown with respect to soil intrusion in Figure 6.3 for middle strength CBR ~ 2-4 soil samples. The expected trend of increasing permanent deformation with increasing intrusion was seen. Permanent deformation actually increased at a faster rate than soil intrusion. Permanent deformation tripled while intrusion only doubled during these tests. Also shown in Figure 6.3 is the corresponding data for low level stress, high cycling tests. Note for comparable degrees of intrusion the permanent deformation for low stress testing was significantly lower than for accelerated tests even though the soils had similar strengths. This was attributable to mechanism of failure/deformation with the two types of loading. Barenberg³⁴ suspected high level loading perhaps caused a different failure mode to take place than does low level loading. In this research, with low level loading, the intrusion appeared to be a slow *upward* process in which the soil gradually moved up into the aggregate. Due to the lengthy testing time (up to 5 days), there was significant slurry formation, leading to easy movement of fine particles. For the high level loading, the soil/aggregate interface weakened quickly and the aggregate was "shoved" *down* into the soil, and to a much greater degree. This was a bearing capacity type of failure in which the aggregate contact stresses exceeded the strength of the top surface of the soil specimen. The soil filled the voids of the newly embedded aggregate. This pumping/intrusion movement can be validated by comparing relative permanent deformations. In the low level loading cases, small permanent deformation occurred, indicating a minimal merging of the two materials. For high level loading cases, significant permanent deformation took place indicating a merging of the two materials, yet intrusion comparable to low level loading occurred. A major advantage of using the clear plexiglas test cylinders was this process could be visually observed as opposed to guessing what was occurring beneath a pavement surface or within an opaque test chamber or neoprene sleeve.

Intruded soil is compared to elastic deflection in Figure 6.4. These tests actually resulted in larger intrusion for smaller elastic deflections. The test results were counter to expectations and atypical for this research. Additionally, the degree of accuracy in measuring elastic deformations was not as great as in measuring permanent deformations. This

measurement inaccuracy was due to occasional problems with the thin (1/8 in.) seating plate. It sometimes would not maintain intimate contact with the open-graded aggregate and would actually come up off the aggregate during the up-stroke of the loading head. This could lead to inaccuracies in elastic deformation measurements. Figure 6.5 shows similar data to Figure 6.3 in permanent deformation is compared to soil strength. Permanent deformation dropped significantly for stronger soils under the accelerated testing method, but minimal change occurred at low level testing. This was a benefit of the accelerated method in degree of material behavior change was magnified and occurred at faster rates than under typical field level loading conditions. The outlying point was suspected to be a result of an aggregate compaction problem with an especially weak soil during specimen preparation.

6.3.2 *Geotextile Separation*

Testing with a geotextile separation layer was conducted for varying strength soil samples. Figures 6.6 through 6.11 show plots of similar parameters as for the previously discussed no separation testing cases. Figure 6.6 shows the degree of soil pumping versus soil strength. For accelerated loading, there was a distinct strength level above which minimal pumping occurred. For the stabilized Mexico Clay the strength level was at a cone index of 200, corresponding to a CBR of around 4. Another interesting point shown in Figure 6.6 was for several samples below this strength threshold, pumping did not occur. This was again suspected to be partially due to the aggregate footprint/contact stress issue previously discussed. At lower stress levels, unlike the case with no separation, the geotextile significantly minimized pumping. For lower strength soils, soil pumping was only about 10% of what it was without separation. Soil pumping for specimens without lime as shown in Figure 6.6 was twice stabilized soil pumping and approached non separated case pumping, indicating the importance of soil modification. Figure 6.7 shows the same parameters with mid and high loading levels and cyclic durations. Notice it took 400,000 cycles at 20 psi to begin to match the failure levels produced with 20,000 cycles at 28 psi. This was part of the reason for the selection of such high loading pressures and low cyclic levels. From here on, the term accelerated loading condition implies this 28 psi load for 20,000 load repetitions.

The amount of soil retained within the geotextiles when tested is shown versus soil strength in Figure 6.8. As expected, with weaker soils a greater amount of soil was retained within the geotextile. Once again, a threshold though not as pronounced as with total pumping was found at cone indices of around 200. Below cone indices of 200, soil retention gradually increased. For the unstabilized soil, the geotextile retained approximately 50% more soil than for stabilized soil of the same strength. For the lower level testing, regardless of soil strength the geotextile retained approximately the same amount of soil, comparable to accelerated testing with strong soils, 0.5 to 1.0 kg/m². Figure 6.8 is plotted to the same scale as Figure 6.6 for comparison purposes. Figure 6.9 shows permanent deformation versus soil pumping. Deformation magnitudes increased from an average of 50 mils for strong soils with cone indices greater than 200 to over 100 mils for soils with cone indices less than 100. Note however this increase was small compared to the cases with no separation. Soil pumping versus elastic deflection is shown in Figure 6.10. This figure shows the trend found during this research and indicates weaker soils exhibited significantly more elastic deflection than the stronger soils. The plot shows pumping for various strength soils. Notice minimal if any pumping occurred when there was a strong soil (CI > 200). Elastic deflections with stronger soils were consistently smaller than with weaker soils. With decreasing soil strengths came increasing elastic deflections and corresponding increased amounts of pumped soil. This threshold turned out to be at a cone index of approximately 200. Finally, Figure 6.11 compares permanent deformation with soil strength. Though not as pronounced as in the non separated cases, deformation levels definitely increased at cone indices below 200 for the accelerated testing levels. Deformations remained low, but slightly increasing for lower soils strengths at lower stress levels.

Figures 6.12 through 6.15 show what this pumping process looks like with geotextiles, for various test conditions. Figure 6.12 shows a moderately plugged geotextile (oven dried) after testing with a stabilized specimen. Note only certain parts of the geotextile were blocked and there were indentations in the geotextile from the aggregate footprints. Figure 6.13 shows the soil underneath this same geotextile. There was ponding of slurry in each of the depressions left by the aggregate footprints. The soil specimen surface was composed mostly of coarser particles, the finer particles having pumped into and through the geotextile. This

may not be readily evident in the photograph however. This coarser underlying soil character was evident in most of the soil samples tested. Figure 6.14 shows a test in which more severe pumping occurred. The aggregate and accompanying slurry shown are just above the geotextile. Figure 6.15 shows a similar situation with an unstabilized soil. Notice the considerable amount of soil retained within the geotextile and the accompanying aggregate was completely coated with soil slurry.

6.3.3 *Dense-Graded Separation*

The performance of the dense-graded separation layers is shown in Figures 6.16 through 6.19. The important observation to note here was the comparative performance of “wet” and “dry” CA 6. As mentioned in Chapter 4, the magnitude of the pumping values cannot be compared with the no separation and geotextile separation cases since the “Material Transfer” values cited here consist of aggregate as well as fine soil weight. Due to chamber height limitations, only a 2 inch layer of CA 6 was tested whereas IDOT specifies a 3 inch layer. From the testing seen in this research, the performance of the thicker layer would likely not have been significantly different from the thinner layer since the material did not perform as a layer and broke down under testing. From Figure 6.16 it was apparent the degree of material transfer was quite variable, with the wet CA 6 material transfer typically much larger than the dry CA 6. The wet CA 6 cycled 20,000 times at 28 psi performed comparably to the dry CA 6 cycled 40,000 times (mid level) at the same pressure. Figure 6.17 shows permanent deformation versus material transfer. Stronger soils ($CI > 200$) exhibited small amounts of permanent deformation compared to weaker soils for the same amount of material transfer. Though some scatter was evident, the general trend of increasing permanent deformation with increasing material transfer for a given soil strength resulted. Material transfer amounts are compared to elastic deformation in Figure 6.18. With the exception of 2 outlying points, the general trend of increasing material transfer with elastic deflection occurred. Also in general, weaker soils tended to have larger elastic deflections than did stronger soils. Lastly, Figure 6.19 shows permanent deformation versus soil strength. As before, with higher cone indices, less permanent deformation occurred. At cone indices above about 200, minimal deformation occurred, implying another threshold of soil strength.

6.4 Wisconsin Silty Clay Till and Separation Layer Performance

Test data for this soil was not as extensive as for Mexico Clay, but similar trends resulted. Long term performance testing with this soil was not completed since Mexico Clay testing showed accelerated testing could give adequate results. Performance analysis is made with respect to the four methods cited in the previous section on Mexico Clay. The deformation versus number of cycle are presented in the Appendix.

6.4.1 *No Separation*

Figures 6.20 through 6.23 show the results of no separation testing for this silty clay till. Figure 6.20 shows soil intrusion with respect to soil strength. As was expected, increases in soil strength resulted in significant decreases in soil intrusion. At 20,000 load cycles, intrusion was reduced by over 50% as soil strength increased from a CBR of 1-2 to a CBR of 6. For the extremely strong samples tested with CBR values greater than 10, next to zero intrusion occurred under accelerated testing even at 60,000 loads (mid level). Figure 6.21 presents permanent deformation versus soil intrusion. For the extremely strong samples, virtually no intrusion occurred. Permanent deformation increased rapidly with increasing soil intrusion, more than 100% for both the stronger and weaker soils, as the intrusion increased by 50% and 100% respectively. Soil intrusion is presented versus elastic deflection in Figure 6.22. As was typical, the weaker the soil, the greater the elastic deflection. The extremely strong samples with cone indices greater than 500 exhibited the lowest elastic deflection with values in the range of 11 mils to 12 mils. The remaining 4 soils exhibited typical elastic deflections in the 25 mil to 30 mil range. Figure 6.23 shows permanent deformation decreasing with increasing soil strength.

6.4.2 *Geotextile Separation*

The performance of the GEOTEX 1101 geotextile when used with the Wisconsin Silty Clay Till is shown in Figures 6.24 through 6.28. Figure 6.24 shows pumped soil versus soil strength. Note how minimal soil intruded when the underlying soil had cone indices

greater than 200. As with the Mexico Clay, there were also cases of minimal pumping with weaker soil as evident with several points on this graph. The circles represent the use of the retaining ring previously described. This ring provided a slightly more restricted flow path for soil through the fabric by reducing the effective fabric diameter and eliminating any potential particle movement up the cylinder wall. However the low levels of pumping seen for those points were also seen for many other pre-ring testing points as well. Much of the lack of pumping for weaker soils can again be partially explained by the footprint left on the geotextile after testing indicating smaller aggregate particles against the soil and correspondingly lower contact stresses. Geotextile soil retention versus soil strength is shown in Figure 6.25. The trends shown here were nearly identical to the Mexico Clay. There was a decreasing retention trend with increasing strength with the retention becoming fairly constant with soils having cone indices above 200. Figure 6.26 presents permanent deformation in relation to soil pumping. As expected, permanent deformation increased rapidly with increasing soil pumping. With weaker soils, significantly more soil had pumped than for the stronger soils, leading to markedly higher deformations, approaching 400 mils. With soils having cone indices greater than 200, regardless of the degree of soil pumping (albeit small), the permanent deformation held fairly constant in the 40 mil to 60 mil range. For this series of tests, elastic deflections did not correlate well with soil pumping as seen in Figure 6.27. Significant scatter exists with a small trend of increasing soil pumping for increasing elastic deflections for the mid-range soil strengths. Figure 6.28 shows permanent deformation versus soil strength. A similar trend was once again produced with minimal deformation occurring at cone indices greater than 200. Tests also showed minimal deformation for weaker soils which can be attributed to aggregate footprints and test variability.

Representative pictures of testing with the Wisconsin Silty Clay Till are presented in Figures 6.29 through 6.32. Figure 6.29 is a picture of the aggregate above the geotextile after an accelerated test on a weak soil. Notice the complete saturation of the aggregate layer with soil slurry which has pumped from beneath the geotextile. Figure 6.30 shows a dried geotextile after testing on a strong soil. Note how clean the geotextile was throughout its surface due to minimal pumping into it from below. A weak soil after testing and after the geotextile was removed is shown in Figure 6.31. Large aggregate indentations were present,

but otherwise no evidence of aggregate material was seen in the soil. This was the advantage of the geotextile in while indentations were occurring, actual aggregate mixing with soil was prevented. Figure 6.32 shows both the geotextile and accompanying aggregate following an accelerated test. The top figure (partial view) was of a stiff underlying soil and minimal soil was evident on the fabric and aggregate. The lower portion of the figure shows the partial saturation of the fabric and aggregate due to pumping from this middle strength (cone index ~150) soil sample.

6.4.3 Dense-Graded Separation

Dense-graded aggregate separation layer performance is shown in Figures 6.33 through 6.36. Material transfer dropped off with increasing soil strength as shown in Figure 6.33. Variability was also higher for the weaker soils as usual, partially due to the effect of contact stresses on the soil. Figure 6.34 presents permanent deformation against material transfer. Regardless of soil strength, increasing material transfer resulted in increased permanent deformation. In this case however it took proportionally higher increases in material transfer to produce comparable increases in permanent deformation. Figure 6.35 shows higher elastic deflections produced higher degrees of material transfer for this set of samples. For the stronger samples, with cone indices greater than 200, a wide variation in elastic deflections occurred which was typical. The sample exhibiting only 13 mils of elastic deflection resulted in the lowest amount of material transfer for a dense-graded separation test case. Again as typical, increased soil strengths produced decreased permanent deformations as seen in Figure 6.36.

6.5 Separation Layer Comparison with Respect to Both Soils

The previous 2 sections detailed the of performance of the 3 separation methods for both Mexico Clay and the Wisconsinan Silty Clay Till individually. In this section, the performance of the 3 separation methods is presented with respect to both soils, i.e. how well does each separation method work for each soil. As before graphs of the 4 analysis methods are presented for each case.

6.5.1 *No Separation*

The performance of non separated soil and aggregate layers tested are presented in Figures 6.37 through 6.40. As shown in Figure 6.37, for a given soil strength the degree of intrusion for the Wisconsin Silty Clay Till was greater than for the Mexico Clay. Permanent deformations versus soil intrusion were comparable for the 2 soils as shown in Figure 6.38 with significant deformation increases of 200% and 300% with increasing soil intrusion. Unfortunately, little correlation occurred with soil intrusion when evaluated versus elastic deflection as in Figure 6.39. There were larger amounts of intrusion for a given elastic deflection for the silty clay till compared to the clay. Figure 6.40 presents permanent deformation versus soil strength. For this limited data, it appears both soils behaved comparably for a given strength and deformation level.

6.5.2 *Geotextile Separation*

Soil pumping is related to soil strength in Figure 6.41. The silty clay till pumped through the geotextile to a greater degree than did the clay. This was not an unexpected behavior due to the problems encountered with geotextiles and silty soils. Also note the threshold at a cone index of 200, above which minimal pumping occurred. Pumping levels stabilized for both materials above cone indices of 200 with the silty clay pumping about twice as much as the clay did, 0.8 kg/m² versus 0.4 kg/m² respectively. The greater degree of pumping with the silty clay till led to greater permanent deformations as shown in Figure 6.42. Deflections were 50% to 100% greater for the silty clay till than the clay for a given amount of pumped soil. Figure 6.43 shows soil pumping versus elastic deflection. Both soils showed considerable variability in pumping for a given elastic deflection. Also, no real comparison between the two soils' performance can be made with this wide spread data. Definite trends occurred when looking at permanent deformations versus soil strength as shown in Figure 6.44. Both soils exhibited comparable deformations for stronger soils with cone indices greater than 200. For weaker soils, the silty clay till exhibited significantly greater, typically about triple the deformation than did the clay for a given soil strength. As before though,

there was a group of silty clay till specimens that behaved comparably to the clay specimens in that minimal permanent deformation occurred during accelerated testing.

6.5.3 Dense-Graded Separation

Dense-graded separation layer performance for both soils is presented in Figures 6.45 through 6.48. Both soils behaved similarly when looking at material transfer versus cone index as shown in Figure 6.45. Significant material transfer occurred with the weak silty clay till samples, while a modest decreasing trend of material transfer with increasing cone index was found. As described earlier, material movement at 2 interfaces occurred and therefore soil strength alone may not adequately determine the degree of material transfer. Figure 6.46 shows permanent deformation with respect to material transfer. Again, the materials behaved comparably with a definite trend of increasing deformation with increasing material transfer. Material transfer though increased at a proportionally faster rate than did permanent deformation during these tests. When looking at material transfer versus elastic deflection as shown in Figure 6.47, no clear trends were evident. There was great variability with the silty clay till data. Similar elastic deflections produced a tighter range of material transfer values, though these varied by upwards of 300%. Finally, Figure 6.48 shows permanent deformation versus cone index. Based upon the data shown, both soils tended to have comparable permanent deformations for given soil strengths.

6.6 Performance Index Based Comparison

In the previous sections, interpretations were made with respect to individual performance parameters such as pumping and deformation. This section analyzes separation performance with respect to a performance index based upon the combination of pumping and permanent deformation. The Separation Performance Index (SPI) was developed by equally weighing pumping and permanent deformation values. Since the numerical magnitudes of pumping and permanent deformation were significantly different (the dimensions were different as well; weight/area and length), permanent deformation values were scaled with respect to pumping quantities as part of the determination of the index. The combined value

was then inverted so higher SPI values would indicate better material performance. SPI values range from 0.005 for very poor performance to over 2 for excellent performance. An example SPI calculation follows:

Mean permanent deformation of series of tests: 90 mils

Mean pumping for same series of tests: 1.1kg/m²

Data for given test: permanent deformation: 100, pumping 0.85

$$SPI = \frac{1}{(100 / (90 / 1.1) + 0.85)} = 0.48$$

6.6.1 Separation Performance Index for Mexico Clay

The SPI is compared to cone index as shown in Figures 6.49 through 6.52 for Mexico Clay. To provide an idea of the performance associated with the SPI values shown in the graphs, the table below presents typical value ranges for the two parameters composing the SPI.

SPI	Pumping (kg/m ²)	Permanent Deformation (mils)	Performance Rating
2.0	0.001 to 0.05	35 to 25	Excellent
1.0	0.23 to 0.25	65 to 50	Good
0.5	0.3 to 1.0	120 to 75	Fair
0.1	1.4 to 5	400 to 170	Poor

In Figure 6.49, the results of no separation testing is shown. As expected the SPI increased with increased soil strength, though large variability, especially at low strengths was present. For a given cone index (approximately 100), the SPI varied from 0.03 to 1.6. Much of this can be attributed to the fact that strength alone may not be adequate for determining strength. Recall from Section 5.2.2 that a soil specimen of a given cone index can have significantly varying densities and moisture contents, hence differing performance capabilities. In this research, once a minimum strength level was reached (CI > 200), then adequate performance resulted. Figure 6.50 shows the same data except 1101 geotextile separation layer was used. Notice the trend of rapidly increasing performance with increasing soil strength. Considerable variability was evident however even though the average SPI at higher

strengths is 4 times the SPI at lower strengths. Again, this variability was attributable to how a single strength can represent differing performance. Note that once a cone index of 200 was reached, the SPI was consistently greater than 1. In this case the variability is insignificant since all these points indicate adequate performance. Dense-graded SPI is plotted in Figure 6.51. Here again, the SPI increased with increasing soil strength. Recall the material transfer with dense-graded separation layers had to be calculated in a different manner than the other 2 separation cases, thereby eliminating direct comparison. There was not as distinct a performance/strength breakpoint for dense-graded separation as previously seen. The condition of the dense-graded layer was more relevant to pumping than the soil strength. Underlying weaker soils simply afforded a more rapid breakdown of dense-graded separation layers by providing less stable support. To compare SPI values, Figure 6.52 plots SPI for both geotextile and no separation cases. At cone indices less than 200, geotextile separation resulted in SPI values 4 times greater than no separation cases. Additionally, very strong soils not separated from the open-graded aggregate did not yield SPI values as high as weak geotextile separated soils. For stronger soils, with cone indices greater than 200, this ratio increased to approximately 8. This data shows the benefit of geotextile separation actually increased with increasing soil strength.

6.6.2 Separation Performance Index for Wisconsin Silty Clay Till

Figures 6.53 through 6.56 show SPI data versus cone index for Wisconsin Silty Clay Till. In Figure 6.53, no separation testing results are presented. A wide range of soil strengths were tested. It was evident from the testing significant soil strength (cone indices of 500) was required to achieve SPI values comparable to geotextile separation with Mexico Clay, as shown in the previous section. Figure 6.54 shows SPI values for geotextile separation. Considerable variability resulted from these tests, but the trend of increased SPI with increasing soil strength is once again present. Note that for cone indices greater than 200, that consistently good performance was exhibited. The performance variability of the specimens weaker than cone index 200 is inconsequential. For dense-graded separation layer testing as shown in Figure 6.55, very low SPI values resulted. These values of 0.04 and less were comparable to Mexico Clay SPI values. Figure 6.56 compares the SPI for geotextile

and no separation testing. As with the Mexico Clay, the SPI values for the geotextile tests were significantly greater than for the non separated tests, by factors of 10 to 25. Also, geotextile separated soils with cone indices less than 200 performed comparably to non separated soils having cone indices around 500.

6.7 Separation Layer Performance Comparison

In this final analysis section, the performance of each separation method is compared against one another for both soils. Graphs depicting the performance of no separation, geotextile separation, and dense-graded separation methods are presented in Figures 6.57 through 6.67.

6.7.1 Separation Layer Performance with Mexico Clay

A comparison of geotextile separation to no separation performance is shown in Figure 6.57. Without exception, the geotextile was able to keep pumping levels down substantially from the non separated cases. For weaker soils, with cone indices of less than 200, this behavior was even more dramatic. The geotextile reduced pumping by 80% from the non separated cases. Without separation, significantly strong soils with cone indices of 300 or more pumped at comparable levels to geotextile separated soils with cone indices of less than 100. Also shown are test cases with unstabilized clay and geotextile separation. The geotextile prevented unstabilized soils from pumping to the same degree as the non separated stabilized soil cases. Figure 6.58 presents the same information as Figure 6.57 but with the inclusion of the dense-graded separation layer data. Keep in mind direct comparisons cannot be made between the dense-graded separation layer and the other 2 methods due to the different means of measuring intrusion. There was a consistent trend of higher intrusions with the wet CA 6 dense-graded separation than with the dry CA 6 separation, indicating the importance of maintaining material in a dry state for it to perform adequately. However, keeping CA 6 in the dry state in the field is not realistically possible as shown in the AASHTO Road Test. Permanent deformation is presented relative to pumped material in Figure 6.59. There were actually few points with common intrusions to make

comparisons. Overall, the geotextile separated test cases deformed less than the non separated cases. There was about a 50% reduction in deformation on average (80 mils to 40 mils) for the non separated versus geotextile separated cases respectively. For higher degrees of intrusion (which there were none with the geotextile separation and stabilized clay), permanent deformations for the non separated cases were on average almost 10 times greater than the geotextile separated cases. This same data is presented in Figure 6.60 but with the inclusion of the dense-graded separation layer. Though there was significant variability, dense-graded test cases exhibited permanent deformations comparable to non separated cases. Permanent deformations with dense-graded separation layers were typically much higher than the geotextile separated test cases. Figure 6.61 presents how pumped material varied with elastic deflections for all 3 separation methods. Typically, with elastic deflections, significant variability was exhibited. As discussed previously pumping for the non separated cases was higher than for geotextile separated cases for a given elastic deflection. Permanent deformations are related to soil strengths in Figure 6.62. It was very apparent, especially for weaker soils, geotextile separation cases had the lowest amount of permanent deformation under accelerated testing conditions. Typical values of less than 100 mils were seen. For the dense-graded and no separation cases however, deformation values ranged from a low of 100 mils to a high of more than 400 mils. There was also greater variability in the performance of those same 2 methods as well. For soils with cone indices greater than 200, for both the geotextile and the dense-graded separation layers, permanent deformation levels appeared to “level-off” at approximately 80 mils.

6.7.2 Separation Layer Performance with Wisconsin Silty Clay Till

As with Mexico Clay, performance of the separation layers with Wisconsin silty clay till is presented with respect to the 4 methods of analysis. Figure 6.63 shows pumped material versus cone index. Though data is limited, the same trends were found as with the Mexico Clay. For a given soil strength, the amount of pumped material was considerably greater for the no separation and dense-graded separation layer cases than for the geotextile. Figure 6.64 shows permanent deformation related to pumped material. For the silty clay till with the

geotextile separation, significant deformations occurred unlike the Mexico Clay. However, these deformations occurred when the amount of pumped material was substantially higher than ever seen with the Mexico Clay. The same data is again presented in Figure 6.65 but with the inclusion of the dense-graded separation layer. The wet dense-graded separation layer yielded significant pumped material and the amount of permanent deformation was comparable with weak soils underlying geotextiles with no separation. Figure 6.66 presents pumped material versus elastic deformations. Typical variations were observed with these tests and no definite trends were seen other than less pumping for the geotextile separation test cases. Permanent deformation is compared to cone index in Figure 6.67. As with the Mexico Clay, at cone indices above 200, permanent deformations stabilized for all 3 separation types. For the weaker soils, all 3 methods showed comparable permanent deformations. Much of the poor performance of the geotextile separation in these tests can also be partially attributed to the silty nature of this soil and the general poor performance of geotextiles with silty soils. Many civil engineering projects have encountered failures when geotextiles were used in conjunction with highly mobile silts. This material responded well to lime stabilization by gaining strength. Its strength gain was through a small yet very active of clay mineral fraction. There remained a large fraction of silty particles available for migration through the geotextile.

6.8 Applicability of Test Results to Field Performance and Use of Index Test

6.8.1 Test Overview

The purpose of this testing was to determine soil strength parameters for use with separation layers and open-graded drainage layers. To facilitate this testing, increased loading stress levels were used. To make these test results correspond to actual field loading, additional testing was performed at more realistic field loading levels.

One important relationship in this research was the significant weakening of both the soil and dense graded separation layers with increasing water contents and levels of saturation. While not revolutionary, the testing performed here has put quantitative values on the performance of saturated materials.

The index test proposed relates field dry strengths to accelerated testing performance. To start, correlate wet and dry soil specimen strengths in the laboratory with the cone penetrometer. Test the wet specimens under accelerated conditions to verify long term performance with the given separation layer type. With the dry strength to wet performance correlation known, field verification can easily be completed. This is done by comparing the dry field soil cone index with the laboratory wet soil cone index. The acceptable wet soil cone index is based upon accelerated laboratory performance testing. If the dry soil from the field is not as strong as required by laboratory testing, poor field performance may result. If the required dry strengths are not reached in the field, separation layer and soil strength properties need to be modified to meet required standards.

6.8.2 *Test Procedure*

The procedure begins with the preparation of 8 in. (200 mm) diameter by 4 in. (100 mm) high cylindrical specimens at optimum moisture and maximum dry density from the lime modified field site soil. This procedure is depicted in Figure 6.68. Cure and vacuum saturate enough specimens to test a small factorial of separation layers with this soil. After vacuum saturation, place the specimens in confining rings and test them with a hand held cone penetrometer. This gives a relationship between wet and dry soil strength. Next, test the wet specimens under accelerated loading to evaluate the performance of various separation layers with these wet soil specimens. Determine the minimum specimen strength criteria required for adequate performance based upon accelerated testing performance. Take dry field cone indices and compare them to the required dry strength from laboratory testing. Decide if additional strength or different separation requirements are needed.

Table 6.1: Performance Evaluation Parameters

Plot	Function
Pumping/Intrusion vs. Cone Index	Relates degree of material movement to underlying soil strength. Expect lower degrees of movement for stronger soils with perhaps a strength threshold above which pumping stops.
Permanent Deflection vs. Pumping/Intrusion	Relates level of consolidation of layers to degree of material movement. Two parameters are directly related in that material movement between layers results in lowering of overall layer thicknesses. With dense separation and no separation a merging of layers occurs.
Pumping/Intrusion vs. Elastic Deflection	Relates degree of material movement to resilient behavior of loaded system. Expect higher elastic deformations to result in higher material movements.
Permanent Deflection vs. Cone Index	Relates consolidation of layered system to underlying soil strength. Expect higher deflections with lower strength materials due to intermixing of layers and pumping of soil.
Pumping/Intrusion vs. "Energy"	Relates degree of material movement to total applied energy to loaded system. Higher imparted energy ideally results in larger pumping values.
Elastic Deflection vs. Cone Index	Relates resilient behavior of loaded system to underlying soil strength. Higher elastic deflections should occur with softer materials.

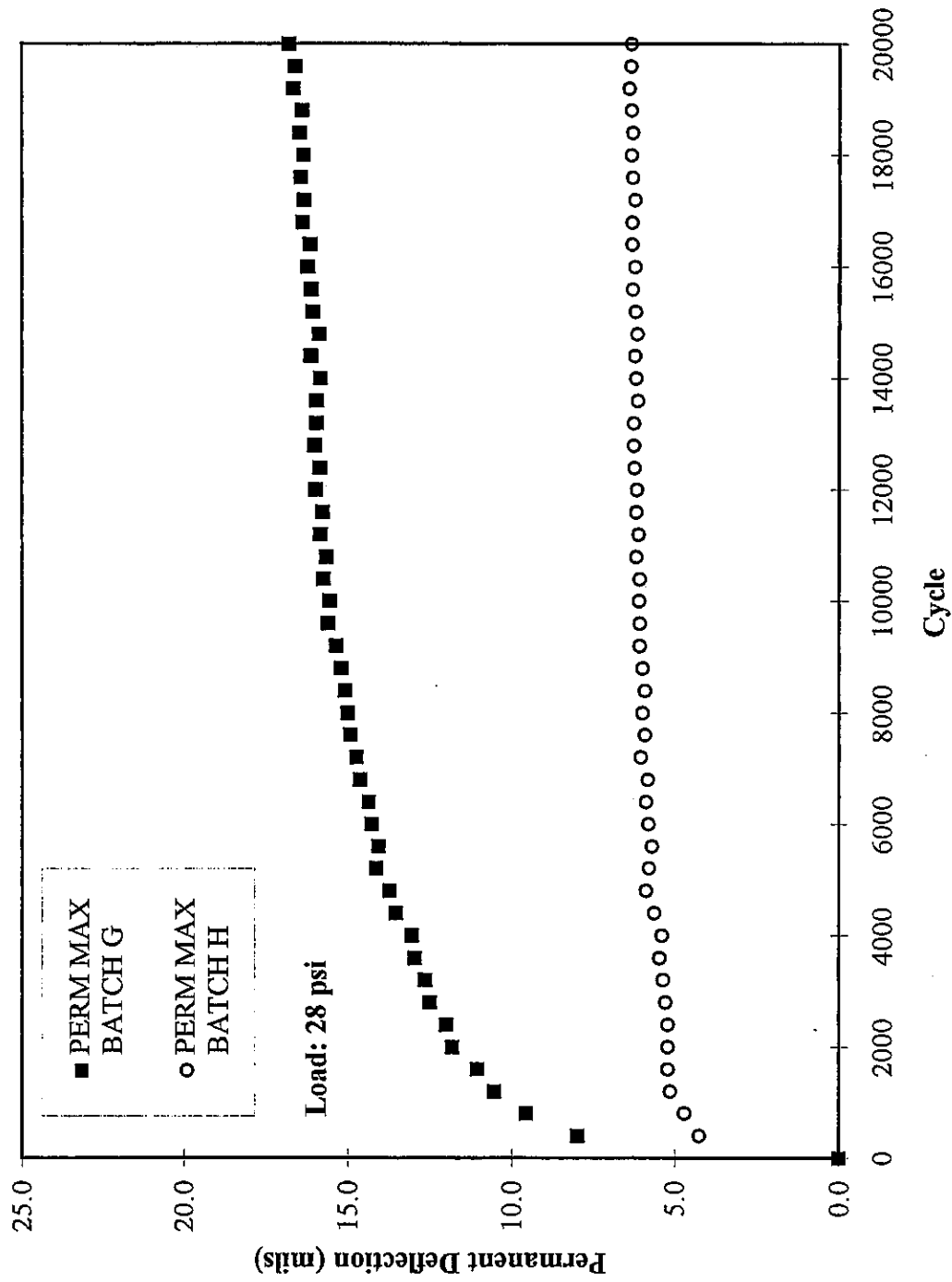


Figure 6.1: CA 7 Aggregate Batches G H, Permanent Deformation vs Load Cycle

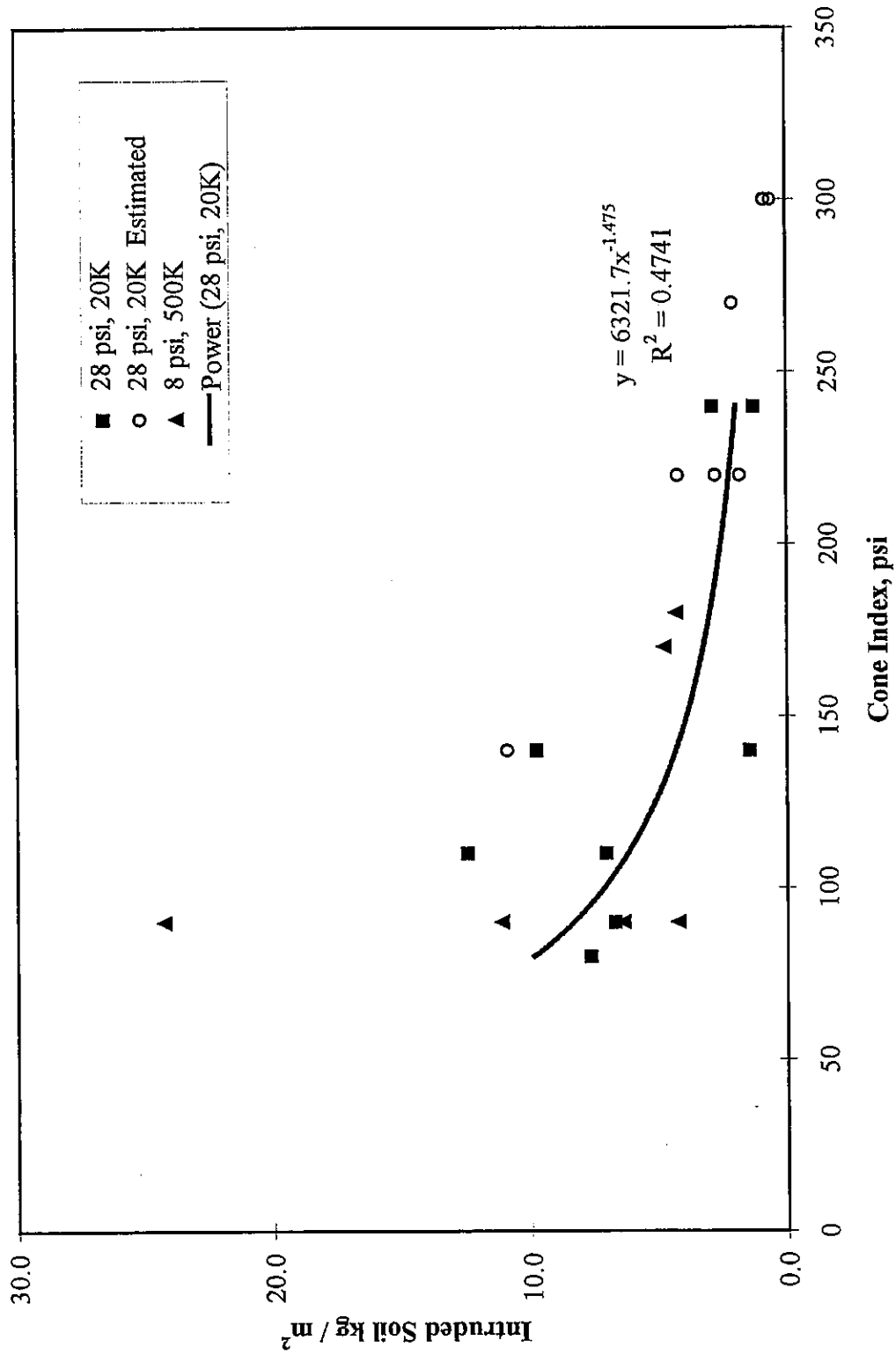


Figure 6.2: Mexico Clay / No Separation / CA 7, Intruded Soil vs Cone Index

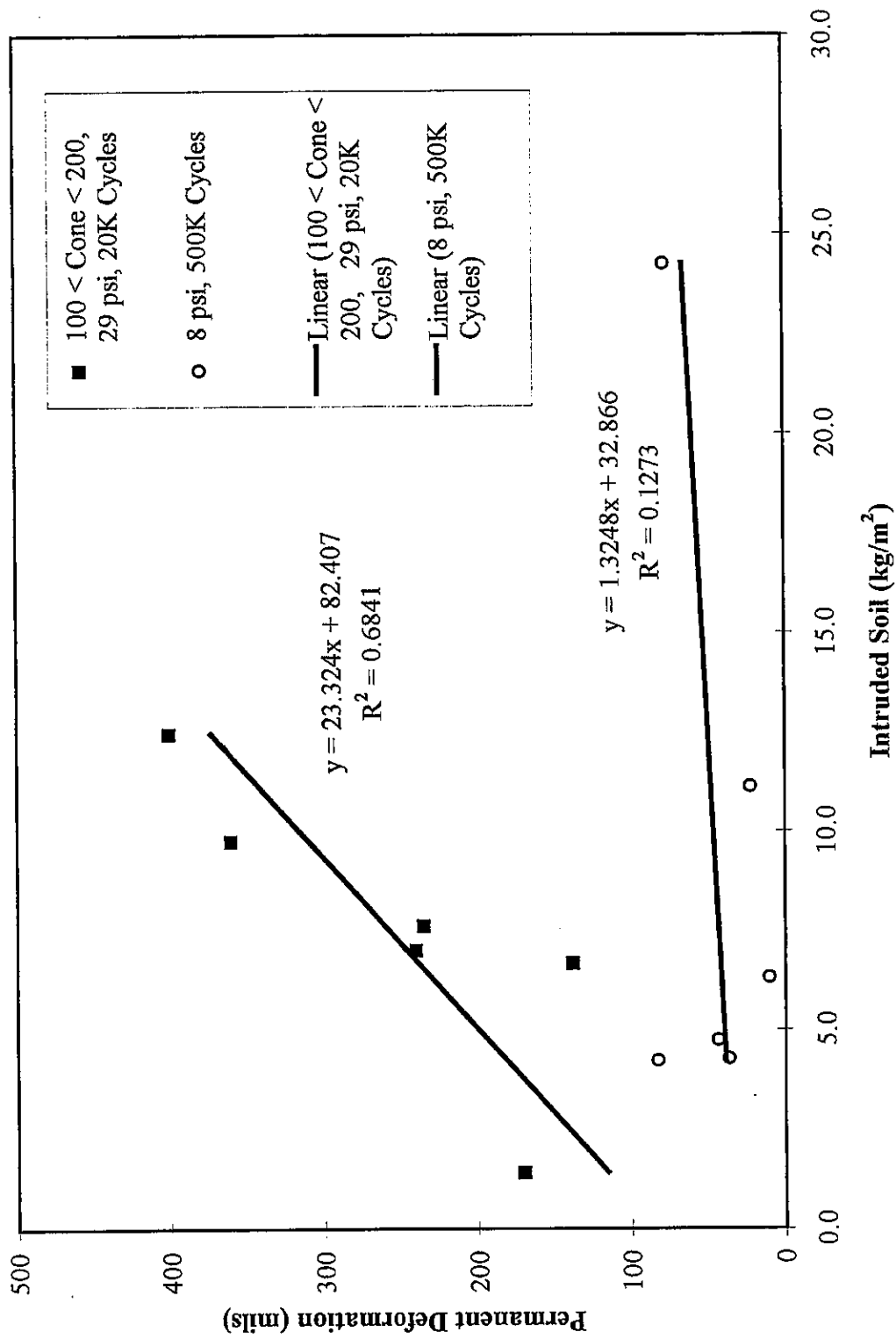


Figure 6.3: Mexico Clay / No Separation / CA 7, Permanent Deformation vs Intruded Soil

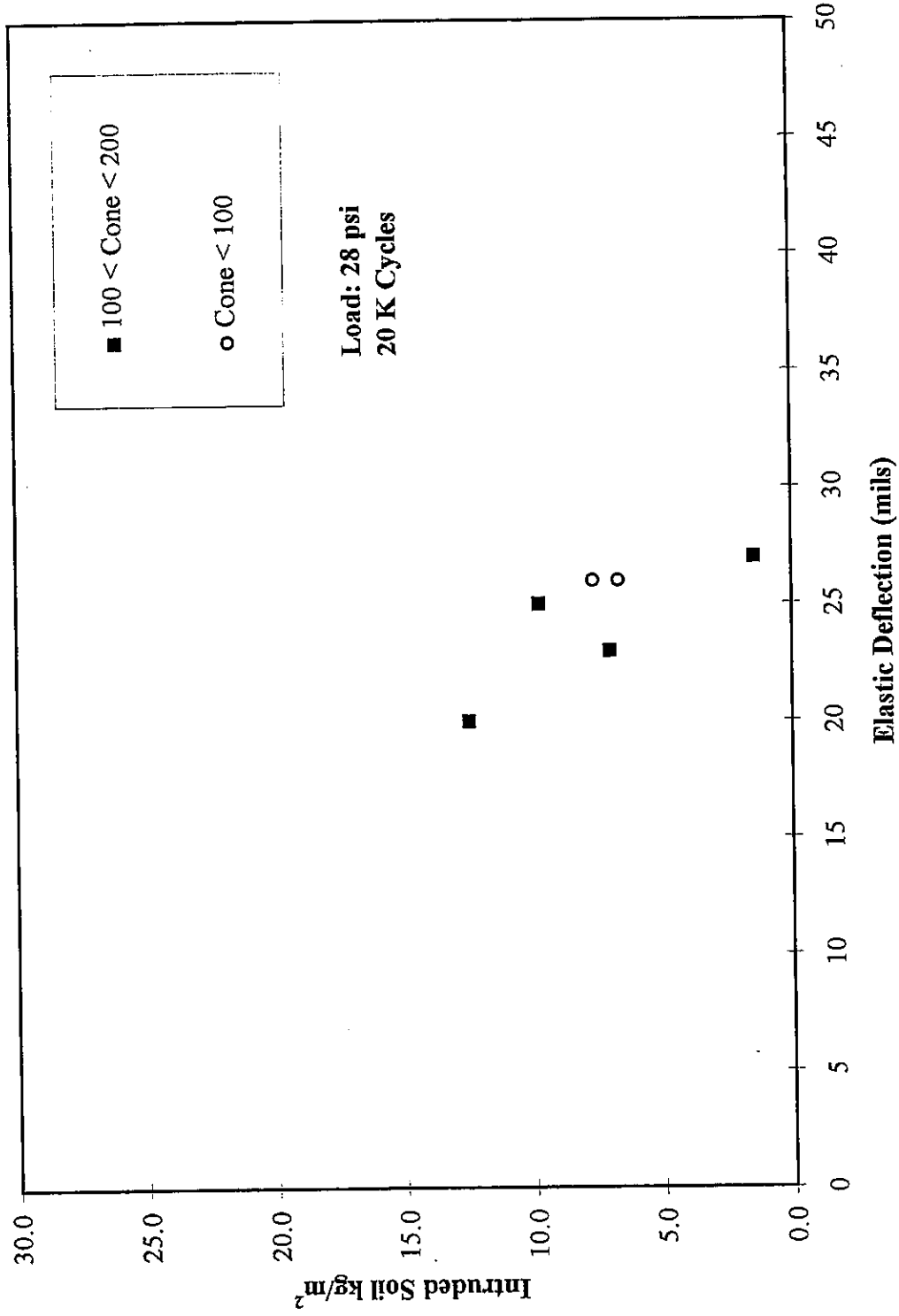


Figure 6.4: Mexico Clay / No Separation / CA 7, Intruded Soil vs Elastic Deflection

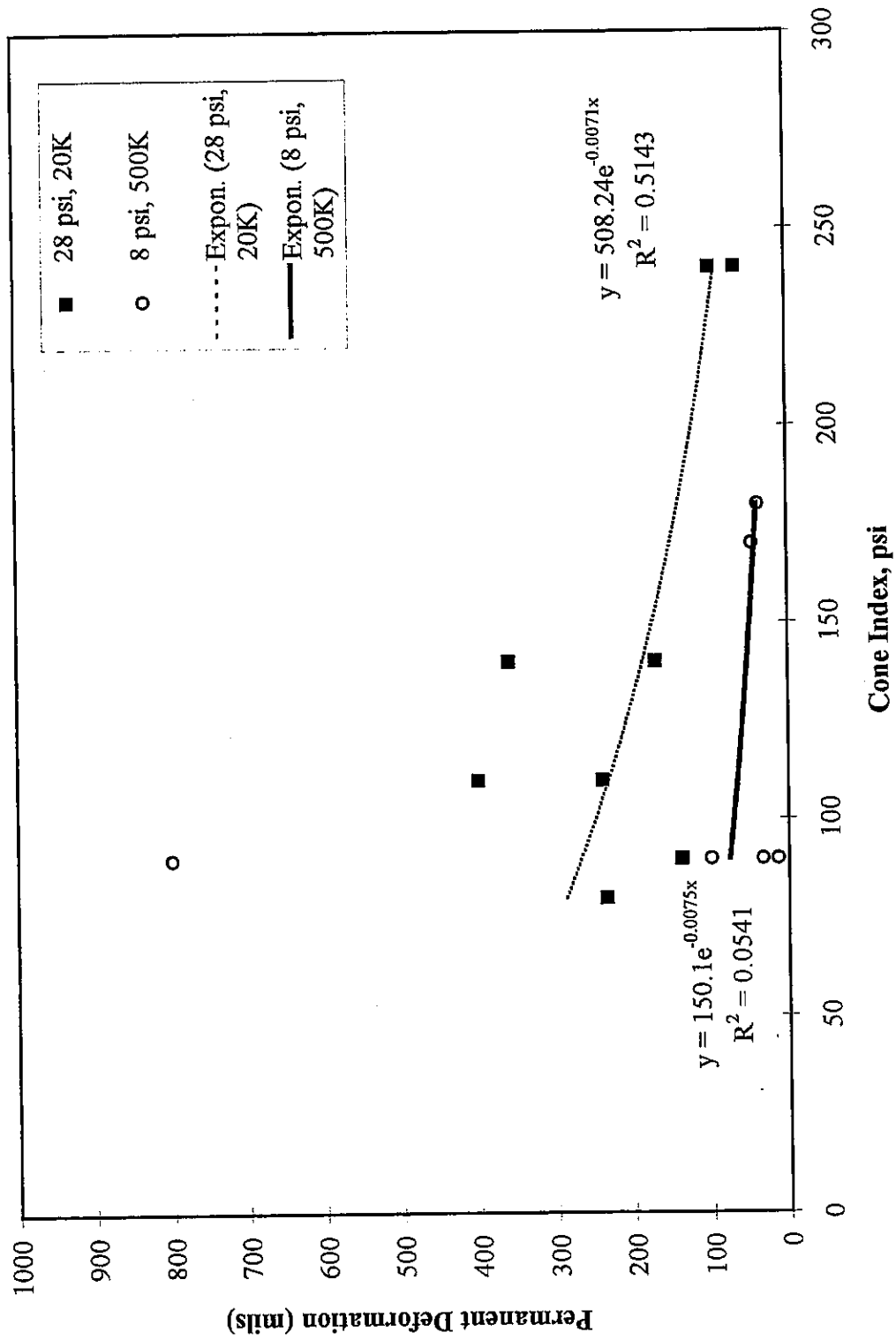


Figure 6.5: Mexico Clay / No Separation / CA 7, Permanent Deformation vs Cone Index

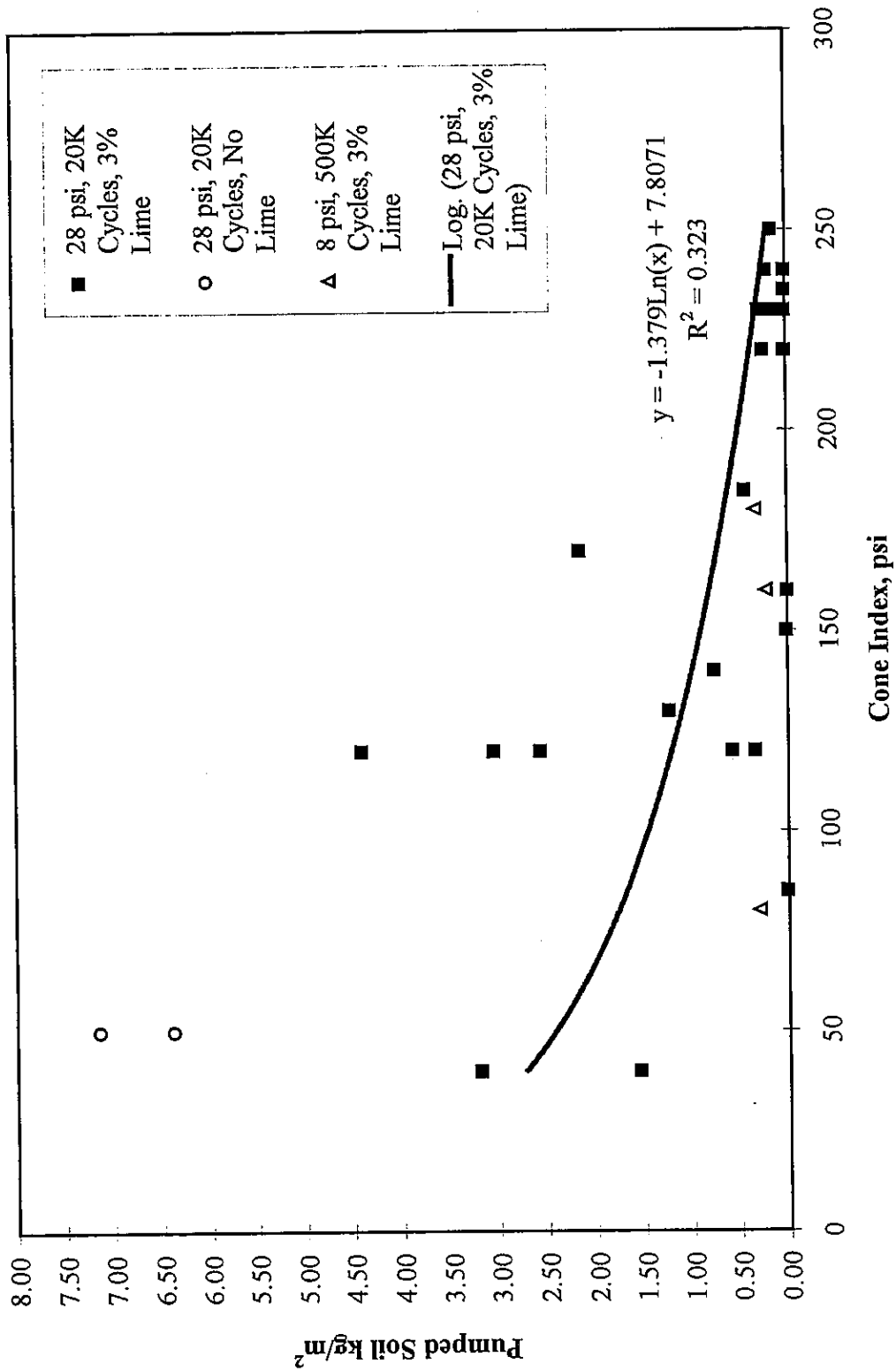


Figure 6.6: Mexico Clay / 1101 Geotextile / CA 7, Pumped Soil vs Cone Index

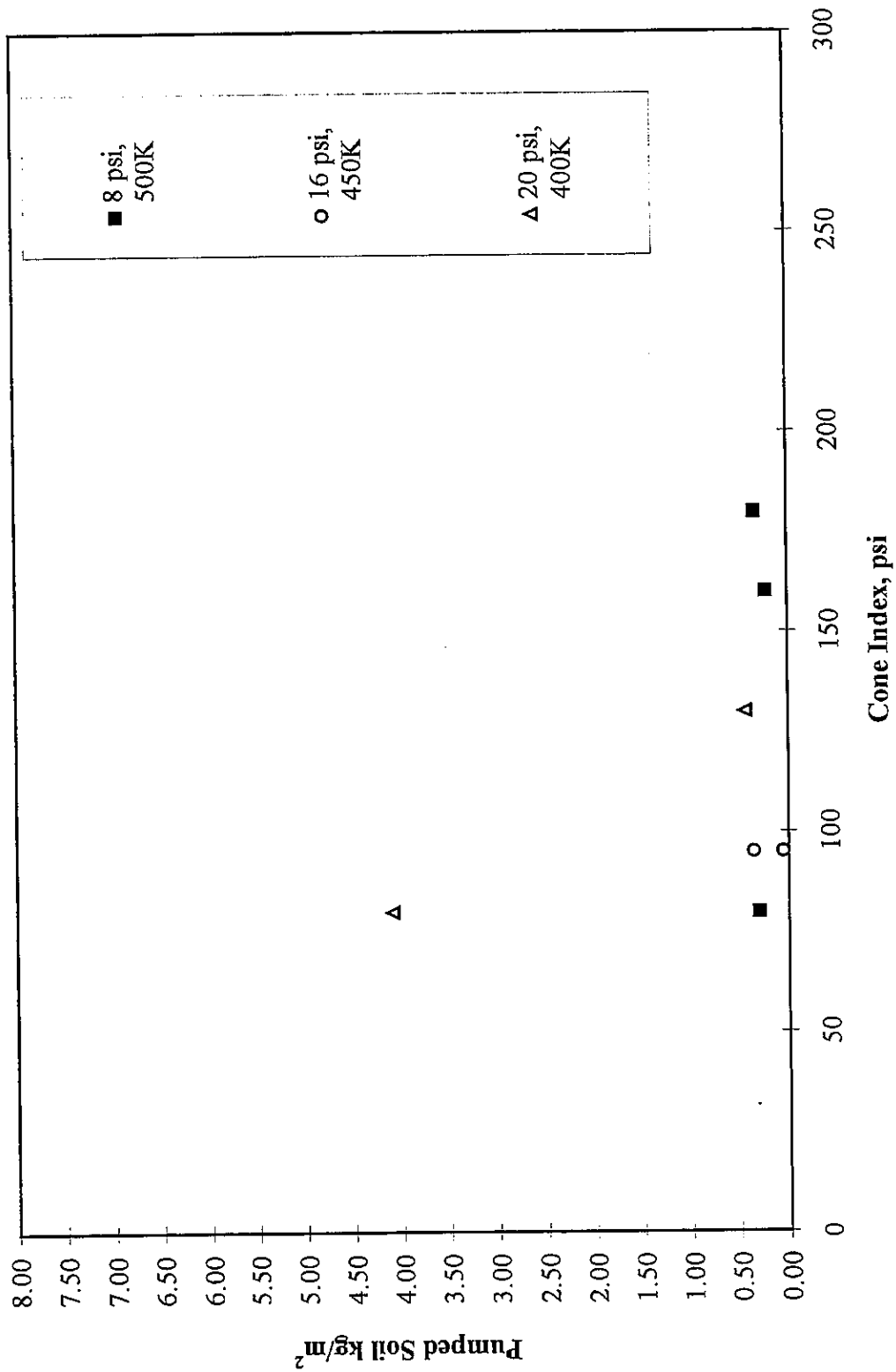


Figure 6.7: Mexico Clay / 1101 Geotextile / CA 7, Pumped Soil vs Cone Index, Long Term

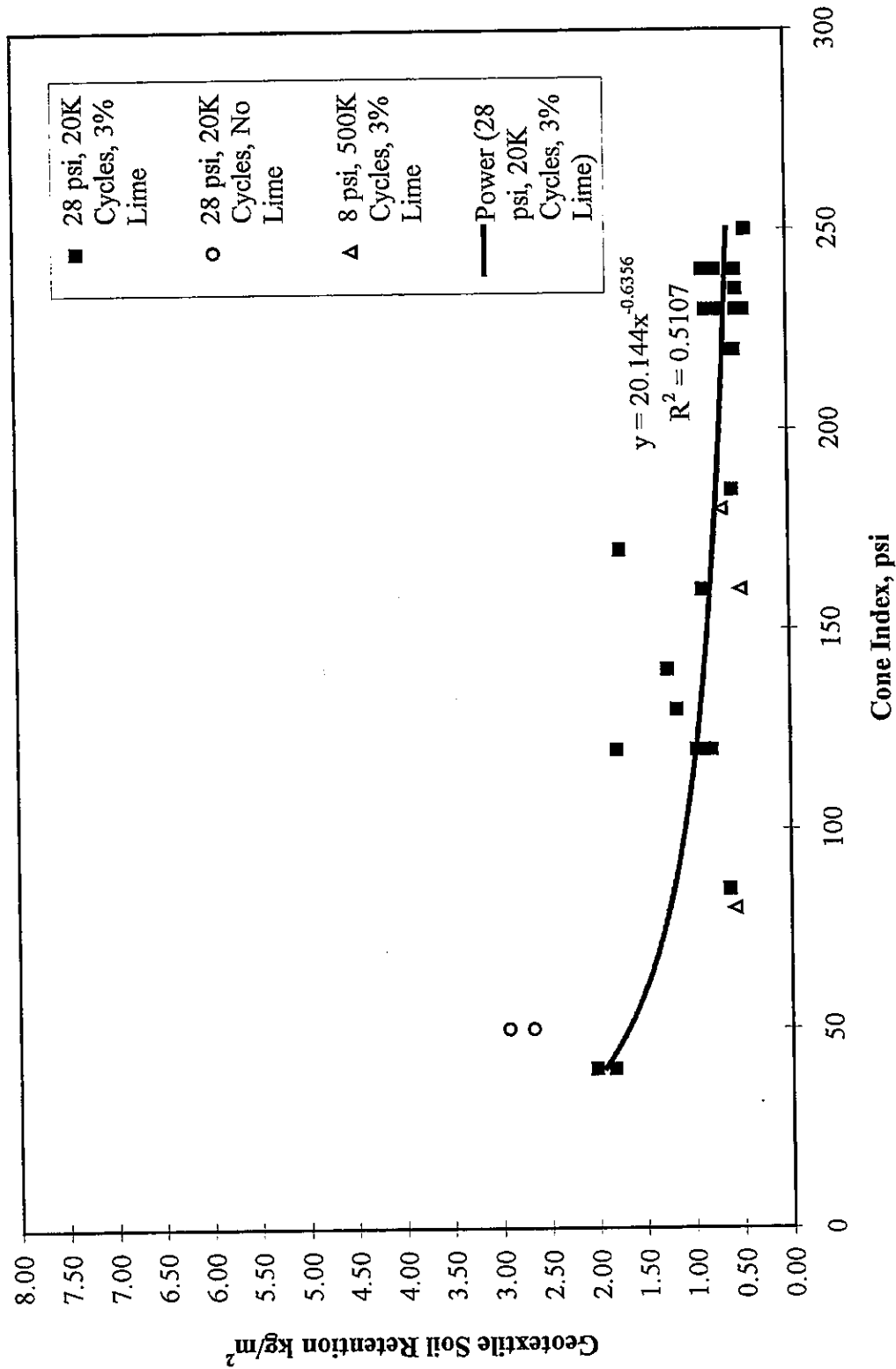


Figure 6.8: Mexico Clay / 1101 Geotextile / CA 7, Geotextile Soil Retention

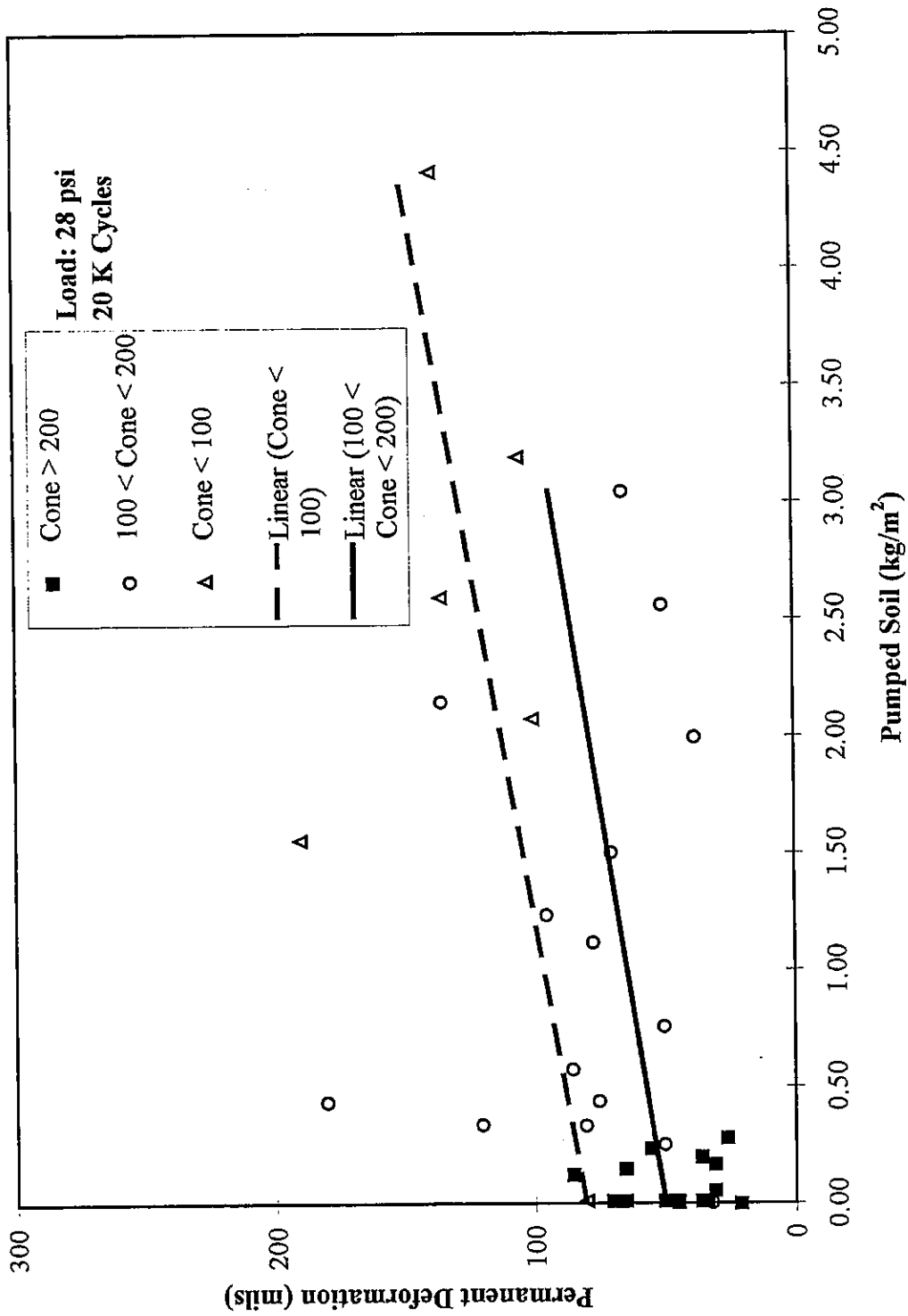


Figure 6.9: Mexico Clay / 1101 Geotextile / CA 7, Permanent Deformation vs Pumped Soil

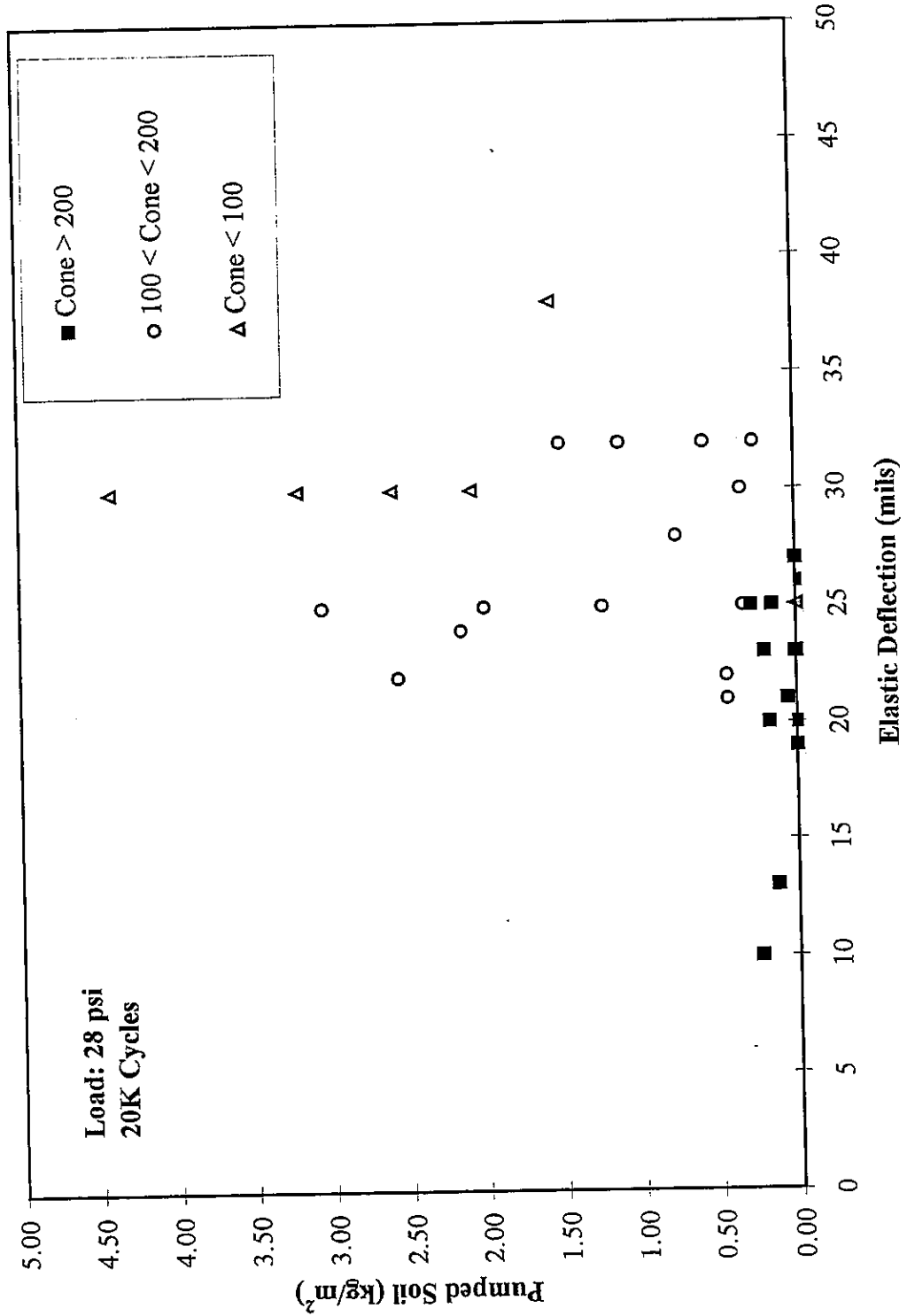


Figure 6.10: Mexico Clay / 1101 Geotextile / CA 7, Pumped Soil vs Elastic Deflection

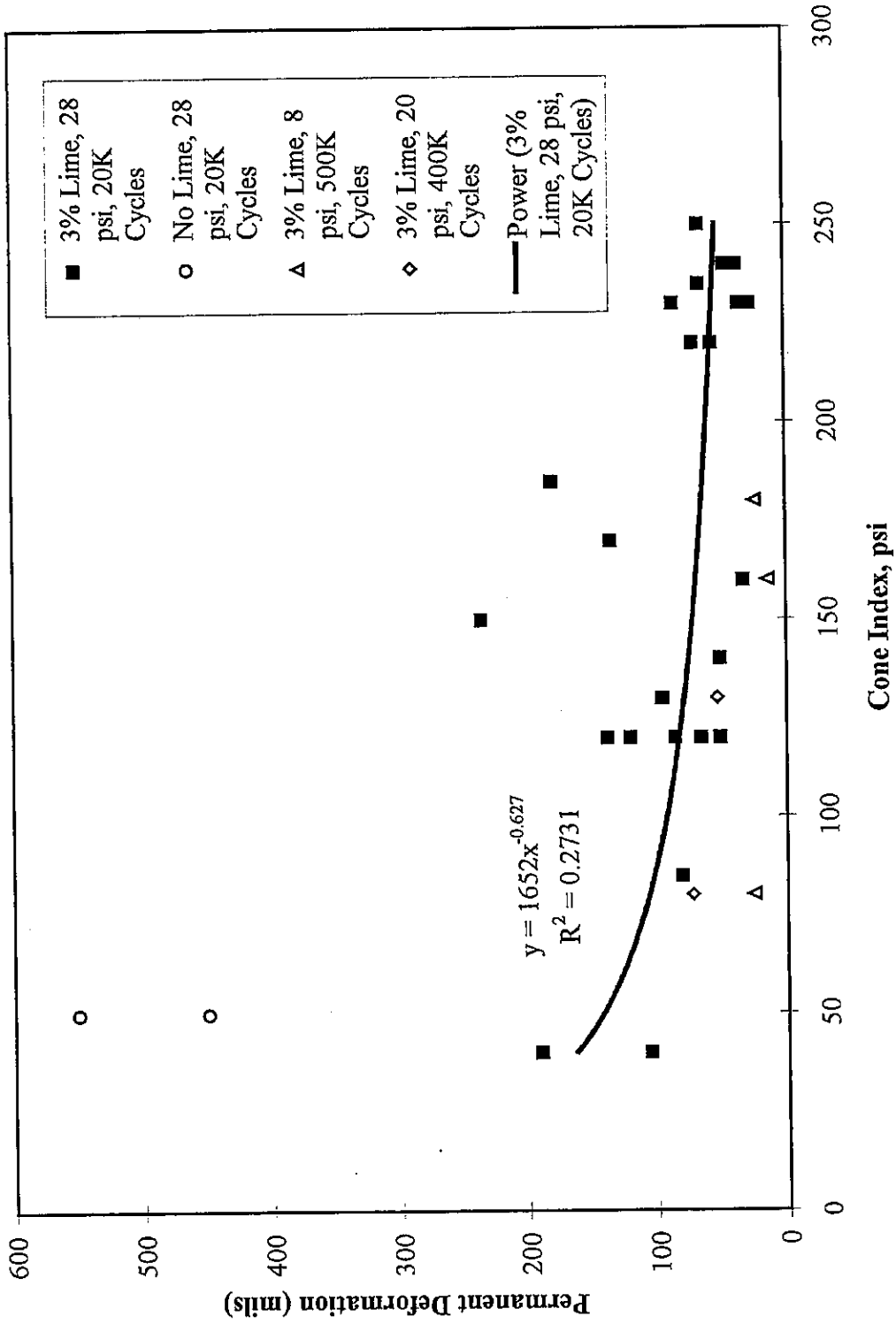


Figure 6.11: Mexico Clay /1101 Geotextile / CA 7, Permanent Deformation vs Cone Index



Figure 6.12: 1101 Geotextile with Pumped Mexico Clay - Post Test

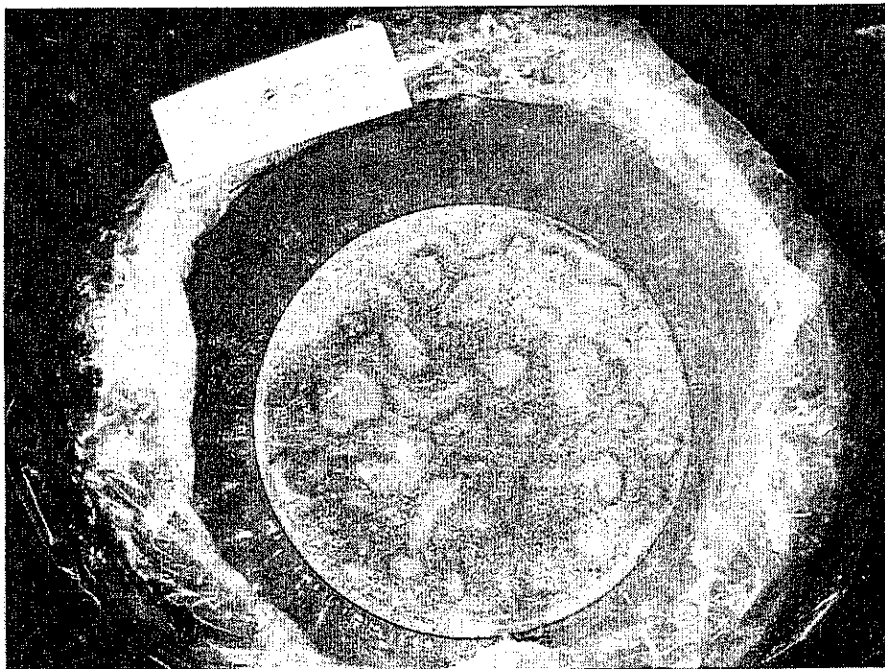


Figure 6.13: Mexico Clay Specimen Surface Underlying 1101 Geotextile - Post Test

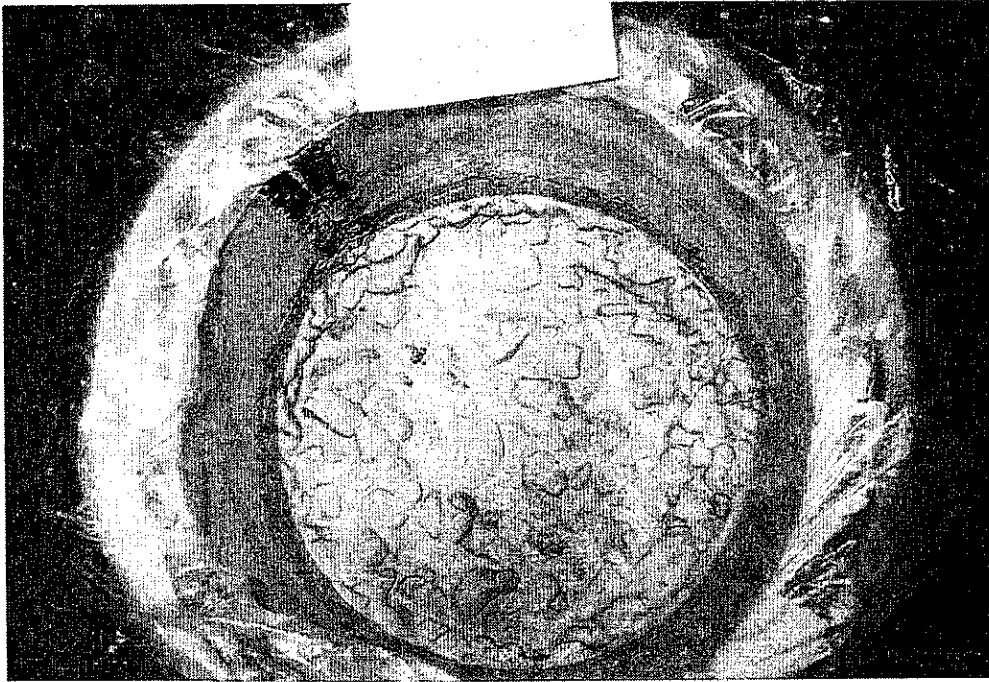


Figure 6.14: Mexico Clay Pumped into 1101 Geotextile and CA 7 - Post Test

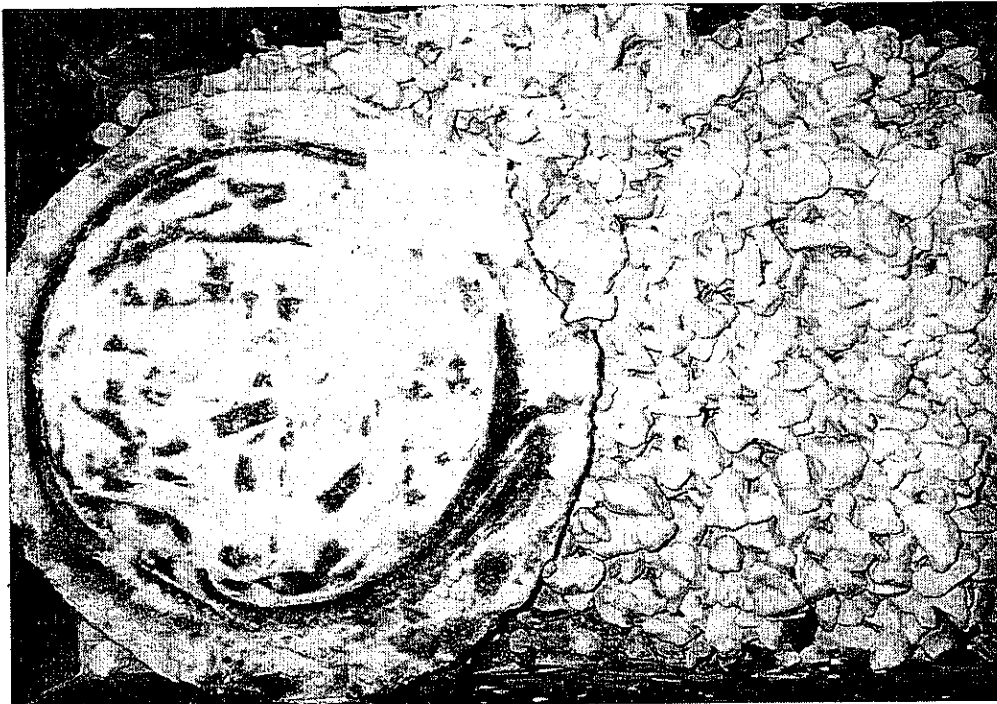


Figure 6.15: Mexico Clay Slurry Coating 1101 Geotextile and CA 7 - Post Test

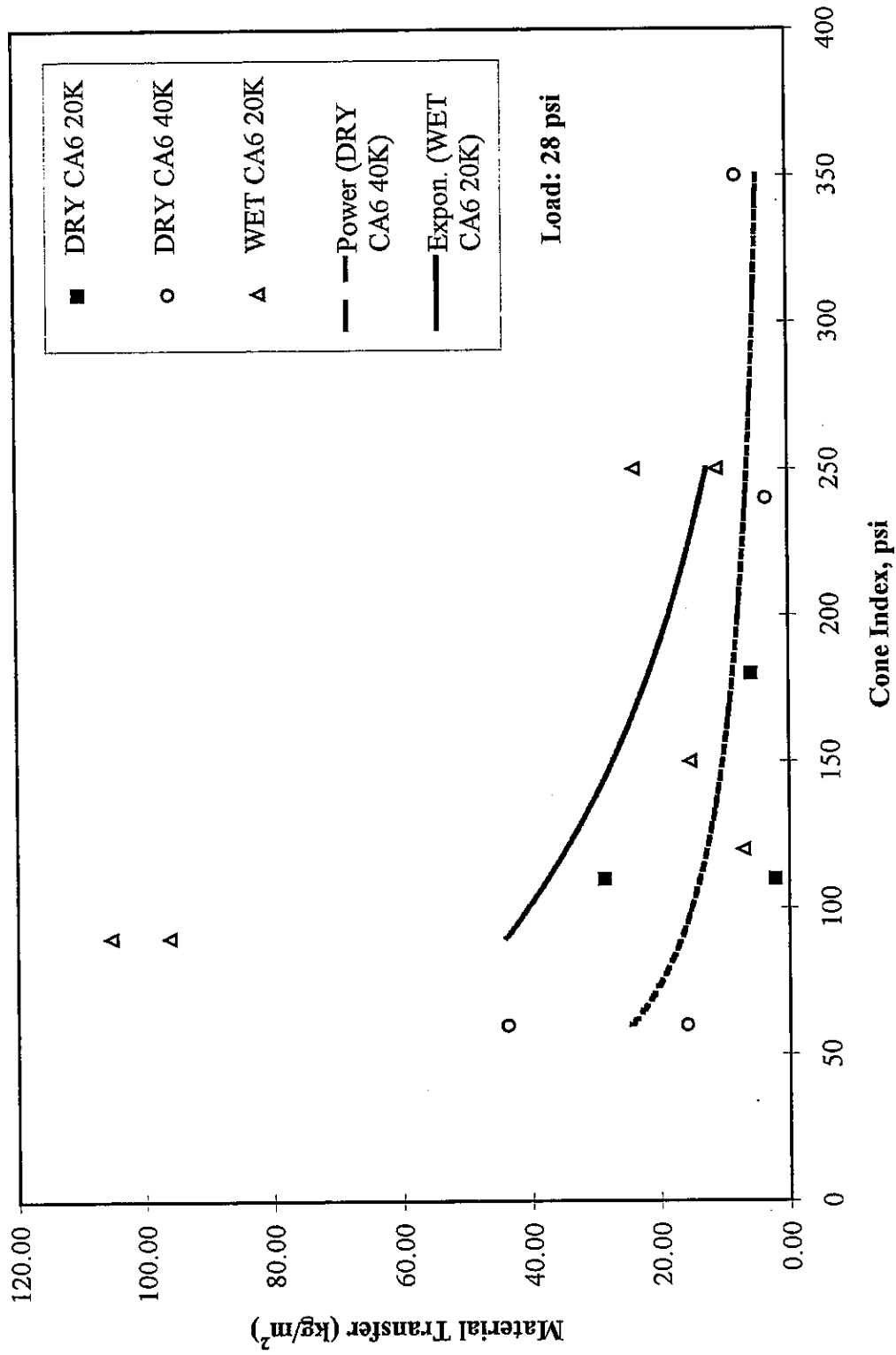


Figure 6.16: Mexico Clay / CA 6 / CA 7, Material Transfer vs Cone Index

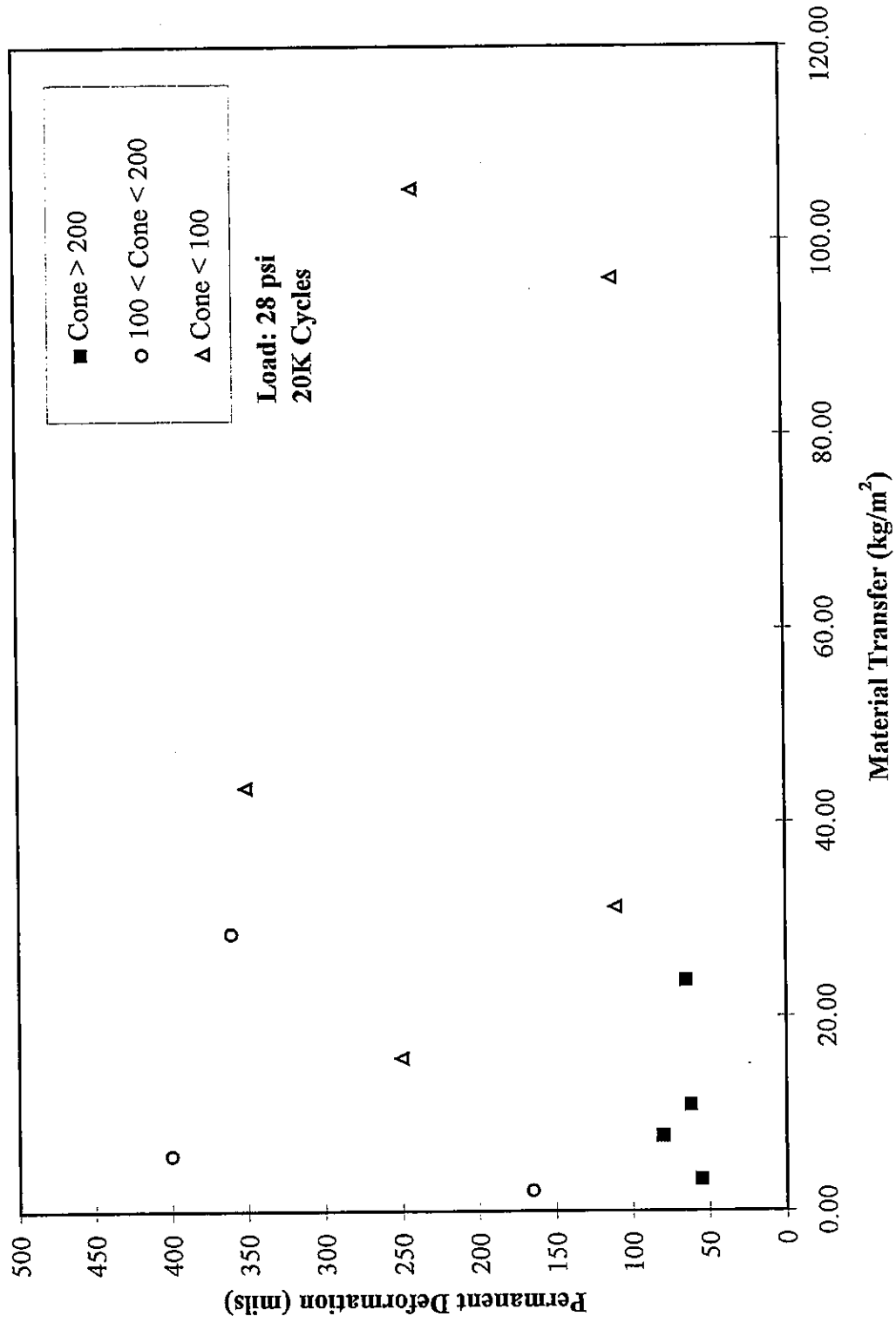


Figure 6.17: Mexico Clay / CA 6 / CA 7, Permanent Deformation vs Material Transfer

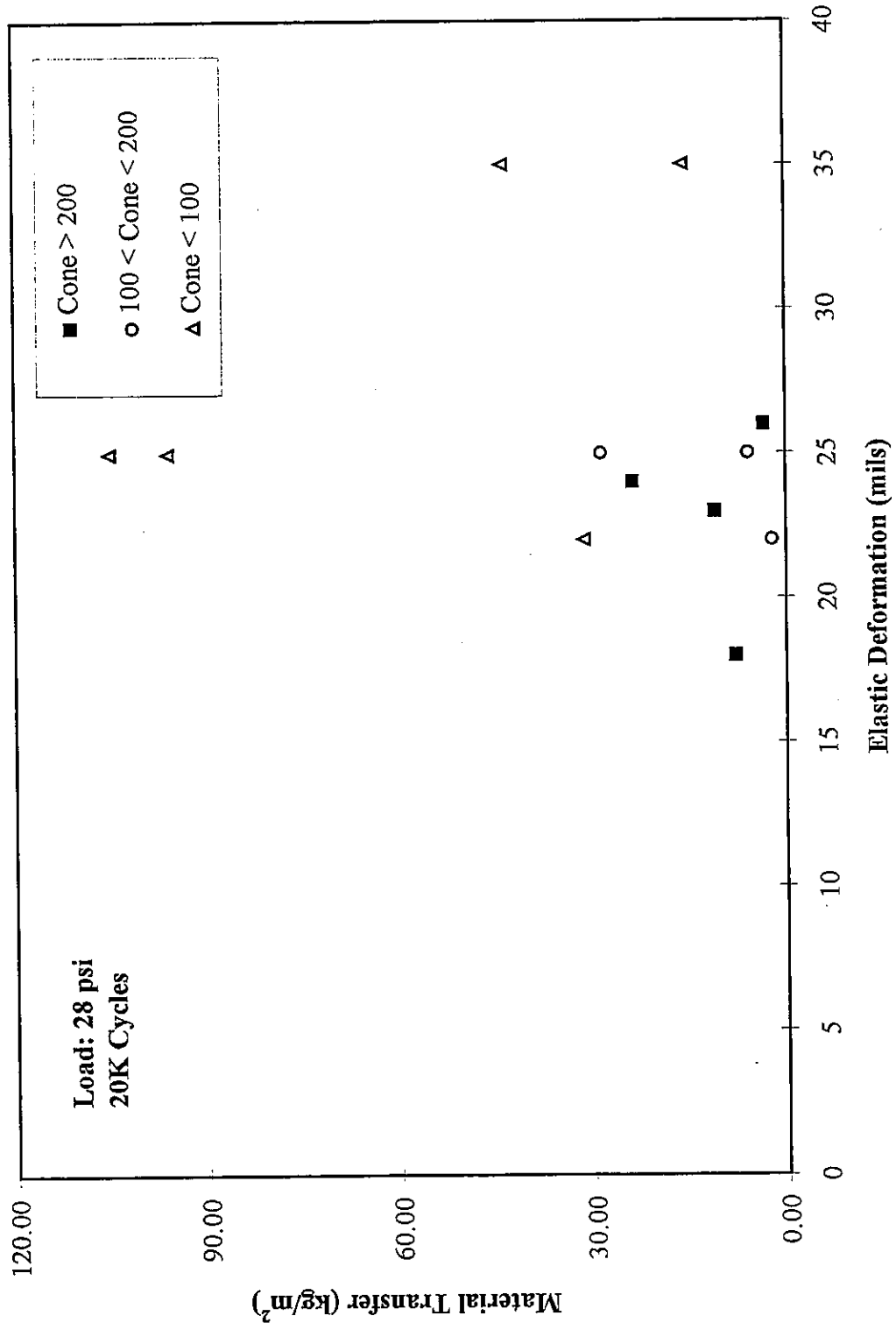


Figure 6.18: Mexico Clay / CA 6 / CA 7, Material Transfer vs Elastic Deflection

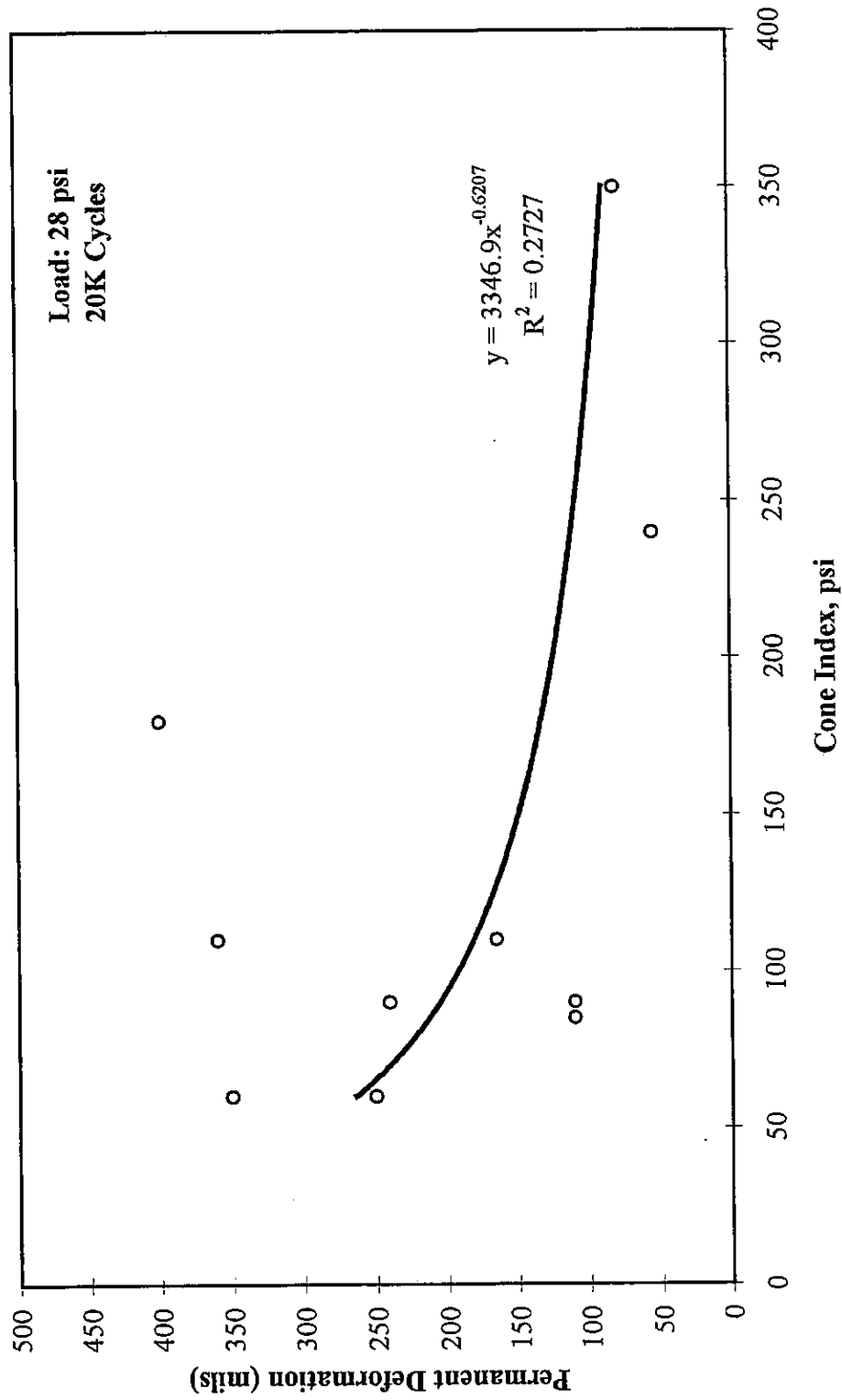


Figure 6.19: Mexico Clay / CA 6 / CA 7, Permanent Deformation vs Cone Index

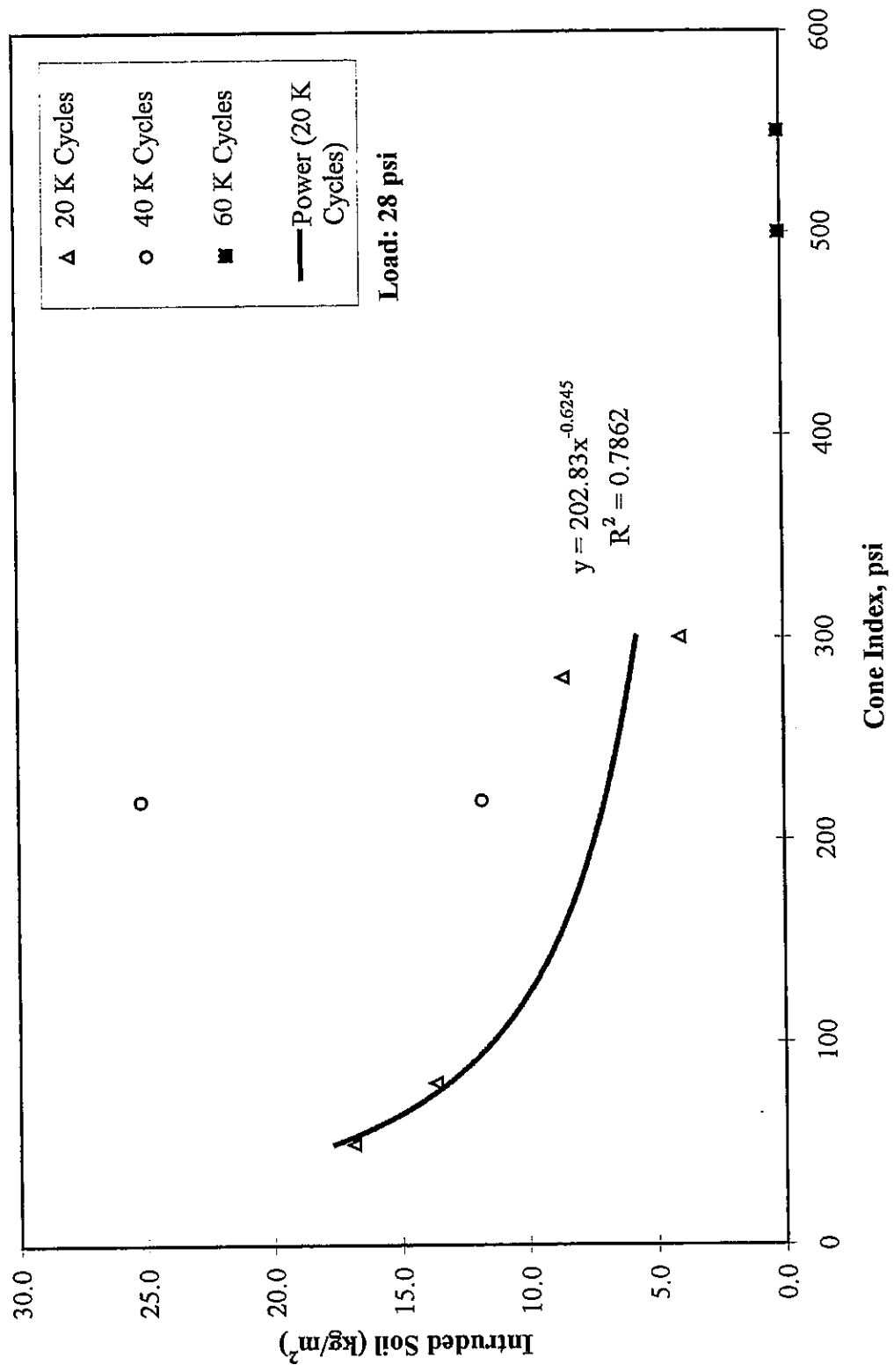


Figure 6.20: Wisconsinan Silty Clay Till / No Separation / CA 7, Intruded Soil vs Cone Index

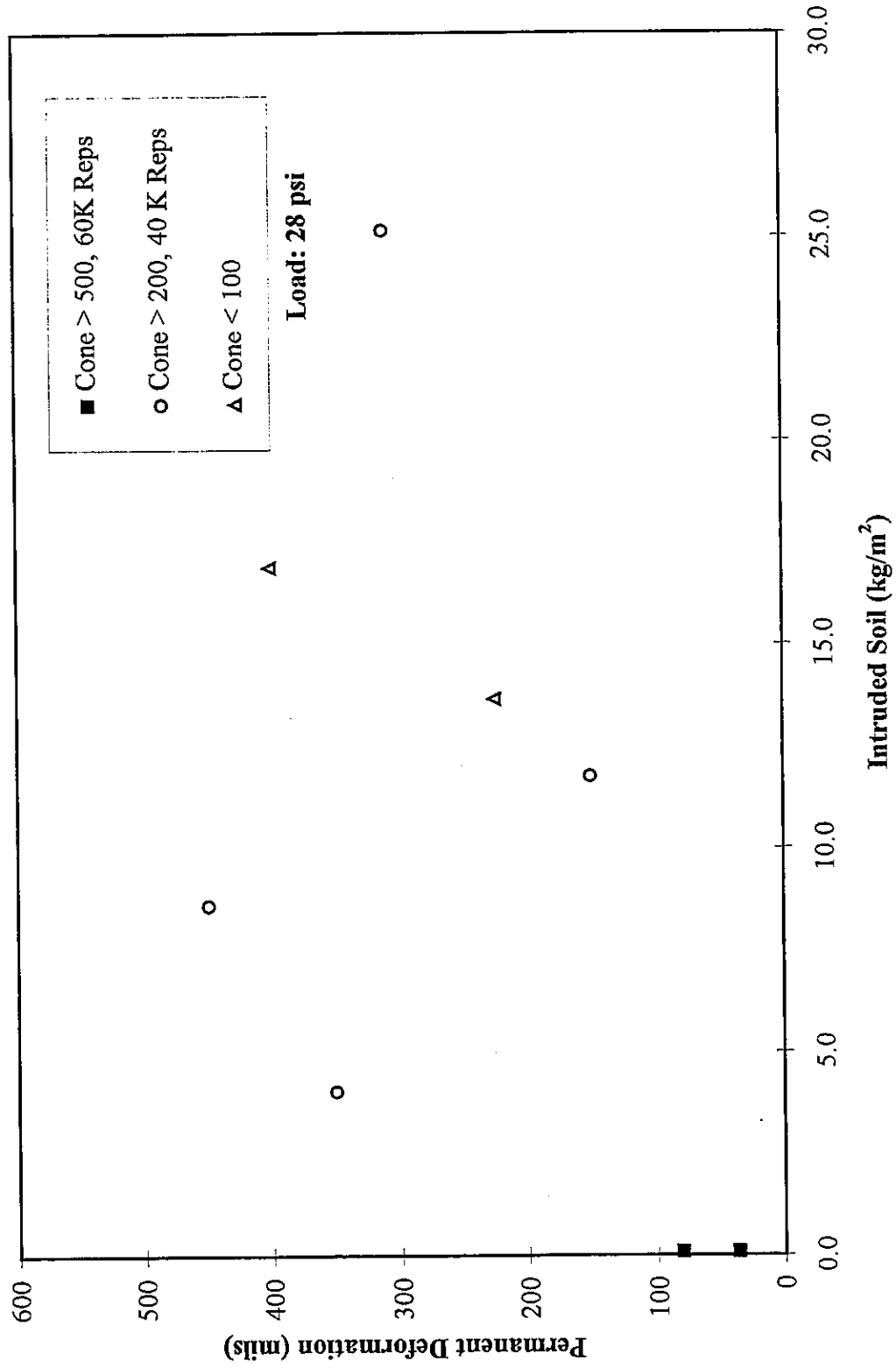


Figure 6.21: Wisconsin Silty Clay Till / No Separation / CA 7, Permanent Deformation vs Intruded Soil

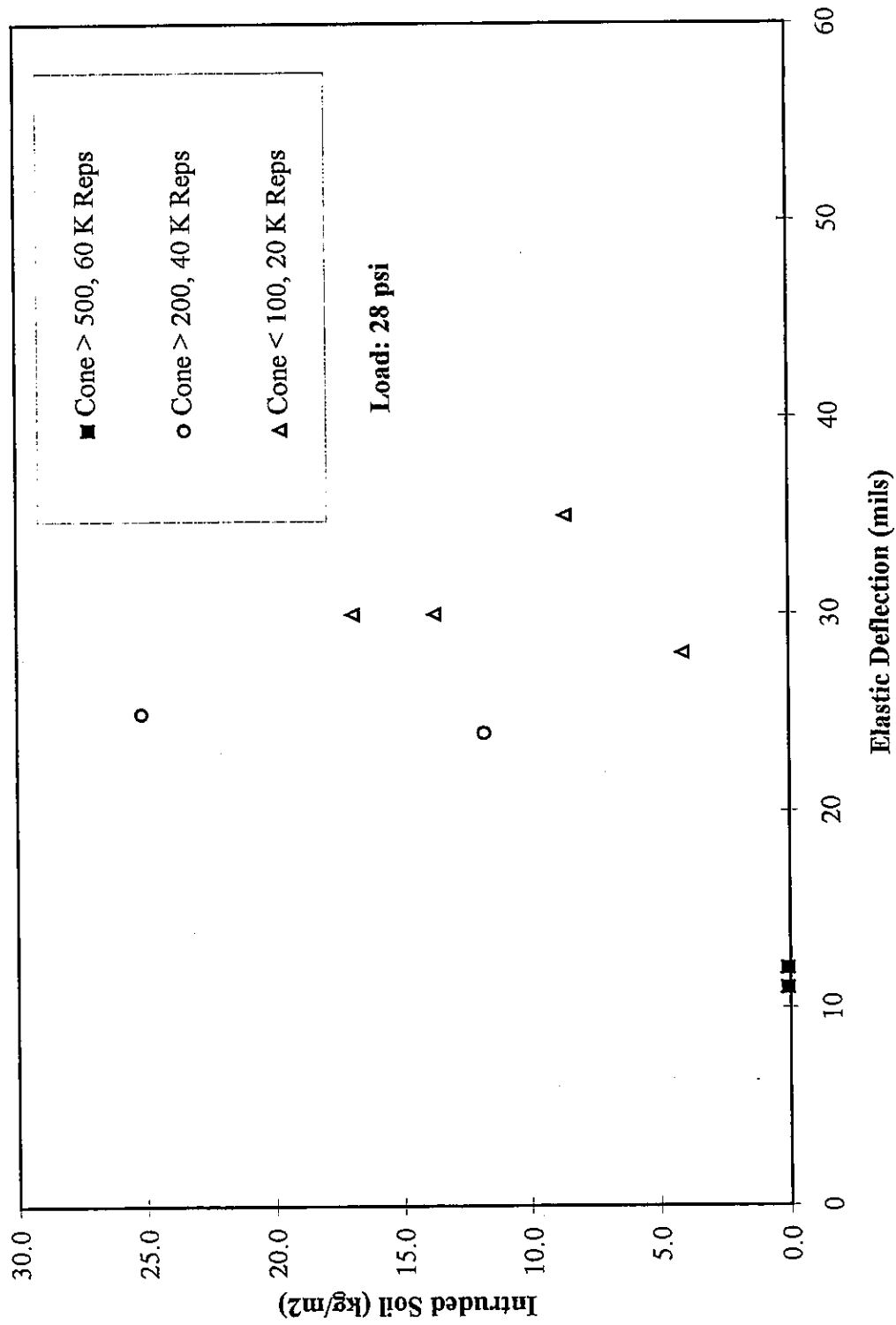


Figure 6.22: Wisconsinan Silty Clay Till / No Separation / CA 7, Intruded Soil vs Elastic Deflection

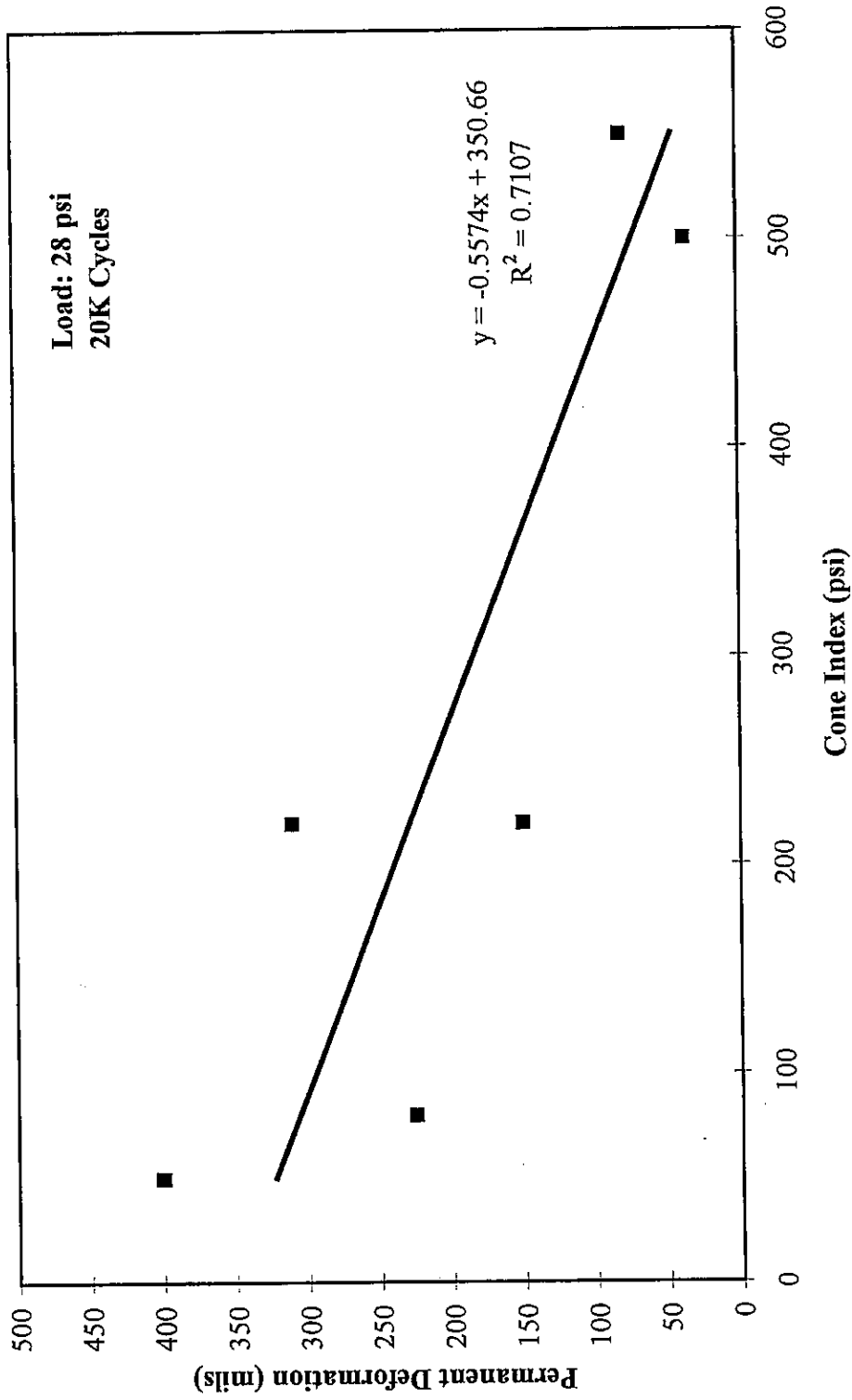


Figure 6.23: Wisconsin Silty Clay Till / No Separation / CA 7, Permanent Deformation vs Cone Index

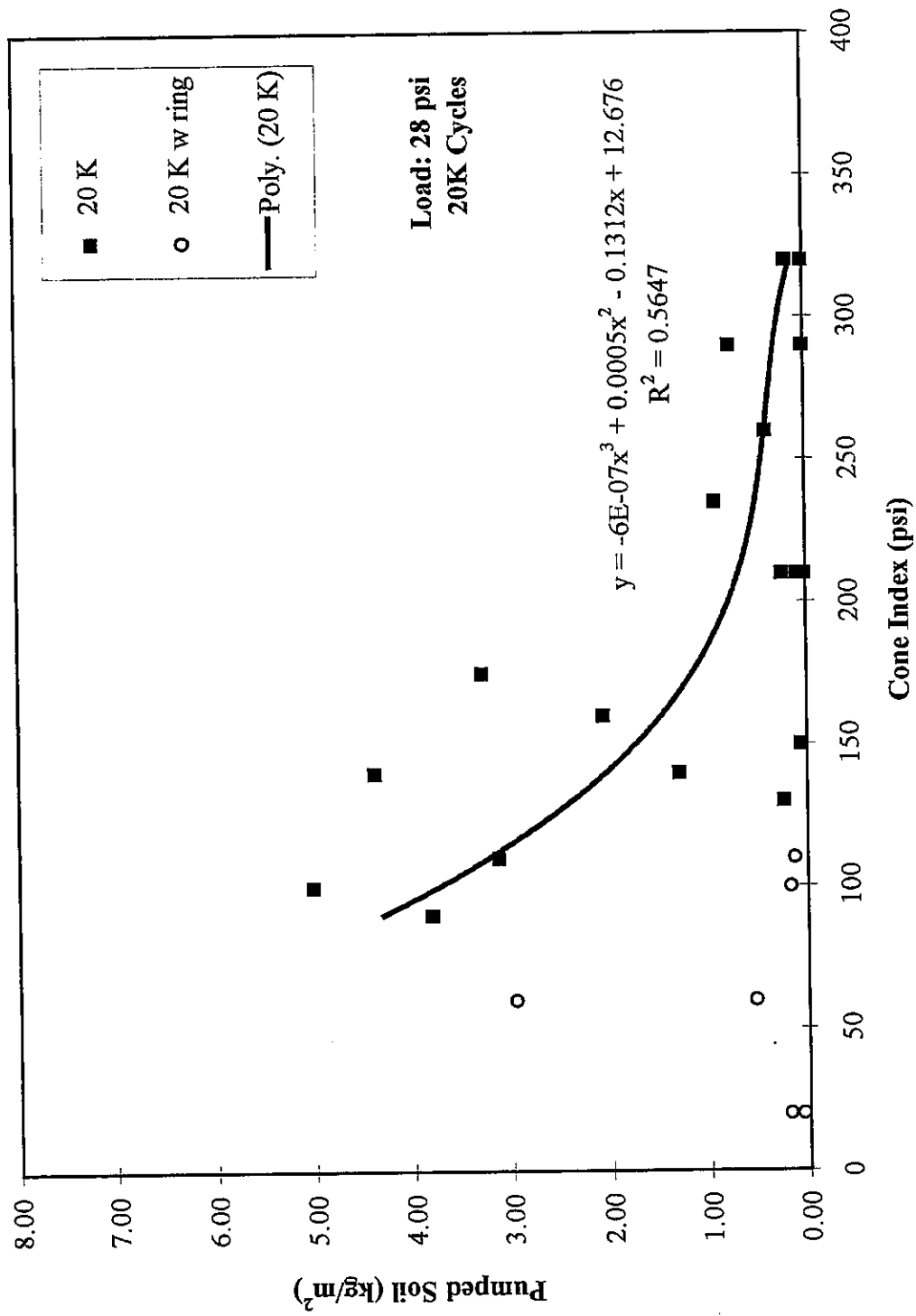


Figure 6.24: Wisconsinan Silty Clay Till / 1101 Geotextile / CA 7, Pumped Soil vs Cone Index

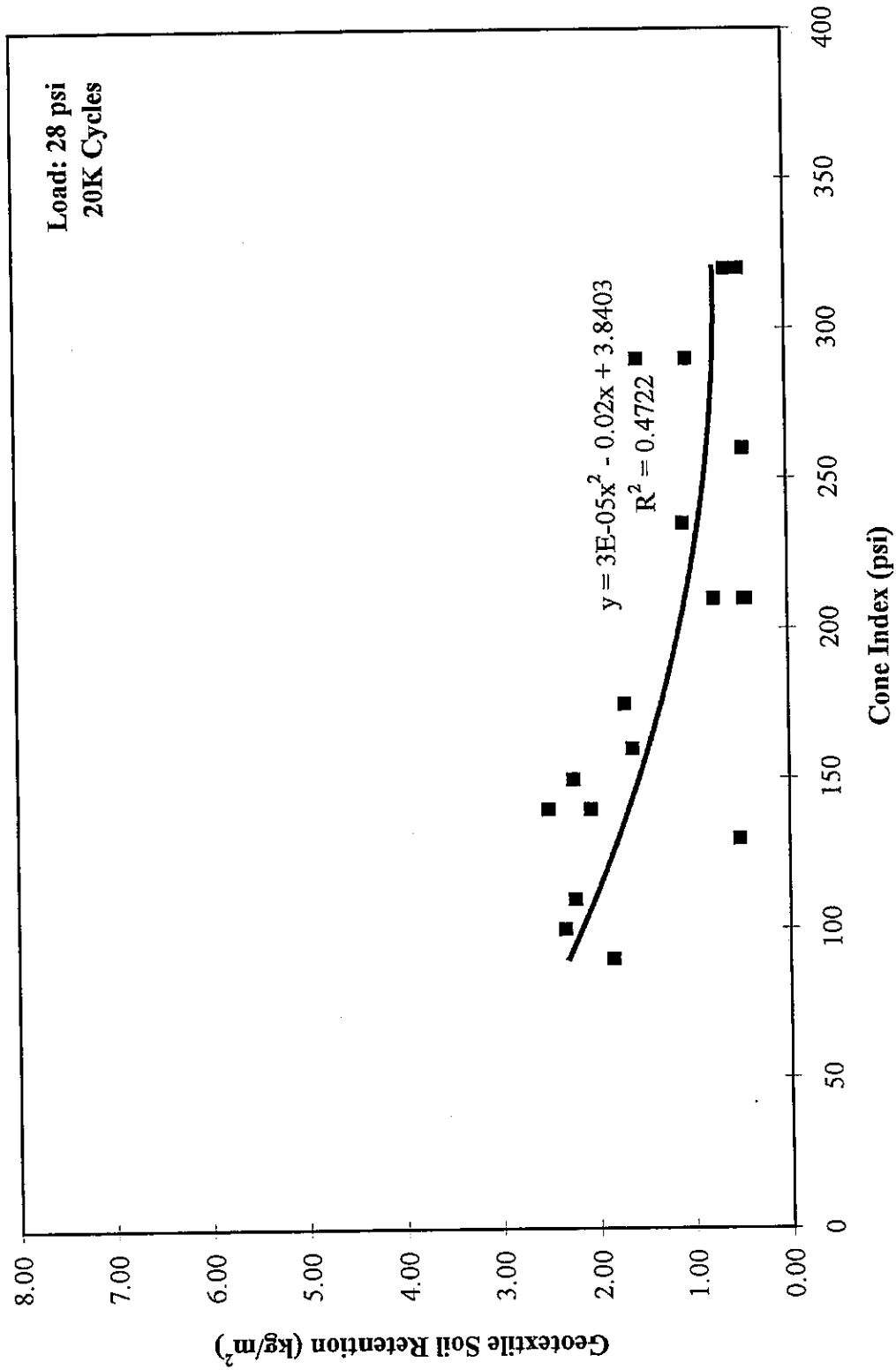


Figure 6.25: Wisconsinan Silty Clay Till / 1101 Geotextile / CA 7, Geotextile Soil Retention vs Cone Index

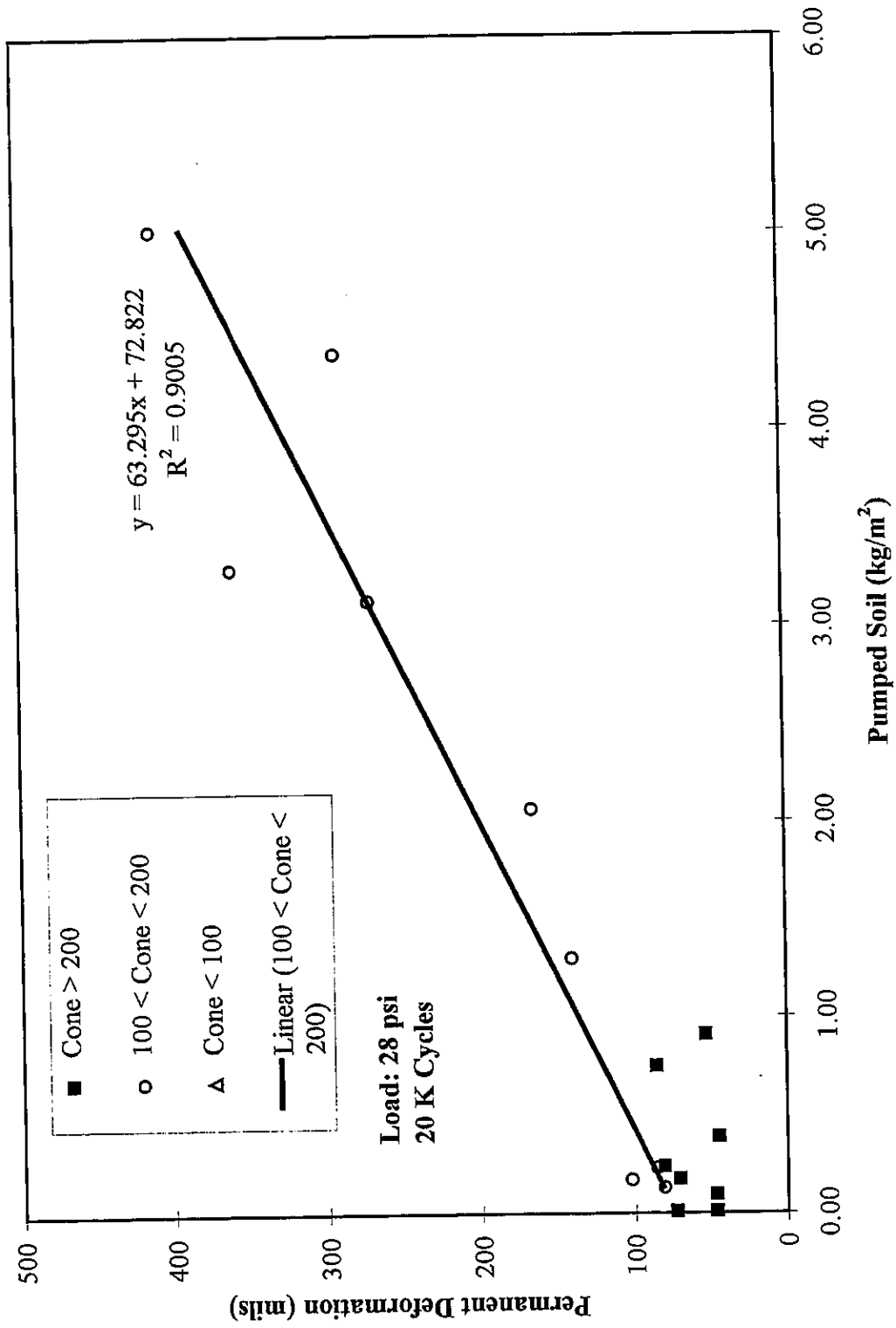


Figure 6.26: Wisconsin Silty Clay Till / 1101 Geotextile / CA 7, Permanent Deformation vs Pumped Soil

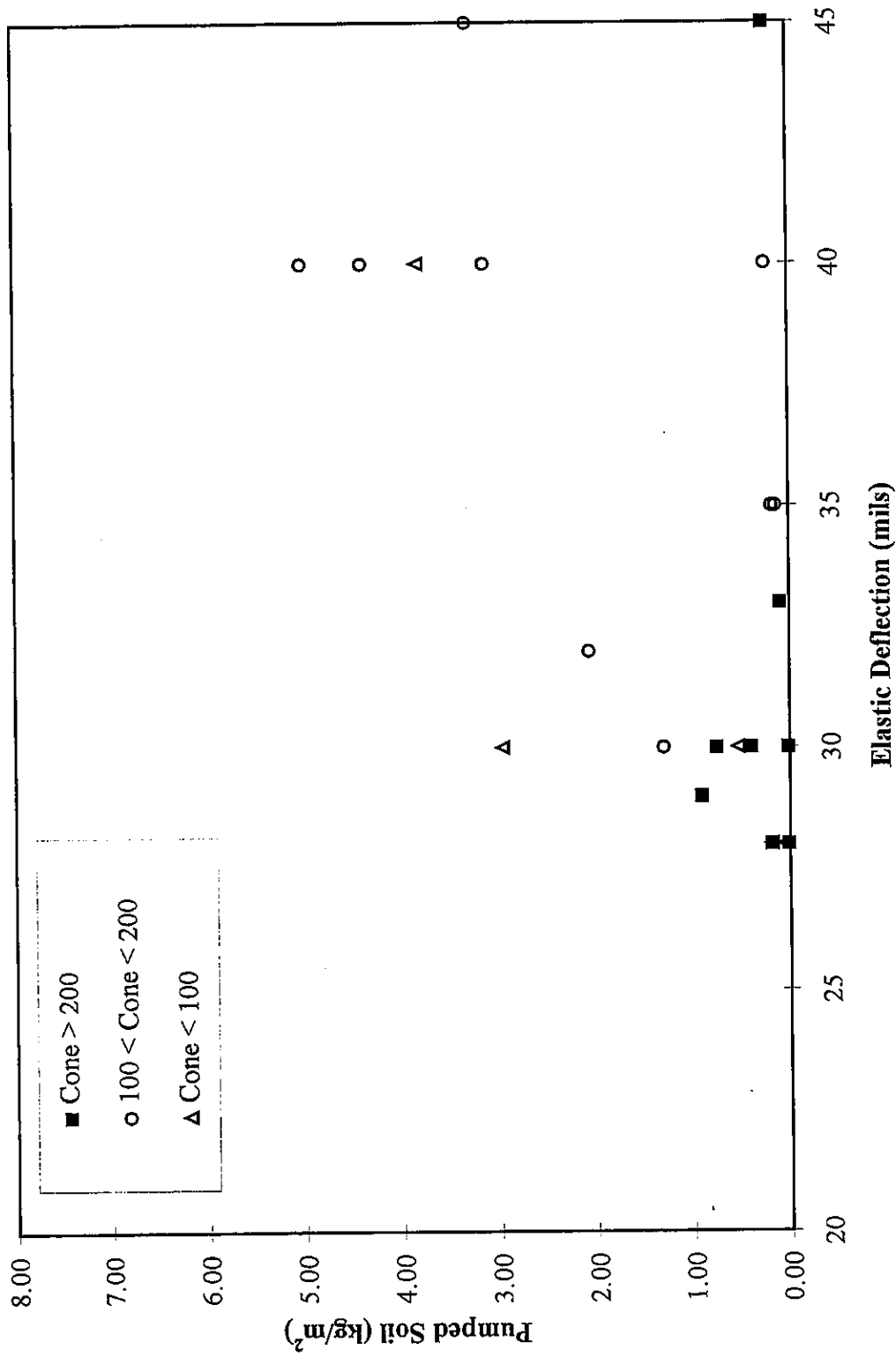


Figure 6.27: Wisconsinan Silty Clay Till / 1101 Geotextile / CA 7, Pumped Soil vs Elastic Deflection

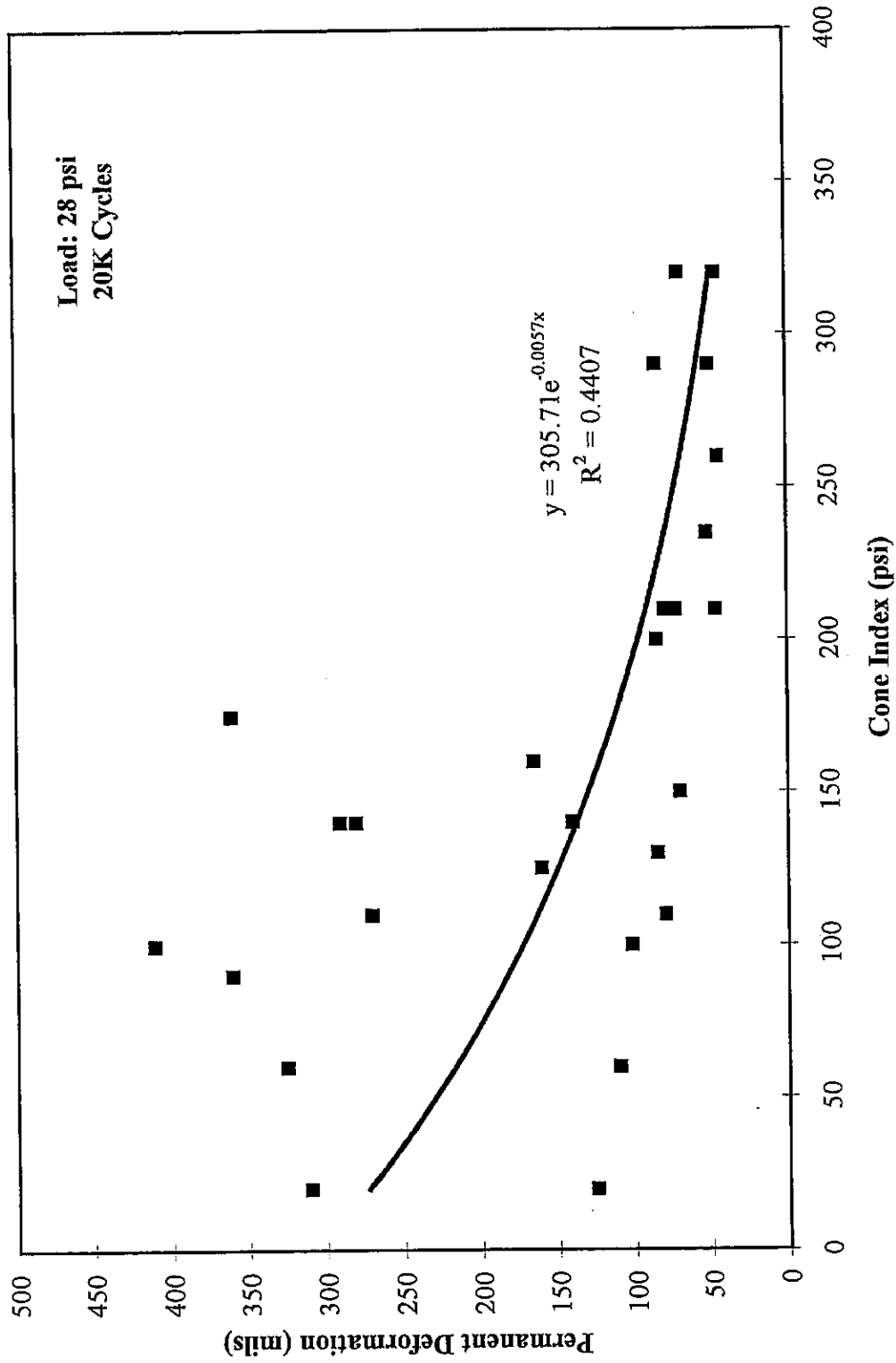


Figure 6.28: Wisconsin Silty Clay Till / 1101 Geotextile / CA 7, Permanent Deformation vs Cone Index

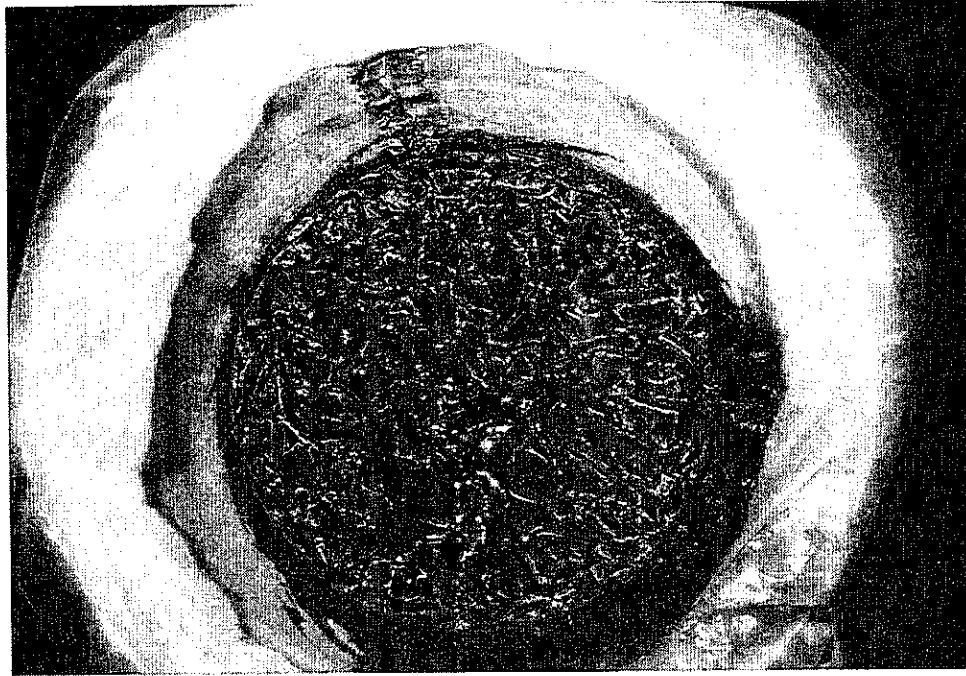


Figure 6.29: Wisconsin Silty Clay Till Slurry Coating 1101 Geotextile - Post Test

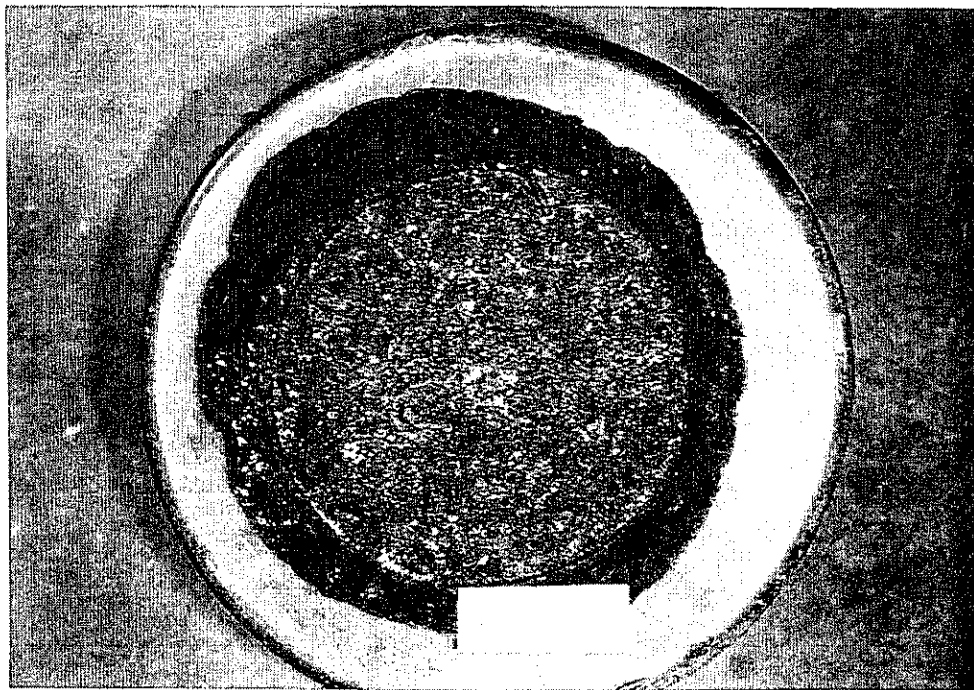


Figure 6.30: Wisconsin Silty Clay Till Pumped into 1101 Geotextile and CA 7



Figure 6.31: Wisconsin Silty Clay Till Specimen Surface Underlying 1101 Geotextile

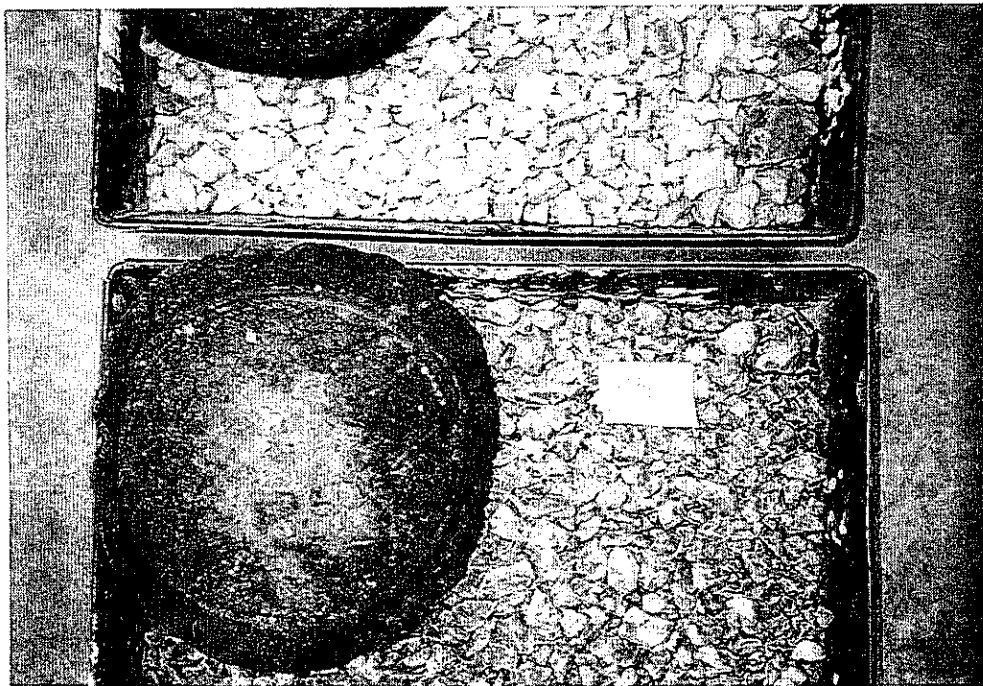


Figure 6.32: 1101 Geotextile and CA 7 with Pumped Wisconsin Silty Clay Till

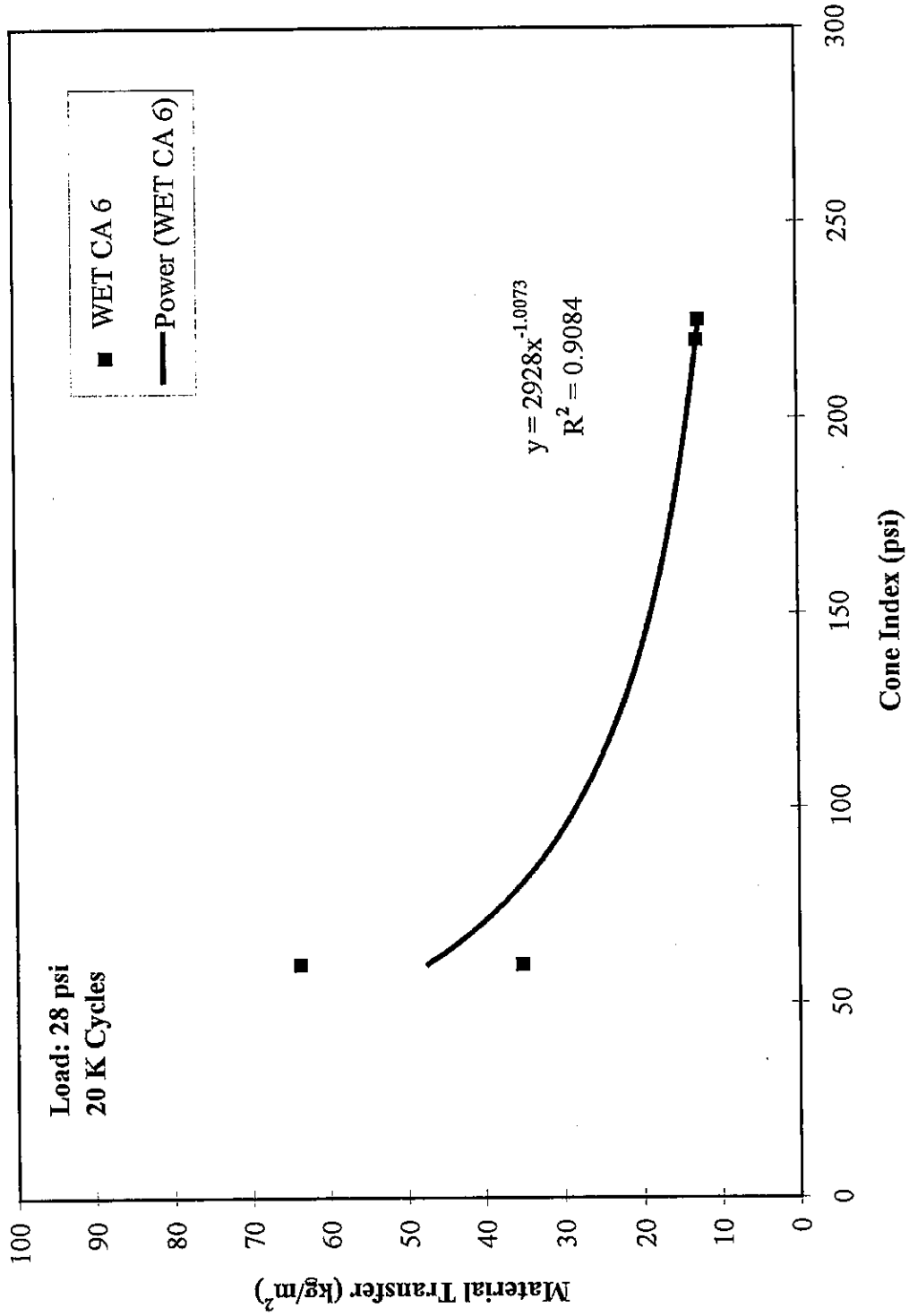


Figure 6.33: Wisconsinan Silty Clay / CA 6 / CA 7, Material Transfer vs Cone Index

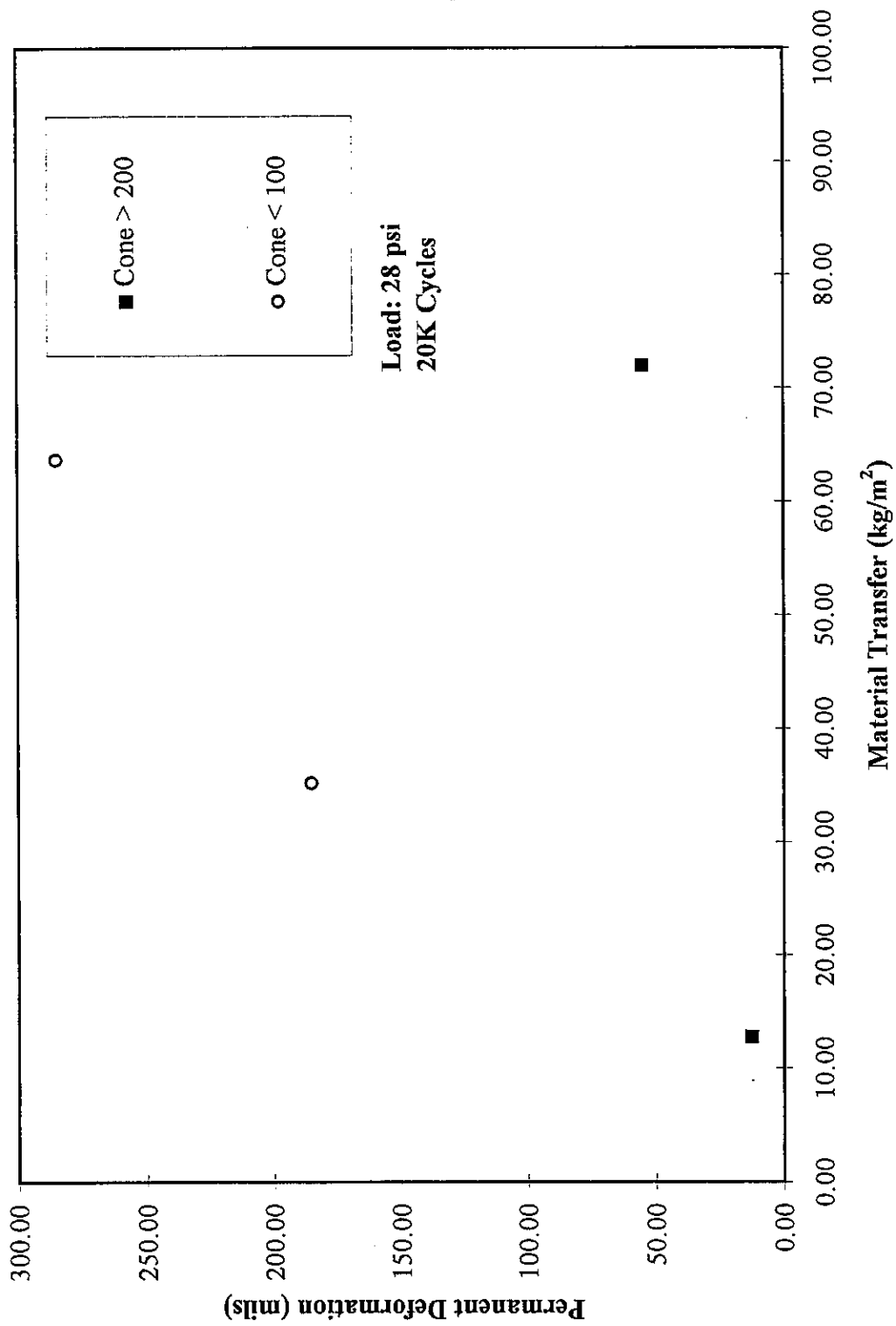


Figure 6.34: Wisconsin Silty Clay Till / CA 6 / CA 7, Permanent Deformation vs Material Transfer

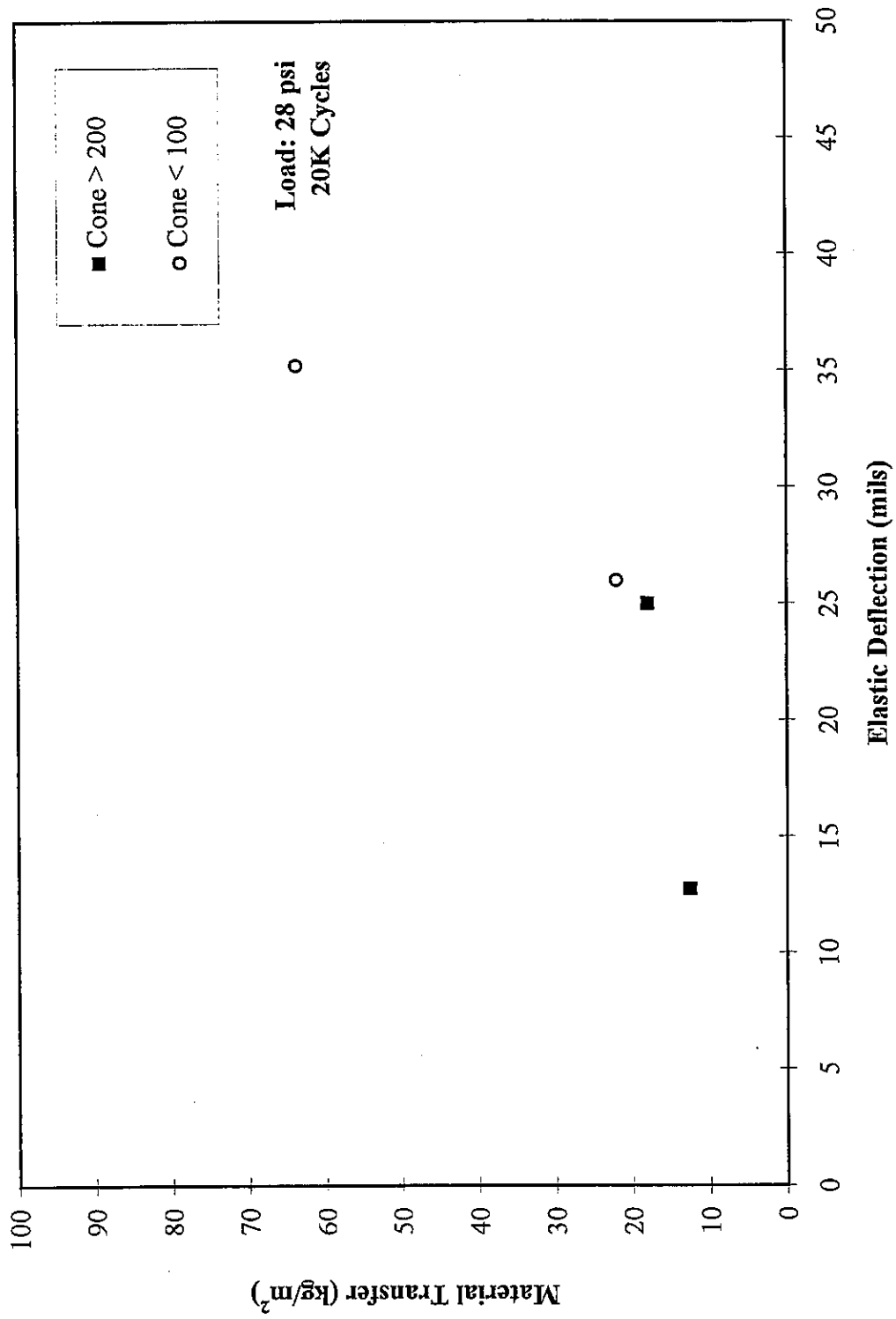


Figure 6.35: Wisconsinan Silty Clay Till / CA 6 / CA 7, Material Transfer vs Elastic Deflection

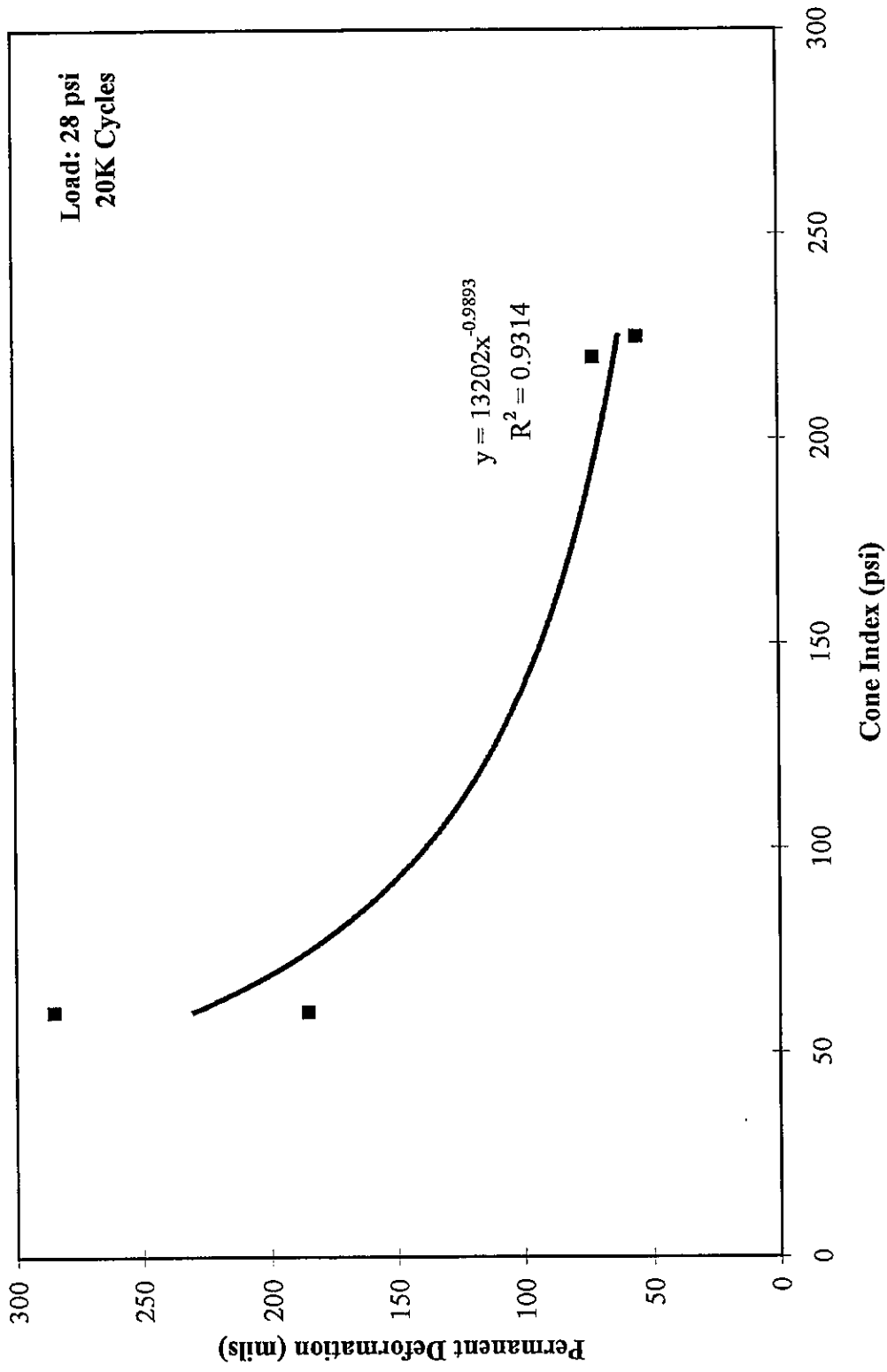


Figure 6.36: Wisconsin Silty Clay Till / CA 6 / CA 7, Permanent Deformation vs Cone Index

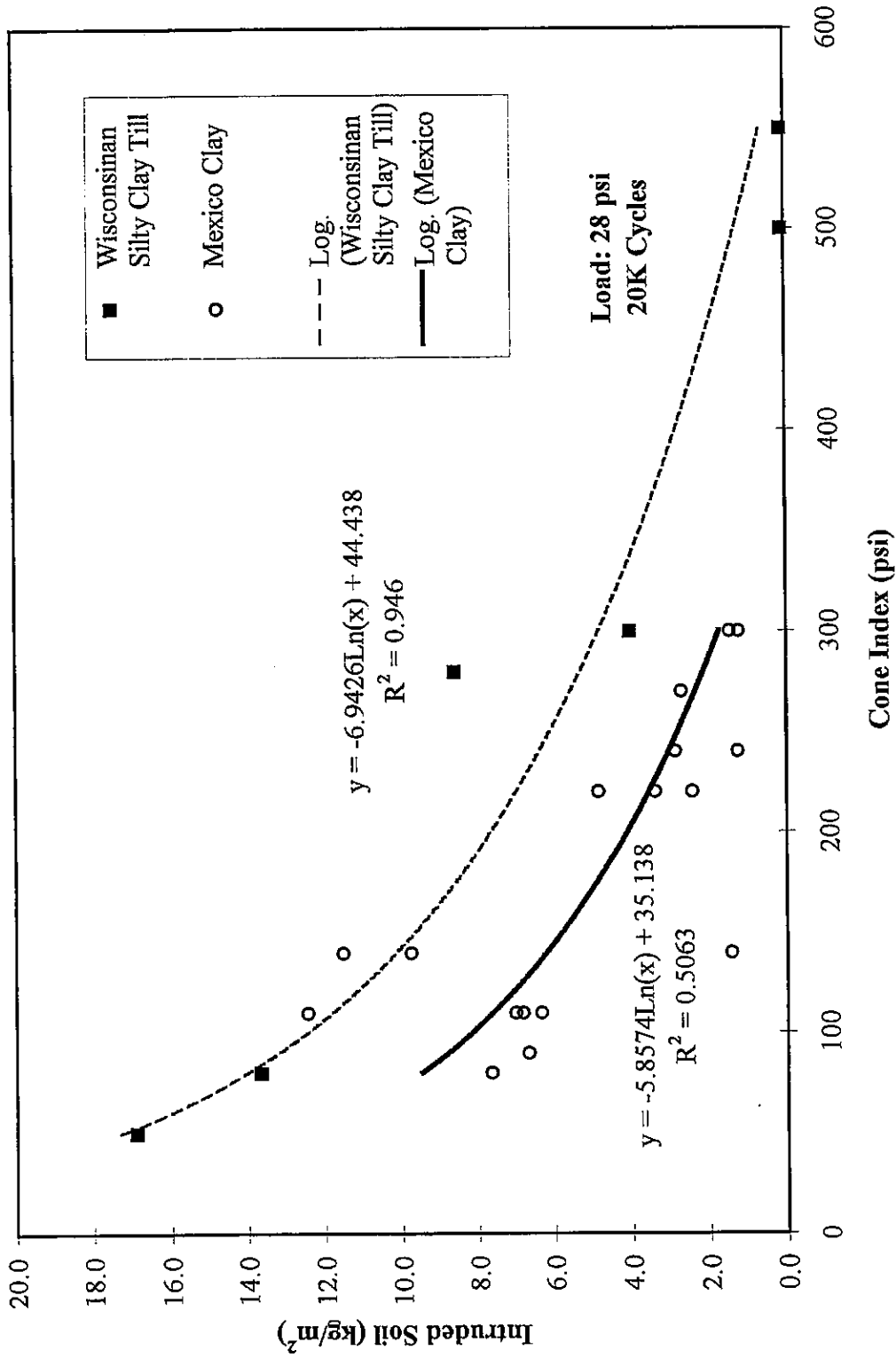


Figure 6.37: Soil / No Separation / CA 7, Intruded Soil vs Cone Index

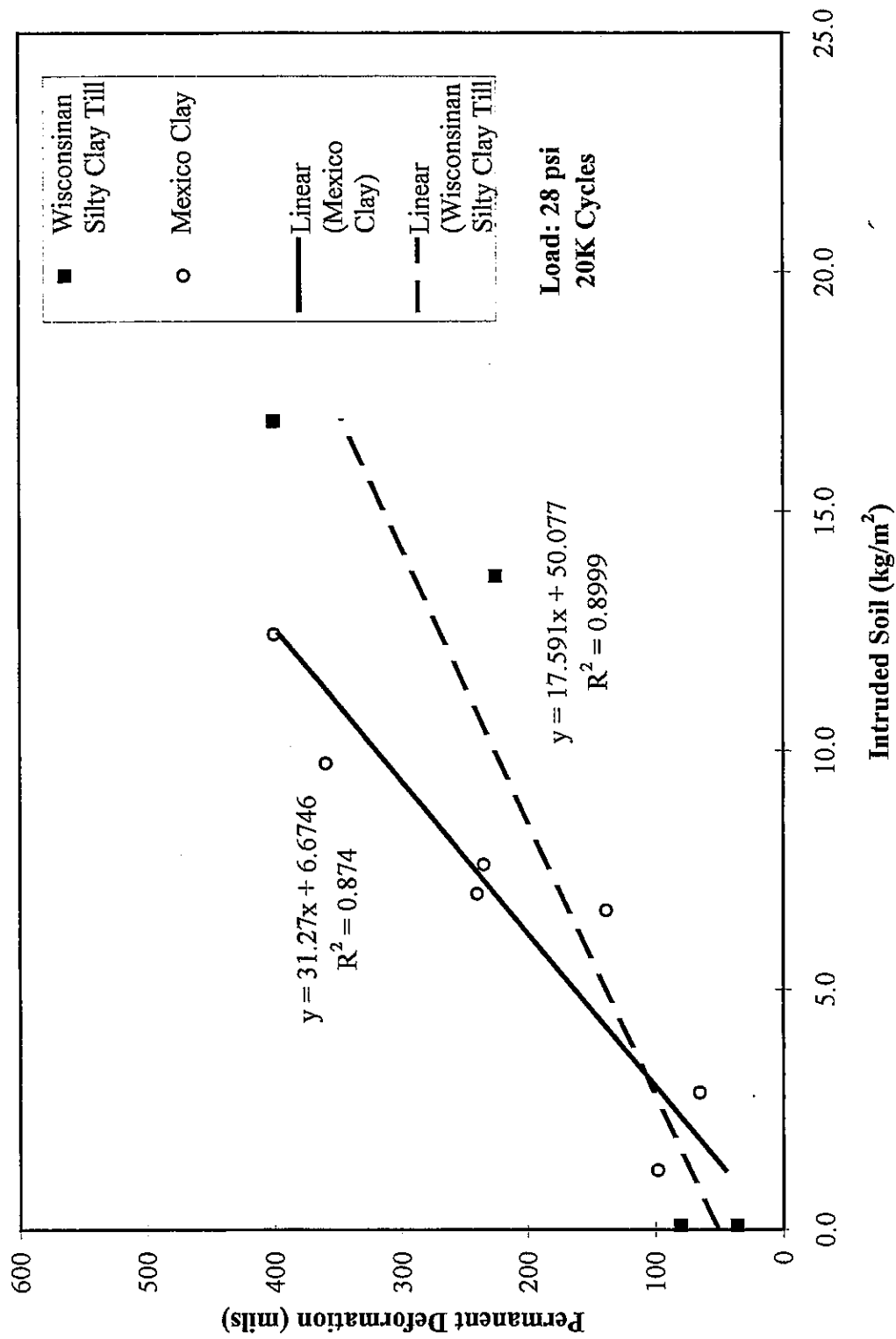


Figure 6.38: Soil / No Separation / CA 7, Permanent Deformation vs Intruded Soil

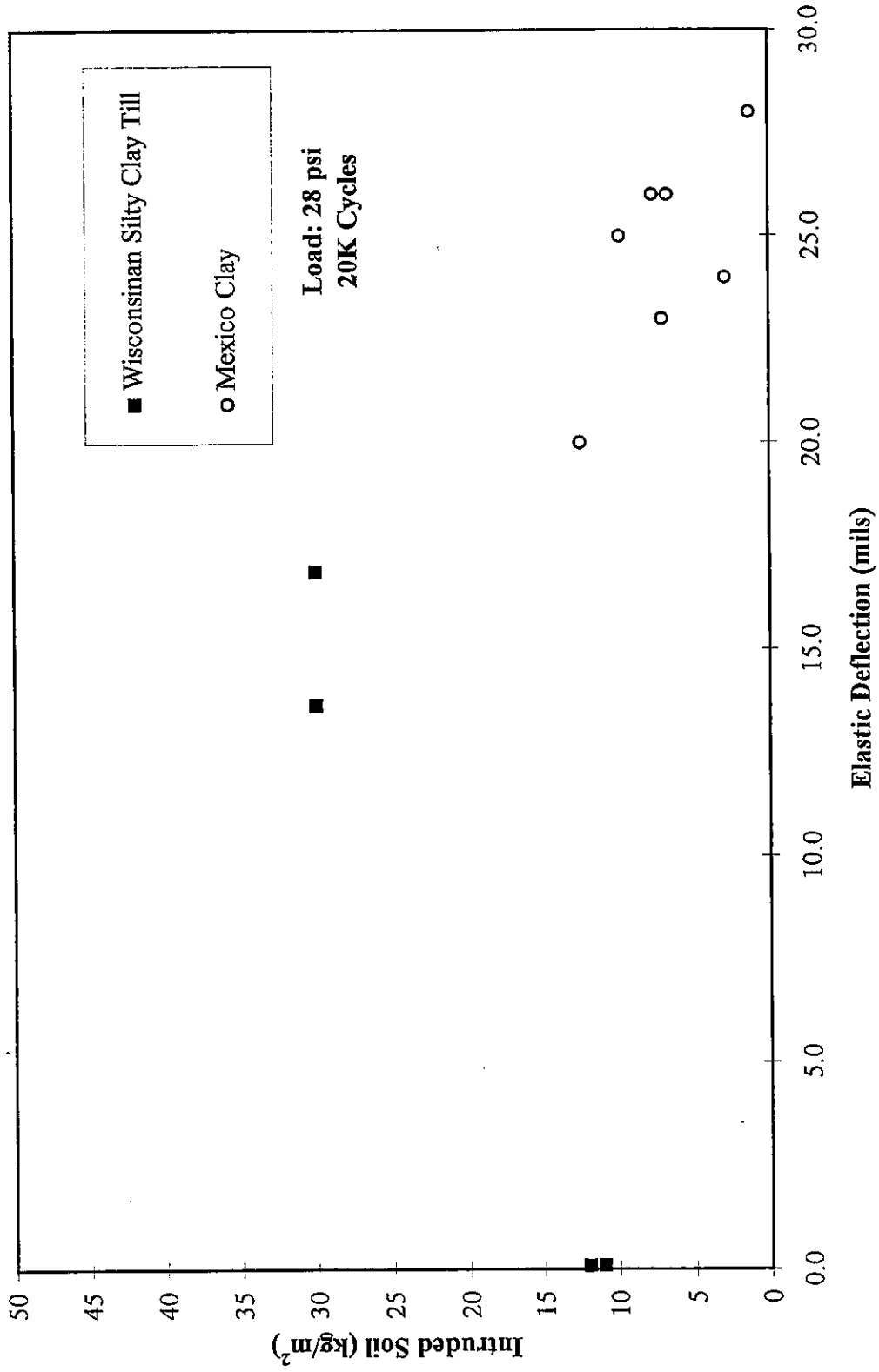


Figure 6.39: Soil / No Separation / CA 7, Intruded Soil vs Elastic Deflection

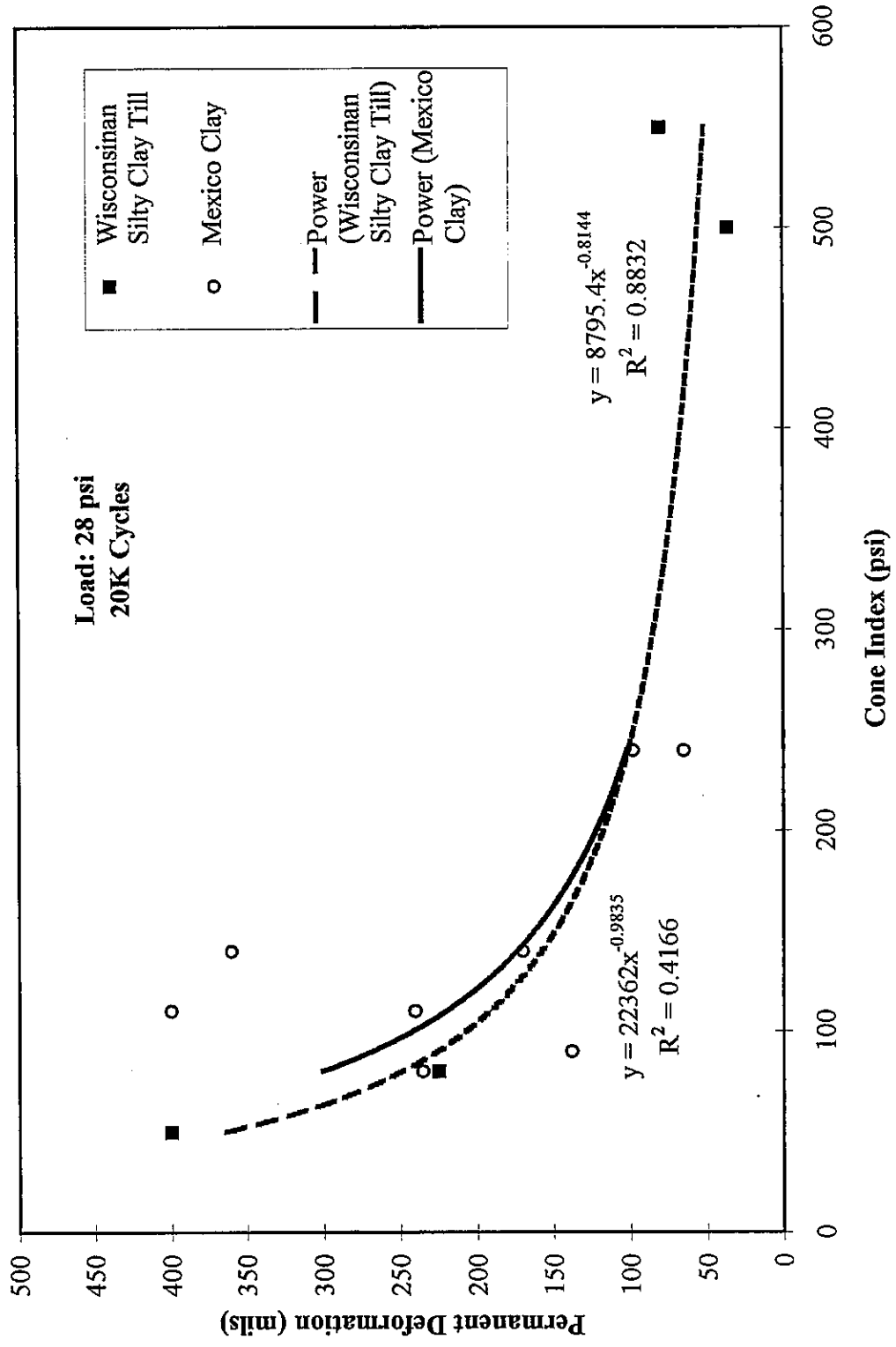


Figure 6.40: Soil / No Separation / CA 7, Permanent Deformation vs Cone Index

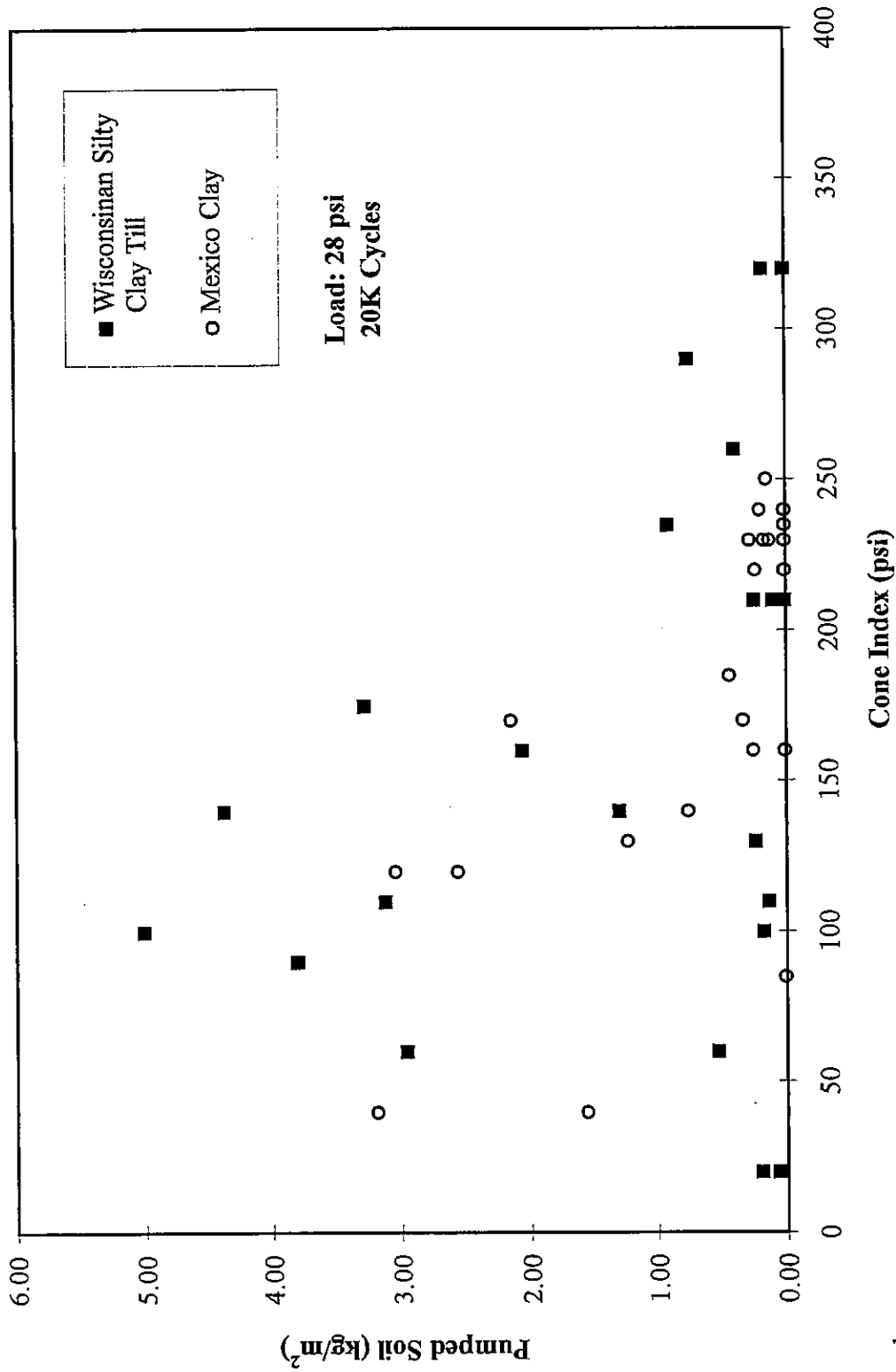


Figure 6.41: Soil / 1101 Geotextile / CA 7, Pumped Soil vs Cone Index

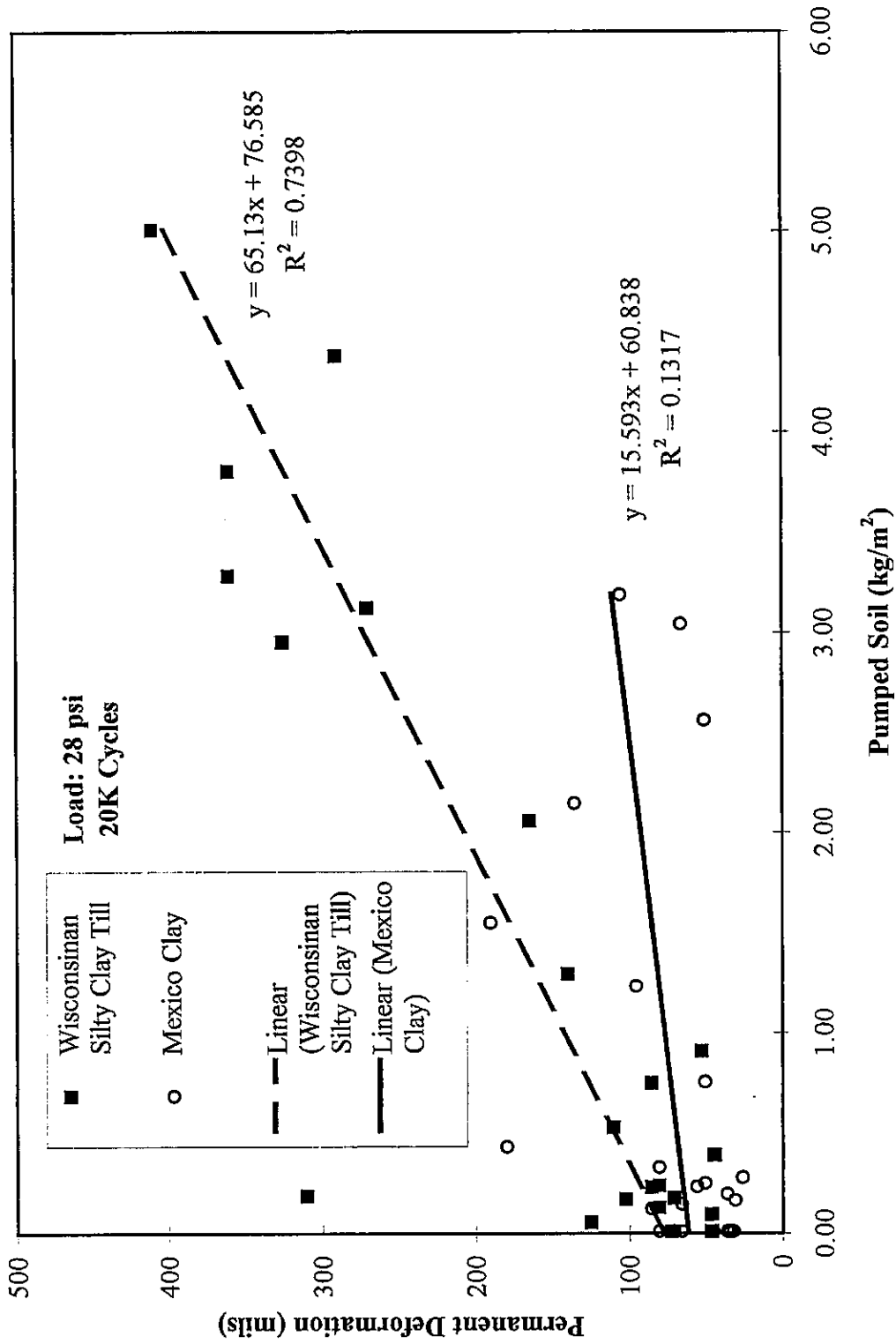


Figure 6.42: Soil / 1101 Geotextile / CA 7, Permanent Deformation vs Pumped Soil

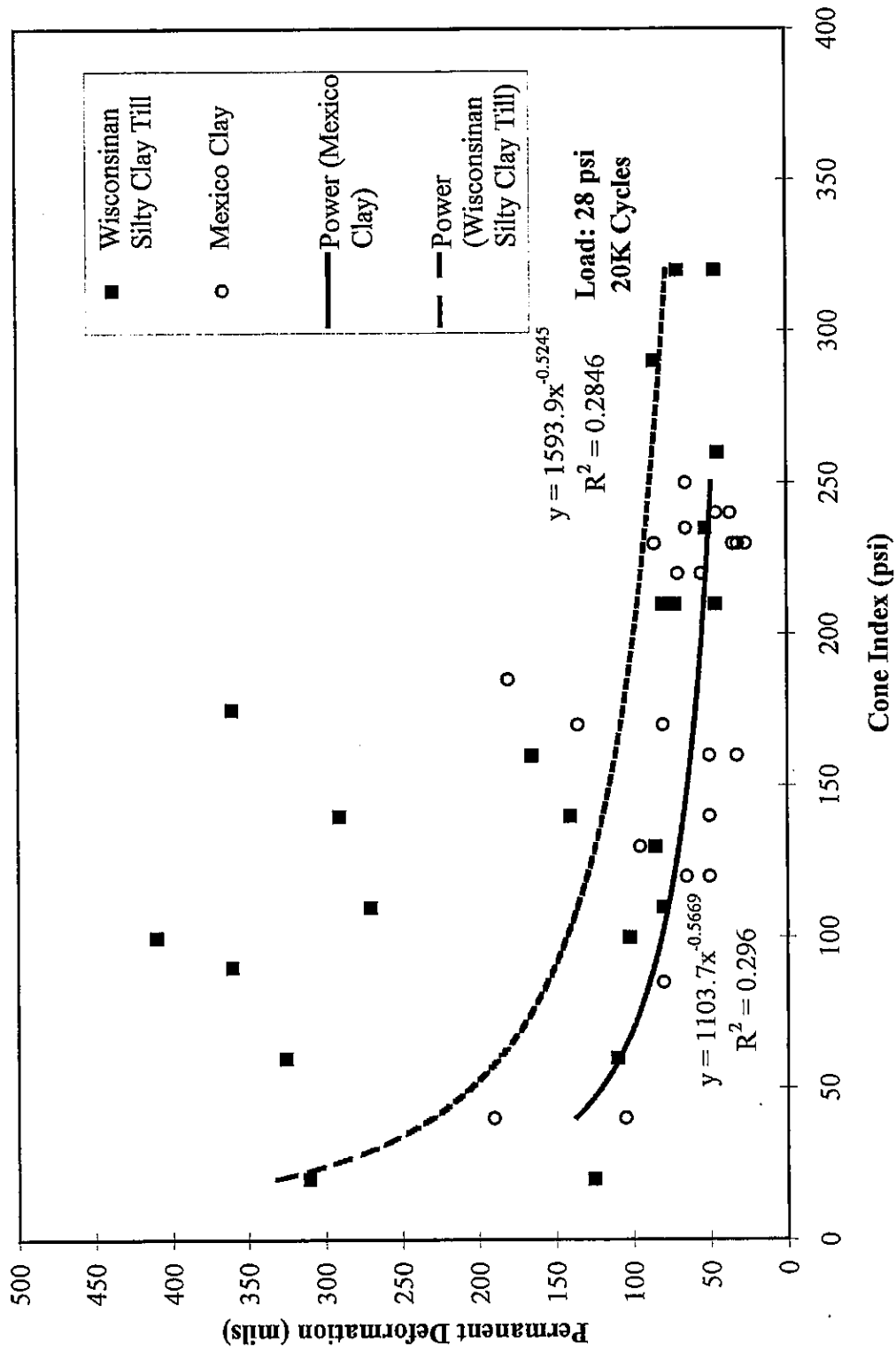


Figure 6.44: Soil / 1101 Geotextile / CA 7, Permanent Deformation vs Cone Index

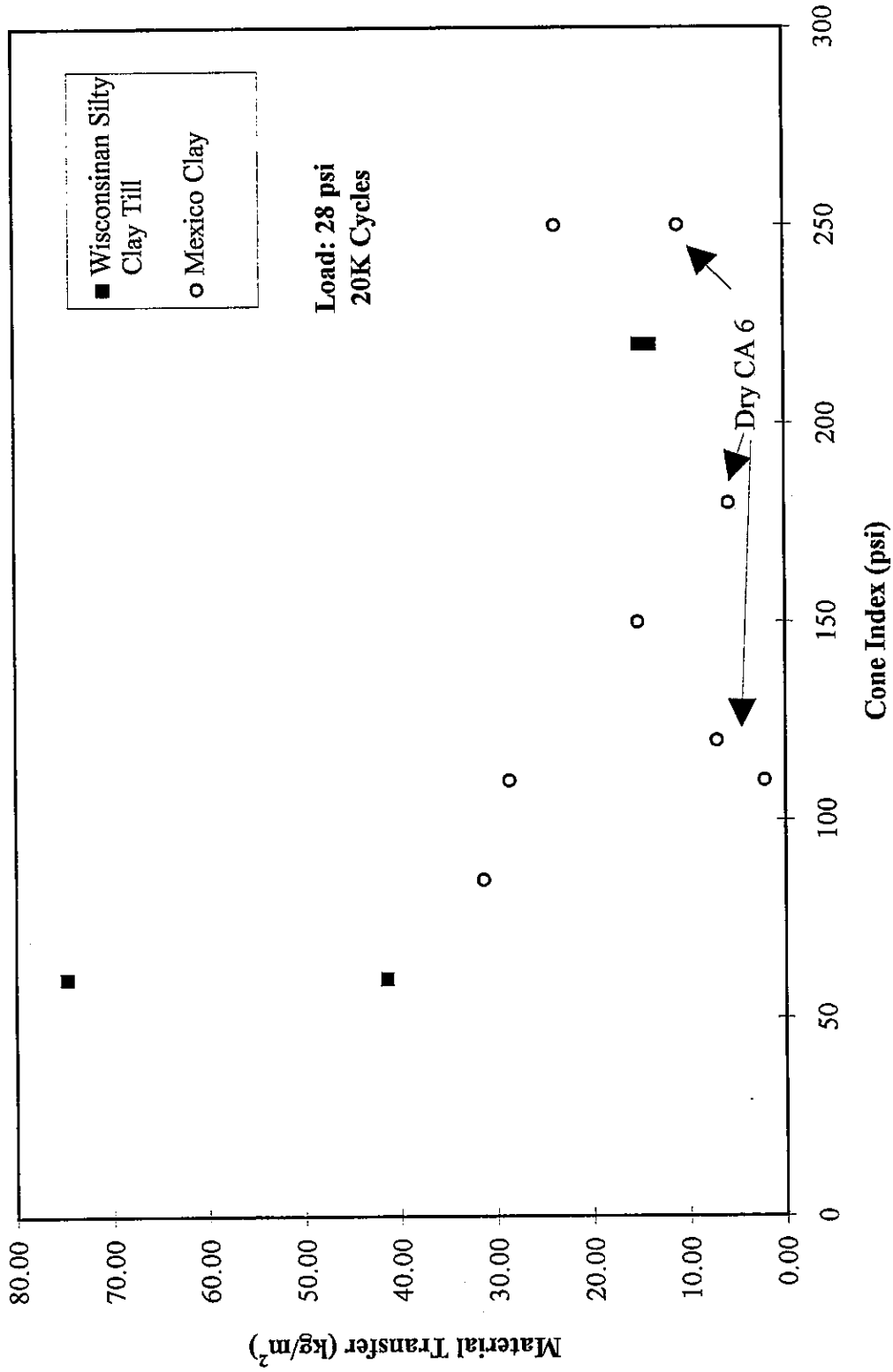


Figure 6.45: Soil / CA 6 / CA 7, Material Transfer vs Cone Index

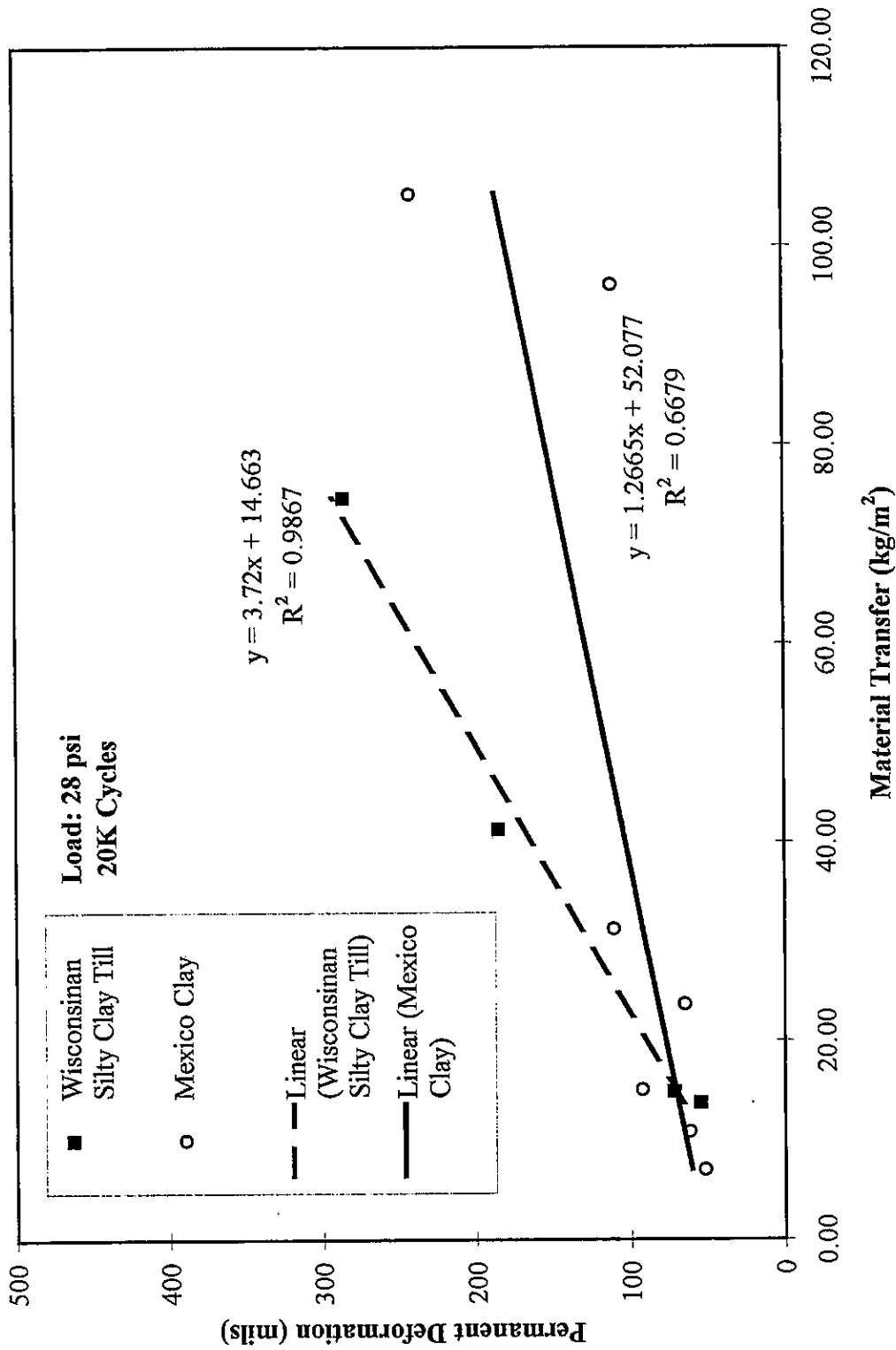


Figure 6.46: Soil / CA 6 / CA 7, Permanent Deformation vs Material Transfer

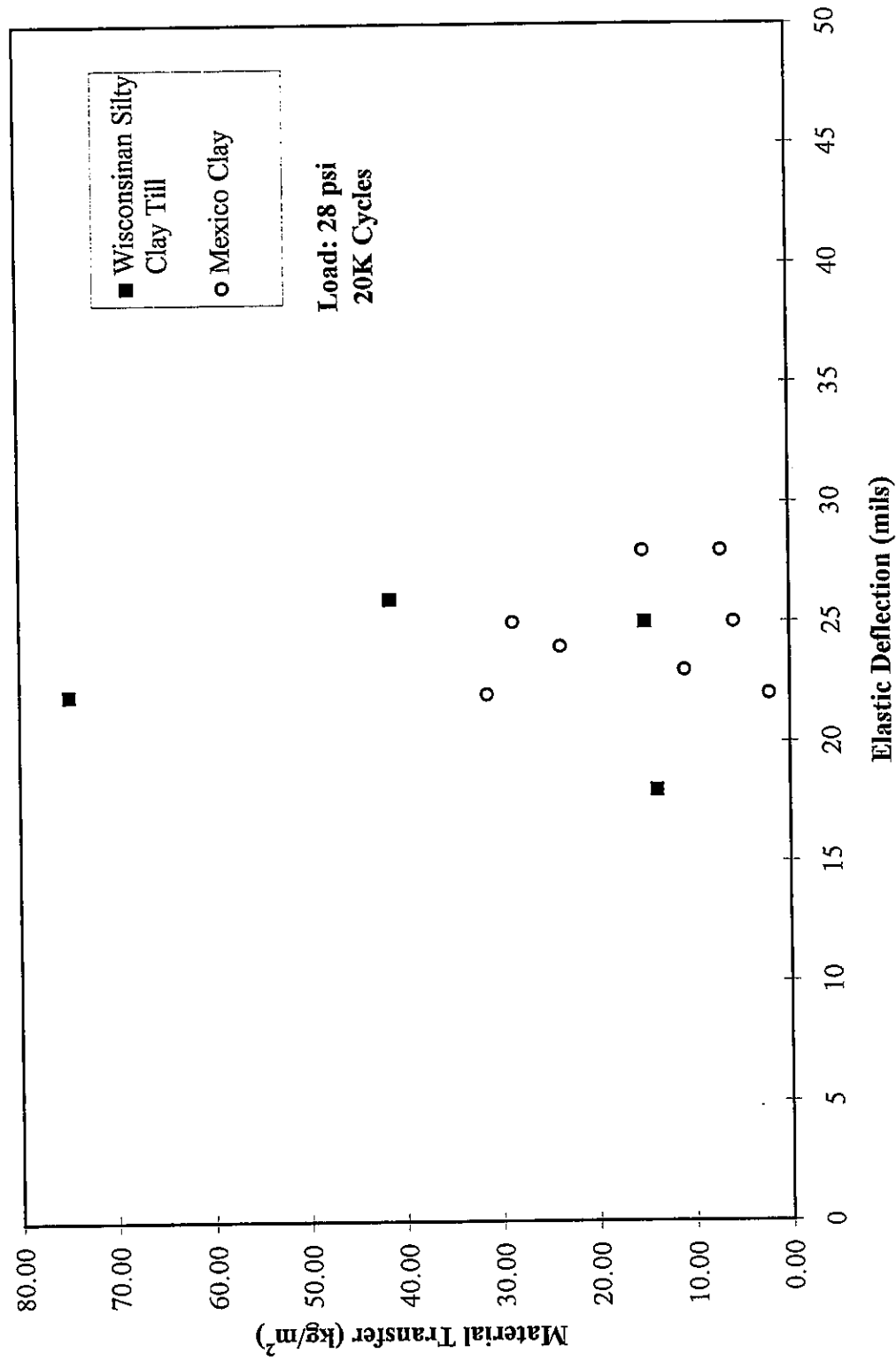


Figure 6.47: Soil / CA 6 / CA 7, Material Transfer vs Elastic Deflection

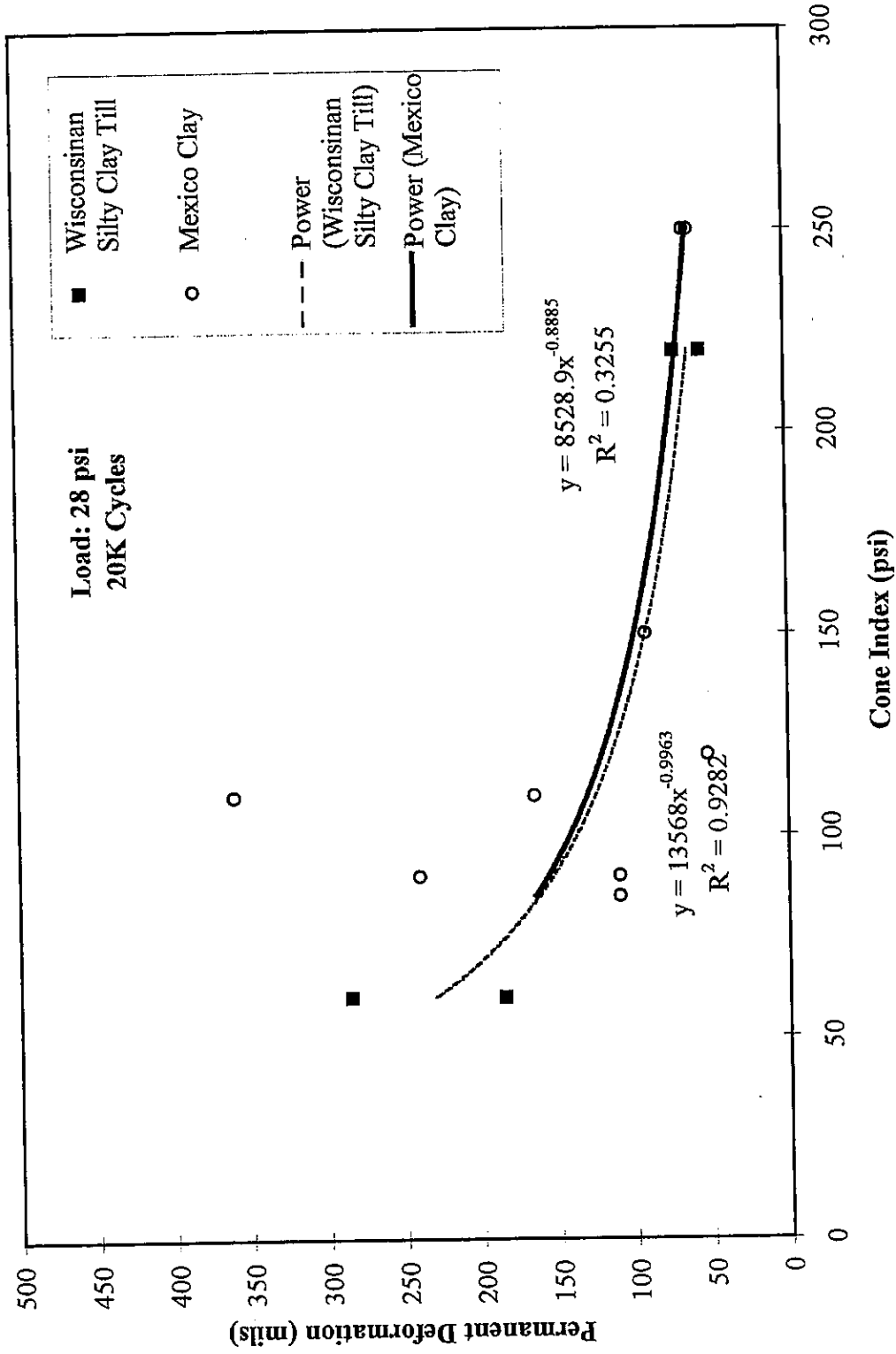


Figure 6.48: Soil / CA 6 / CA 7, Permanent Deformation vs Cone Index

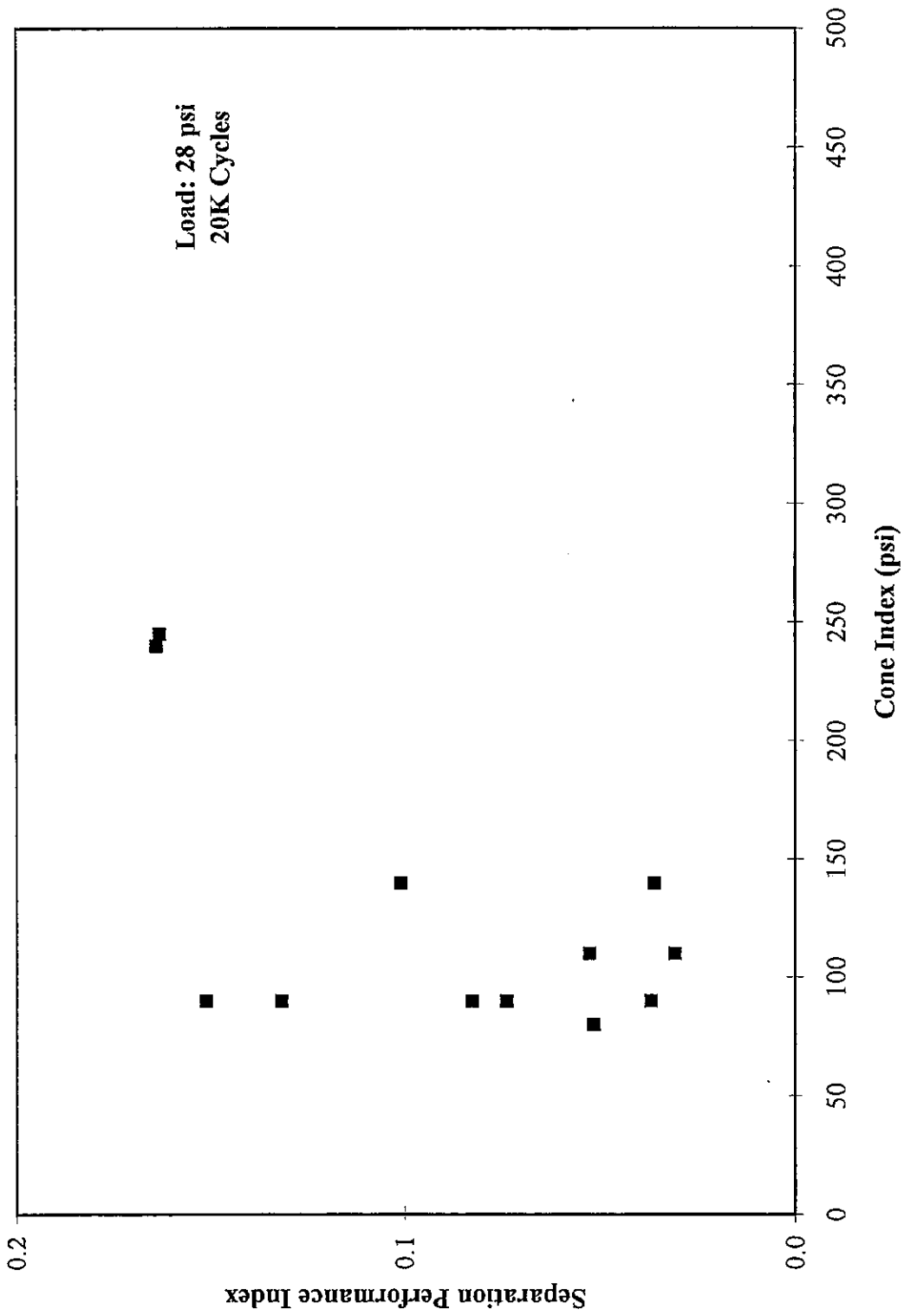


Figure 6.49: Mexico Clay / No Separation / CA 7, Separation Performance Index vs. Cone Index

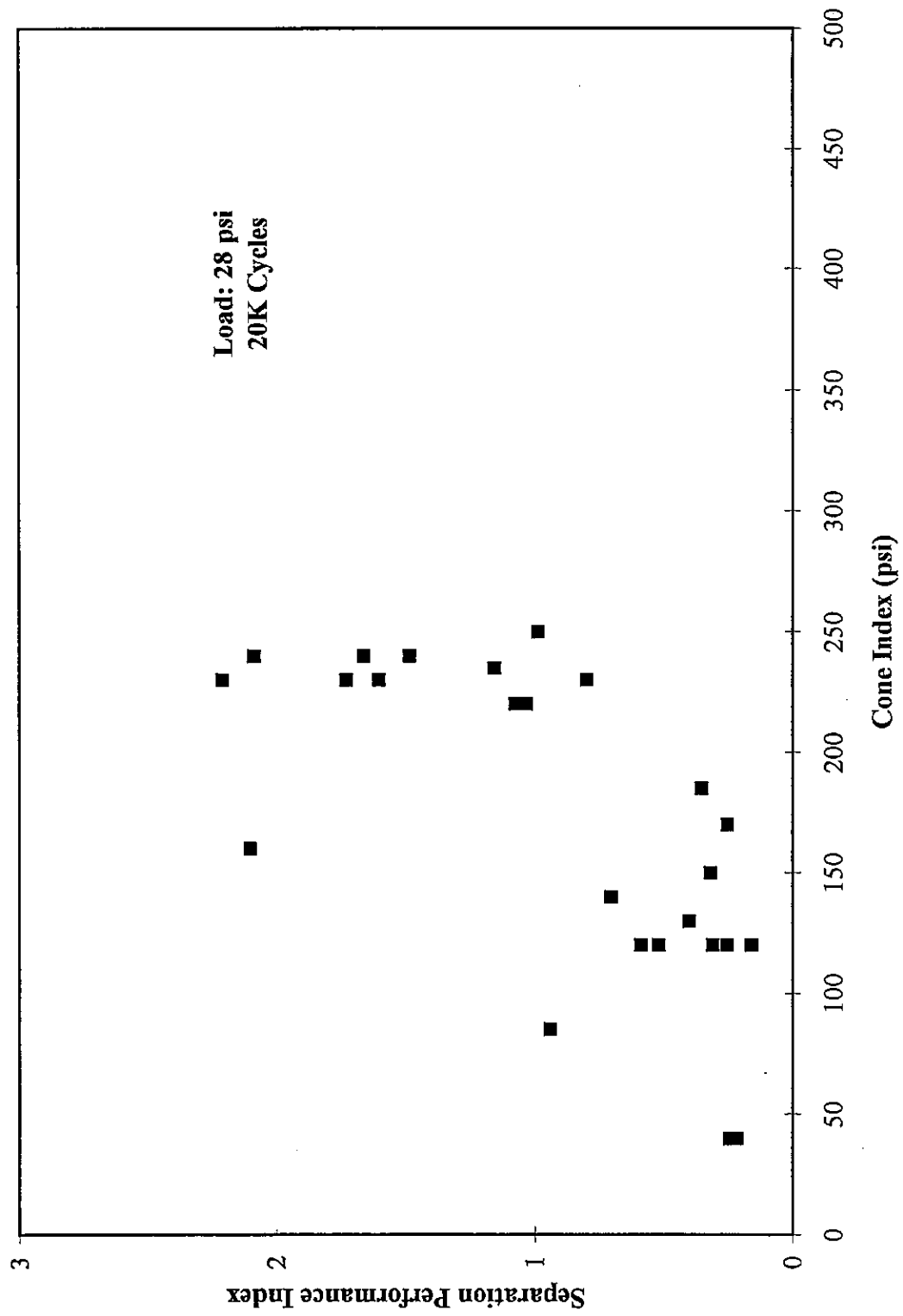


Figure 6.50: Mexico Clay / 1101 Geotextile / CA7, Separation Performance Index vs Cone Index

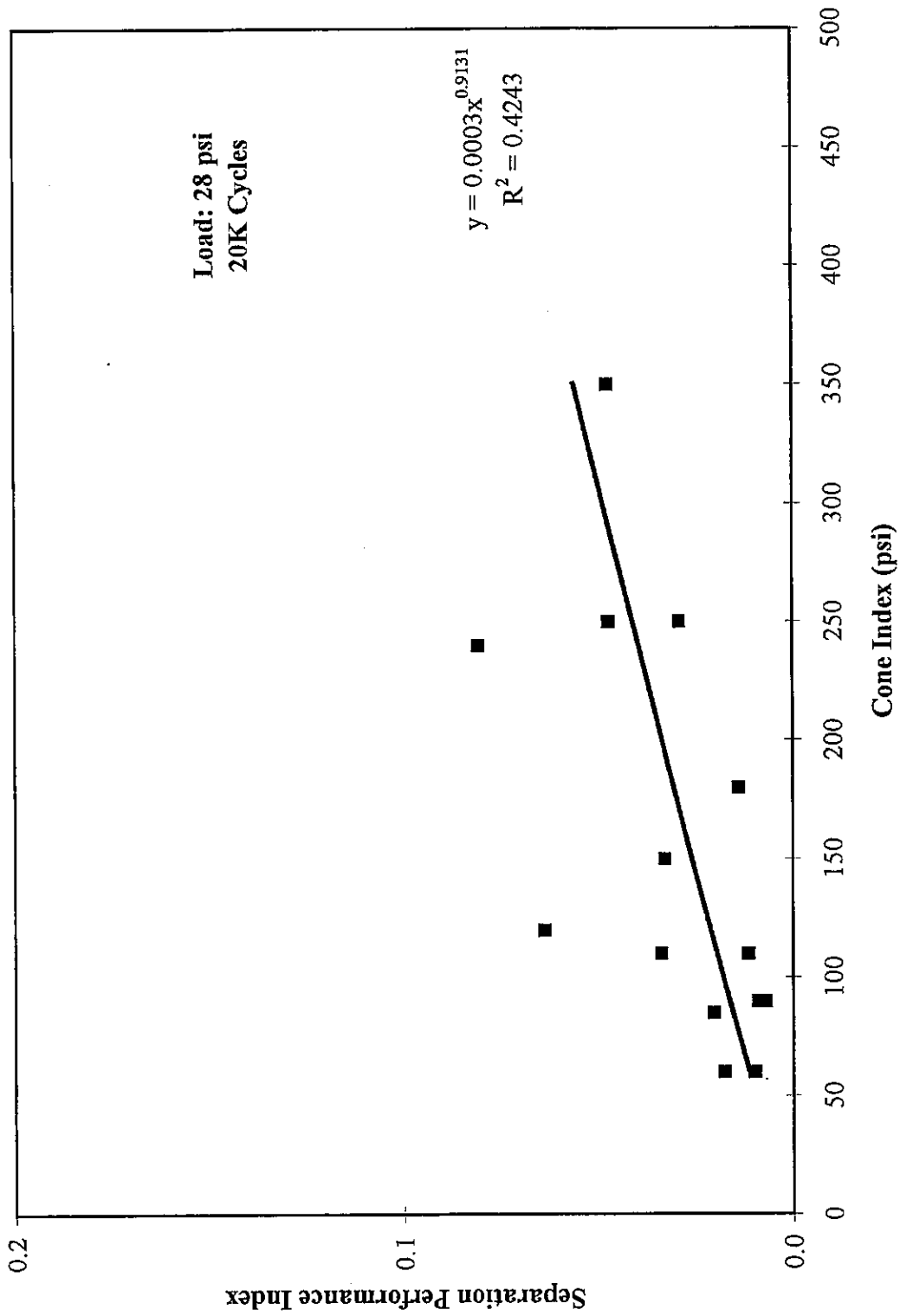


Figure 6.51: Mexico Clay / CA 6 / CA 7, Separation Performance Index vs. Cone Index

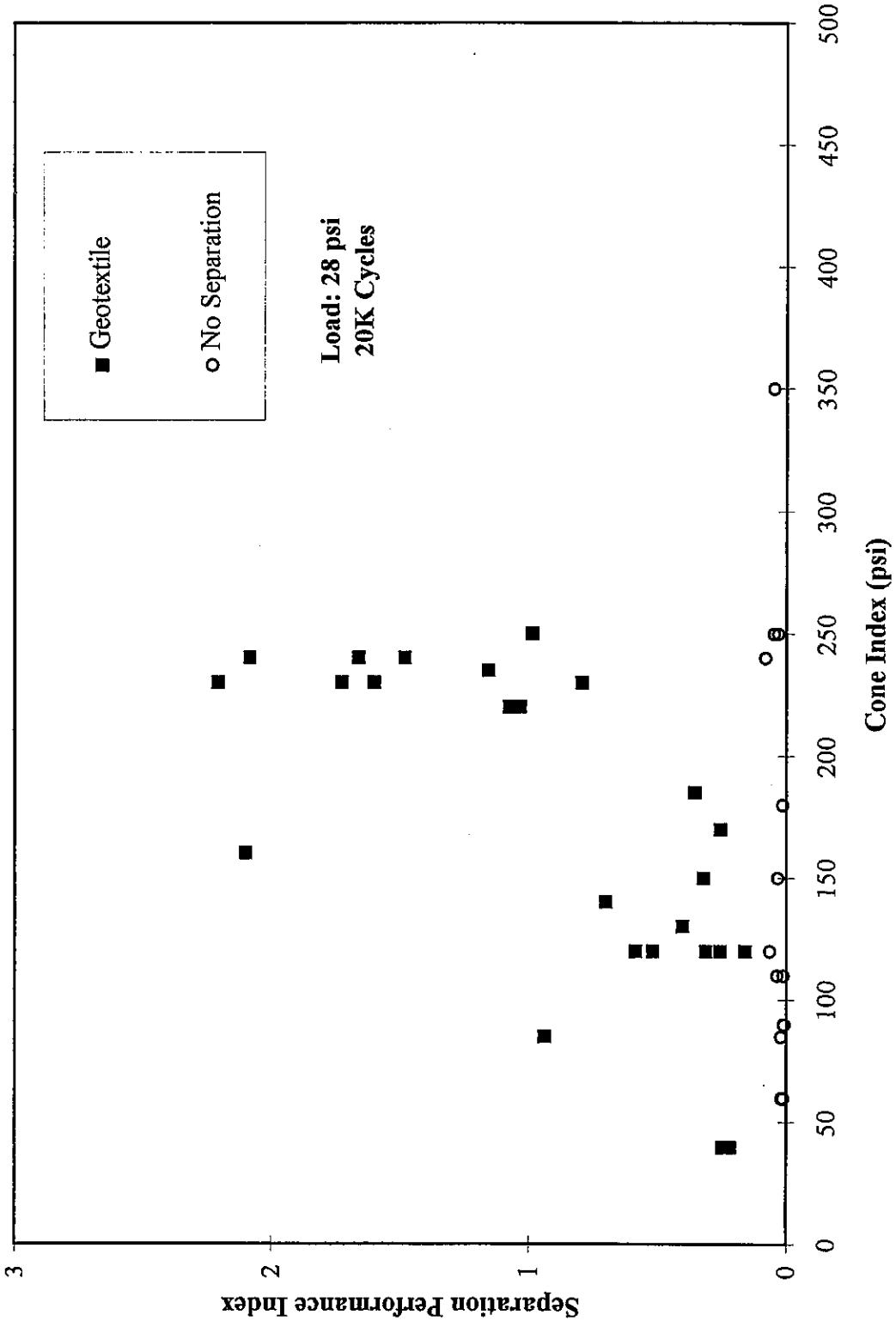


Figure 6.52: Mexico Clay / Separation / CA 7, Separation Performance Index vs. Cone Index

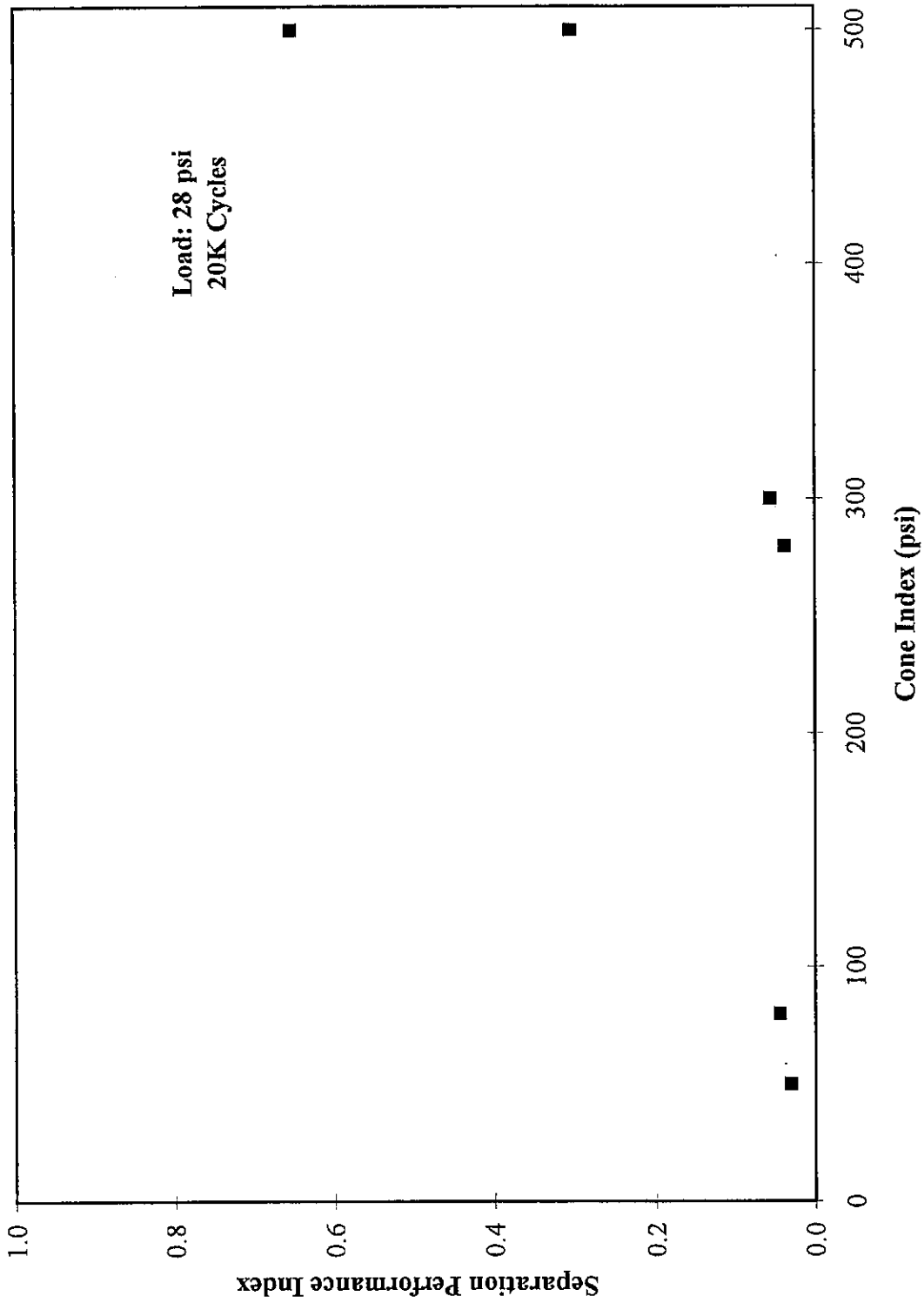


Figure 6.53: Wisconsin Silty Clay Till / No Separation / CA 7, Separation Performance Index vs. Cone Index

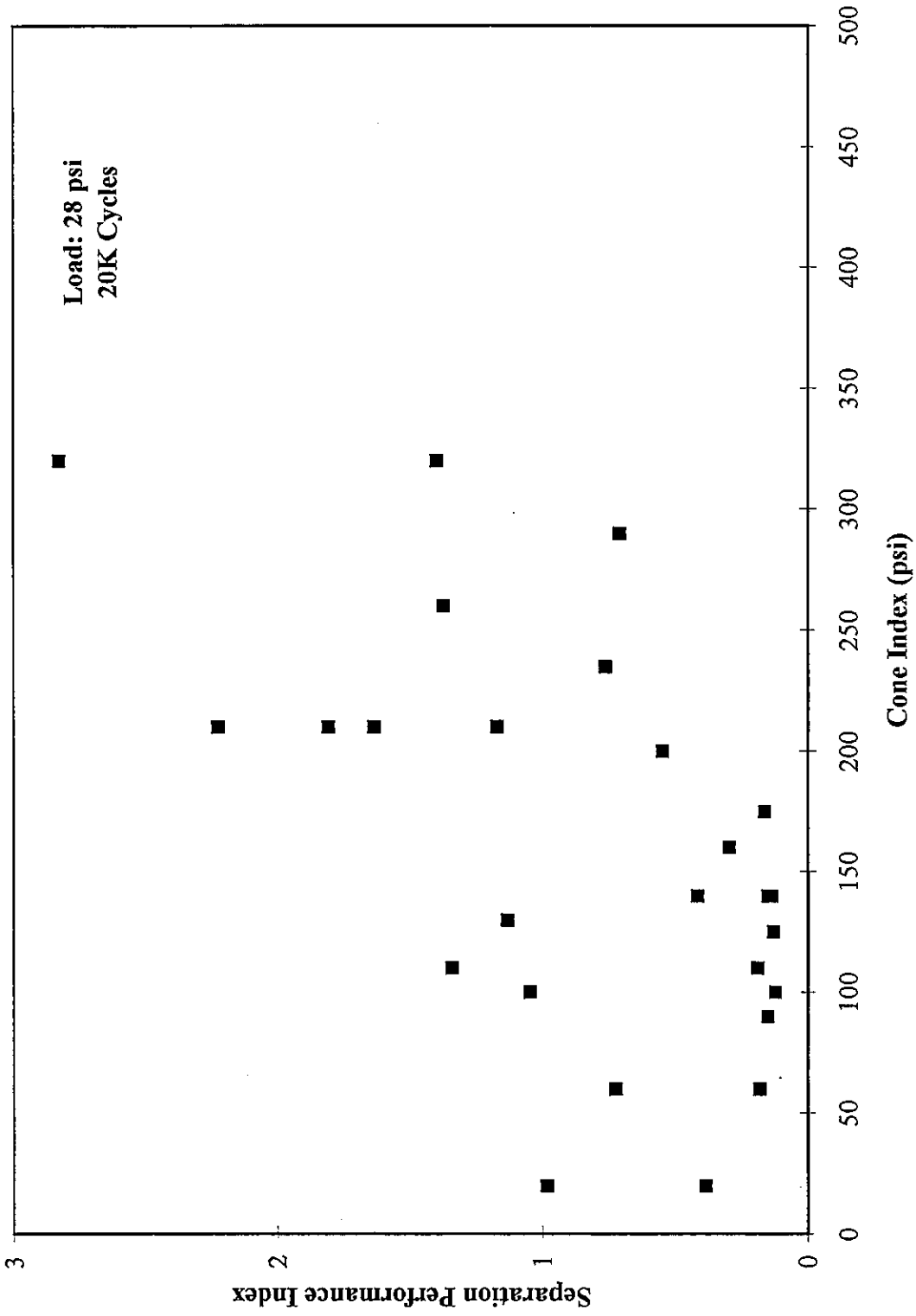


Figure 6.54: Wisconsin Silty Clay Till / 1101 Geotextile / CA 7, Separation Performance Index vs. Cone Index

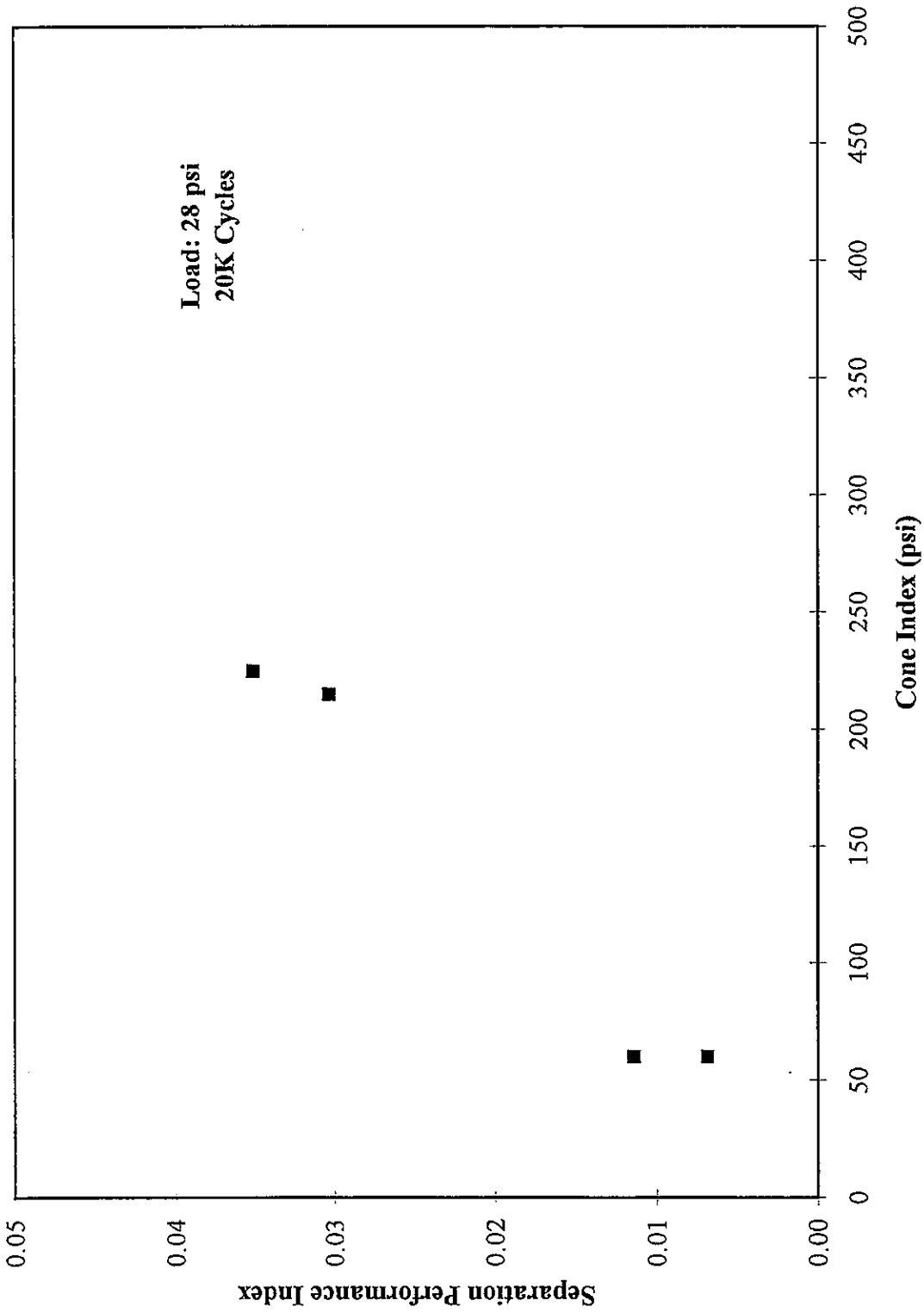


Figure 6.55: Wisconsin Silty Clay Till / CA 6 / CA 7, Separation Performance Index vs. Cone Index

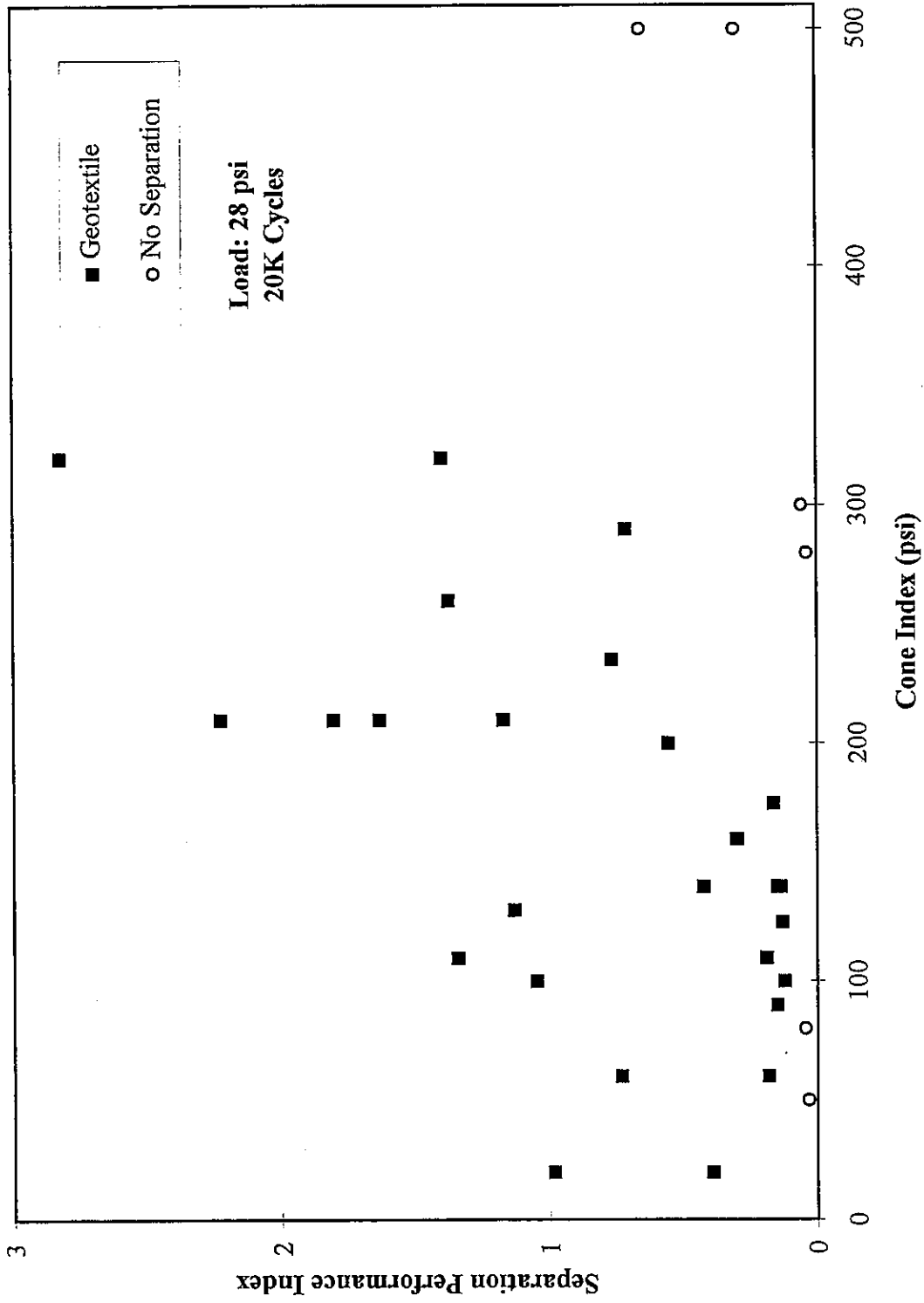


Figure 6.56: Wisconsinan Silty Clay Till / Separation / CA 7, Separation Performance Index vs. Cone Index

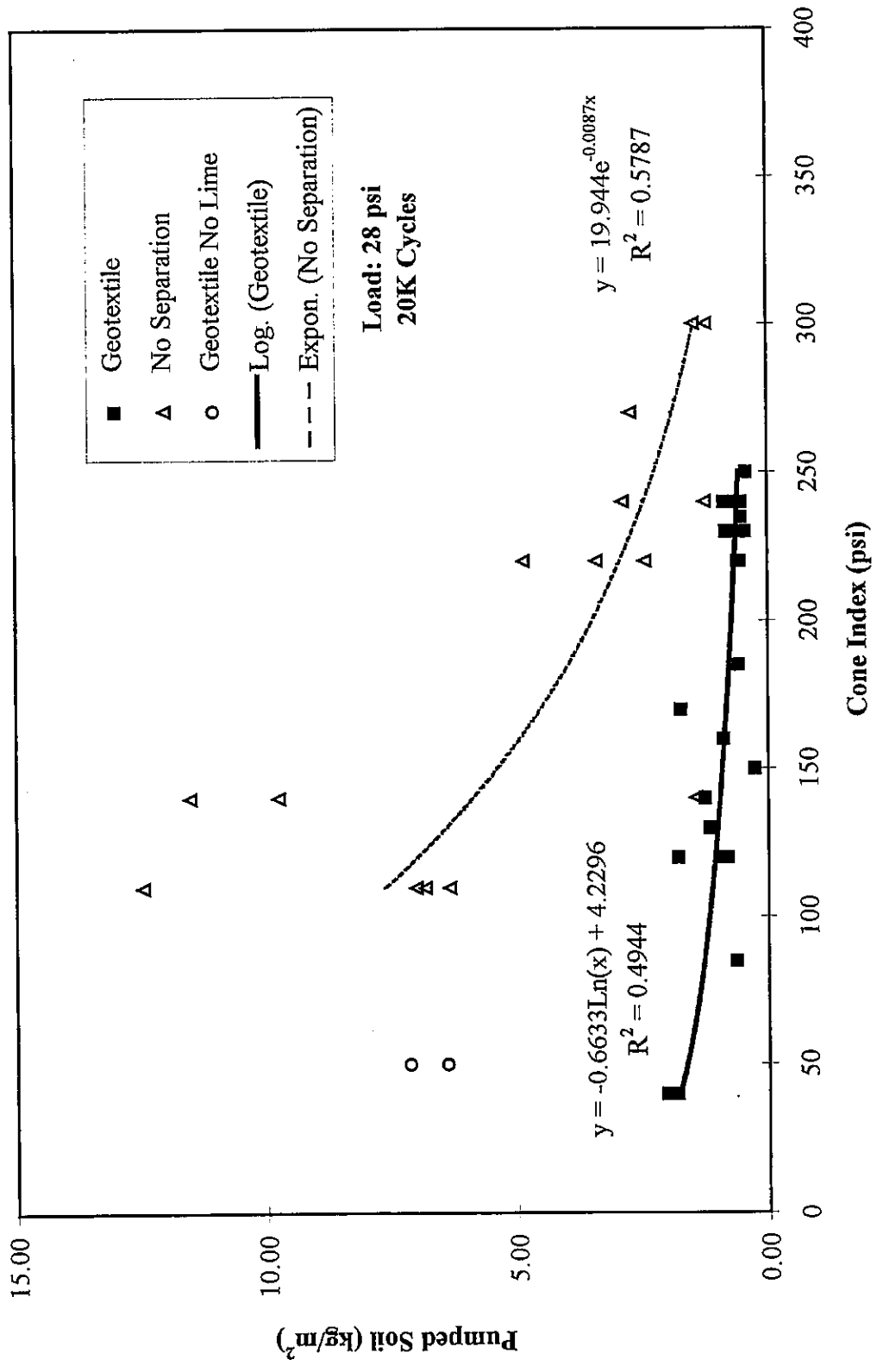


Figure 6.57: Mexico Clay / Separation / CA 7, Pumped/Intruded Material vs Cone Index

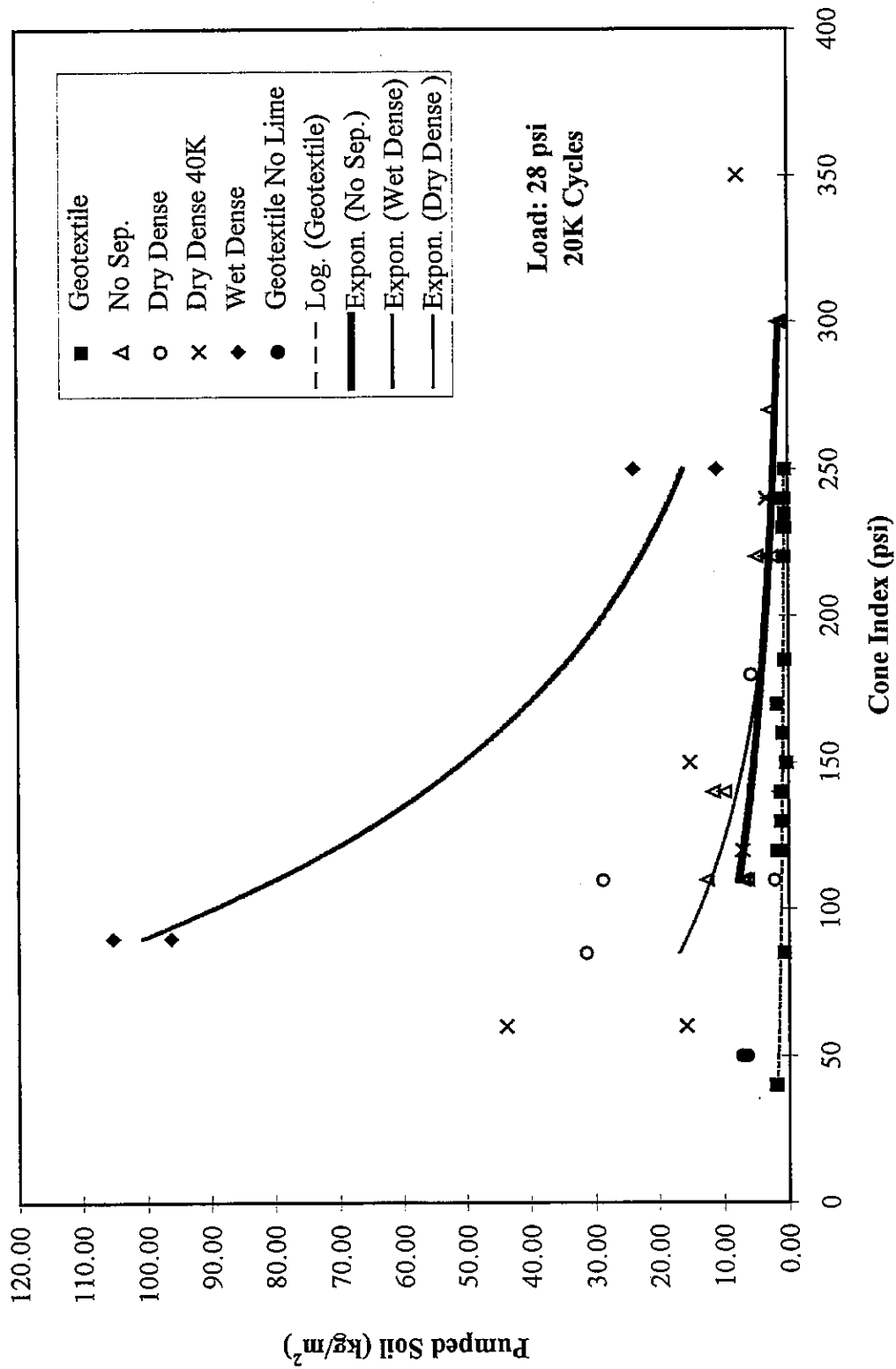


Figure 6.58: Mexico Clay / Separation / CA 7, Pumped/Intruded Material/Material Transfer vs Cone Index

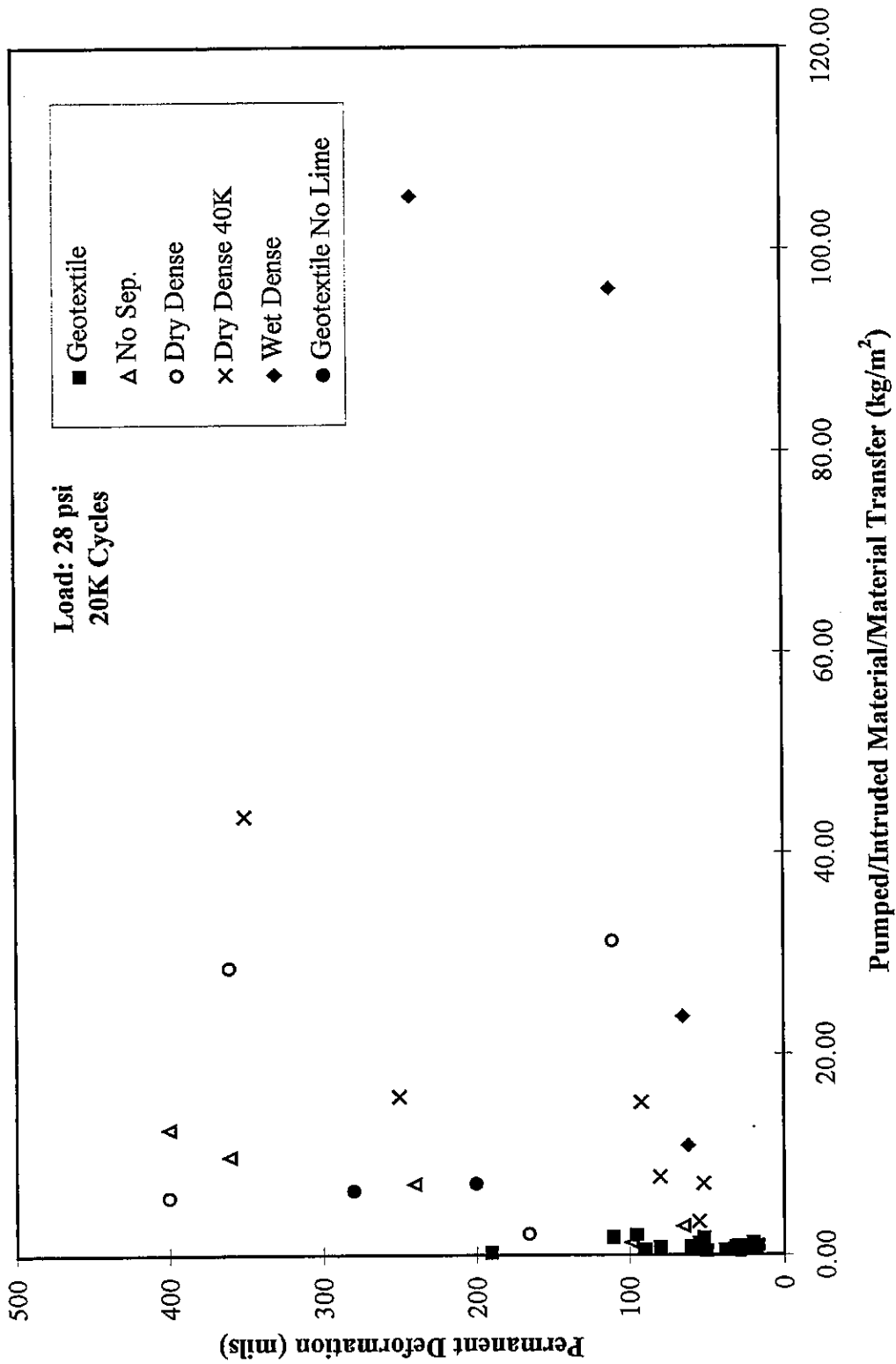


Figure 6.60: Mexico Clay / Separation / CA 7, Permanent Deformation vs Pumped/Intruded Material/Material Transfer

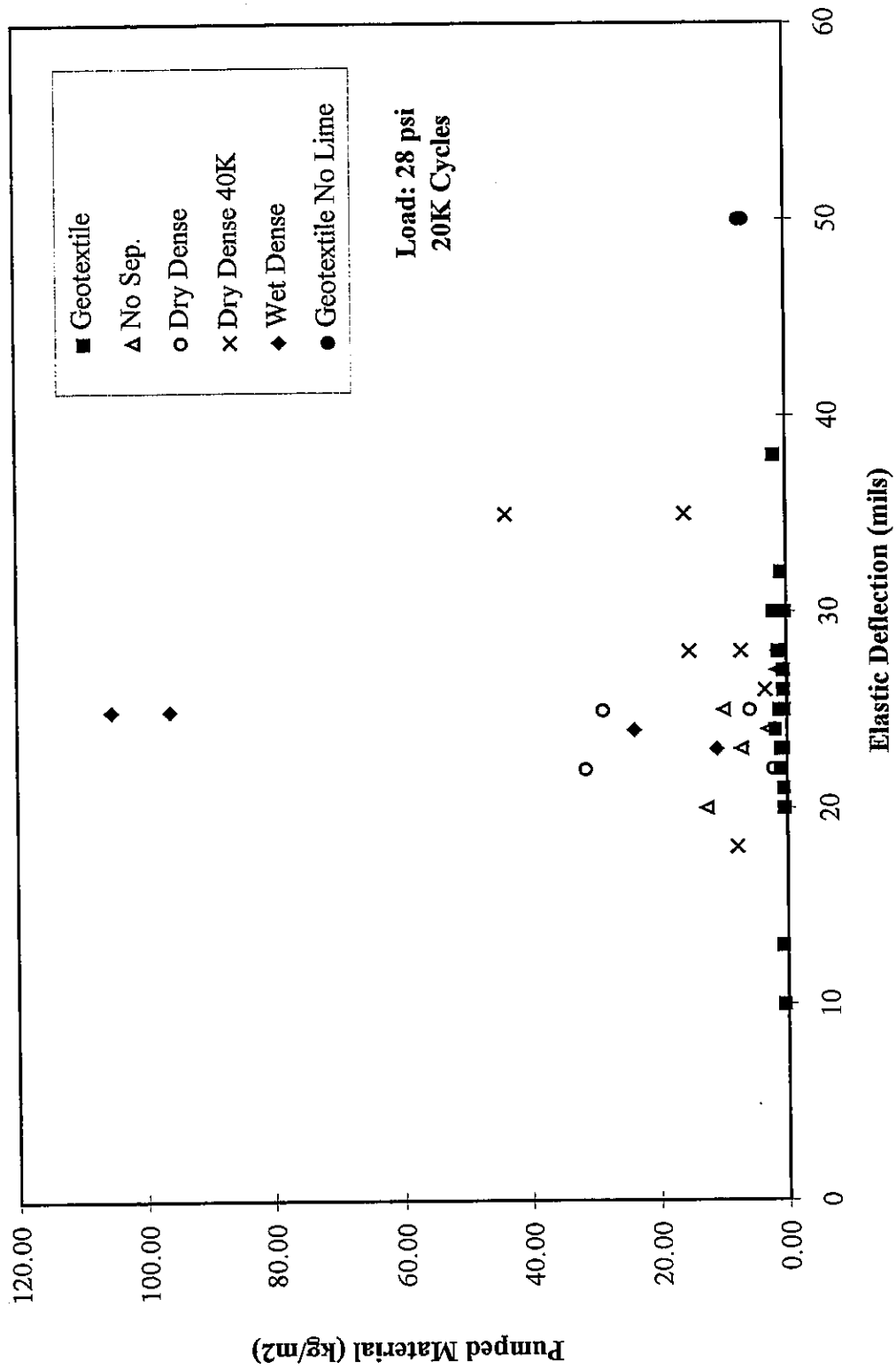


Figure 6.61: Mexico Clay / Separation / CA 7, Pumped/Intruded Material/Material Transfer vs Elastic Deflection

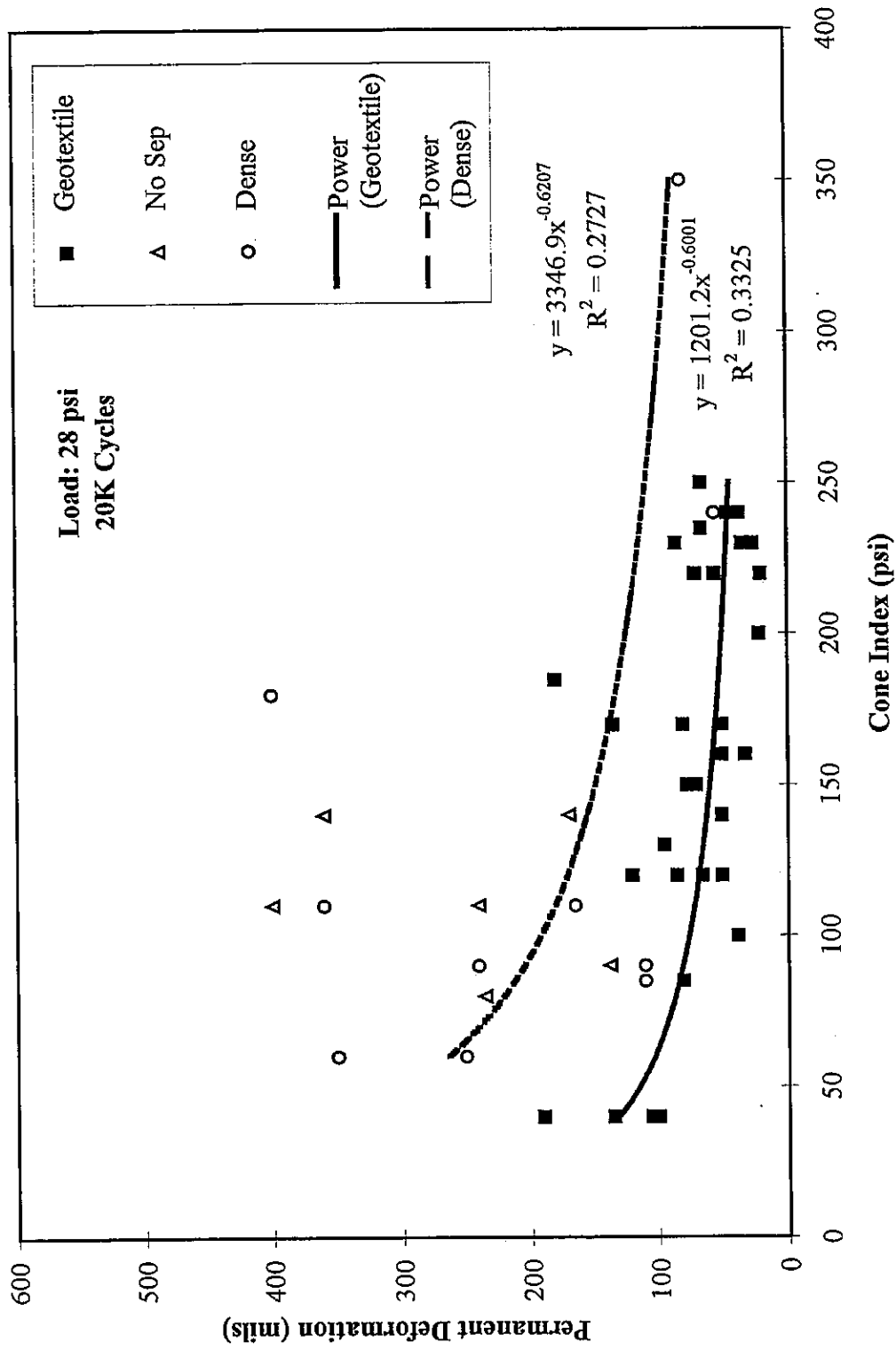


Figure 6.62: Mexico Clay / Separation / CA 7, Permanent Deformation vs Cone Index

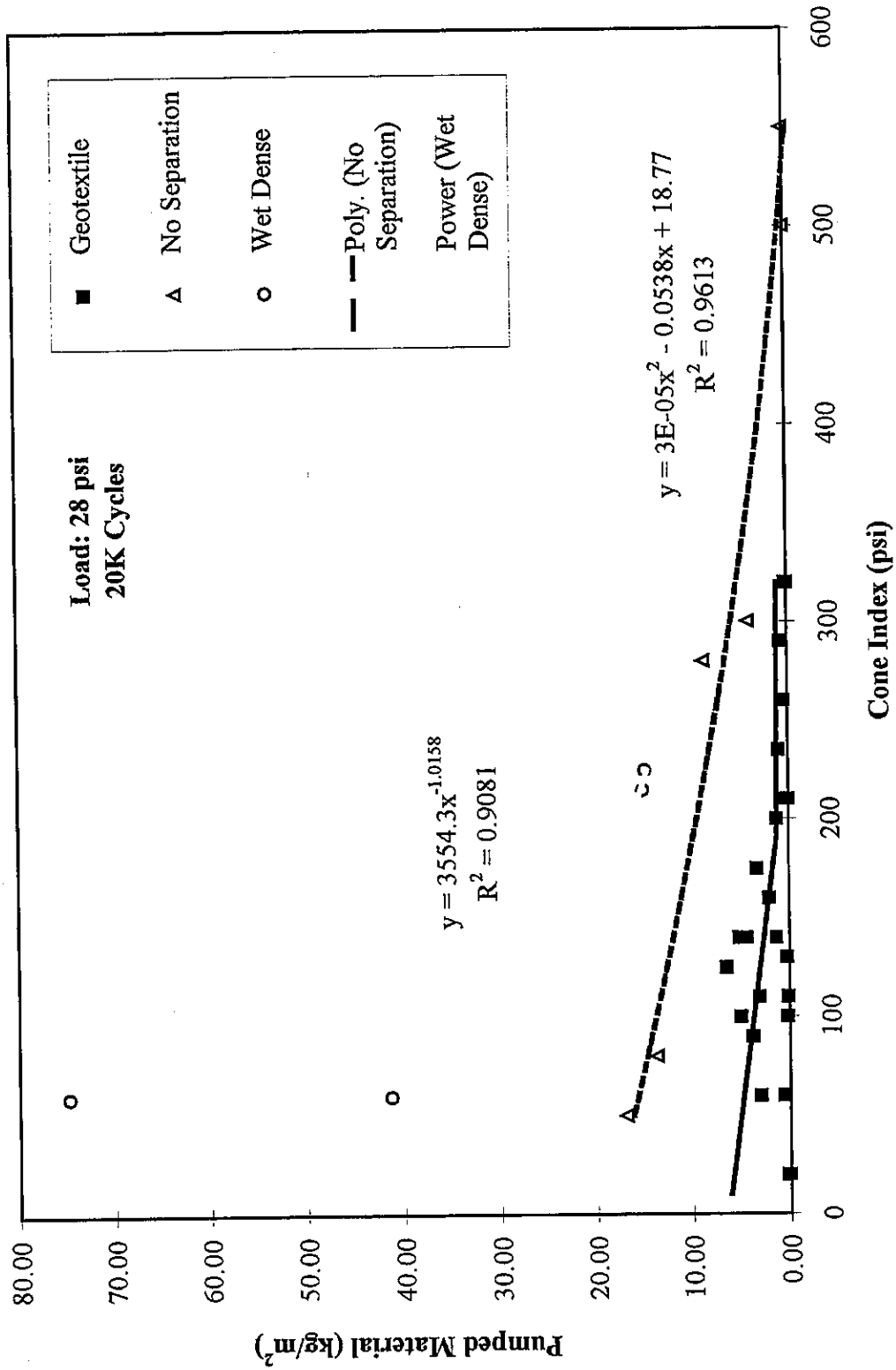


Figure 6.63: Wisconsinan Silty Clay Till / Separation / CA 7, Pumped/Intruded Material/Material Transfer vs Cone Index

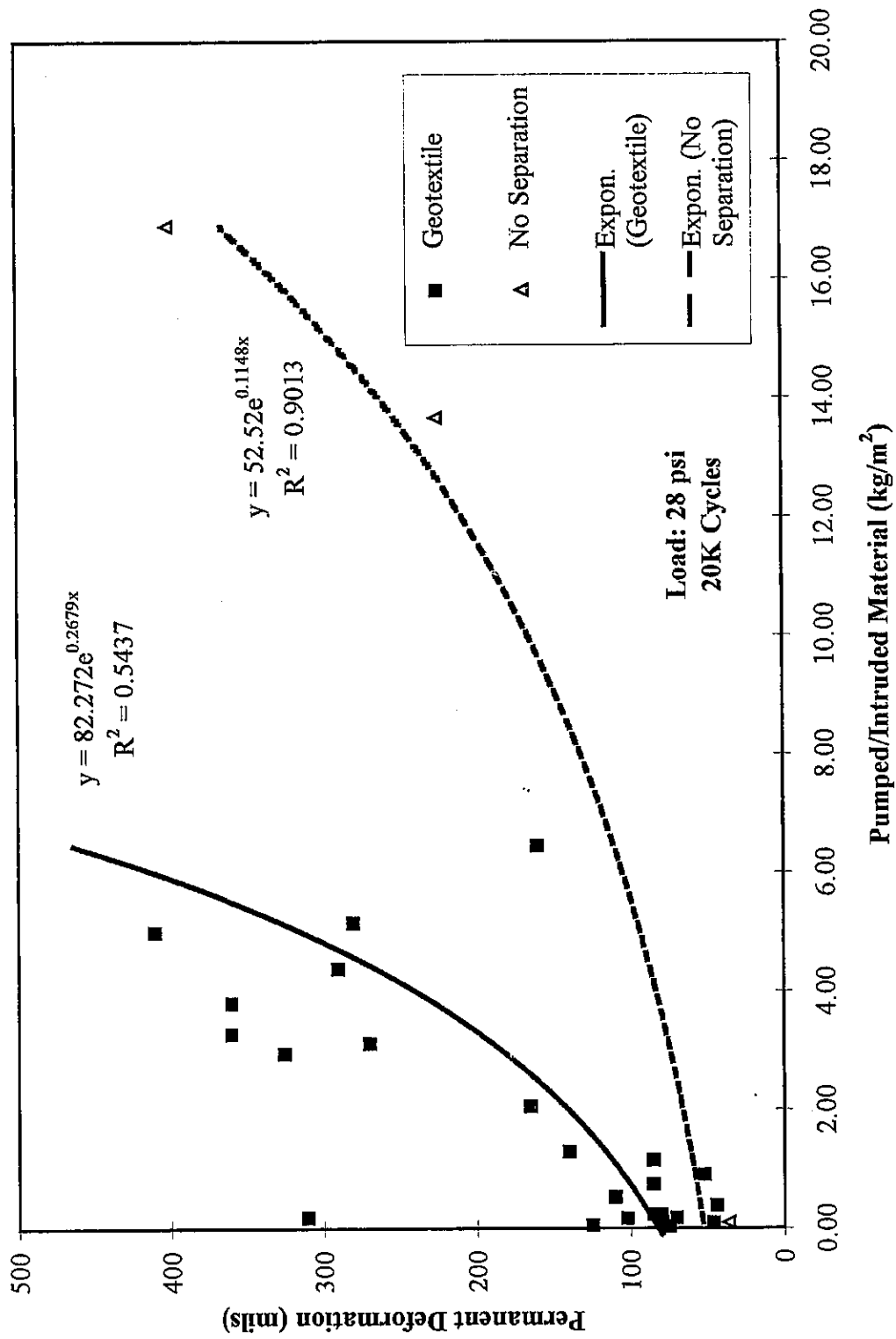


Figure 6.64: Wisconsinan Silty Clay Till / Separation / CA 7, Permanent Deformation vs Pumped/Intruded Material

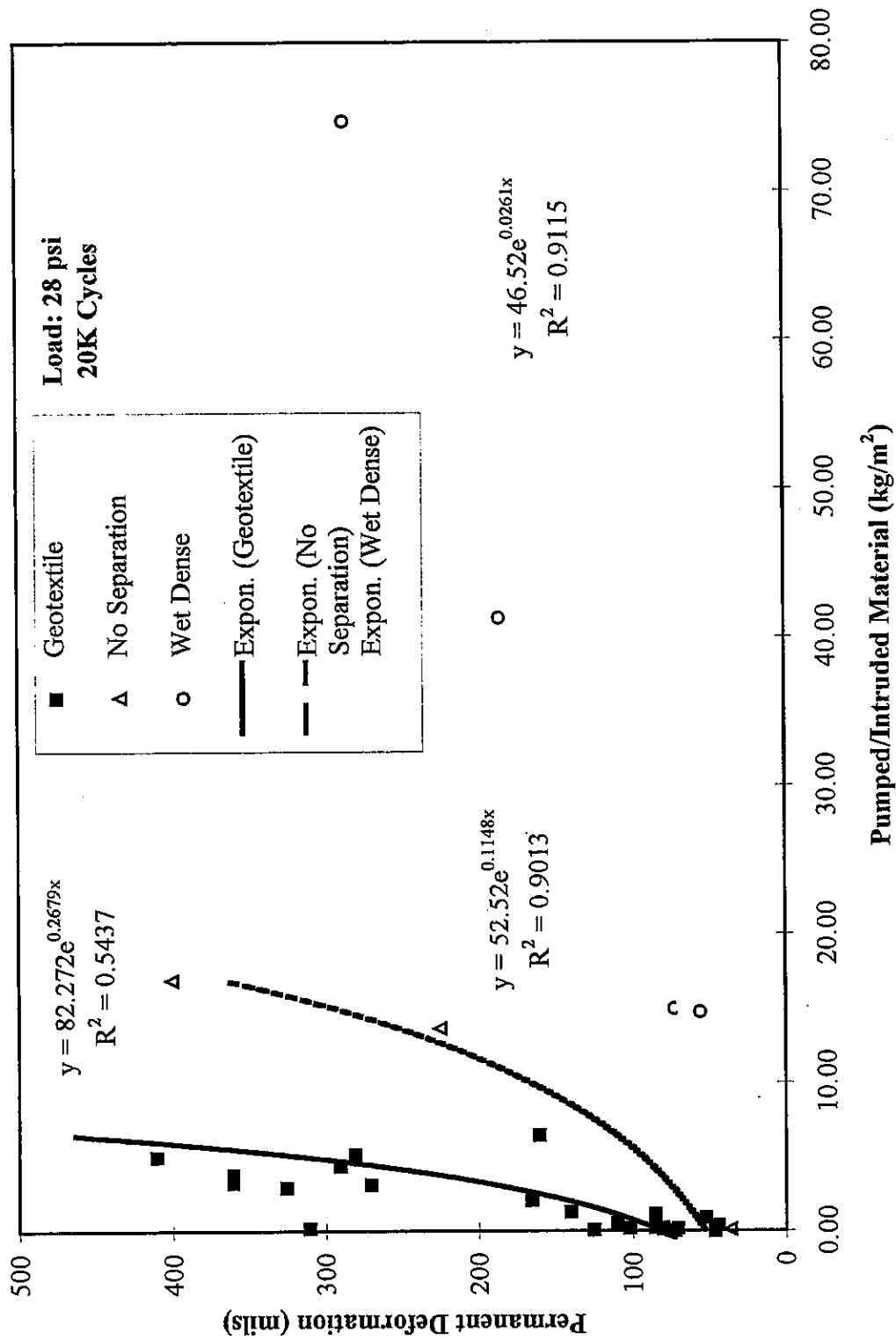


Figure 6.65: Wisconsin Silty Clay Till / Separation / CA 7, Permanent Deformation vs Pumped Material/Material Transfer

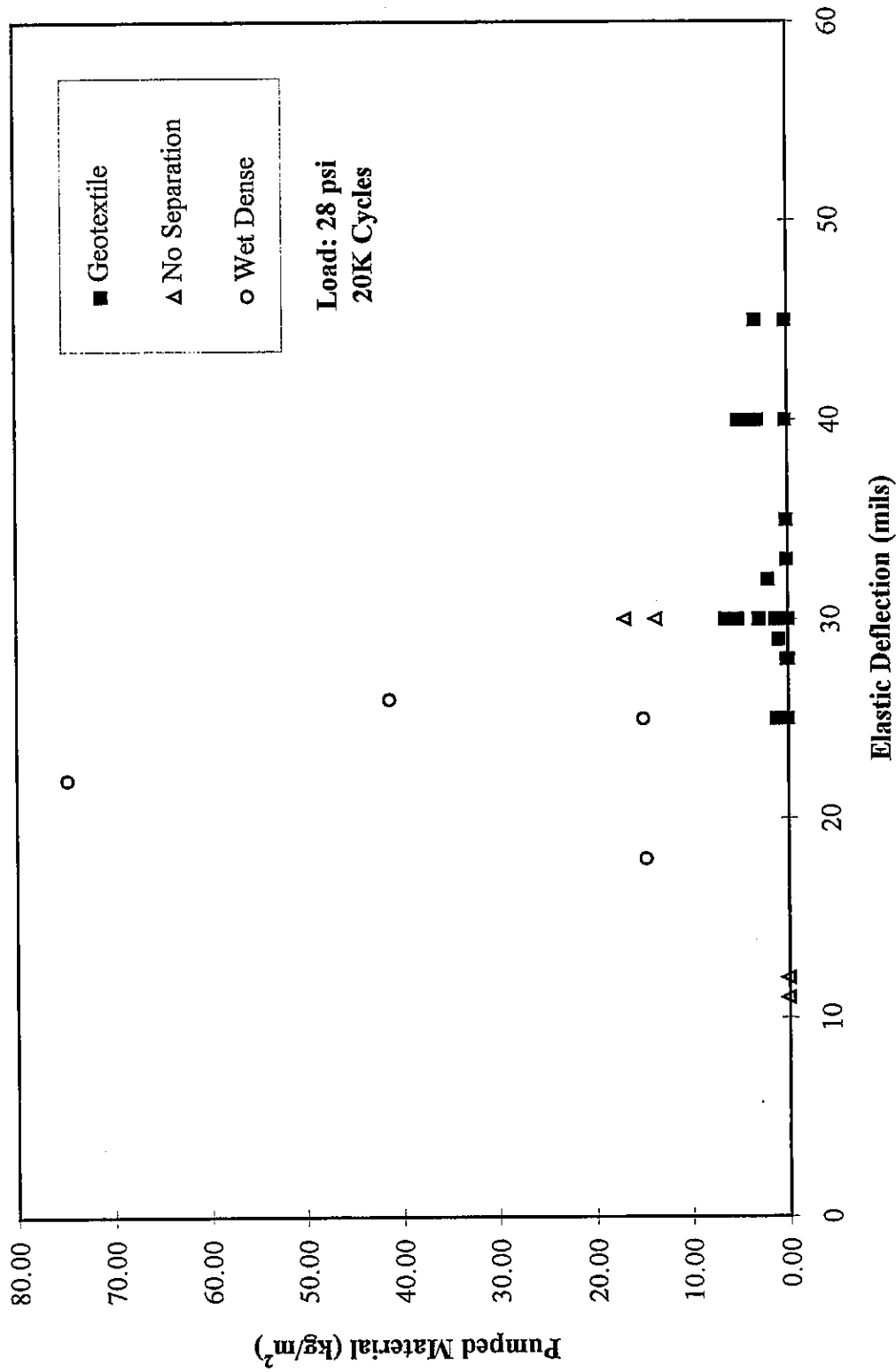


Figure 6.66: Wisconsinan Silty Clay Till / Separation / CA7, Pumped Material/Material Transfer vs Elastic Deflection

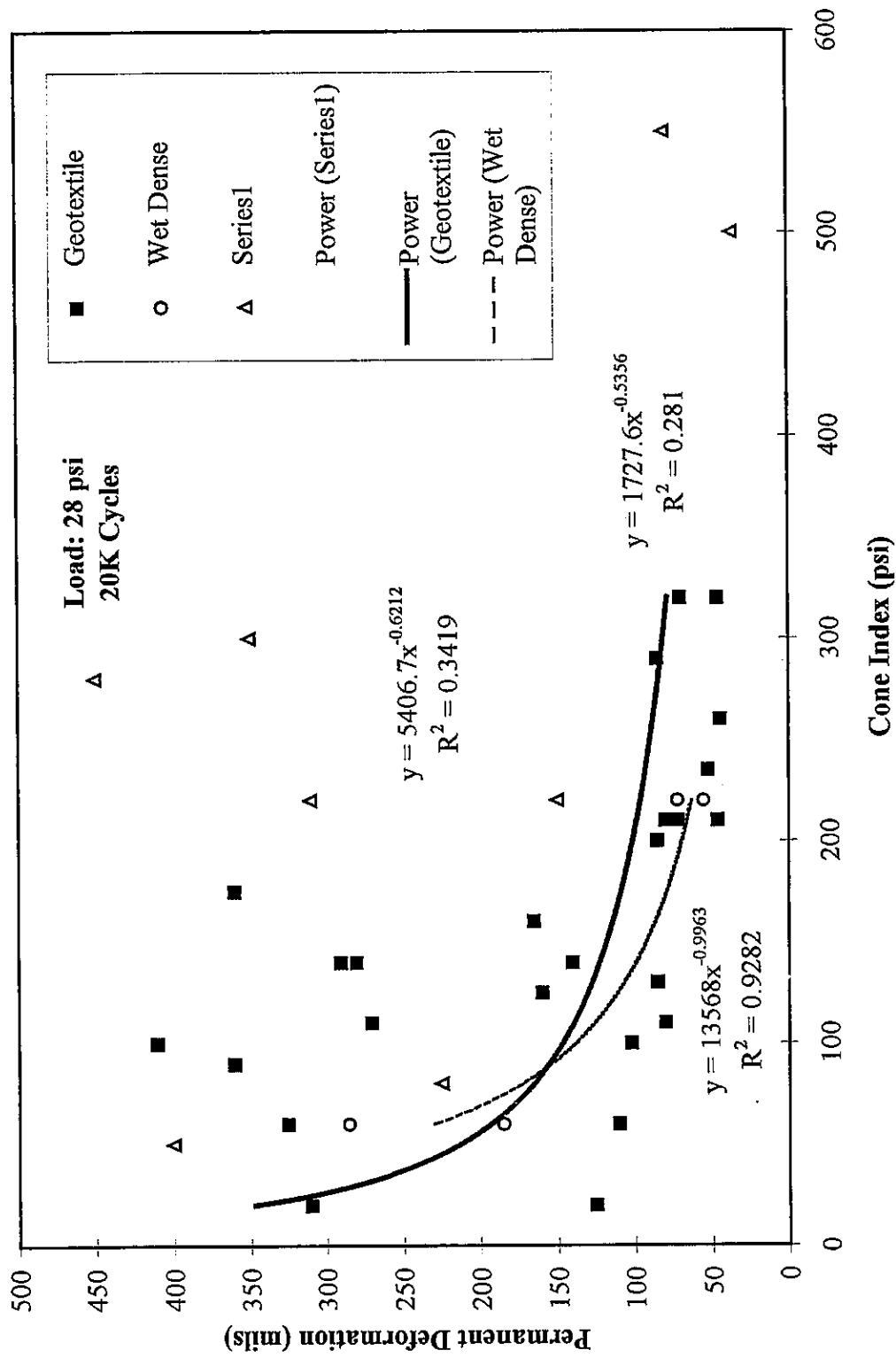


Figure 6.67: Wisconsinan Silty Clay Till / Separation, Permanent Deformation vs Cone Index

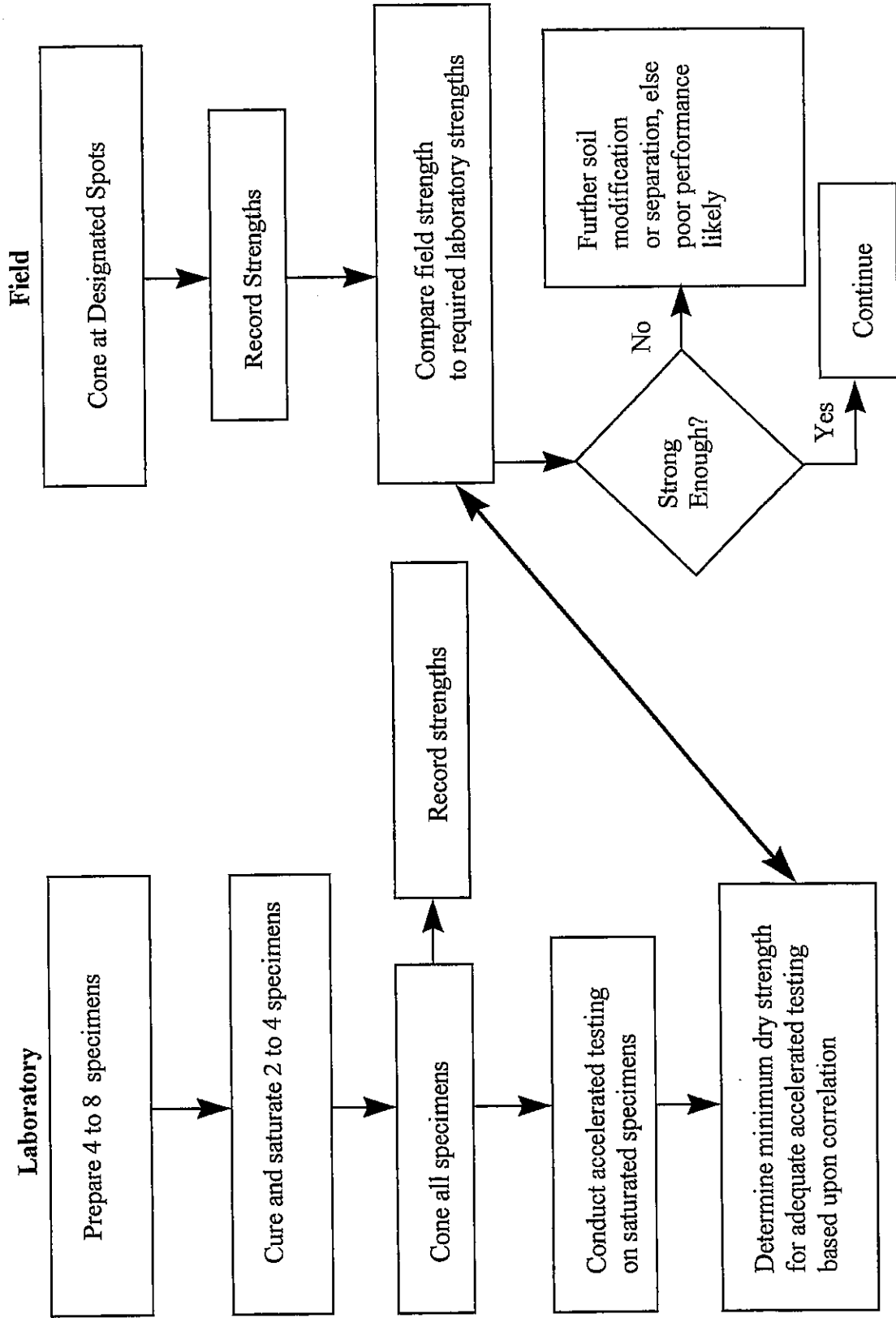


Figure 6.68: Proposed Index Test Flow Chart

7. SUMMARY AND SIGNIFICANT FINDINGS

7.1 Summary

Geotextile and dense-graded separation layers were tested in the laboratory under accelerated conditions to assess their performance with lime stabilized soil subgrades and open-graded aggregate base courses. When no separation was placed between the subgrade and open-graded aggregate, aggregate intrusion and pumping occurred consistently and to a degree directly dependent upon soil strength. With geotextile separation, minimal amounts of pumping occurred and the amount decreased in proportion to soil strength. Regardless of soil strength, the geotextile maintained separation between the subgrade and open-graded aggregate and minimized total permanent deformations. Dense-graded separation layers performed differently depending upon the condition of the layer. When dry, the dense-graded layer sufficiently prevented fines from pumping into the open-graded aggregate. When wet, the dense-graded layer often merged with the open-graded layer under accelerated testing. For stronger soils with $CBR > 4$, minimal pumping occurred for all 3 separation methods. Below this value, pumping tended to increase with decreasing soil strength. Overall, the geotextile performed the best separation function in this research by yielding on average the least amount of soil pumping and permanent deformation.

7.2 Significant Findings

1. Accelerated testing can be used to evaluate the performance of separation layers used in conjunction with stabilized soils and open-graded aggregates provided key points are kept in mind:

A. The accelerated test conditions used in this research hastened the failure modes commonly seen for these materials in the field. Many more testing combinations can be evaluated under these conditions than under normal field loading conditions.

B. The rate of permanent deformation increase and the magnitude of permanent deformation with accelerated testing were both significantly higher than seen under

field loading levels. Comparisons made in Chapter 6 for low level and accelerated loading showed a consistently higher amount of permanent deformation for accelerated loading than for typical loading. Laboratory permanent deformations were not equivalent to field deformations, however the accelerated test gives an indication of a sections' field performance.

C. The magnitude of soil pumping under these accelerated testing conditions (20,000 cycles at 28 psi) were comparable to those seen at lower stress levels and higher durations (500,000 cycles at 8 psi). Due to this behavior, laboratory soil pumping magnitudes were a good indicator of performance under field loading conditions for large numbers of loading cycles.

D. A different mode of failure occurred under accelerated loading conditions than under a low magnitude of loading. Parts B and C must be viewed in relation to this fact. During low level loading, soil pumping/intrusion was an *upward* process. Due to the lengthy testing time and subsequent slurry formation, the soil was gradually forced a small amount at a time upward into the bottom of the aggregate base layer. Minimal permanent deformations occurred indicating the materials maintained their integrity. For accelerated conditions, the aggregate was shoved downward into the soil and the soil simply filled the voids existing in the aggregate or the locally stretched areas of the geotextile. This would explain why under accelerated loading conditions significantly higher permanent deformations occurred yet pumping was comparable. This mechanism was a bearing capacity type failure in which the contact stresses of the aggregate exceeded the soil strength.

E. Soil strength can be obtained through a number of methods. Soils with equivalent cone indices may possess markedly different densities and moisture contents. Soils with comparable strengths as measured by the cone penetrometer may possess significantly different performance capabilities with regard to accelerated loading. Accelerated loading tests soil durability, erosion potential, and strength. For example, strength obtained through increased density and short curing times may not be equivalent to strength obtained with decreased density and long curing times. In the latter case, strength is developed from the formation of

cementing agents which increases durability. However, the lower density may result in higher moisture contents which increases erosion potential due to higher pore water pressures and porosity which tends to offset this durability gain.

2. Subgrade intrusion was a direct function of soil strength, all other conditions being equal. For the high load levels used in this accelerated testing research, a distinct breakpoint occurred at a CI of 200 (CBR 4), above which minimal intrusion occurred, and below which significant intrusion took place.

3. The degree of saturation, and perhaps more importantly the soil moisture content was directly related to soil strength and performance in this research. Soils approaching saturation, even those compacted to maximum dry density and lime treated, suffered significant weakening on the order of 80+% strength loss. This strength loss at saturation translated directly into the increase degree of pumping.

4. Samples prepared at lower levels of compaction showed a higher percentage strength loss at saturation than did samples compacted at higher (AASHTO T99 and greater) levels. The higher void ratios in these soils allowed for easier penetration of water into the soil pores.

5. The mid-gradation open-graded aggregate tested in this research imparted severe contact stresses on the underlying separation layers and subgrade soils. These stresses decreased as the size of aggregate contacting the underlying layers decreased. Variability in the aggregate gradation and position of the aggregate relative to the subgrade affected the testing results. A more uniform or well graded open-graded aggregate might have imparted a more consistent footprint and lower stresses on the separation layers. The lower soil contact stresses may result in significantly better separation layer performance.

6. A non-woven geotextile such as that tested in this research prevented intermixing of soil and aggregate under heavy repeated loading conditions. However, penetrations or indentations into the soil and pumping through the fabric at these points of indentation did occur. Ponding of water occurred at these penetration or indentation points. A geotextile separating non-stabilized weak soils showed lower pumping than did stronger stabilized specimens not separated.

7. Dense-graded aggregate (CA 6) separation layers offered significant separation benefits while “dry”, at optimum moisture and maximum dry density. Upon saturation or lowering in strength however, this layer allowed for significant intermixing of the open-graded layer into the dense-graded layer. Comparisons made in Chapter 6 with “dry” and “wet” CA 6 showed a marked drop-off in performance upon wetting of the dense-graded layer. Though the dense-graded layer often prevented the soil layer from intruding into the open-graded layer, the dense-graded layer itself intermixed into the open layer. It was not realistically possible to determine how much of the material that mixed into the open-graded layer was subgrade soil and dense-graded material due to the comparable fineness of both materials.

8. Intermixing at the dense-graded layer/soil interface was not as dramatic as in the dense-graded/open-graded interface due to the lower contact stresses imparted on the soil by the dense-graded layer. This was one important benefit of the dense-graded separation layer. Provided this material could be kept dry and intact, minimal soil appeared to intrude into the open-graded layer from below the dense-graded layer. However, in field conditions saturation is probable.

9. Soils of considerable strength ($CBR > 15$) showed no intrusion characteristics even when saturated and tested under accelerated conditions without any separation layer between the soil and the open-graded layer. However, long curing times are not practical in the field and quality control is more difficult.

10. The clay soil in this research consistently showed lower degrees of pumping and corresponding permanent deformations under accelerated testing conditions than did the silty clay till. However, selecting a geotextile to compliment each soil particle distribution could increase the separation layer performance.

11. The use of a separation layer between stabilized and lime modified soils and open-graded aggregate drainage layers is imperative. Geotextiles, specifically non-woven, heavy ($>10 \text{ oz./yd}^2$) fabrics will provide separation between the two layers, keeping them from intermixing. Pumping through the fabric occurred to some degree in this study, but large amounts of soil intrusion was mitigated. Dense-graded separation layers showed an adequate degree of separation potential provided the material did not approach saturation levels. At high moisture contents, the strength of this material significantly diminished and the dense-

graded layer and open-graded layer intermixed to a great degree and poor performance resulted.

12. The pumping/intrusion mechanism was shown to be a surface effect. In this research, the principal region of material interaction was the top two inches of soil. It may be possible to mitigate much of these types of failures by significantly increasing the strength of just the top layer of subgrade soil. This may be done by mechanical stabilization with Portland cement for example.

7.3 Suggestions for Further Research

Several research items not addressed in this research should be considered to complete and follow-up this study.

1. Conduct tests with varying gradations of drainable base course materials.
2. Evaluate additional soils, specifically characterize and test a low-PI silty soil that does not lime stabilize or modify easily.
3. Perform accelerated tests with geotextiles of varying weights and types.
4. Run additional low-level tests to enhance the comparison between accelerated loading and field loading, especially with dense-graded separation layers. Consider loading levels as low as 2-3 psi with loading repetitions up to and perhaps greater than 2,000,000 cycles.
5. Examine the applicability and practicality of the index testing procedure discussed in Chapter 6.
6. Sand has consistently been shown in the literature to provide adequate separation between soil and base layers. Conduct tests with properly graded sand filters to determine another reference performance capability.

APPENDIX

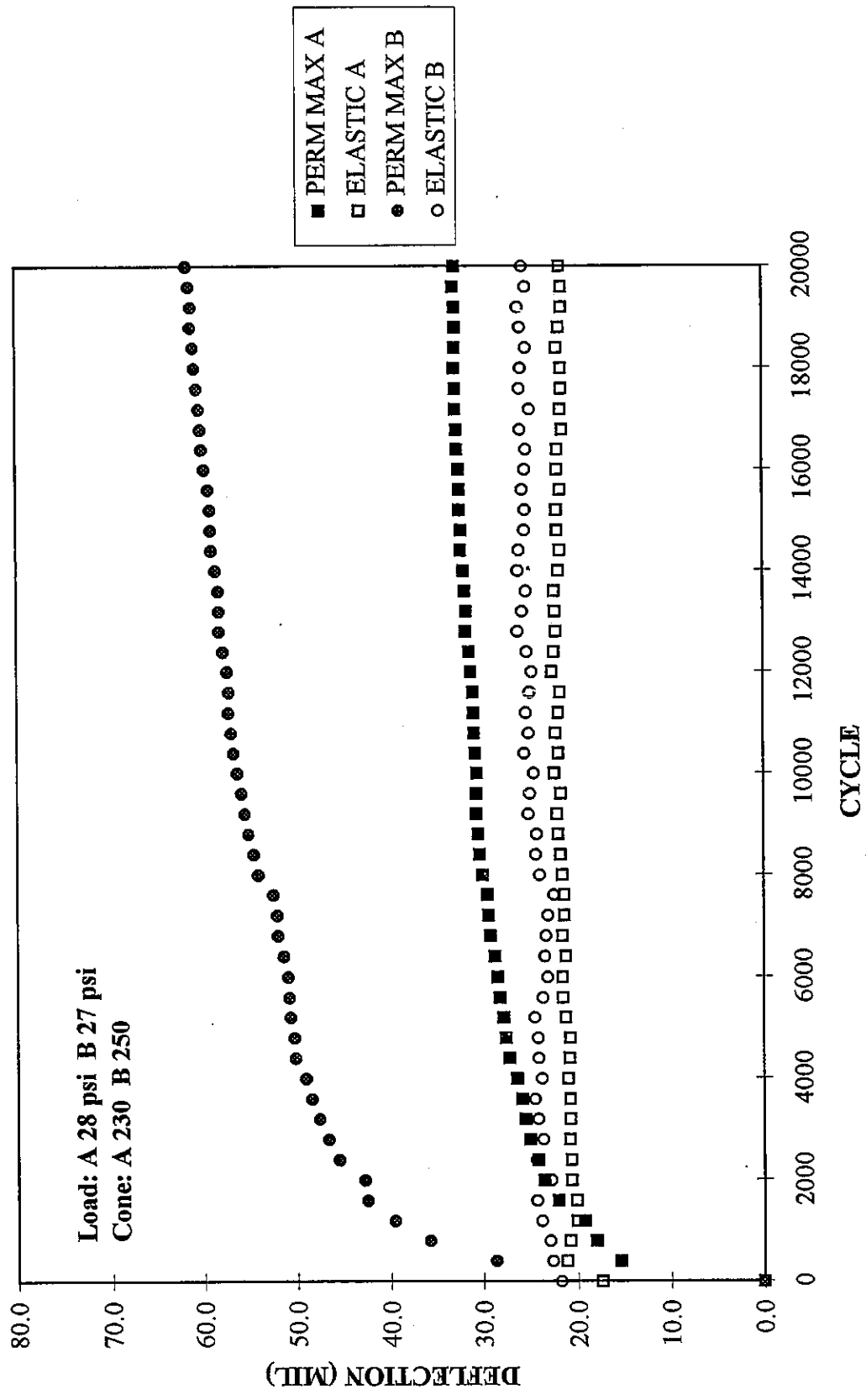


Figure A1: C0405AB / 1101 Geotextile / CA7, Deflection vs Cycle

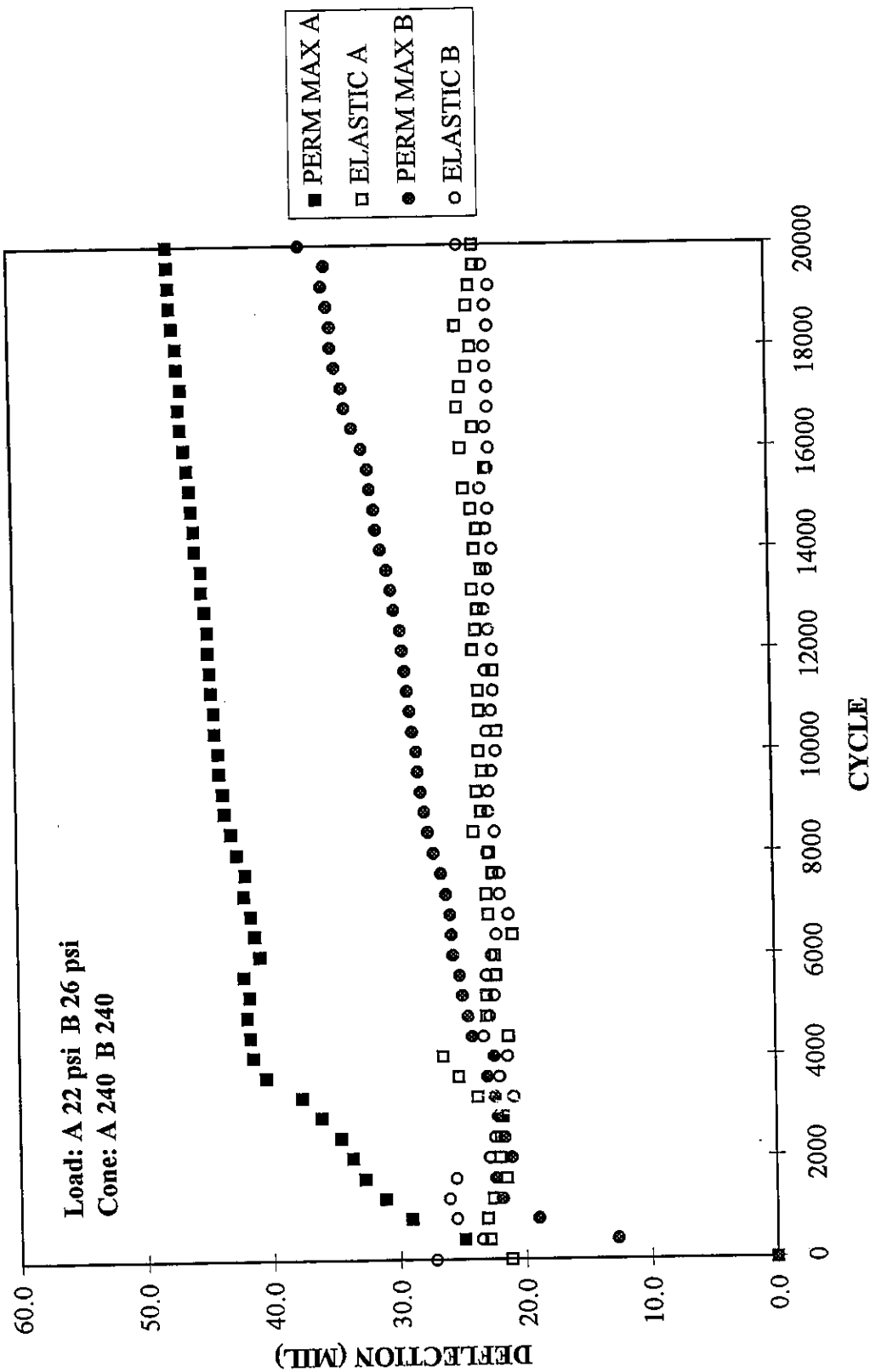


Figure A2: C0407AB / 1101 Geotextile / CA7, Deflection vs Cycle

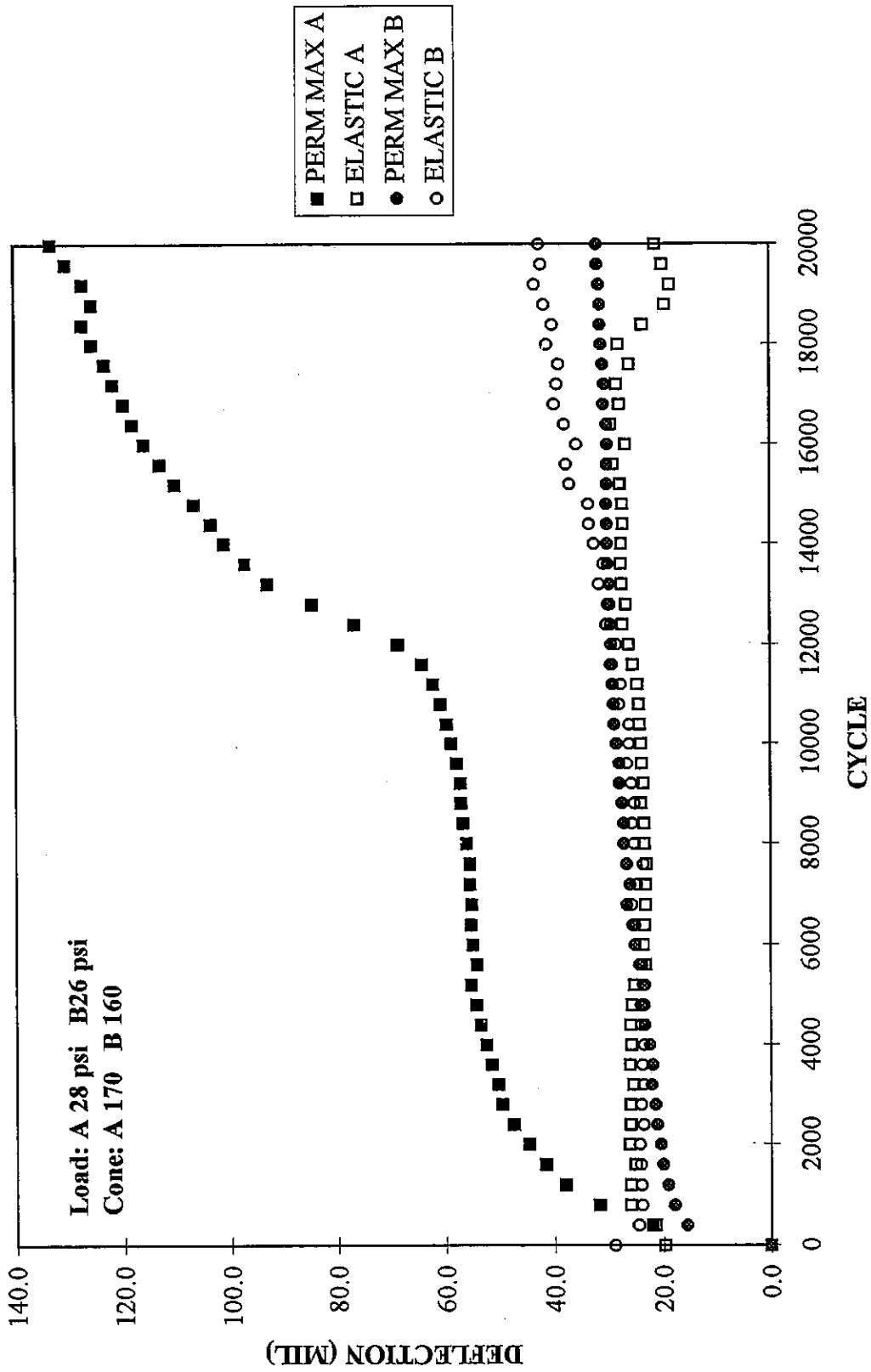


Figure A3: C0410AB / 1101 Geotextile / CA7, Deflection vs Cycle

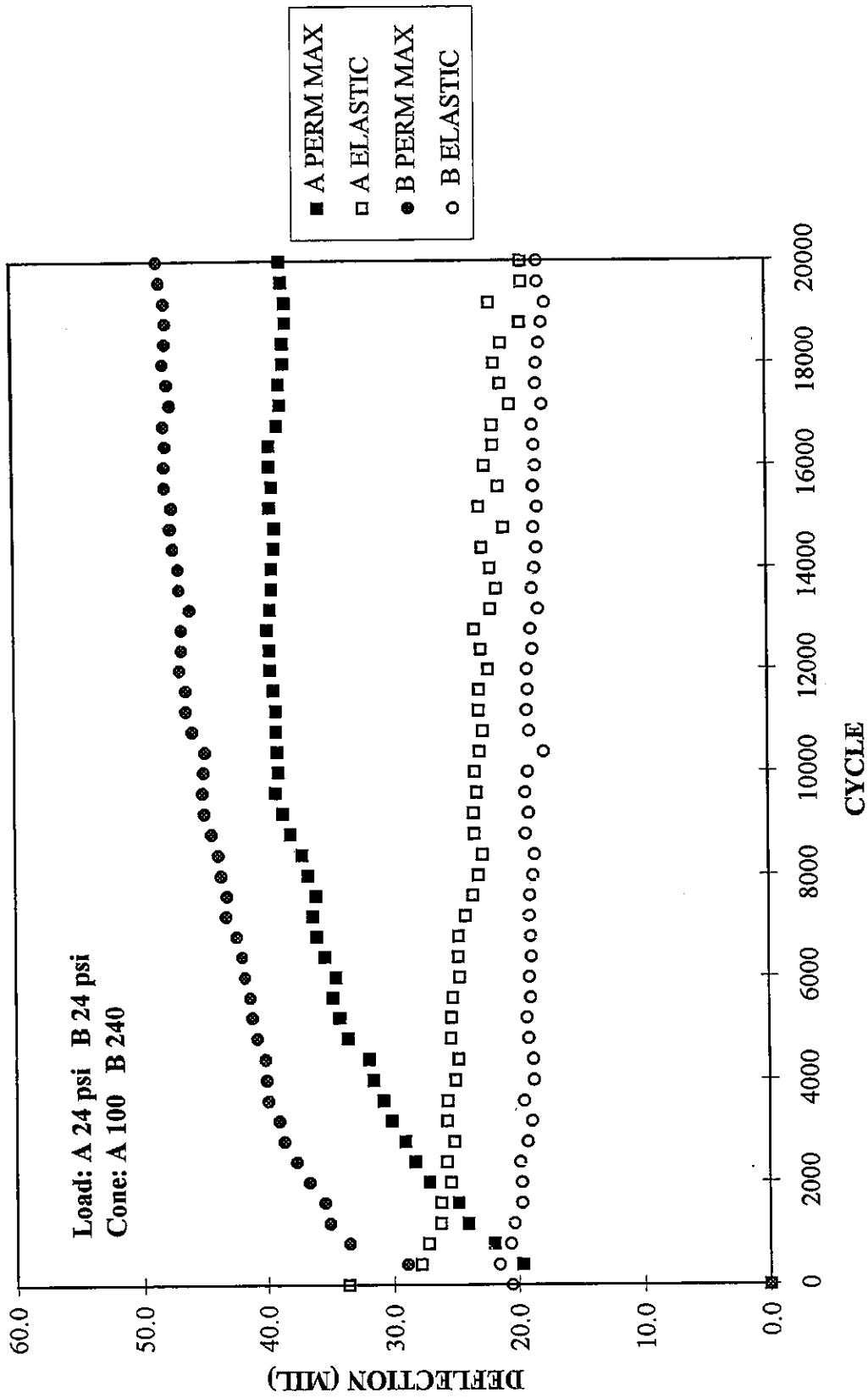


Figure A4: C0429AB / 1101 Geotextile / CA7, Deflection vs Cycle

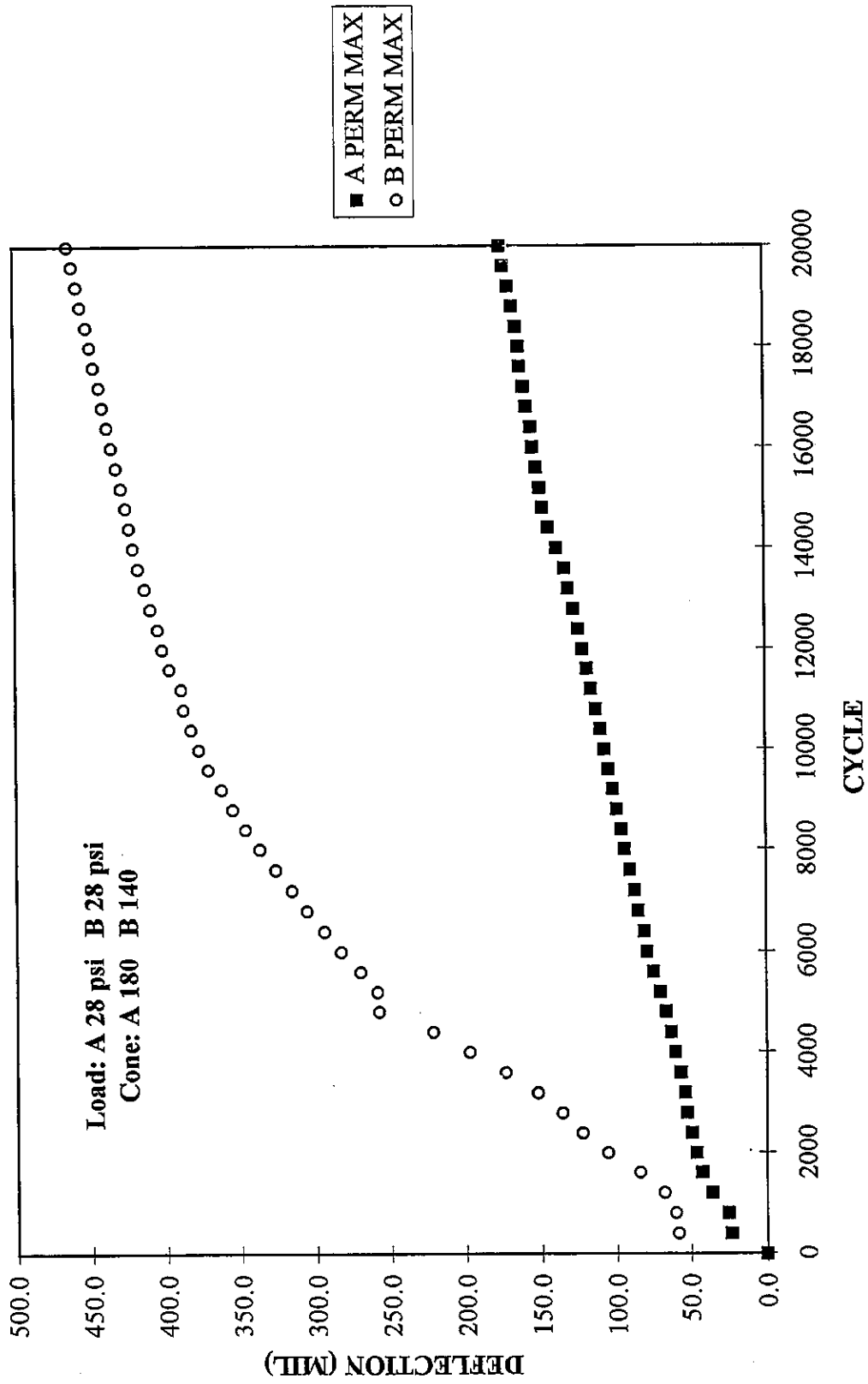


Figure A5: C0605AB / No Separation / CA7, Deflection vs Cycle

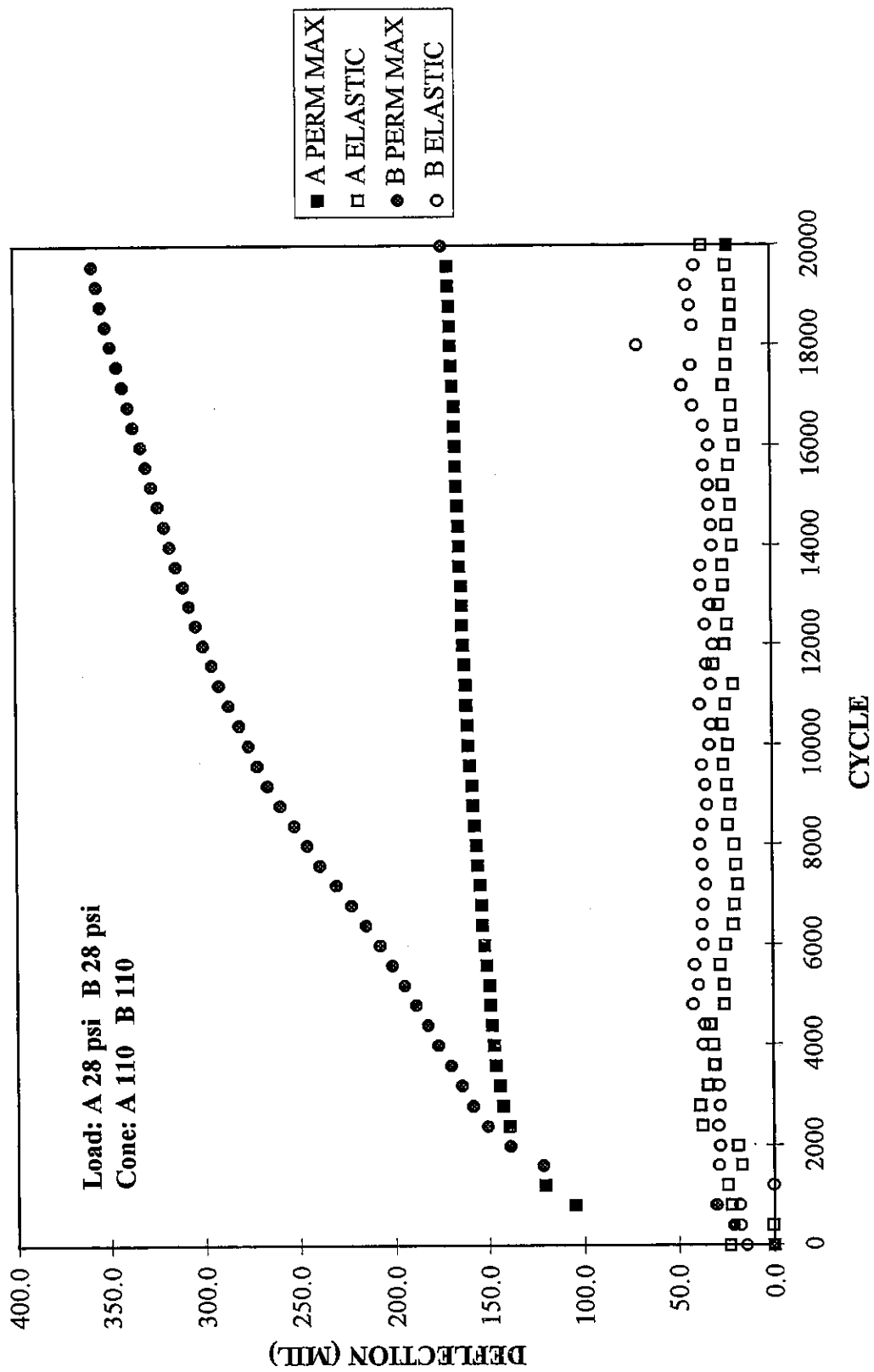


Figure A6: C0610AB / CA6 / CA7, Deflection vs Cycle

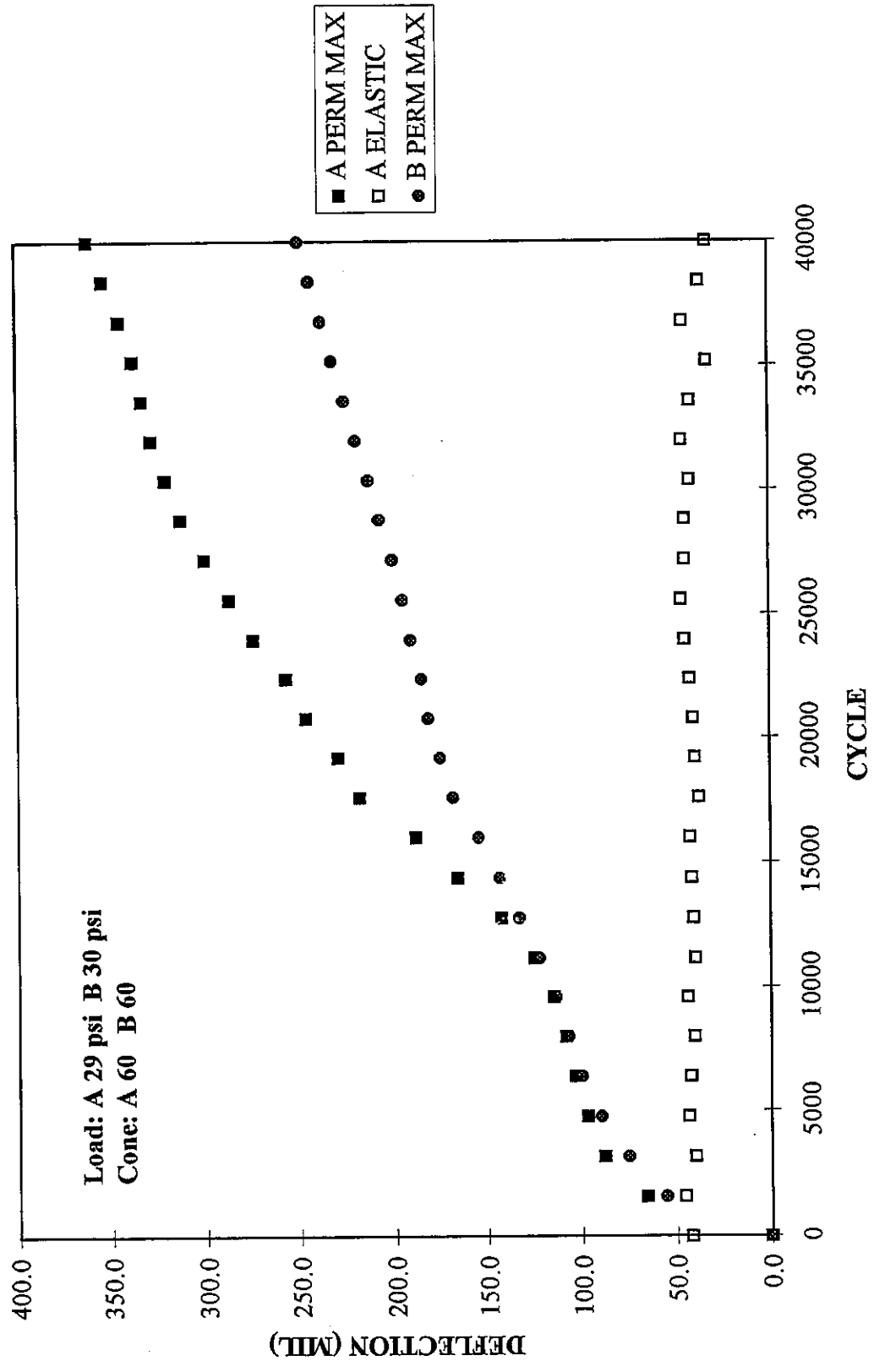


Figure A7: C0621AB / CA6 / CA7, Deflection vs Cycle

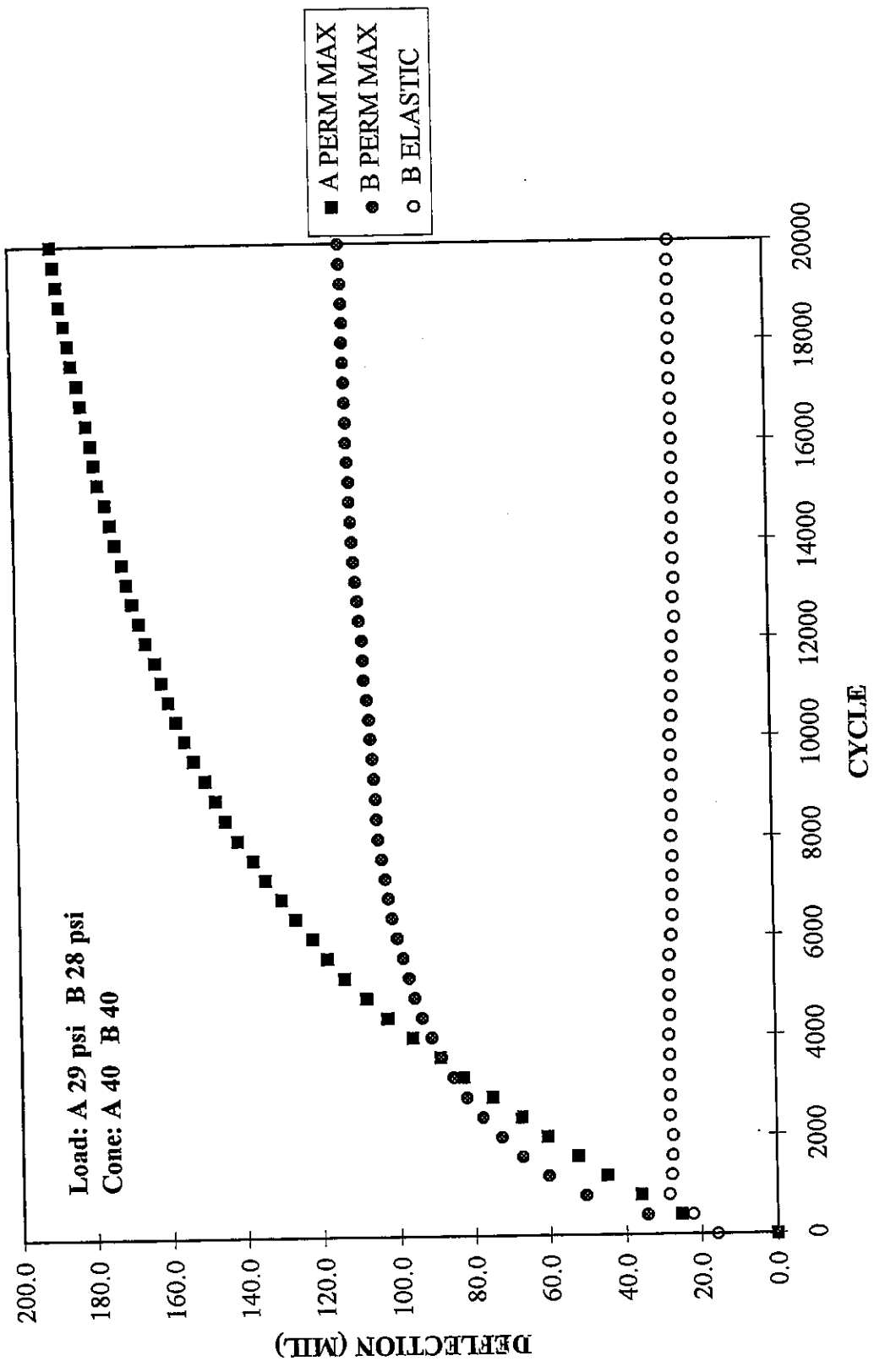


Figure A8: C0730AB / 1101 Geotextile / CA7, Deflection vs Cycle

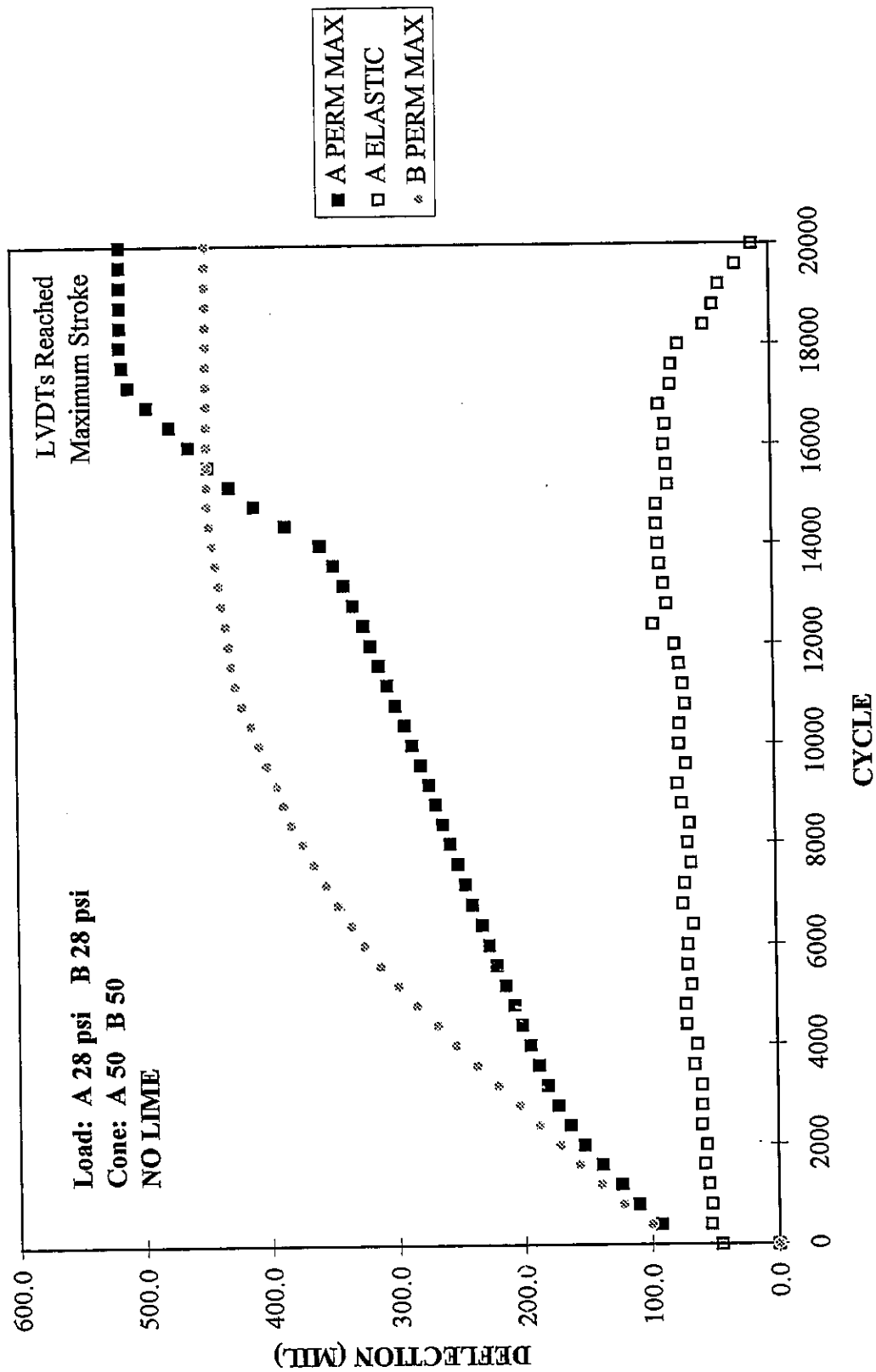


Figure A9: C0731AB / 1101 Geotextile / CA7, Deflection vs Cycle

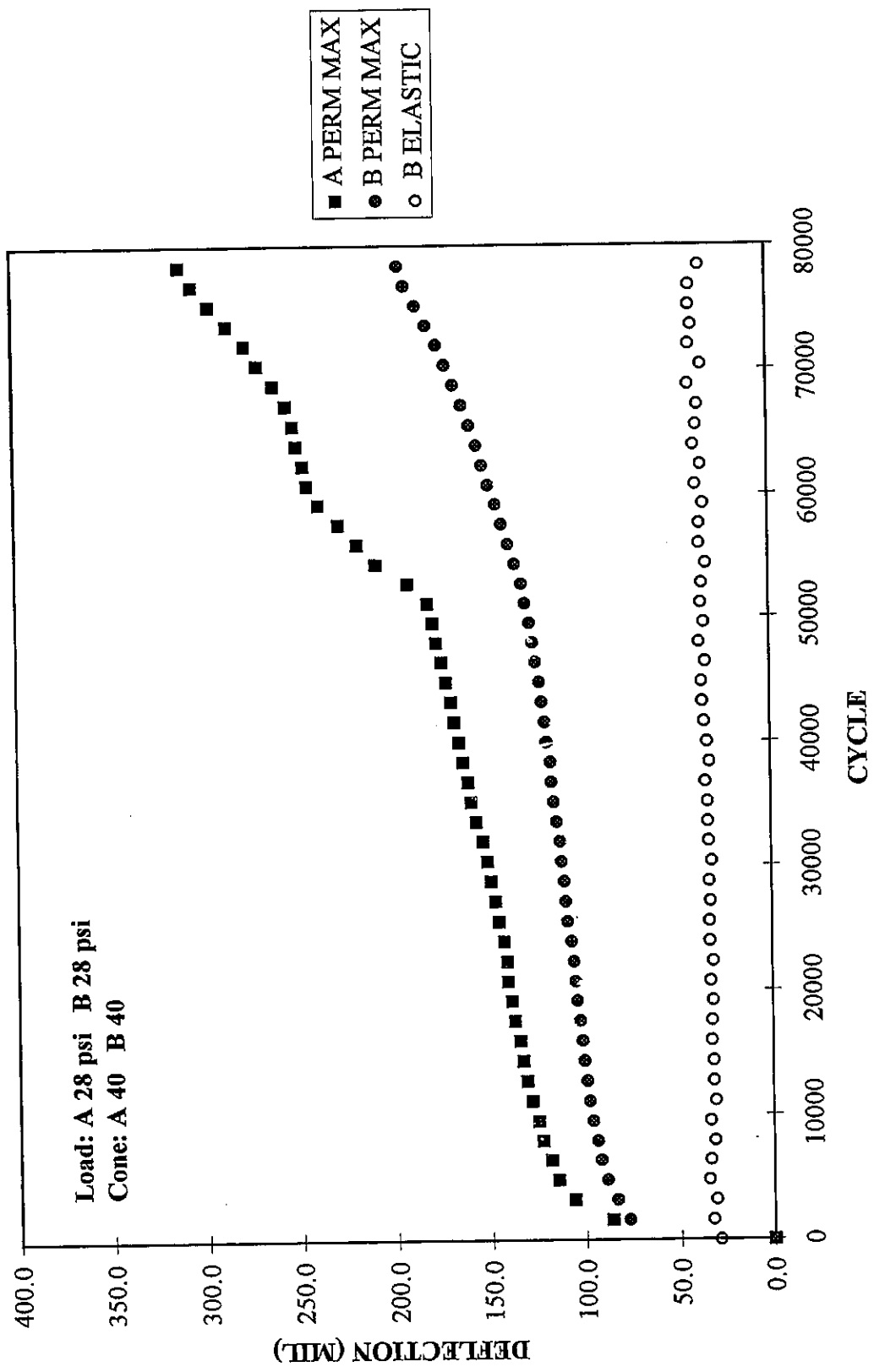


Figure A10: C0802AB / 1101 Geotextile / CA7, Deflection vs Cycle

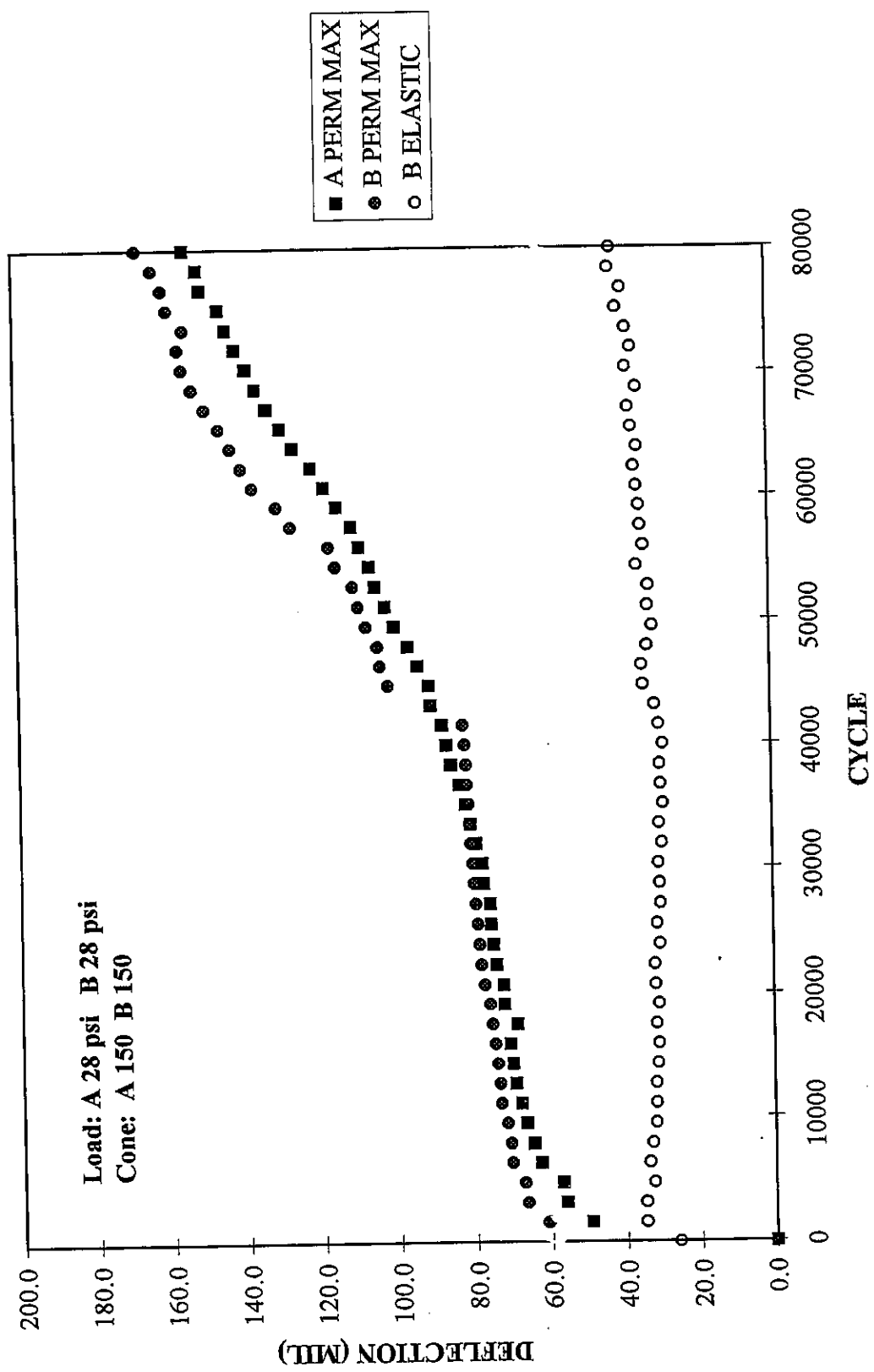


Figure A11: C0805AB / 1101 Geotextile / CA7, Deflection vs Cycle

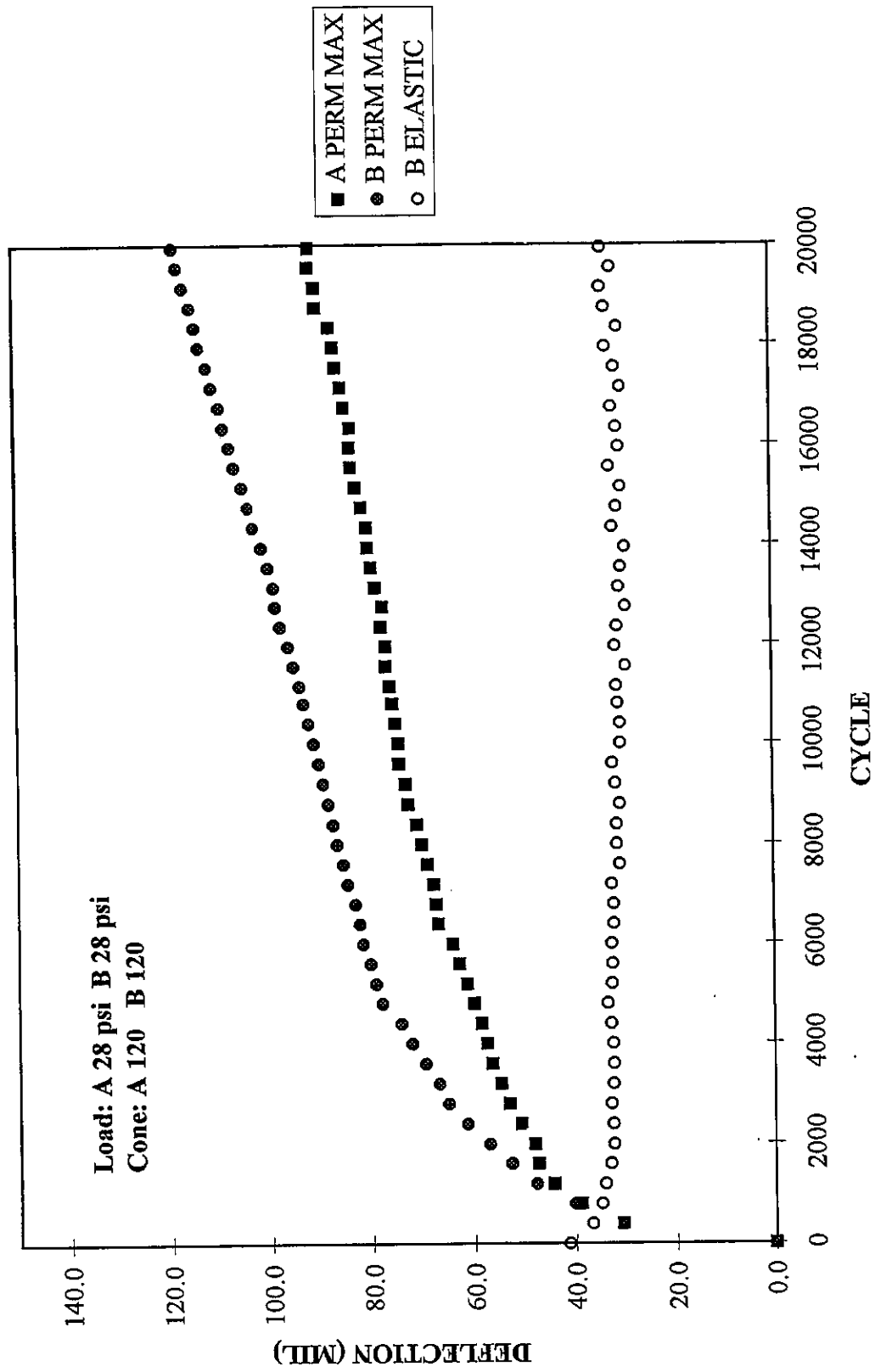


Figure A12: C0808AB / 1101 Geotextile / CA7, Deflection vs Cycle

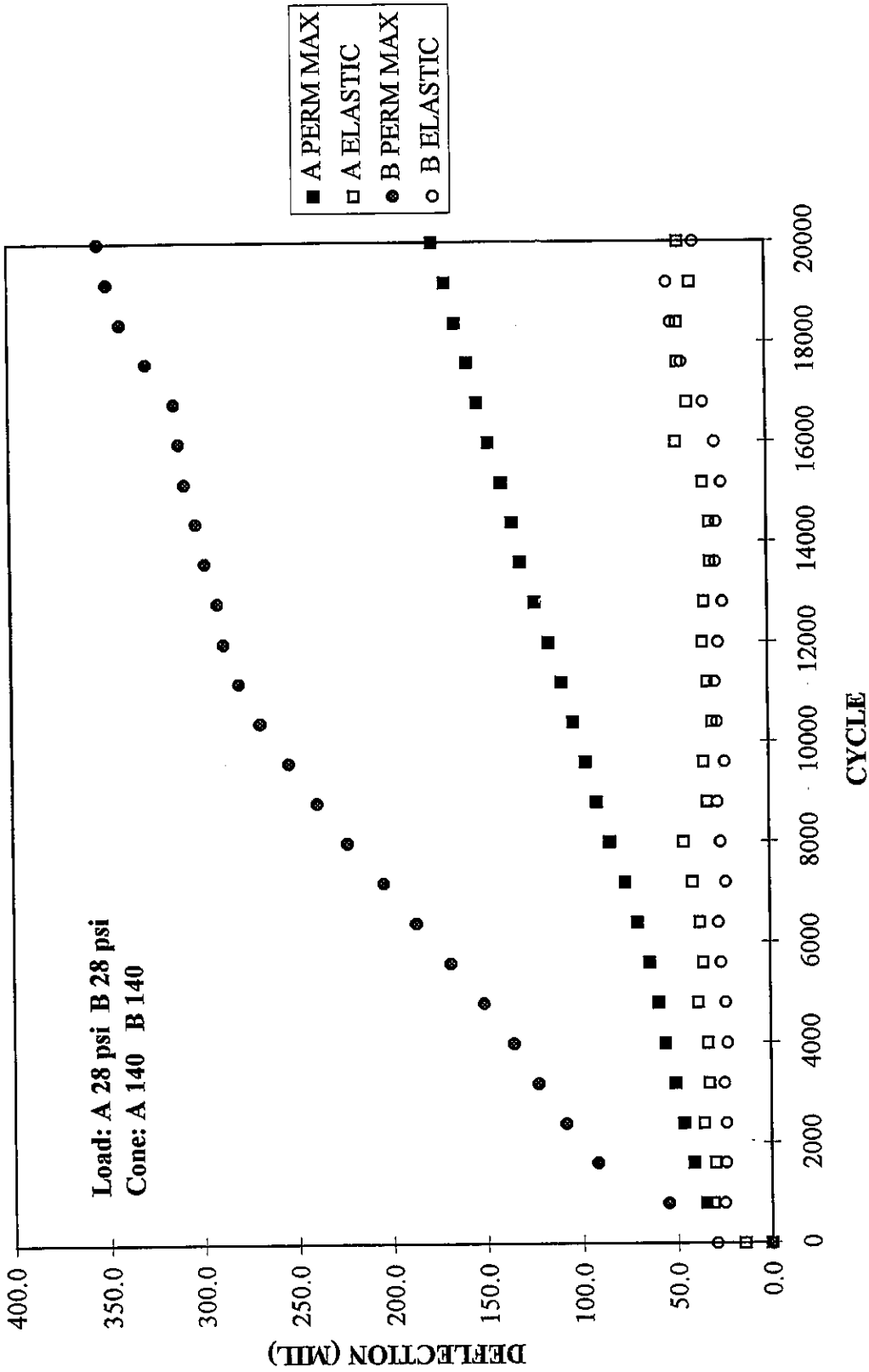


Figure A13: C0814AB / No Separation / CA7, Deflection vs Cycle

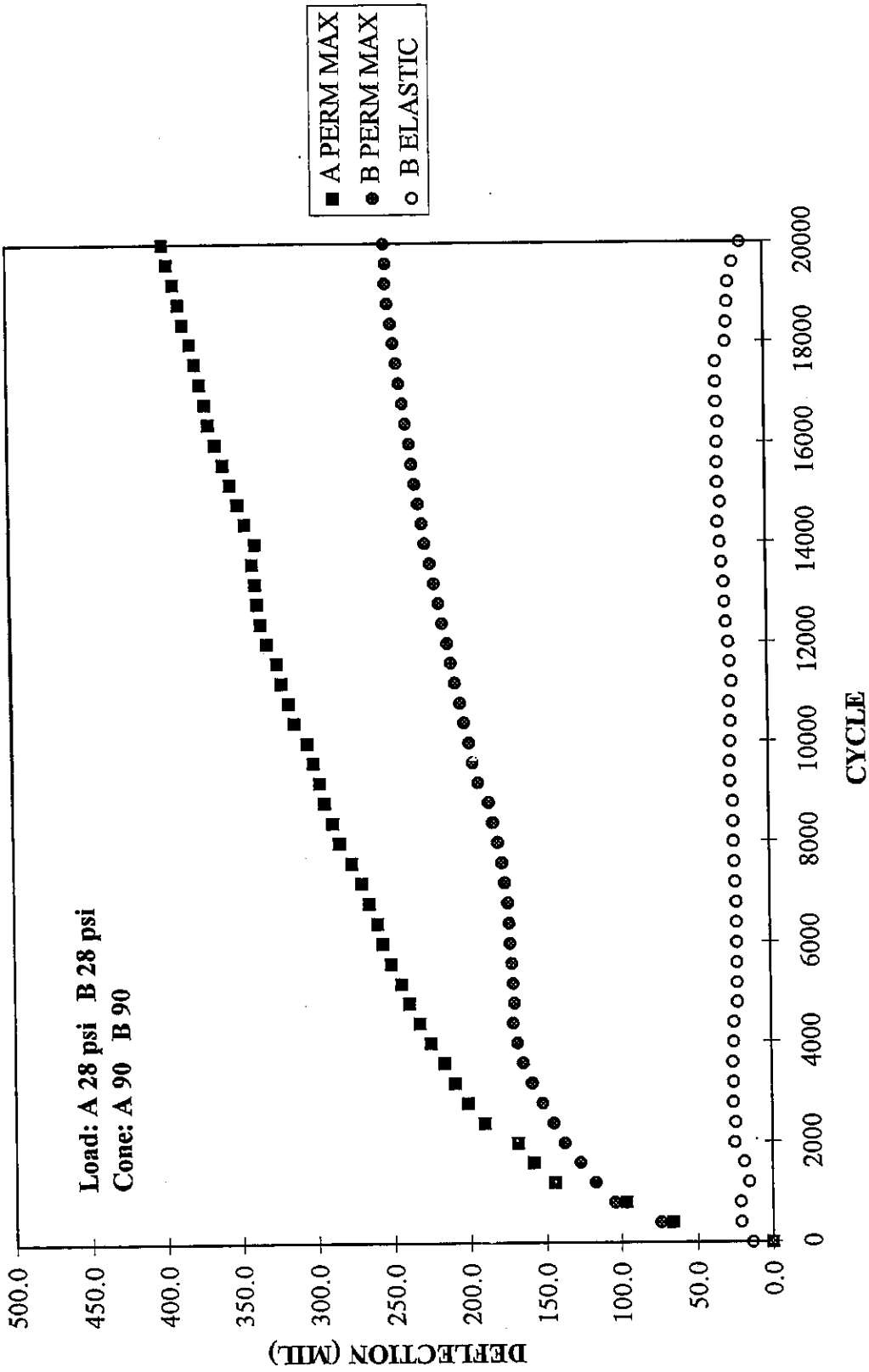


Figure A14: C0816AB / No Separation / CA7, Deflection vs Cycle

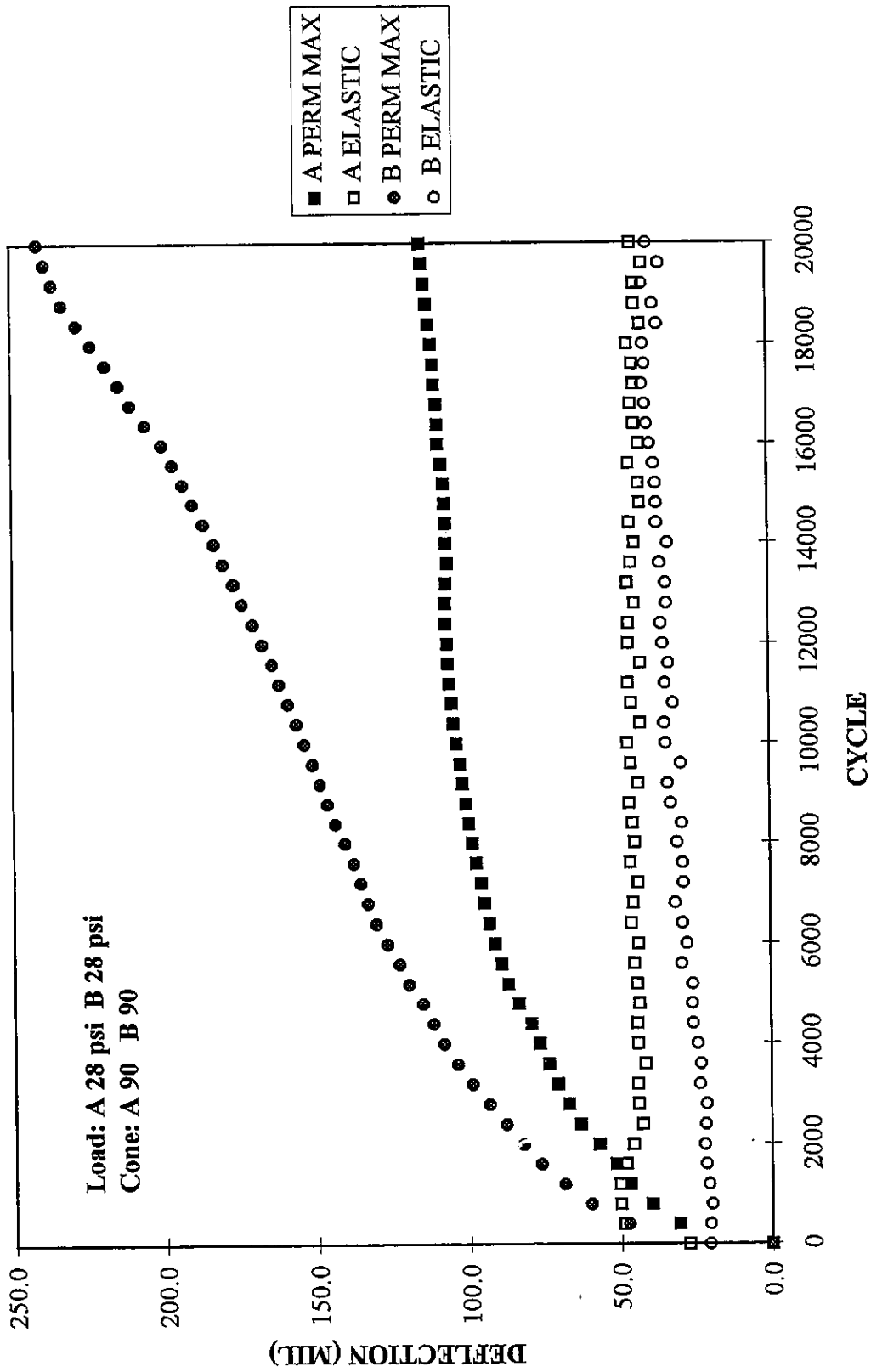


Figure A15: C0820AB / CA6 / CA7, Deflection vs Cycle

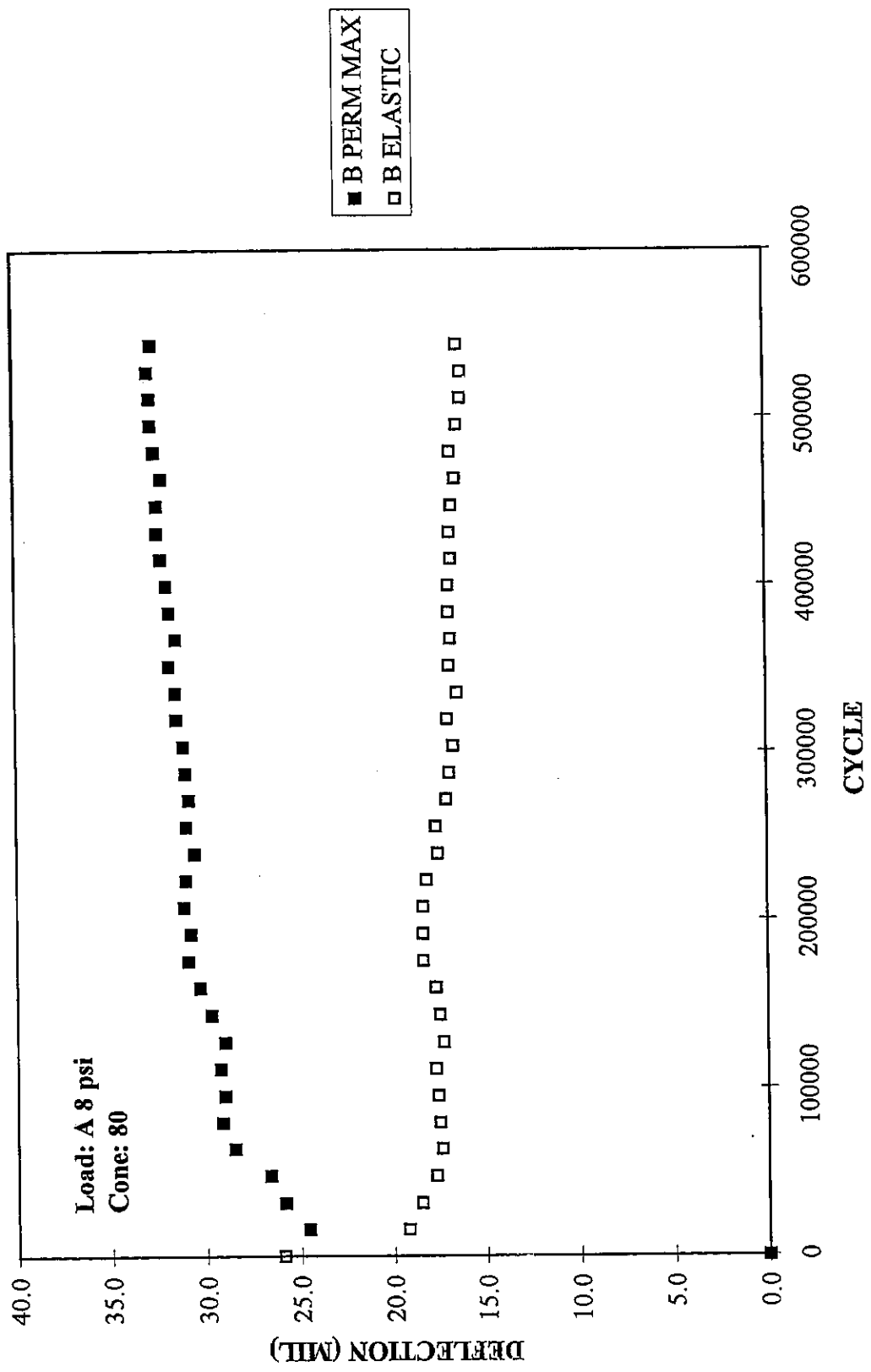


Figure A16: C0822B / 1101 Geotextile / CA7, Deflection vs Cycle

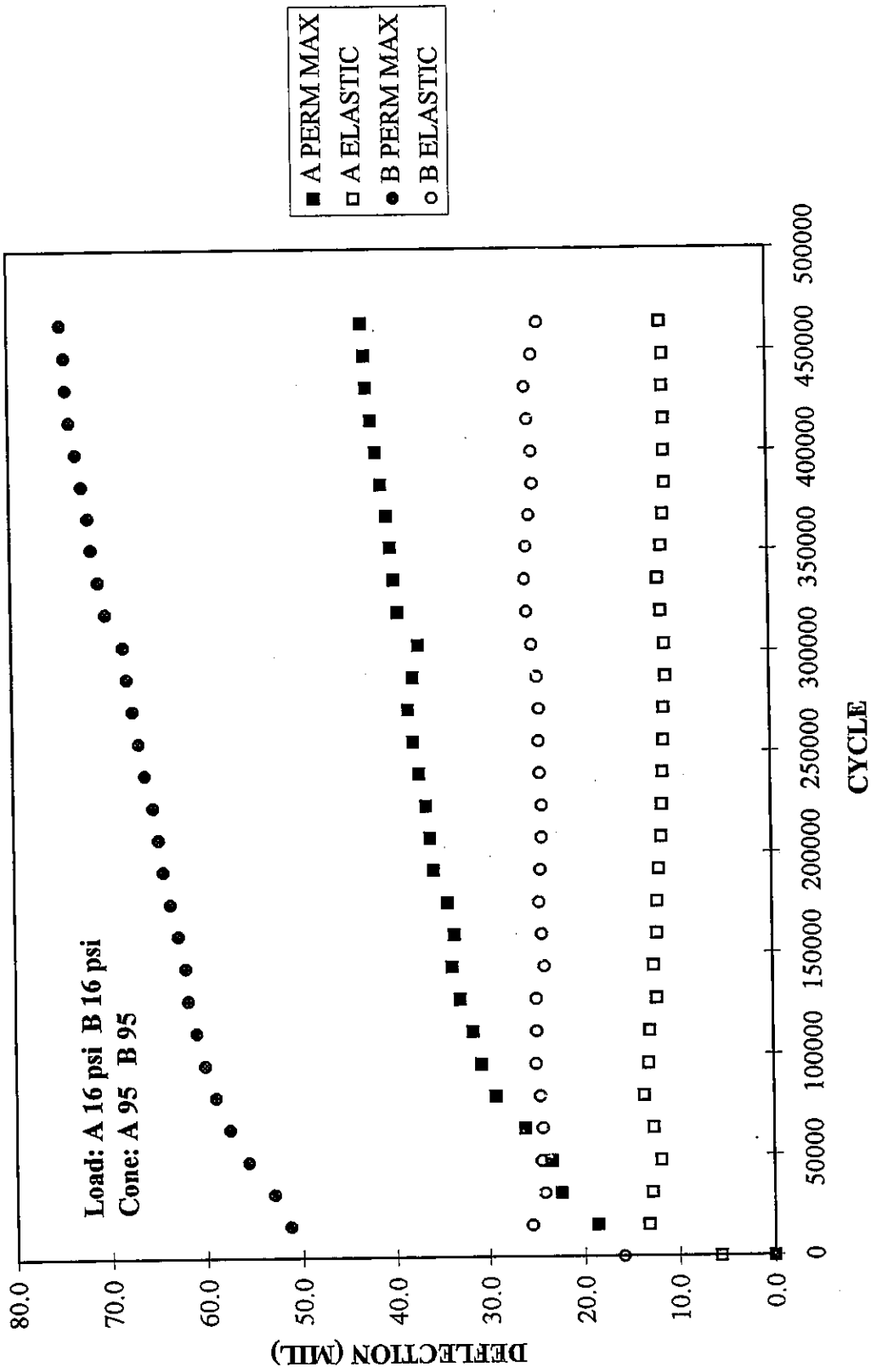


Figure A17: C0908AB / 1101 Geotextile / CA7, Deflection vs Cycle

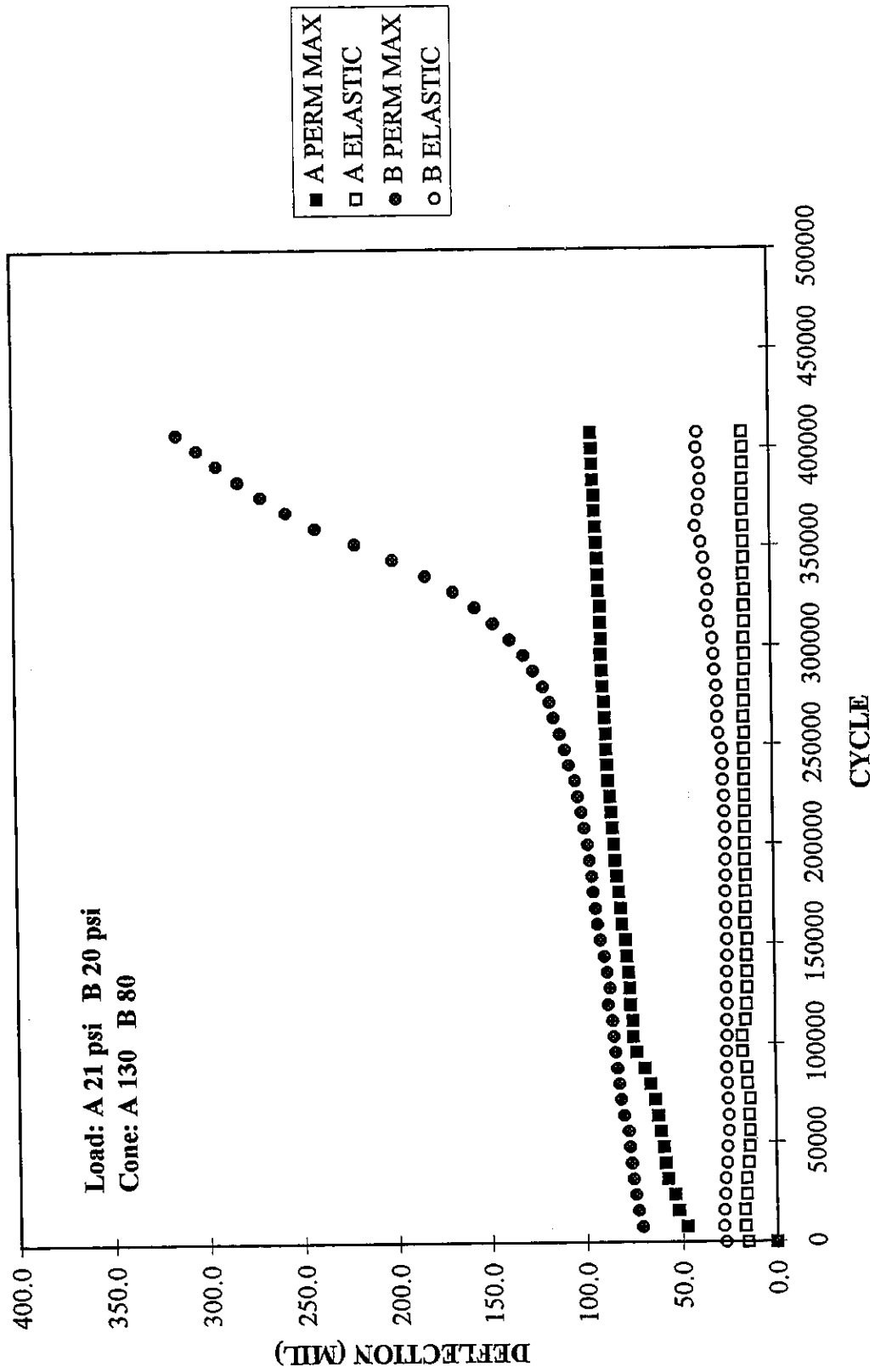


Figure A18: C0916AB / 1101 Geotextile / CA7, Deflection vs Cycle

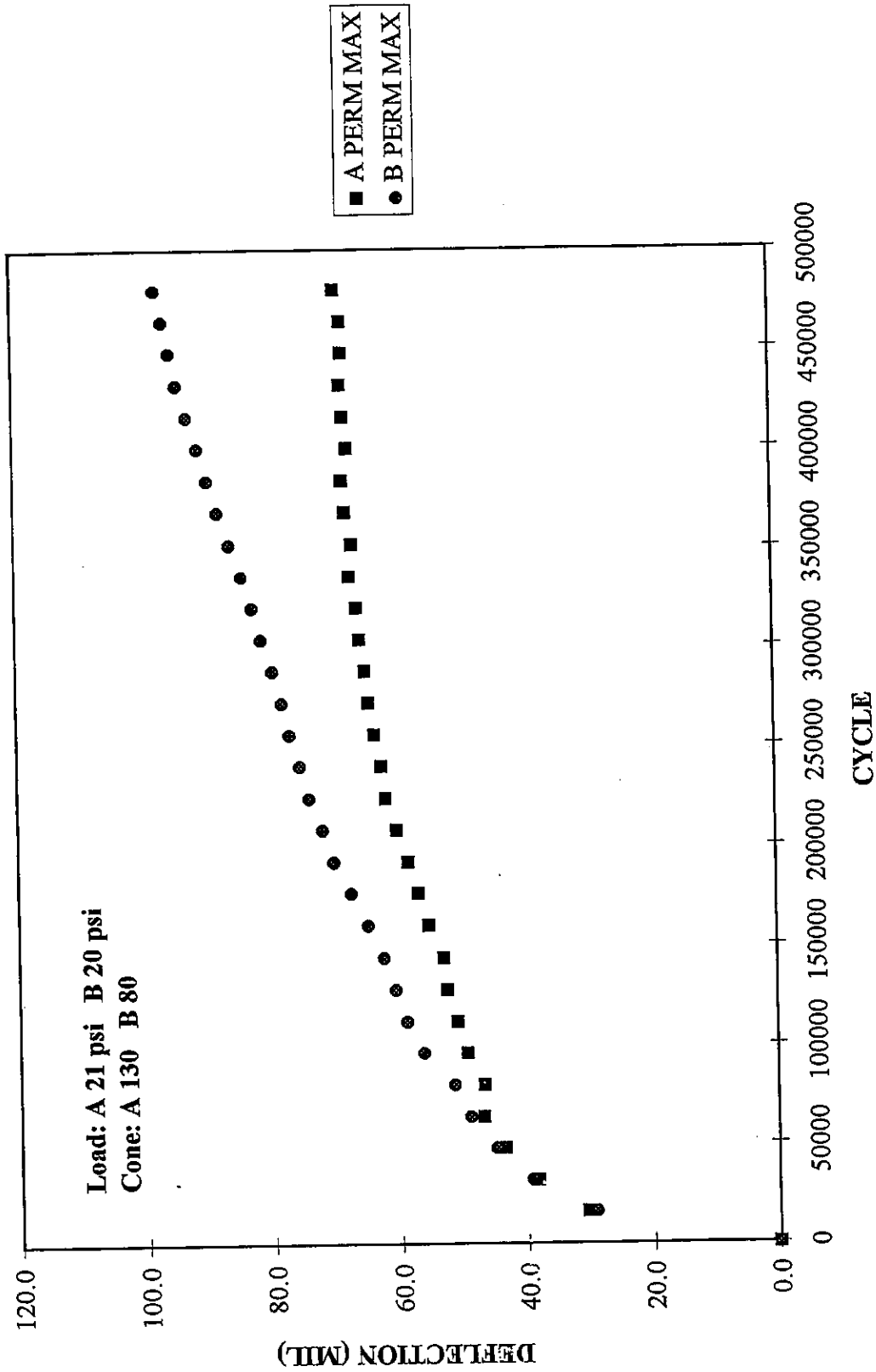


Figure A19: C0923AB / 1101 Geotextile / CA7, Deflection vs Cycle

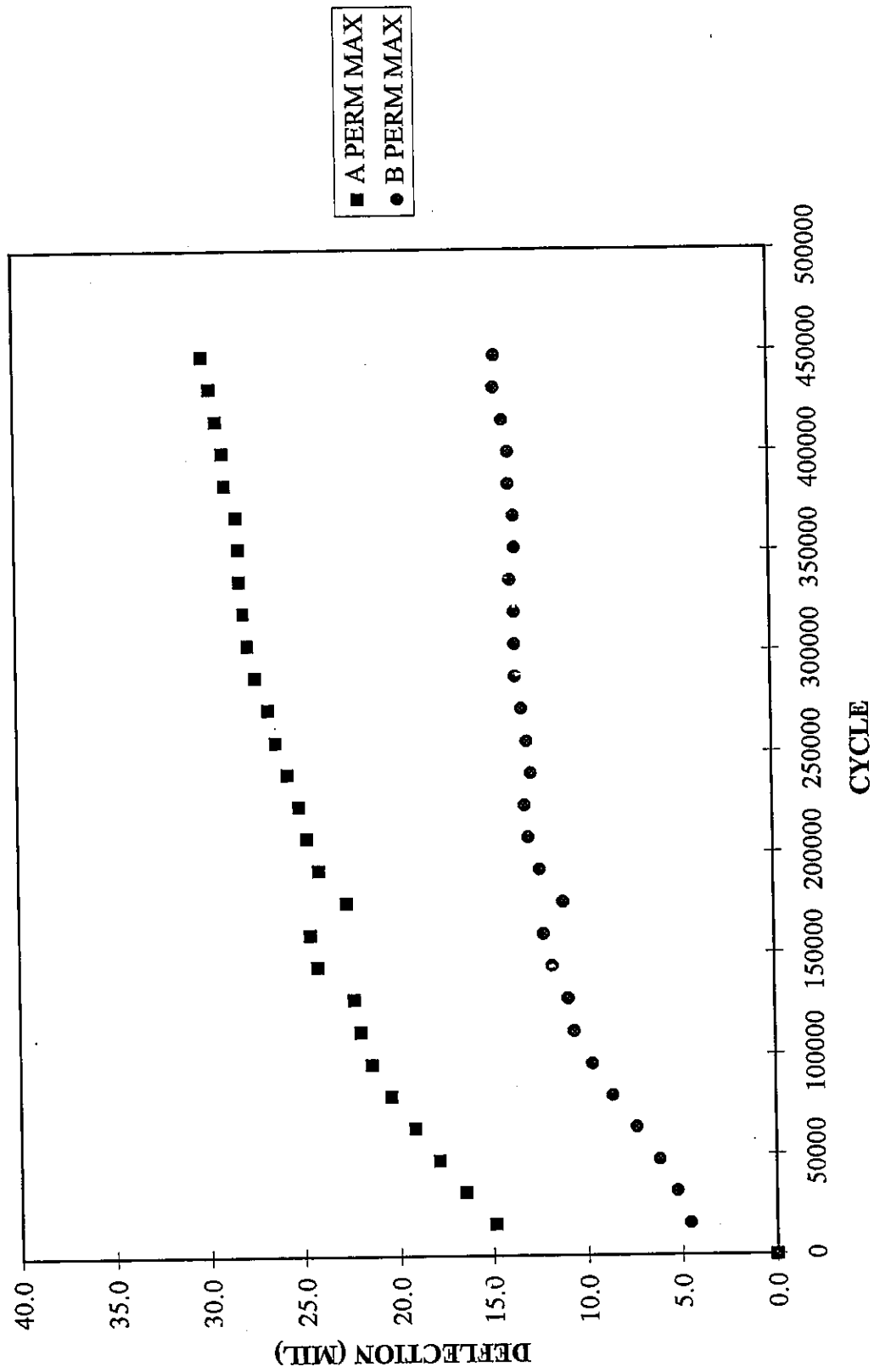


Figure A20: C1001AB / No Separation / CA7, Deflection vs Cycle

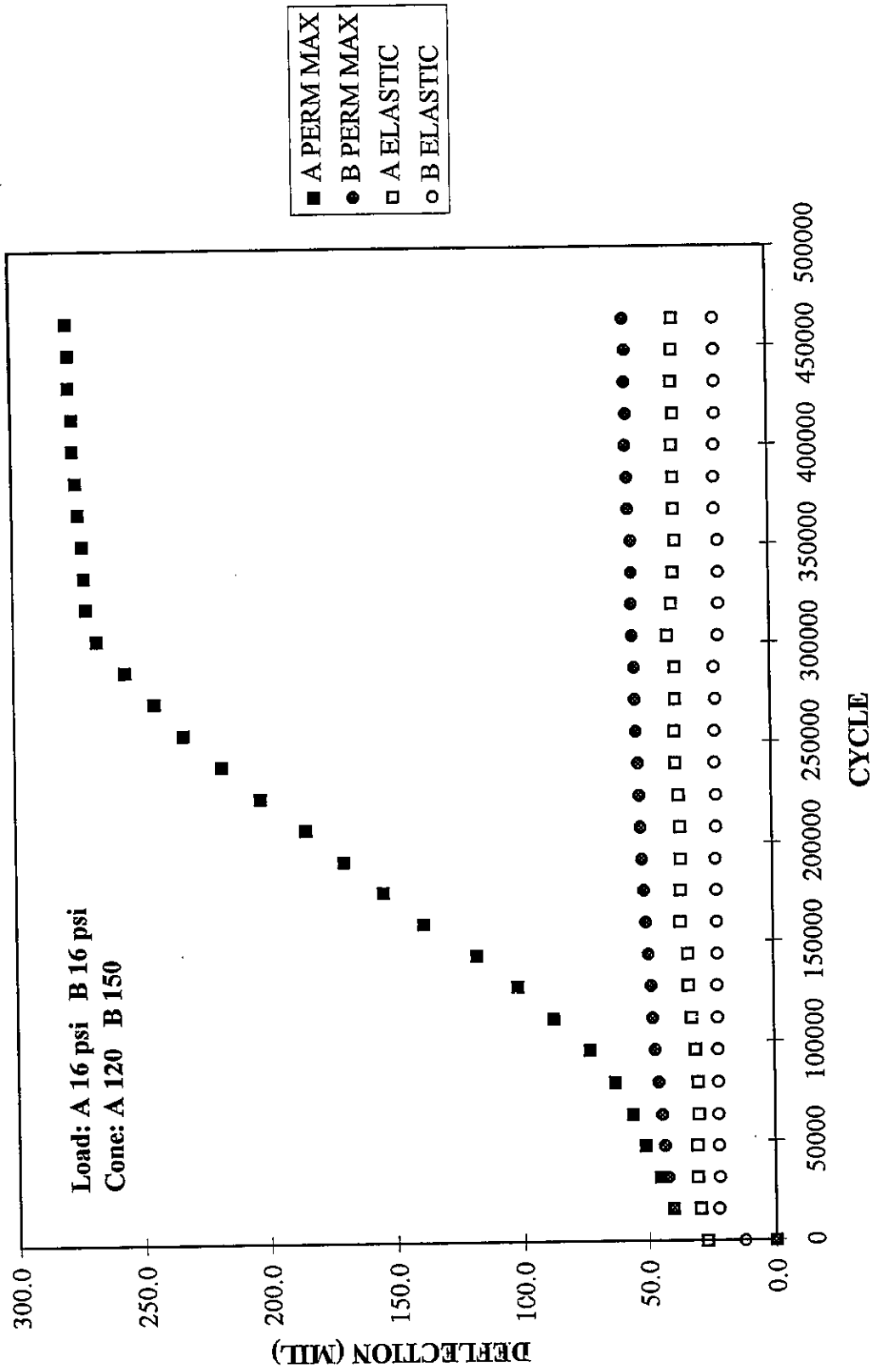


Figure A21: C1017AB / 1101 Geotextile / CA7, Deflection vs Cycle

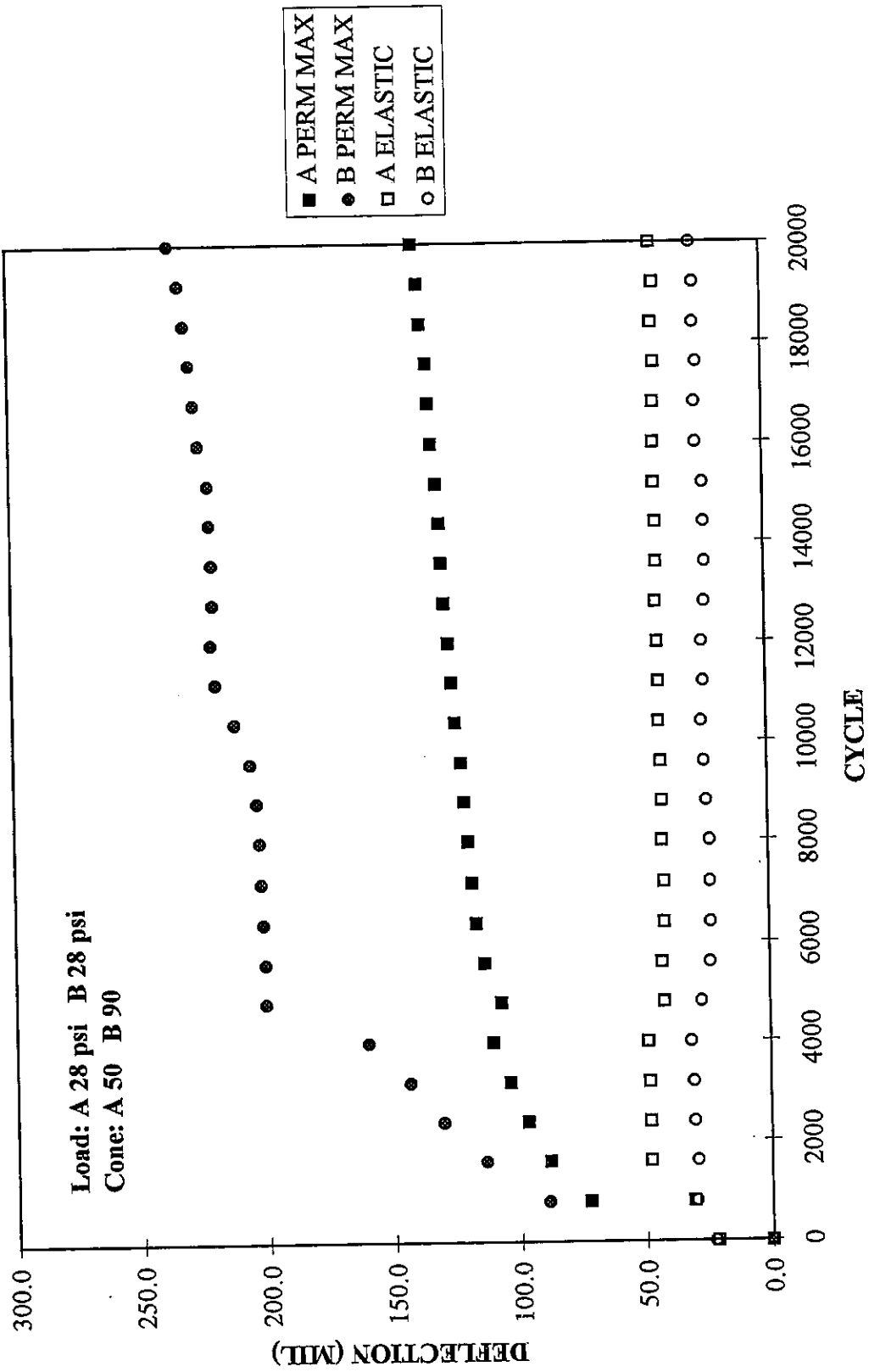


Figure A22: C1027AB / No Separation / CA7, Deflection vs Cycle

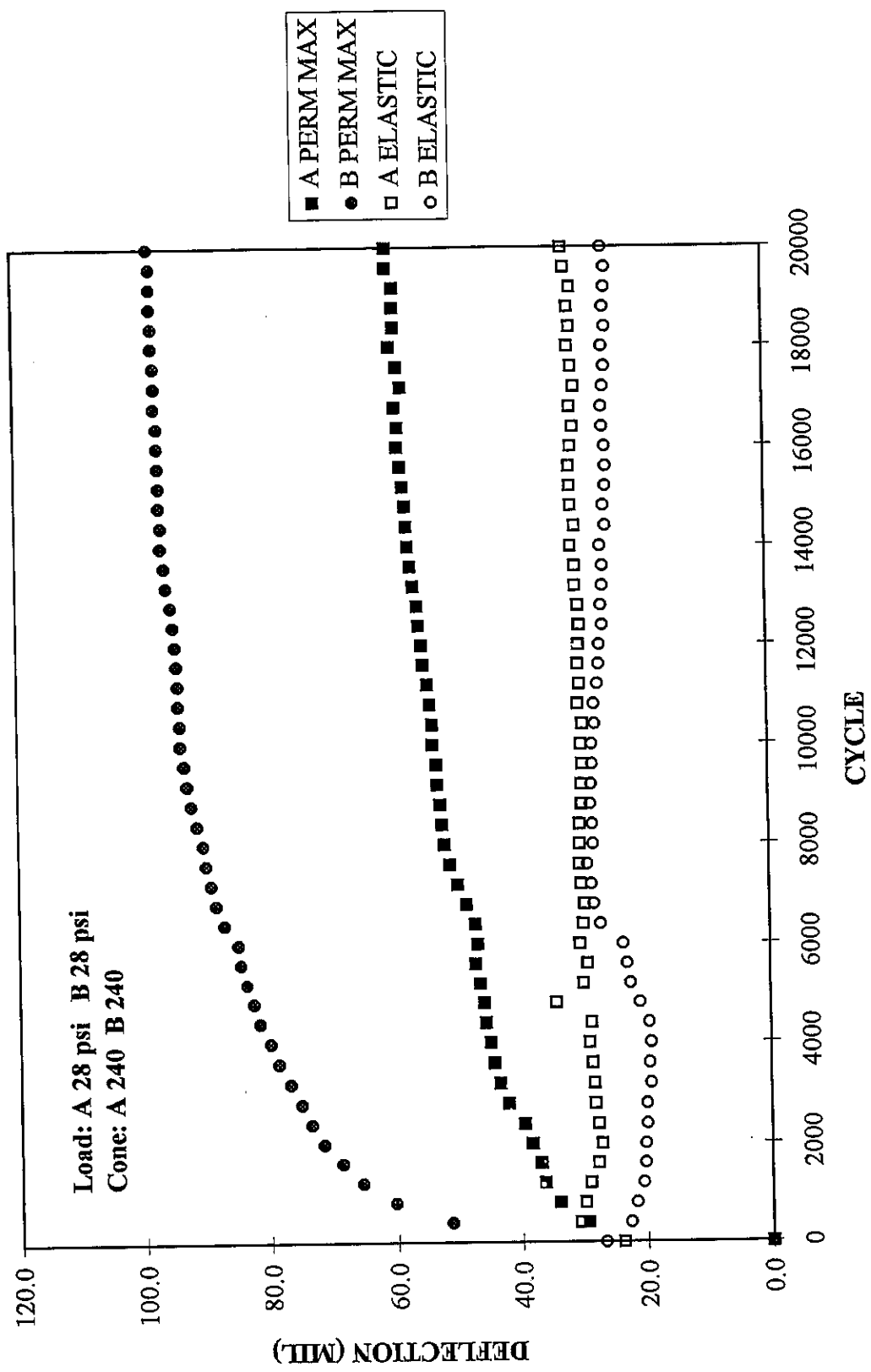


Figure A23: C1029AB / 1101 Geotextile / CA7, Deflection vs Cycle

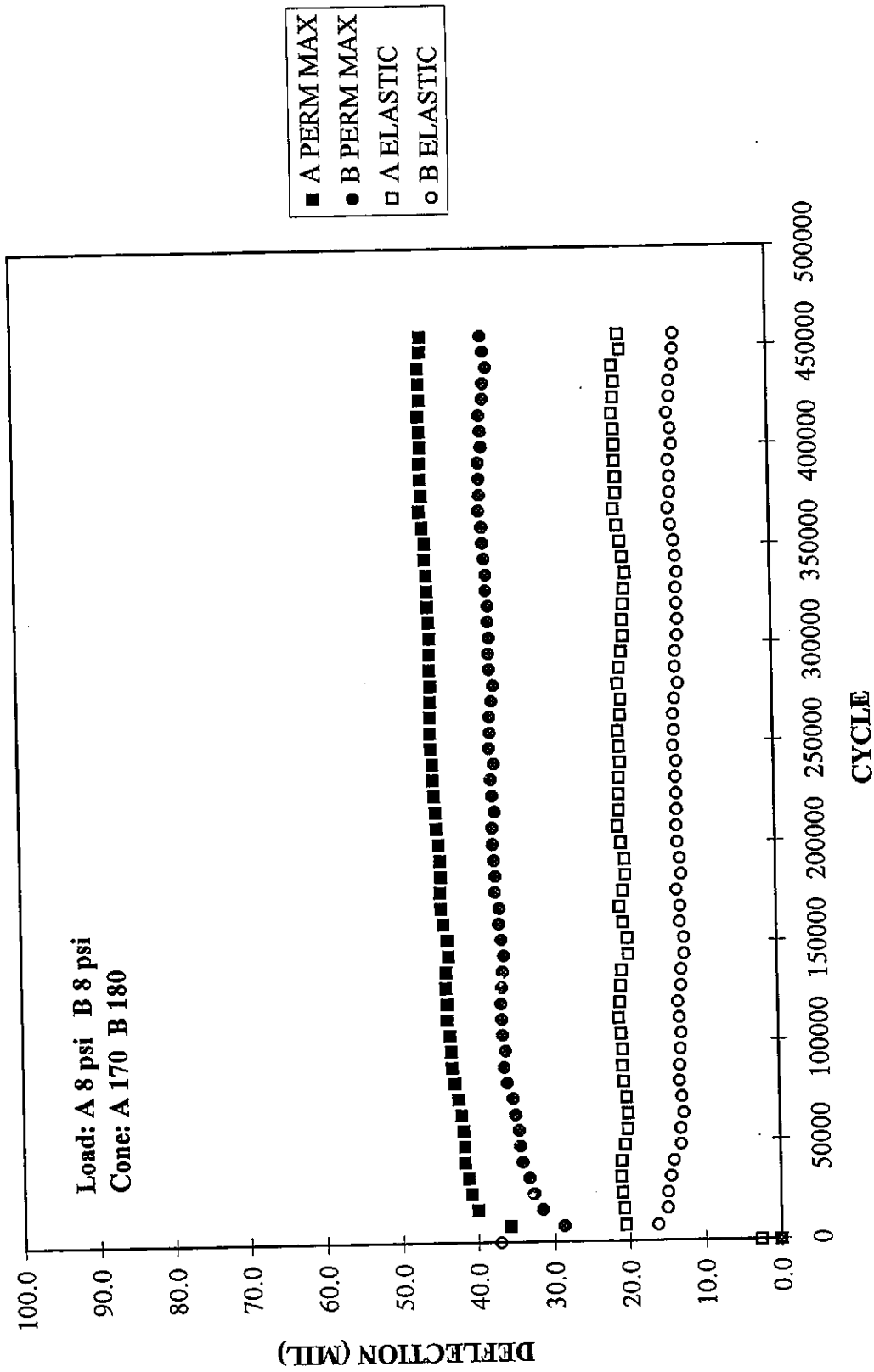


Figure A24: C1104AB / No Separation / CA7, Deflection vs Cycle

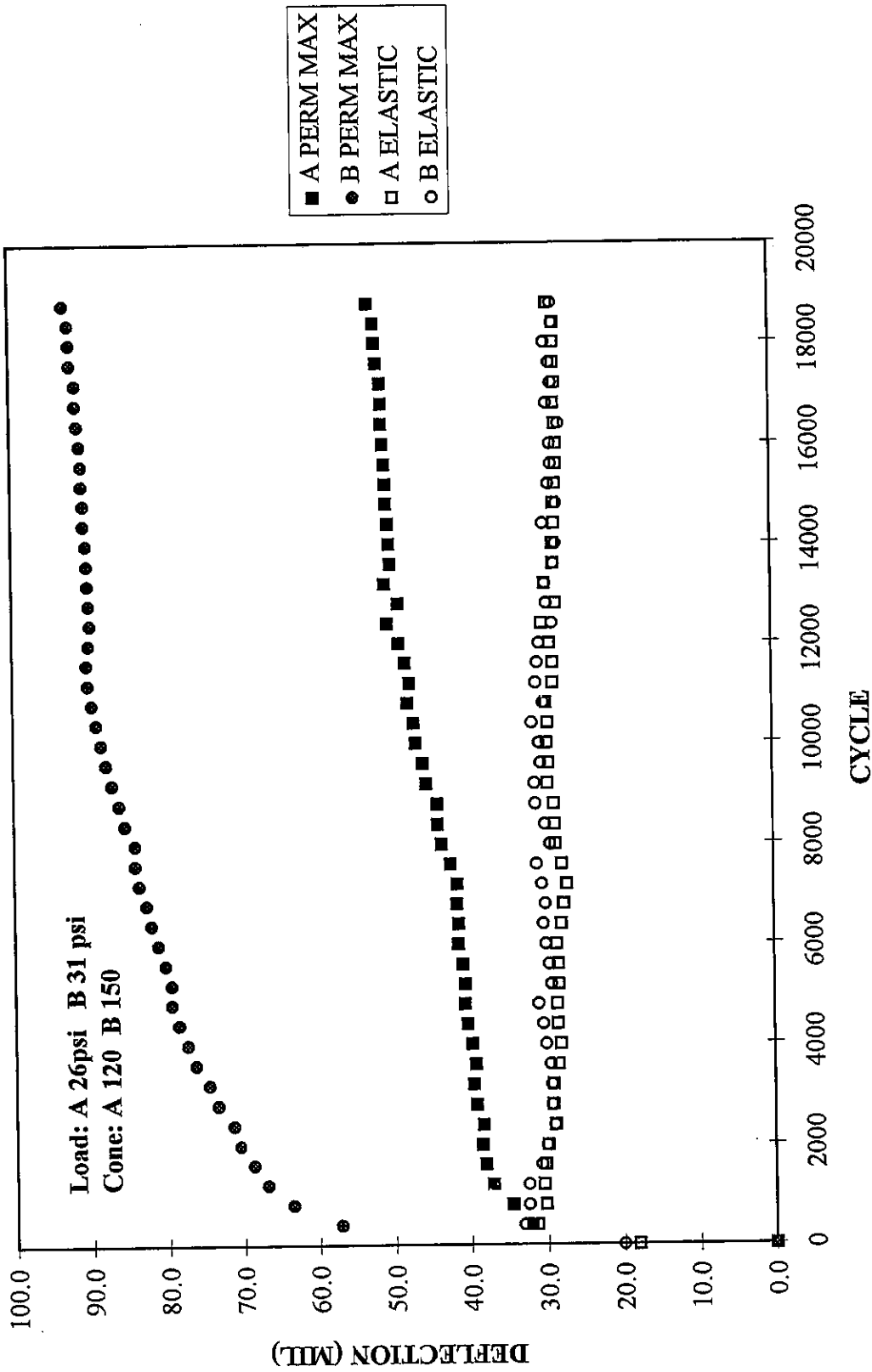


Figure A25: C01116AB / CA6 / CA7, Deflection vs Cycle

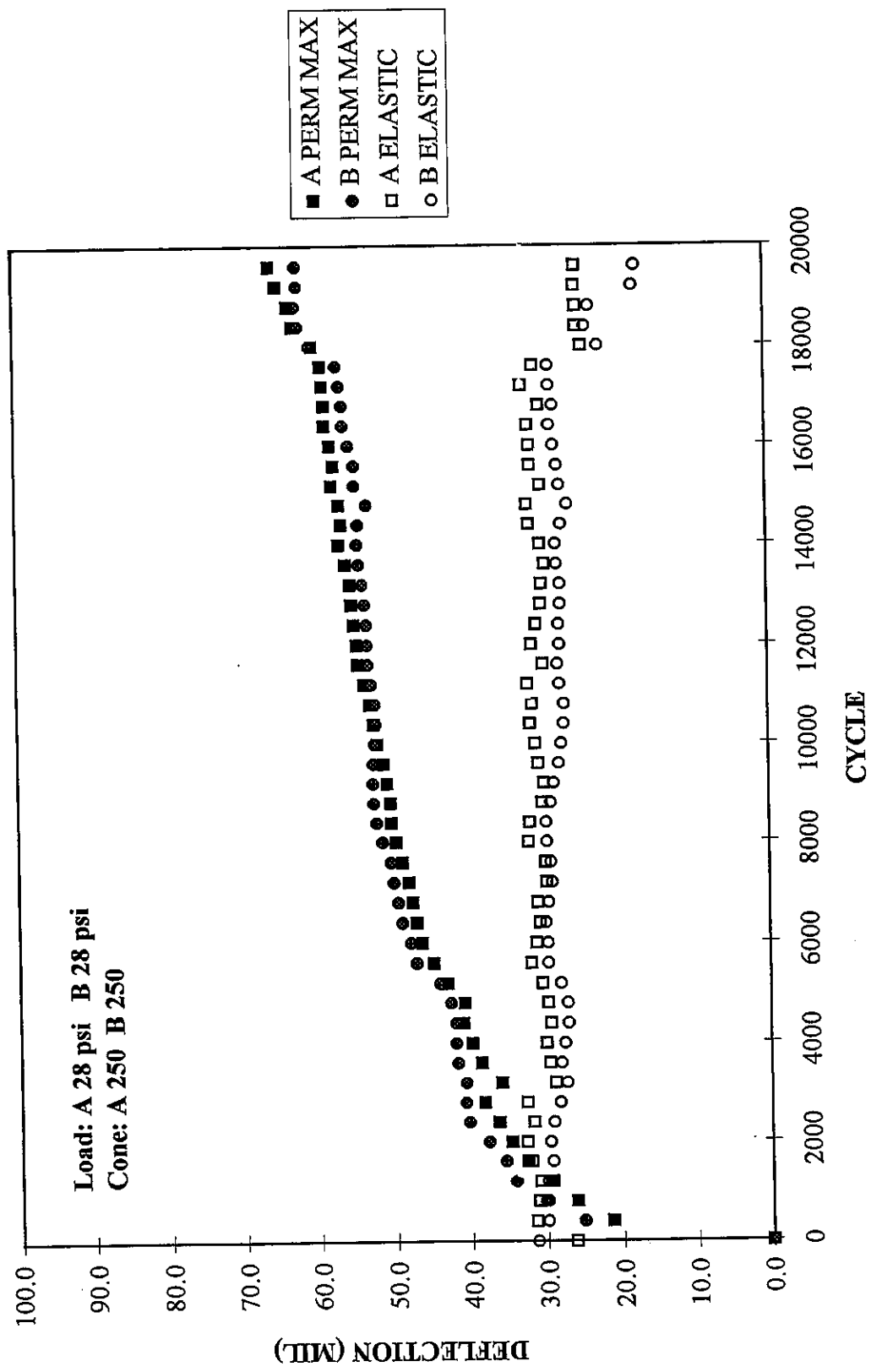


Figure A26: C1117AB / CA6 / CA7, Deflection vs Cycle

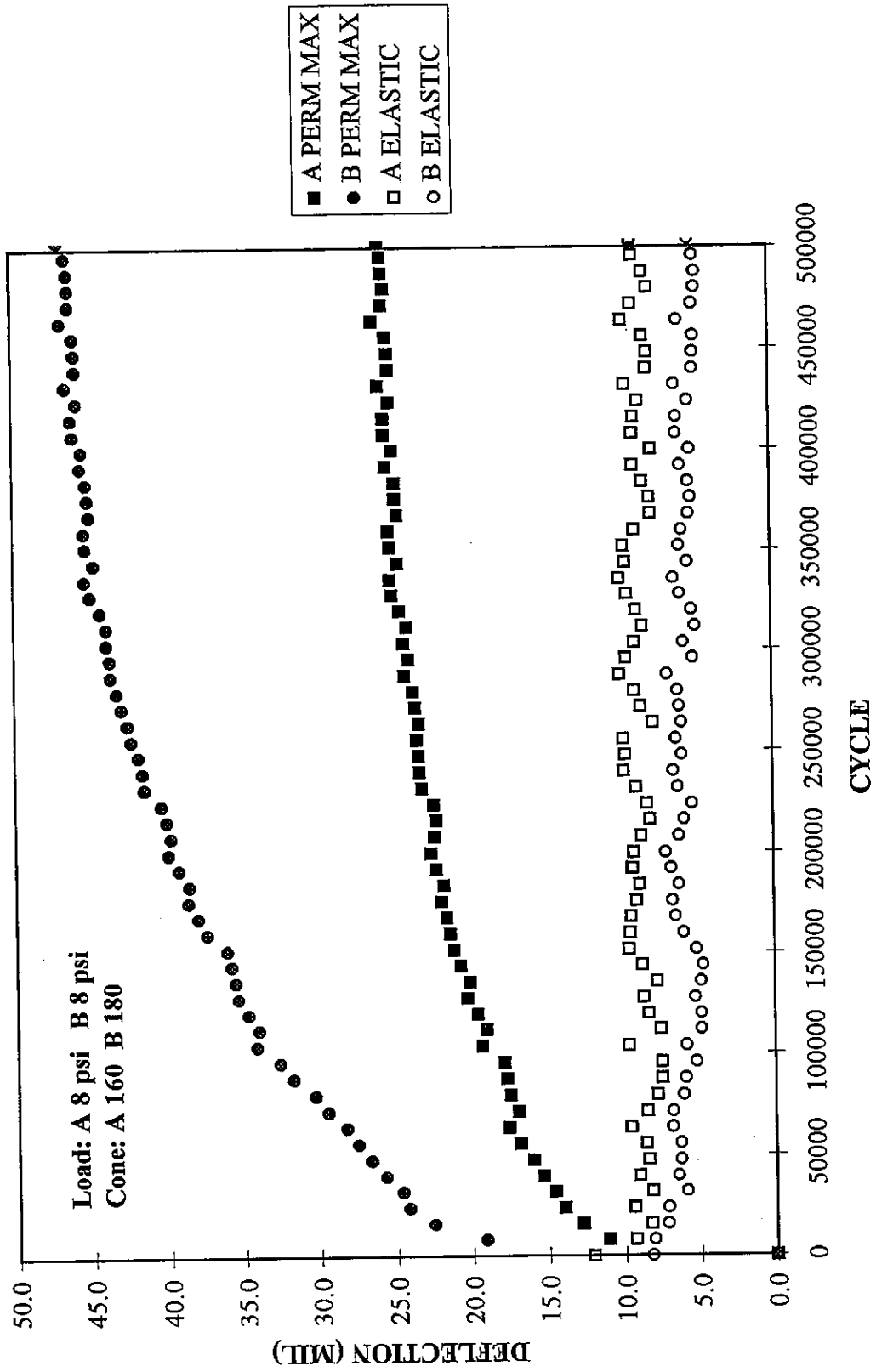


Figure A27: C1120AB / 1101 Geotextile / CA7, Deflection vs Cycle

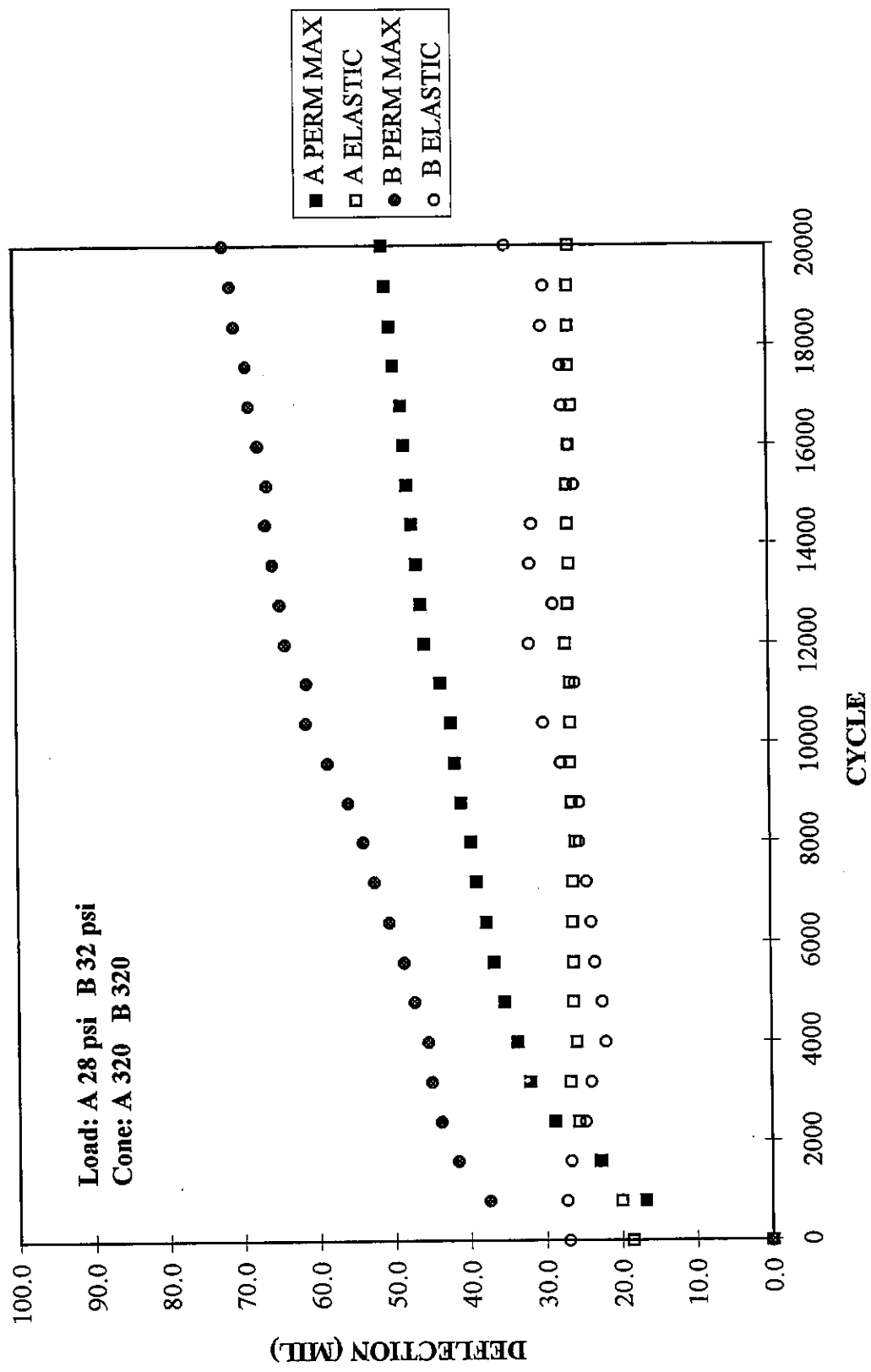


Figure A28: S0707AB / 1101 Geotextile / CA7, Deflection vs Cycle

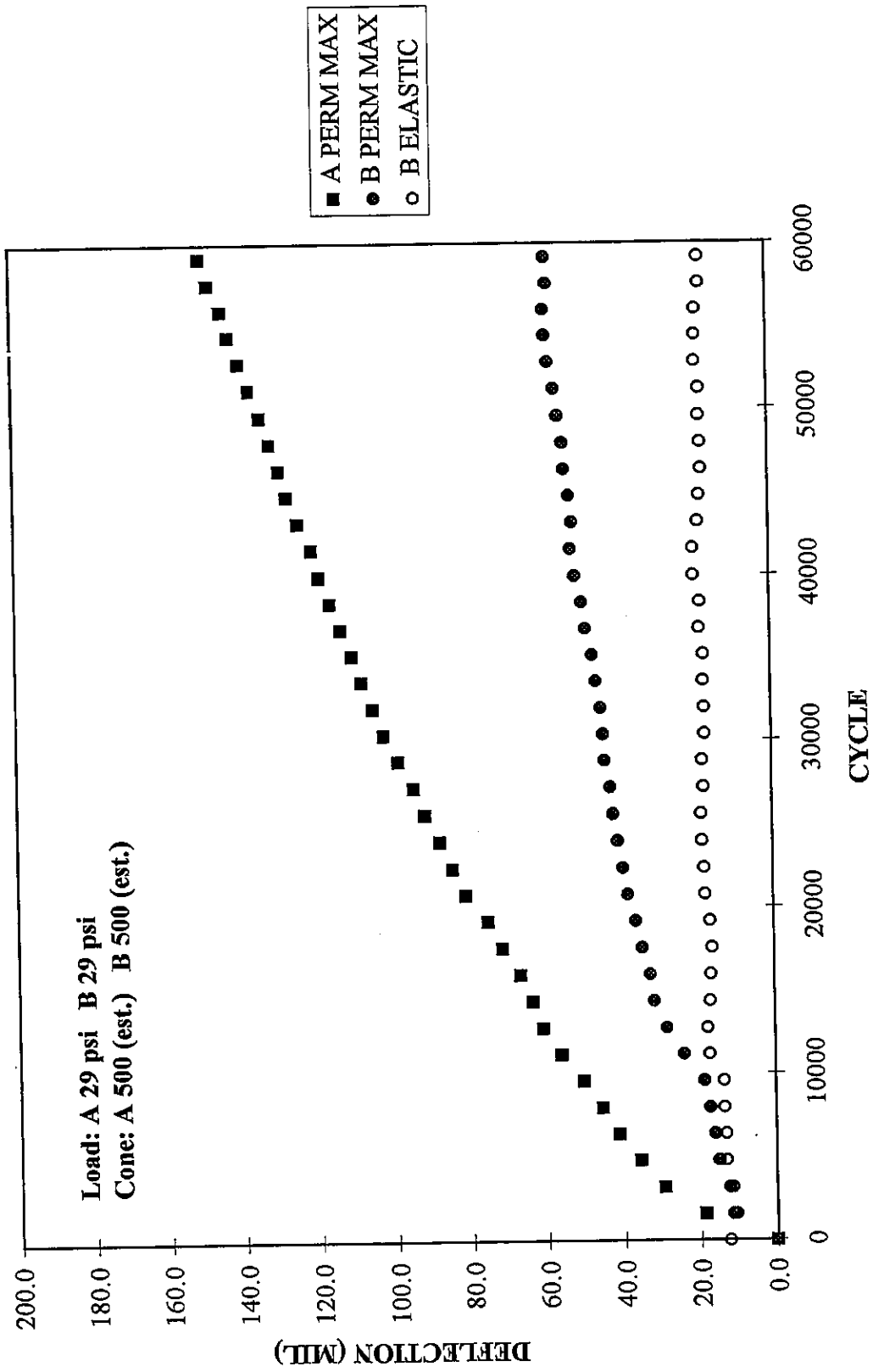


Figure 29: S0707CD / No Separation / CA7, Deflection vs Cycle

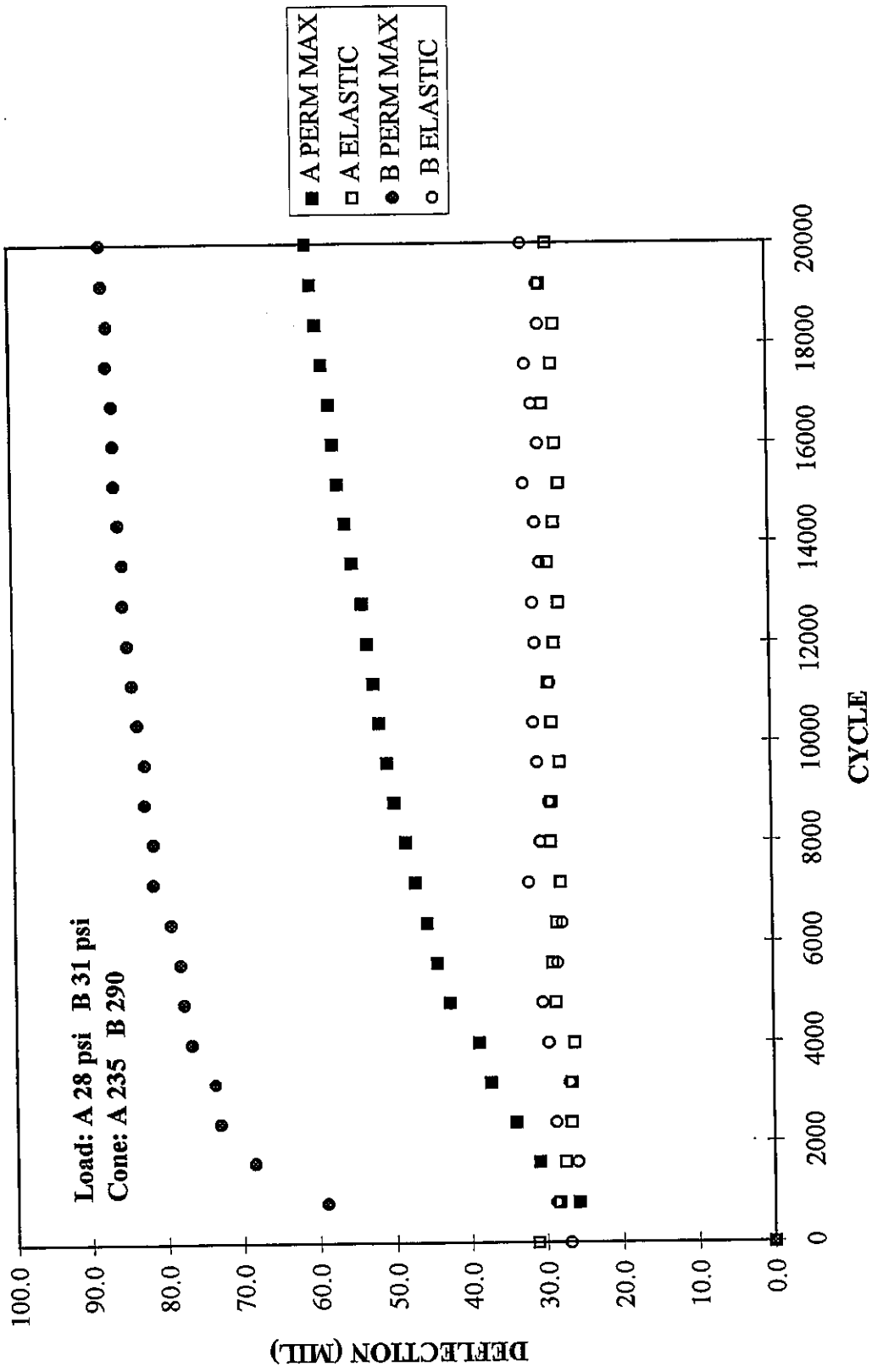


Figure A30: S0708AB / 1101 Geotextile / CA7, Deflection vs Cycle

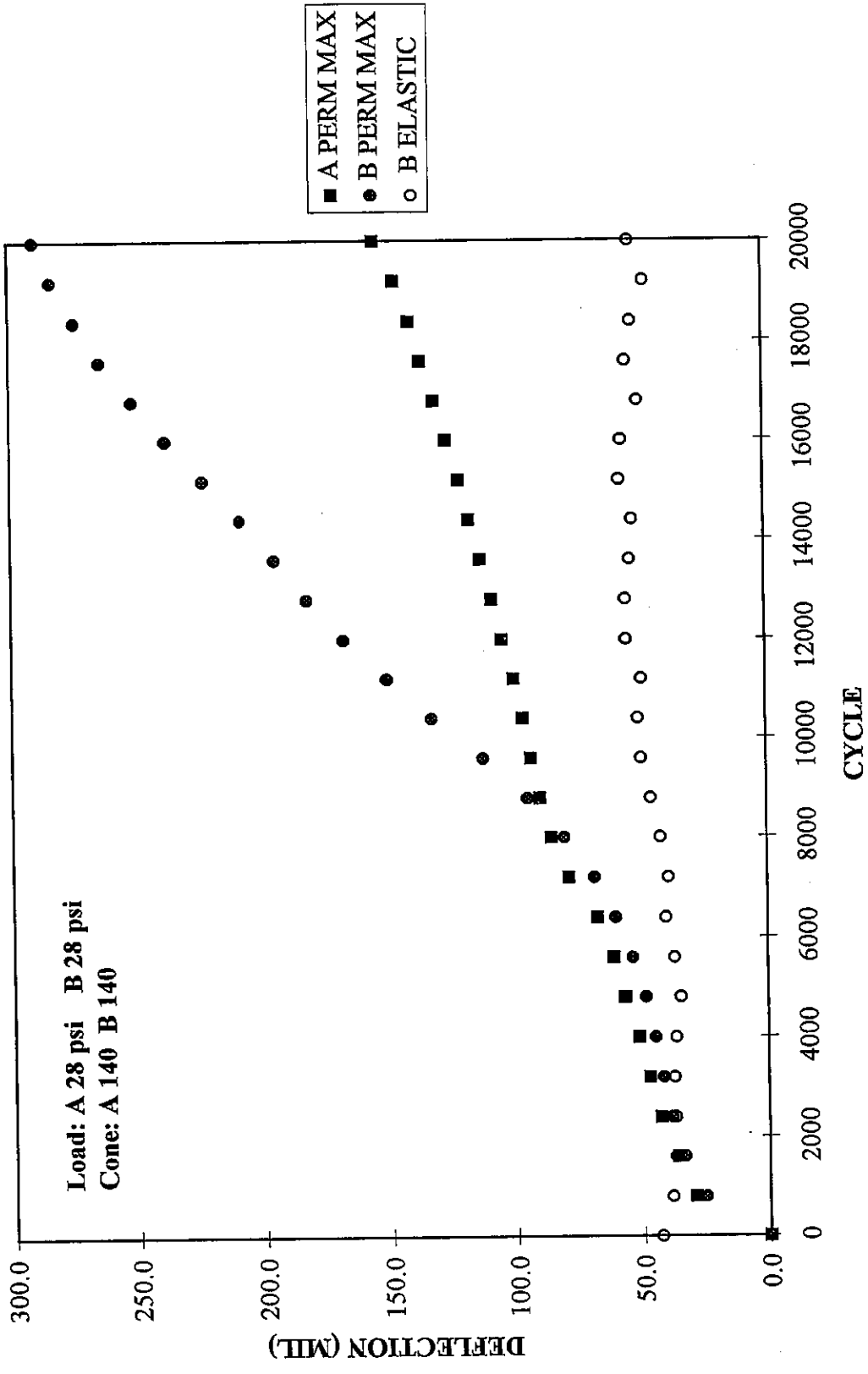


Figure A32: S0722AB / 1101 Geotextile / CA7, Deflection vs Cycle

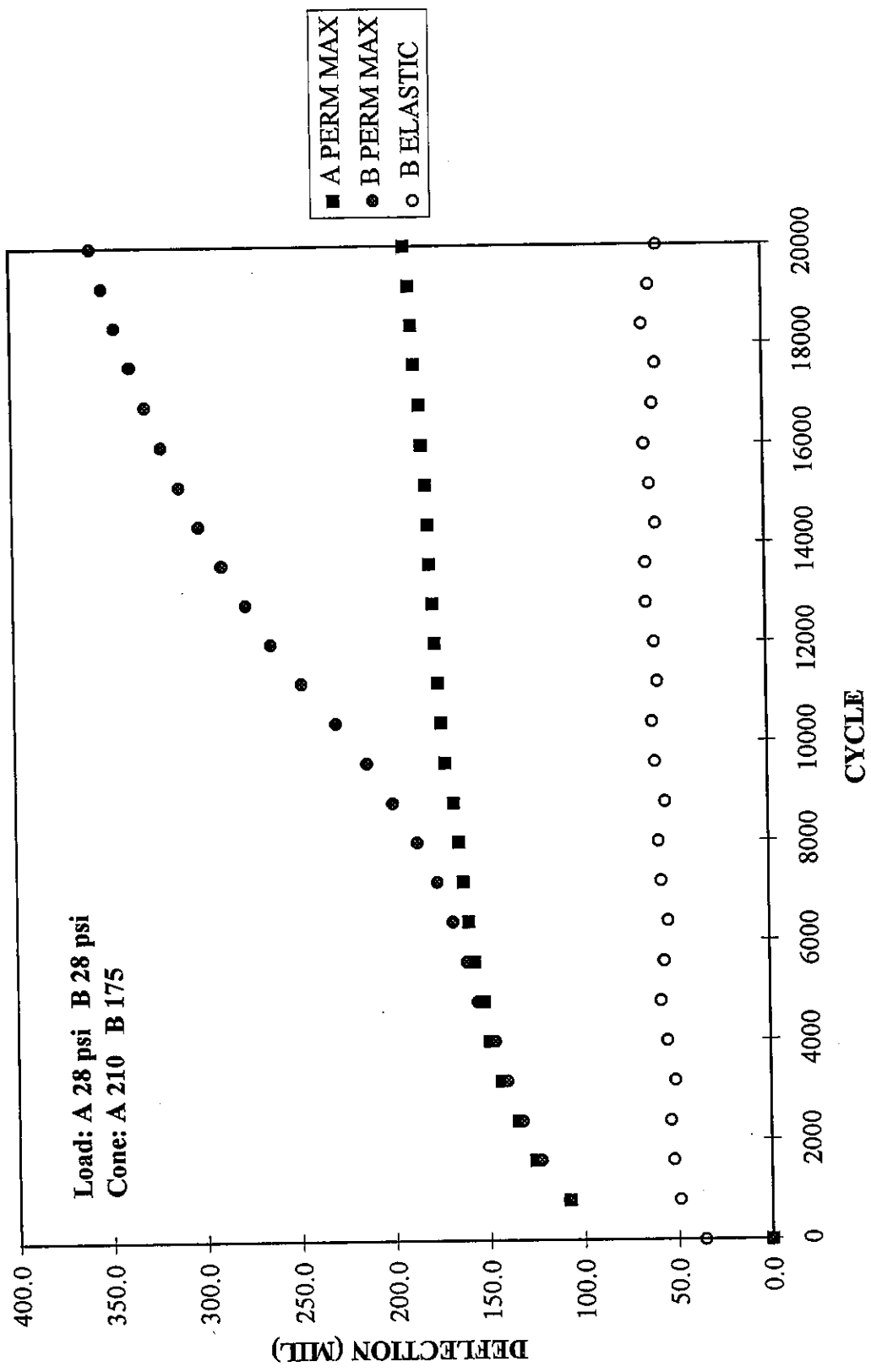


Figure A33: S0723AB / 1101 Geotextile / CA7, Deflection vs Cycle

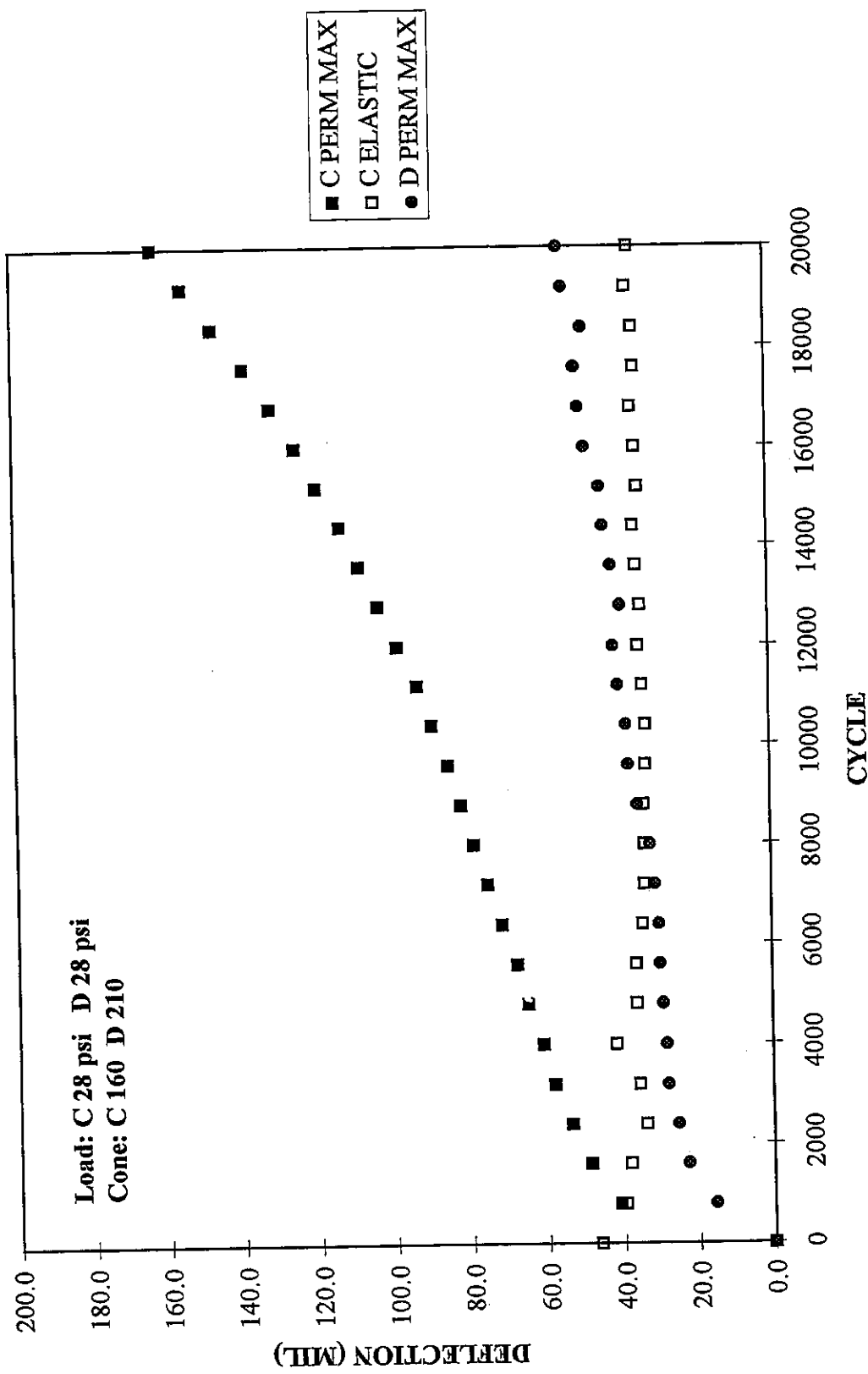


Figure A34: S0723CD / 1101 Geotextile / CA7, Deflection vs Cycle

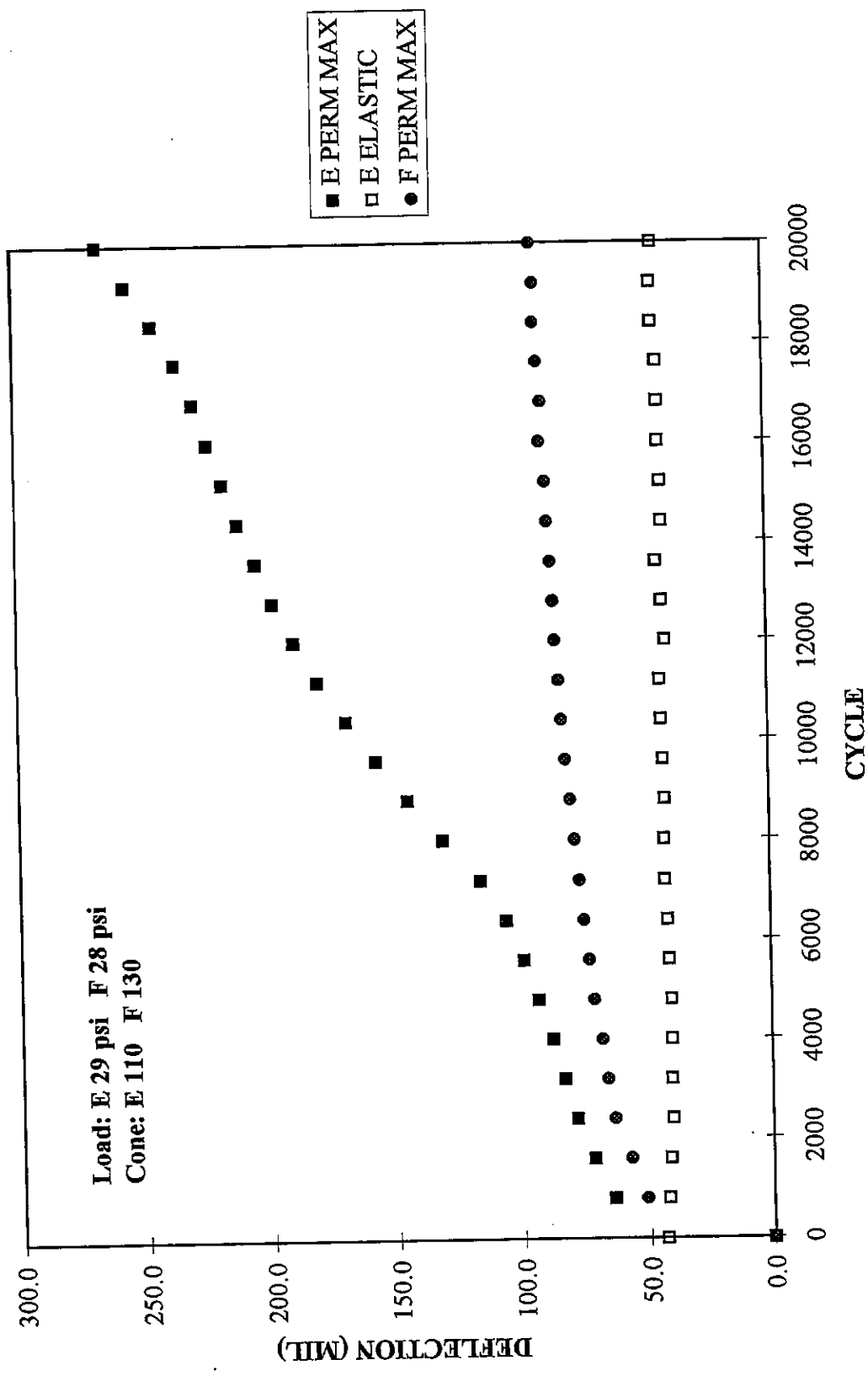


Figure A35: S0723EF / 1101 Geotextile / CA7, Deflection vs Cycle

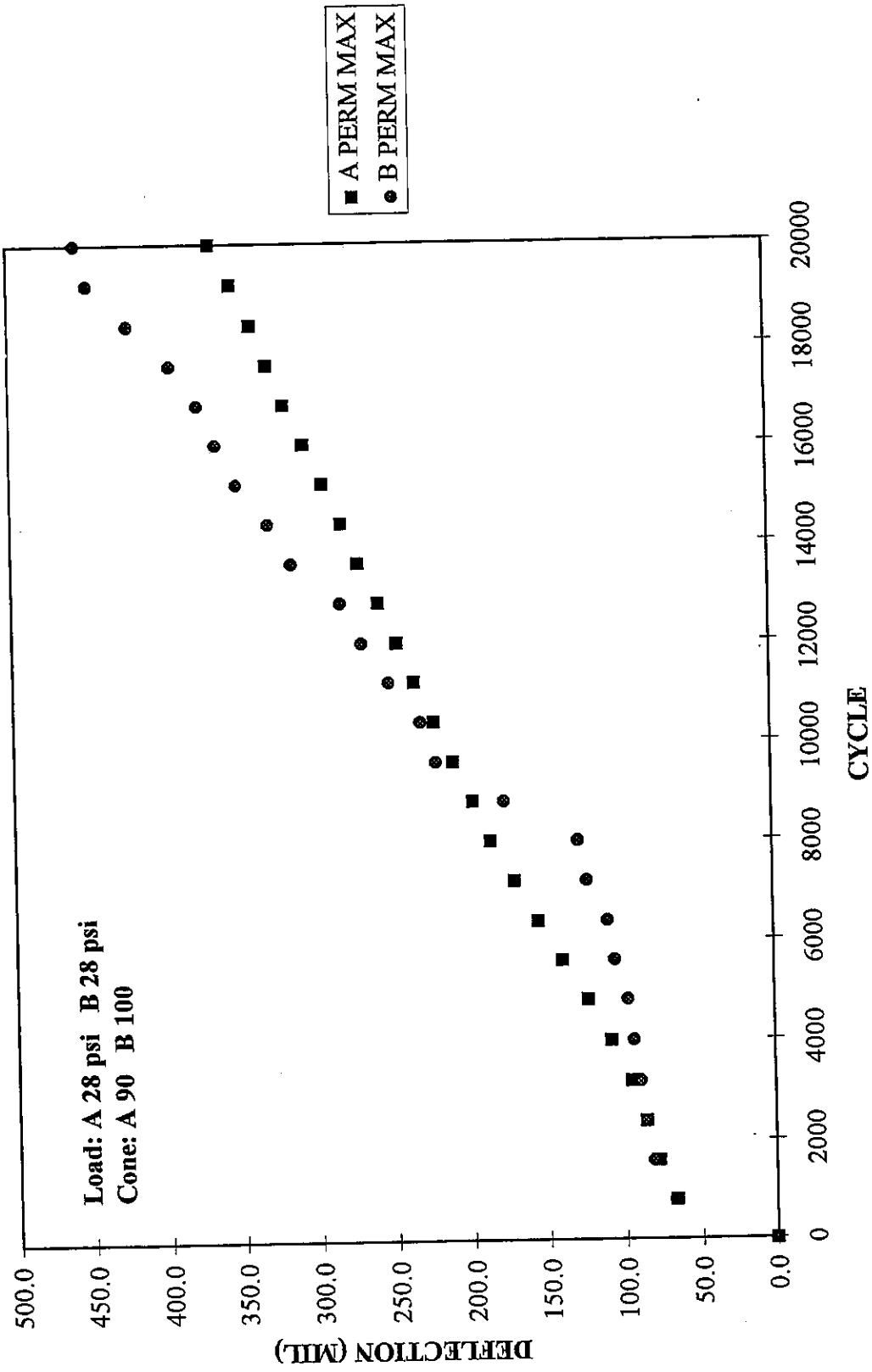


Figure A36: S0725AB / 1101 Geotextile / CA7, Deflection vs Cycle

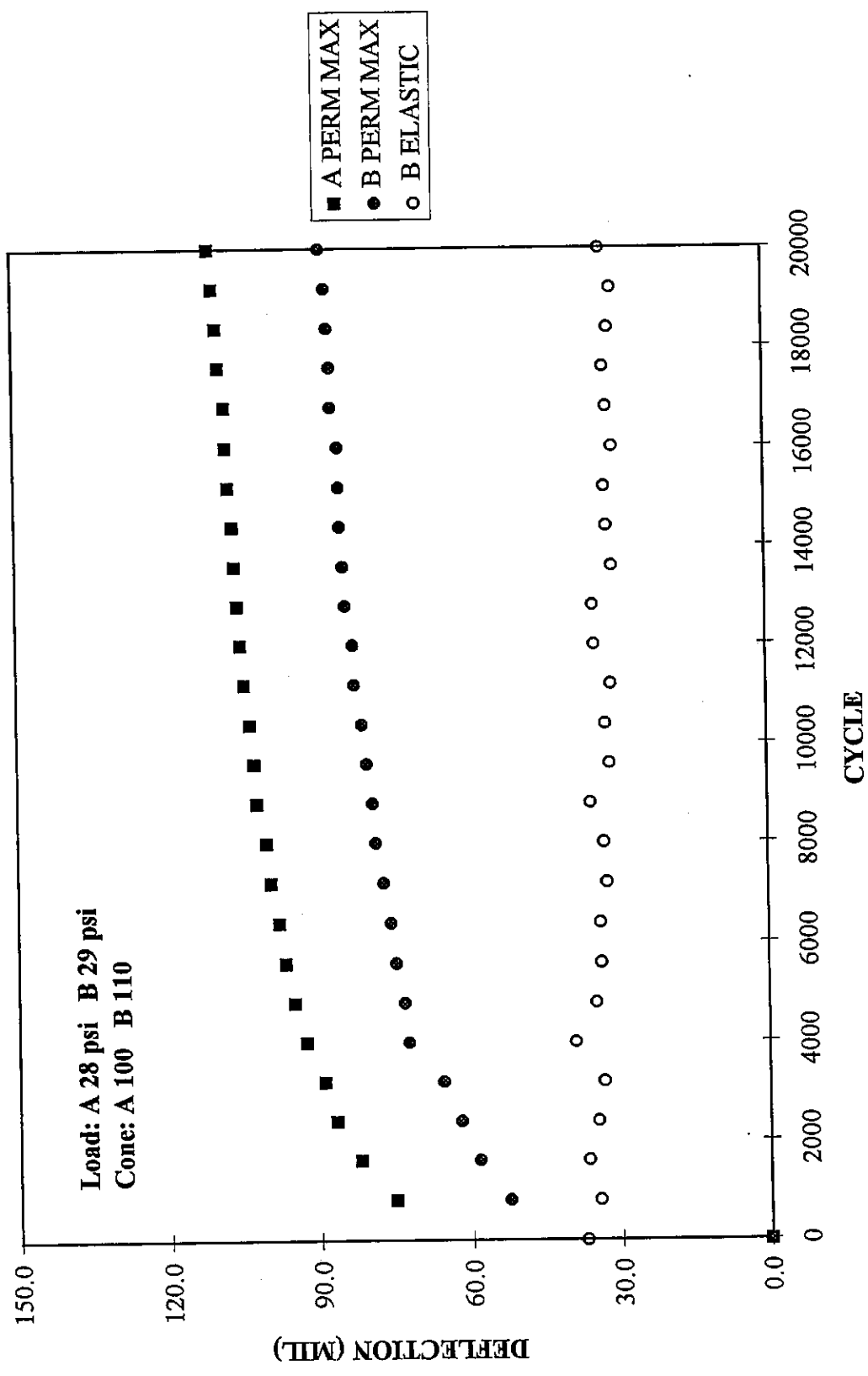


Figure A37: S0728AB / 1101 Geotextile / CA7, Deflection vs Cycle

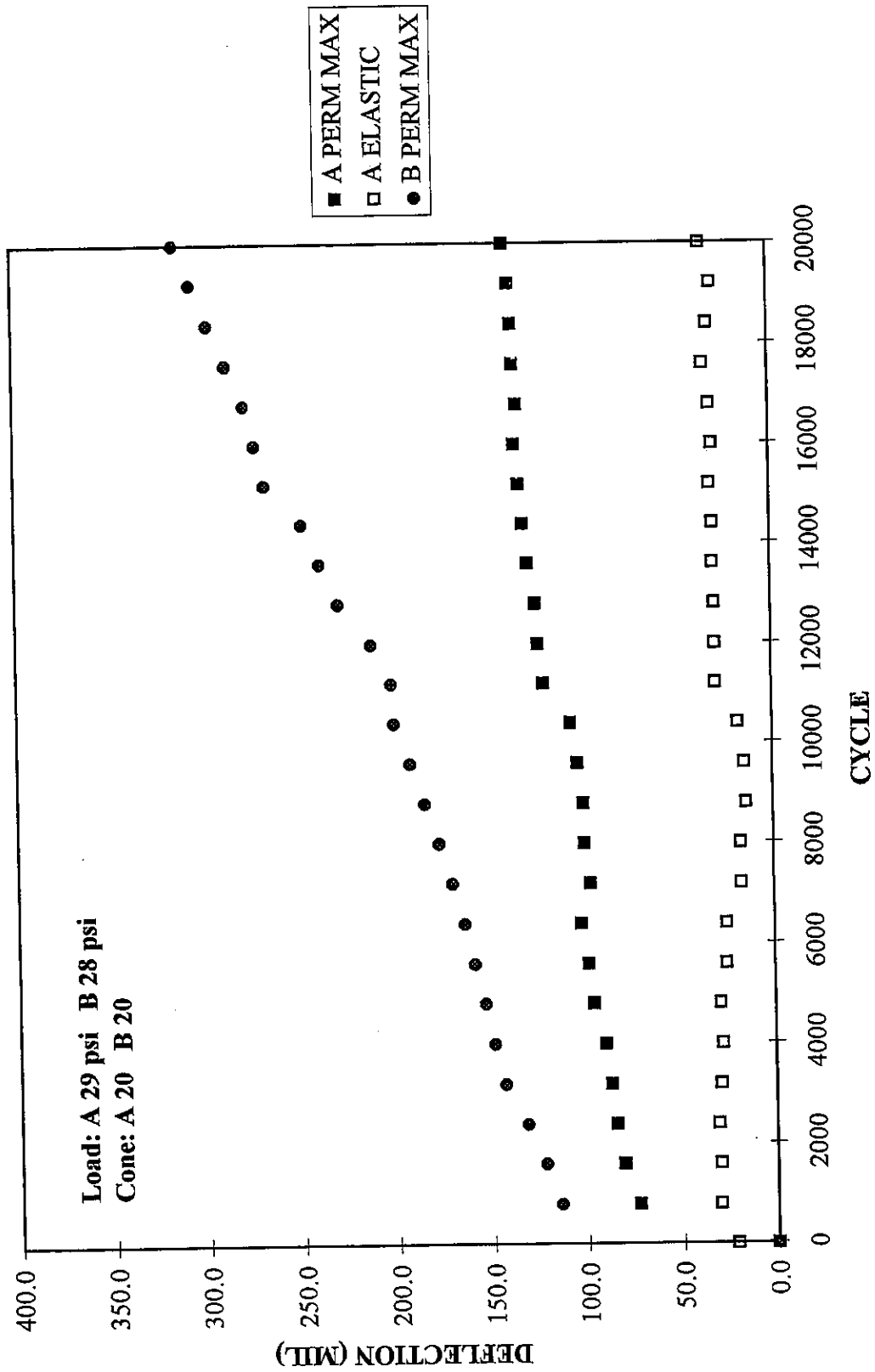


Figure A38: S0729AB / 1101 Geotextile / CA7, Deflection vs Cycle

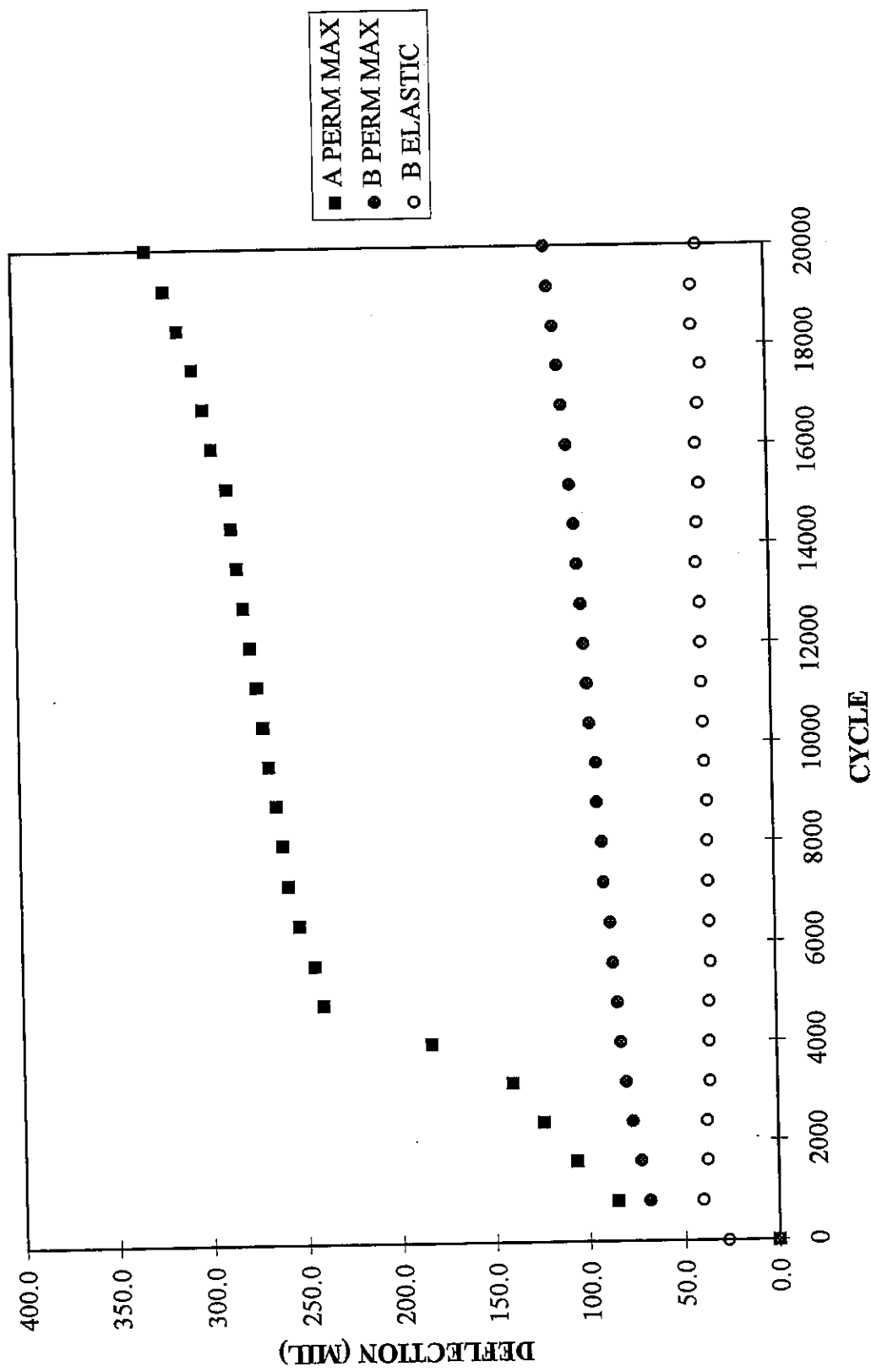


Figure A39: S0801AB / 1101 Geotextile / CA7, Deflection vs Cycle

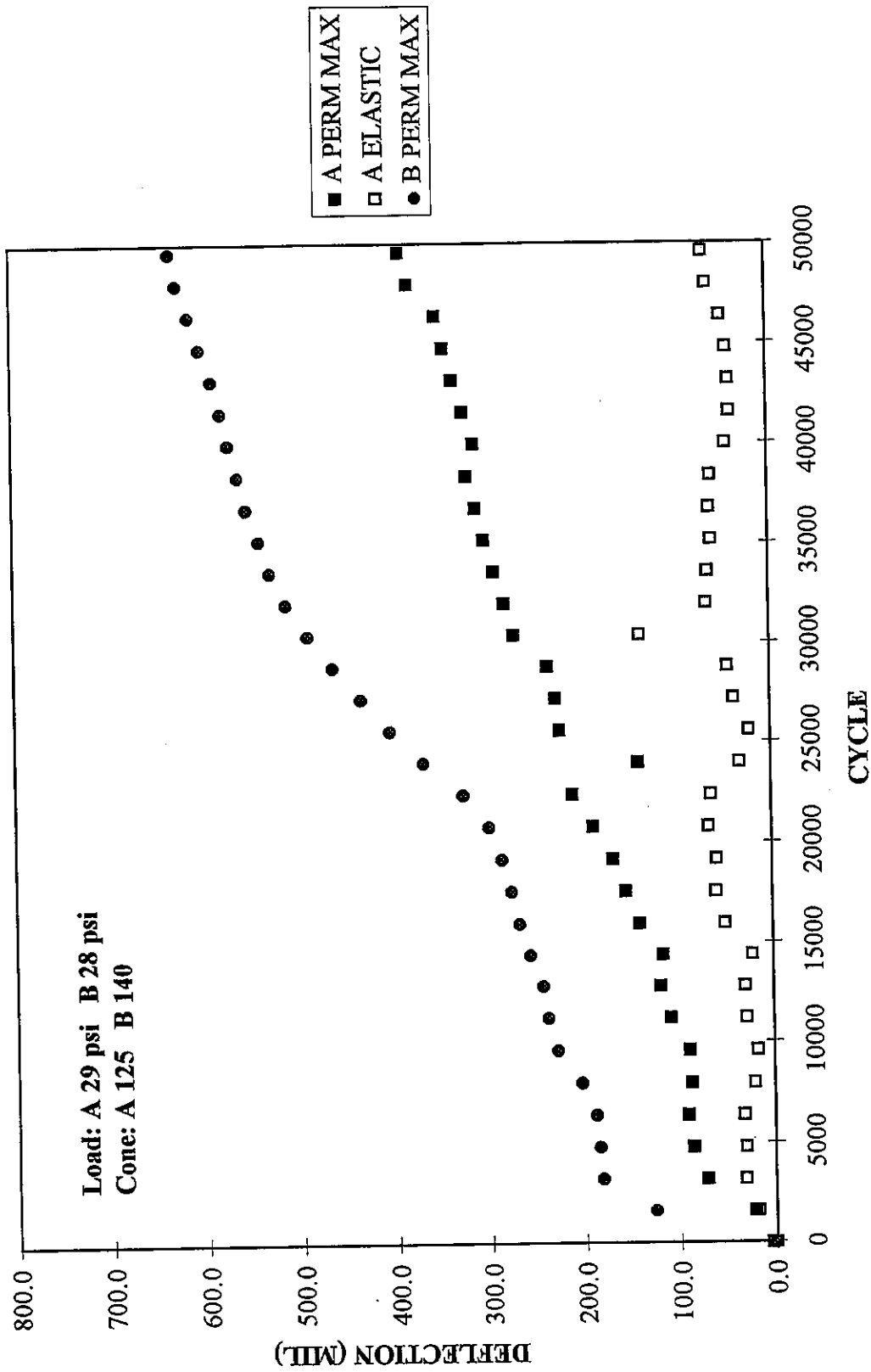


Figure A40: S0804AB / 1101 Geotextile / CA7, Deflection vs Cycle

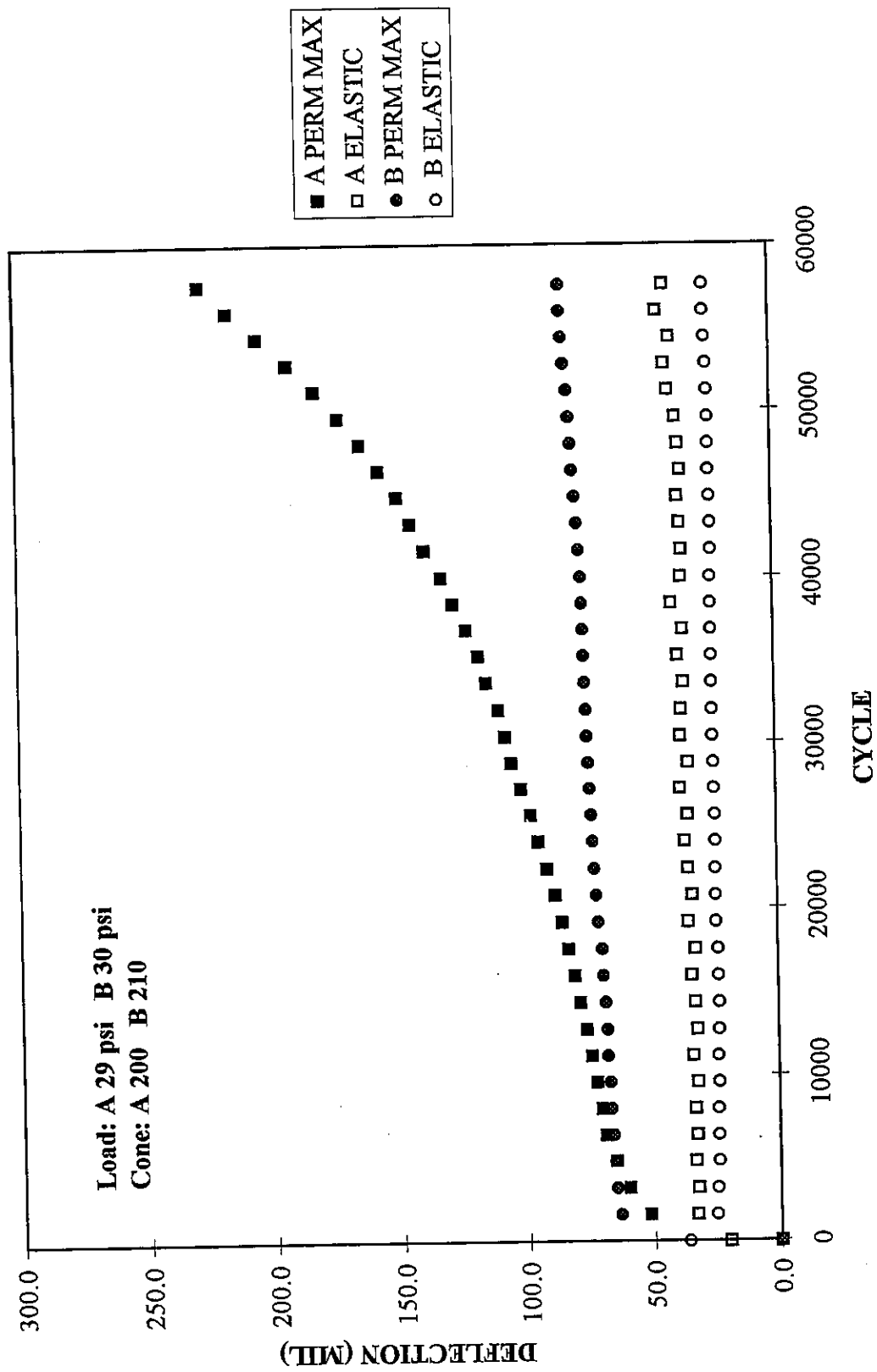


Figure A41: S0806AB / 1101 Geotextile / CA7, Deflection vs Cycle

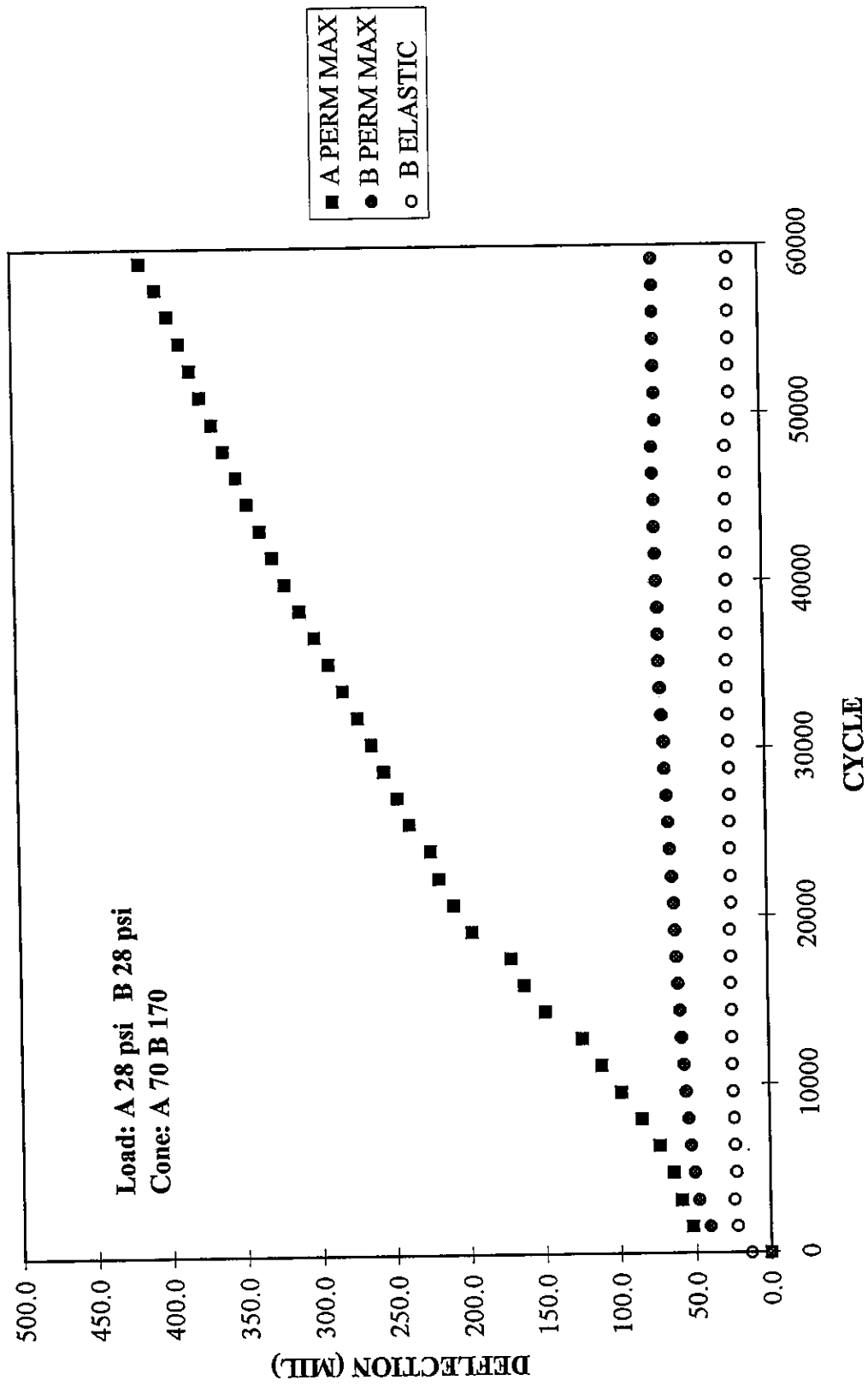


Figure A42: S0811AB / No Separation / CA7, Deflection vs Cycle

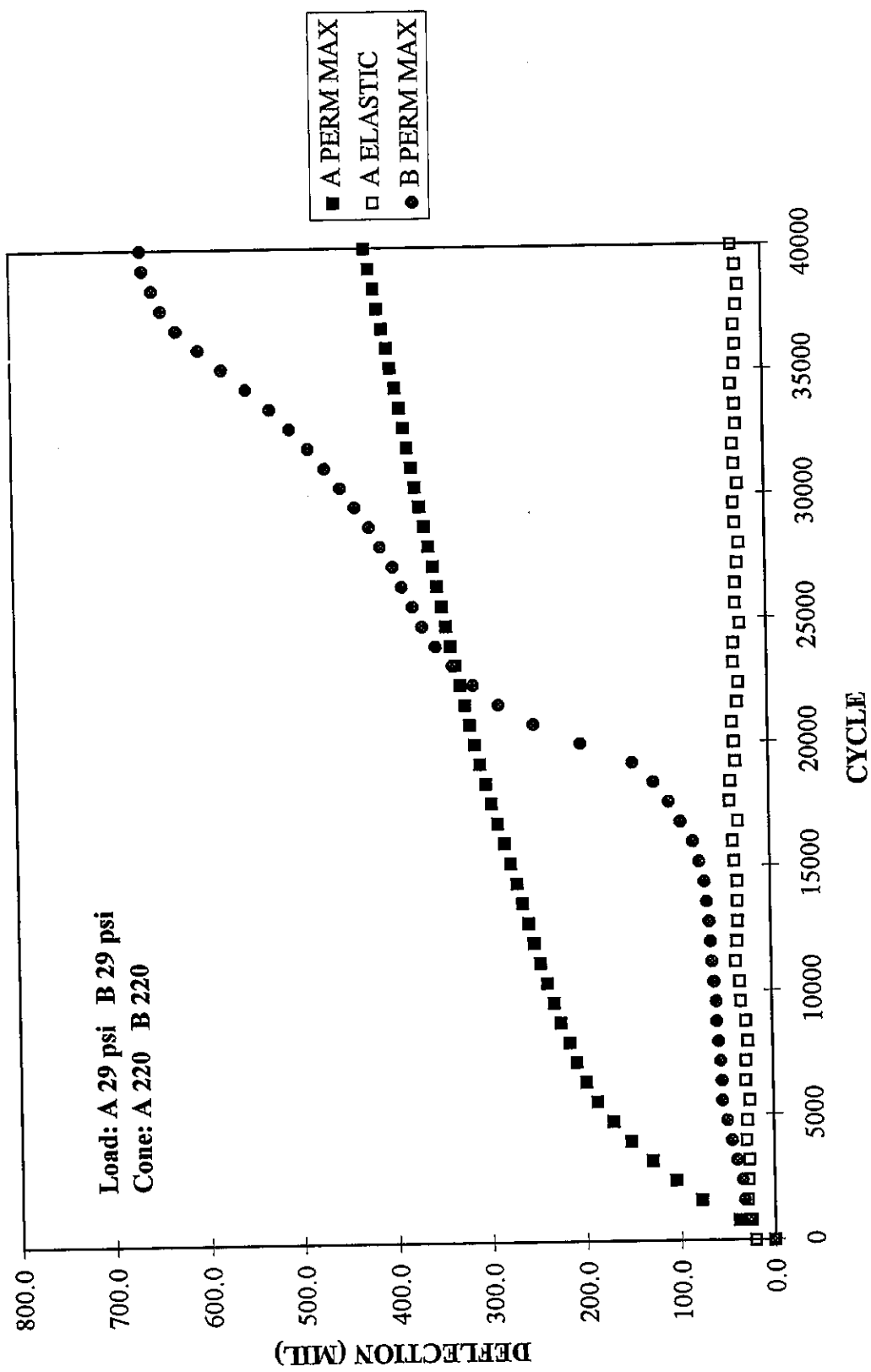


Figure A43: S0813AB / No Separation / CA7, Deflection vs Cycle

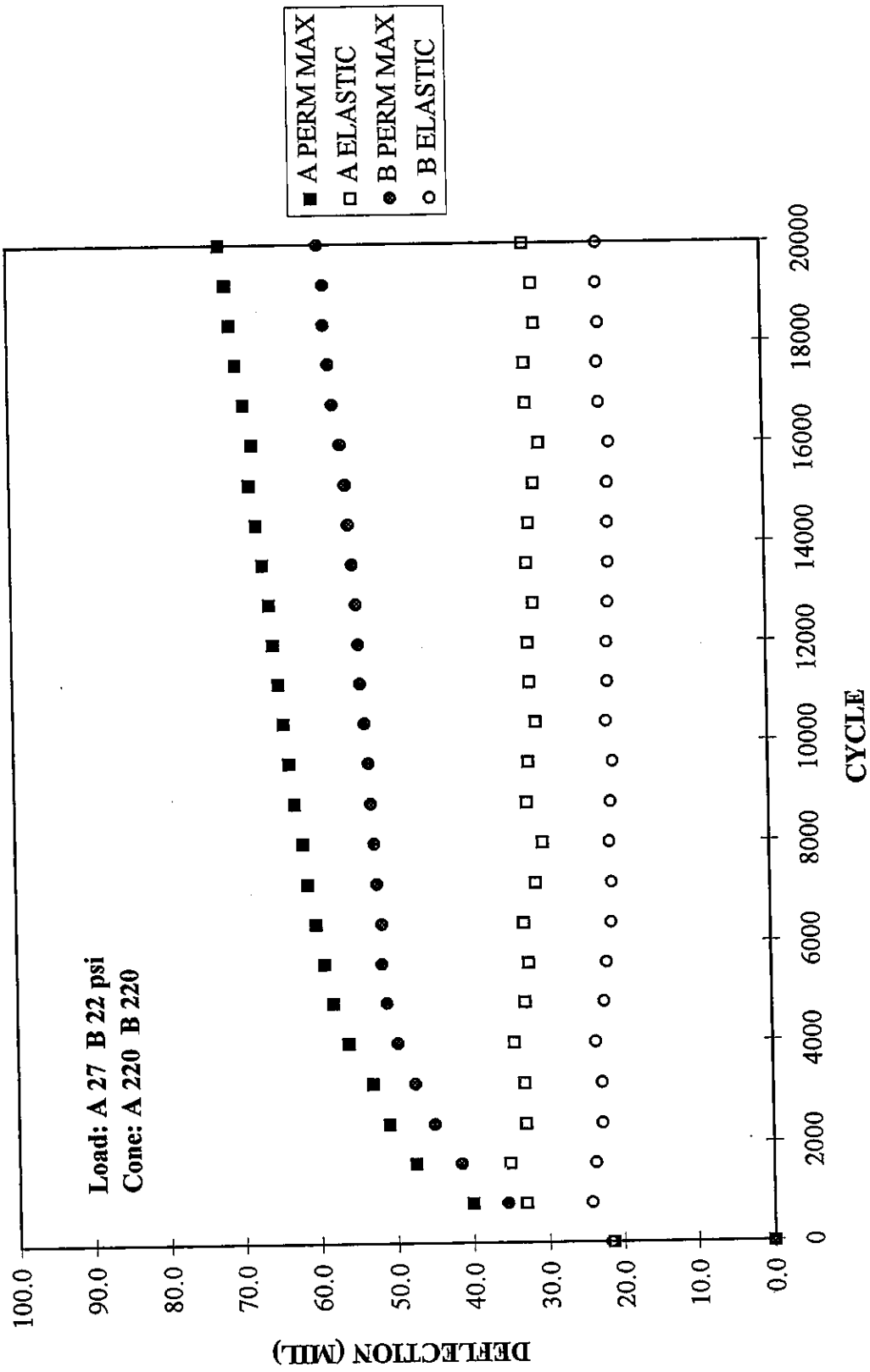


Figure A44: S0815AB / CA6 / CA7, Deflection vs Cycle

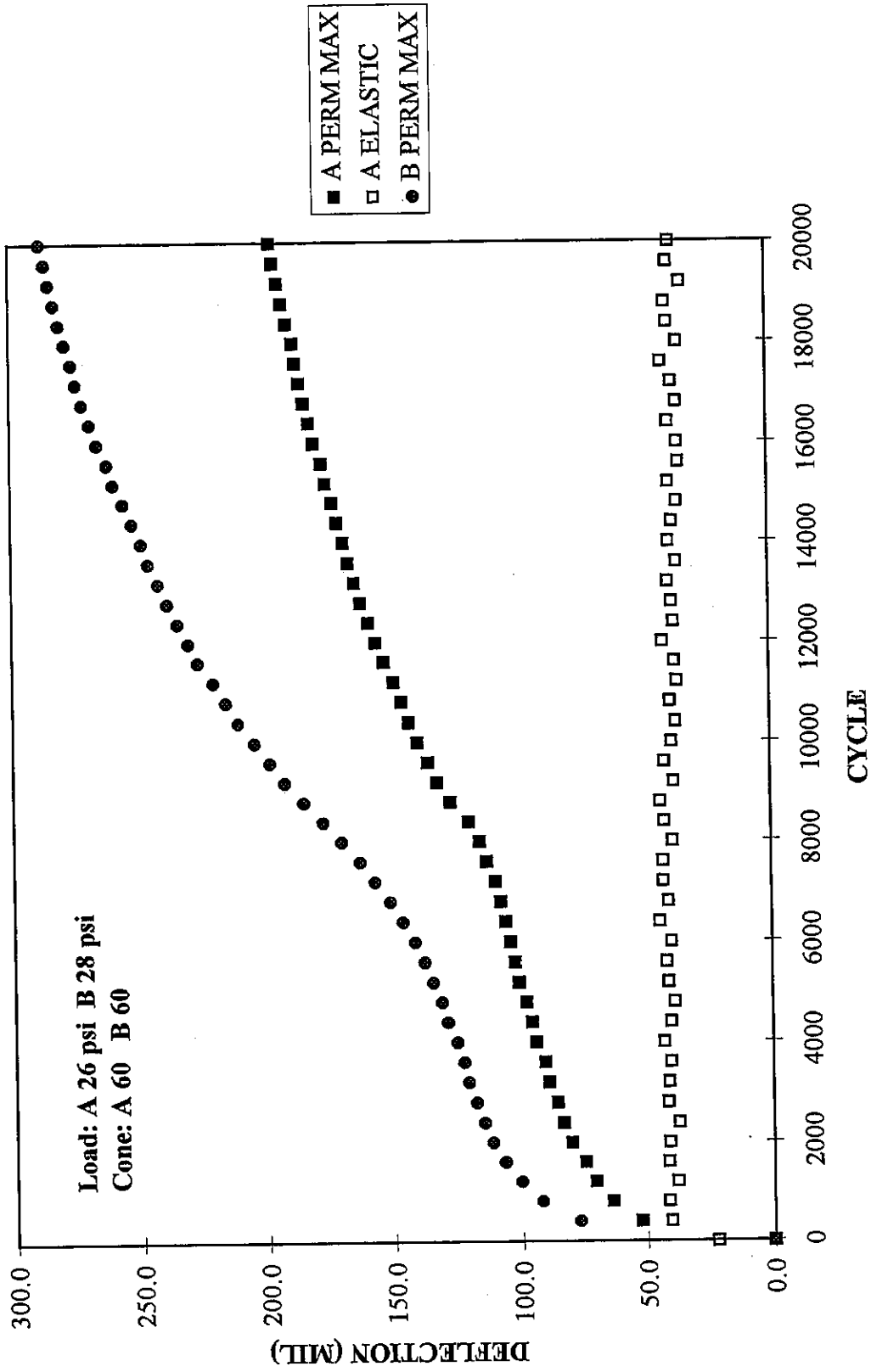


Figure A45: S0819AB / CA6 / CA7, Deflection vs Cycle

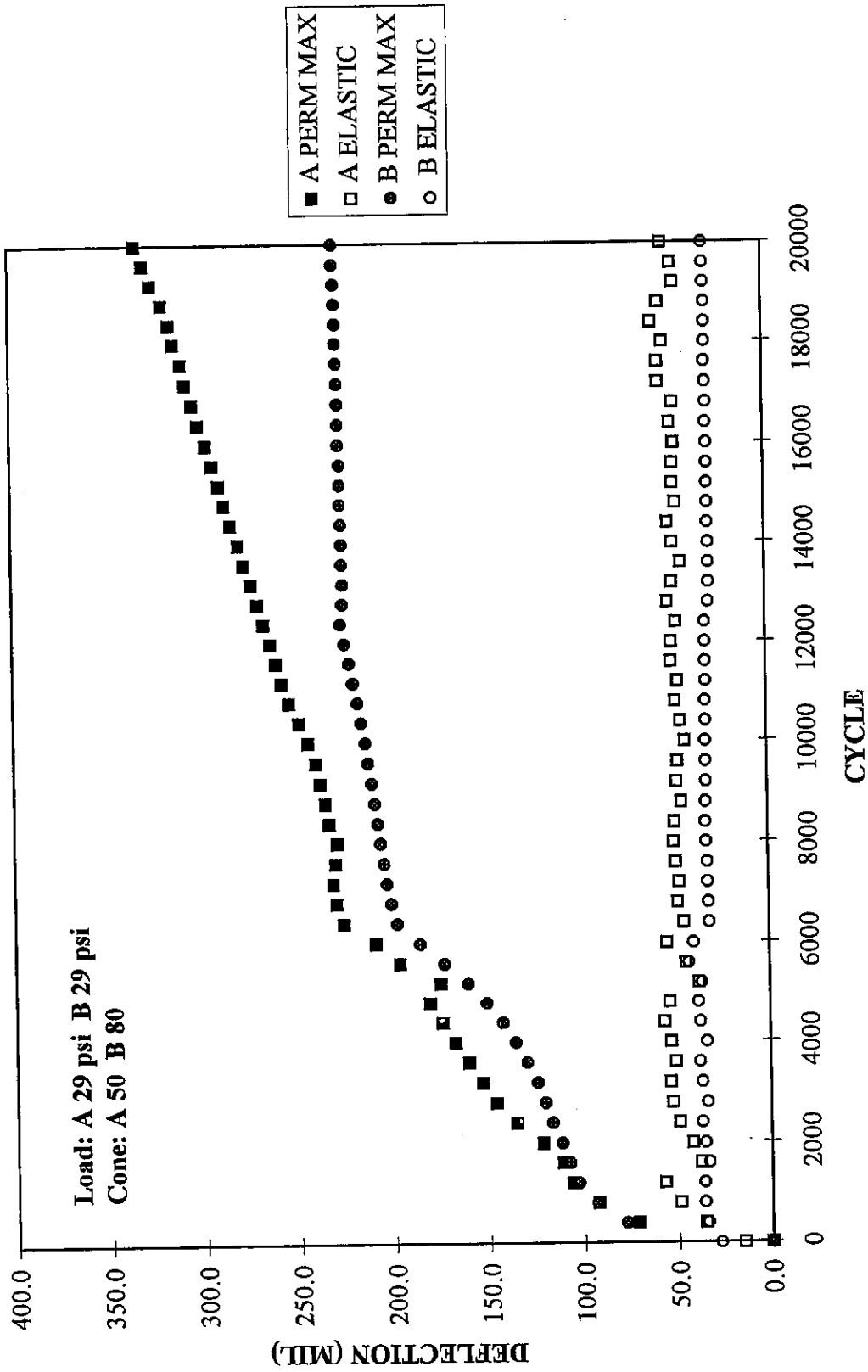


Figure A46: S0821AB / No Separation / CA7, Deflection vs Cycle



REFERENCES



-
- ¹ Cedergren, H. R., *Drainage of Highway and Airfield Pavements*, 1974, pp. 23.
- ² Hewes, L.I., and Oglesby, C.H., *Highway Engineering*, 1954, pp. 3-4.
- ³ McAdam, John L., "Report to the London Board of Agriculture", (from Cedergren)
- ⁴ Hewes, L.I., and Oglesby, C.H., *Highway Engineering*, 1954, pp. 440-441.
- ⁵ Reed, C. M., "Impact of Open-Graded Drainage Layers on the Construction of Concrete Pavements in Illinois", *Transportation Research Record # 1478*, 1995, pp. 67-75
- ⁶ Heckel, L., "Open-Graded Drainage Layers: Performance Problems under Continuously Reinforced Concrete Pavements in Illinois", *Sixth International Purdue Conference on Concrete Pavement Design and Materials for High Performance*, 1997, pp. 97-111.
- ⁷ Dempsey, B. J., "Laboratory and Field Studies of Channeling and Pumping", *Transportation Research Record*, No. 849, pp. 1-12, 1982.
- ⁸ The AASHTO Road Test: Report 7, HRB, Special Report 61G, 1962.
- ⁹ McMorrow, J., "Filtering Action of Non-Woven Geotextiles Under Dynamic Loading", *Geotextiles, Geomembranes and Related Products*, 1990 Rotterdam, pp. 233-238.
- ¹⁰ Hoare, D. J., "A Laboratory Study into Pumping Clay through Geotextiles under Dynamic Loading", *Second International Conference on Geotextiles*, Las Vegas, 1982, pp. 423-428.
- ¹¹ Bell, A. L., McCullough, L. M., Snaith, M. S., "An Experimental Investigation of Sub-Base Protection Using Geotextiles", *Second International Conference on Geotextiles*, Las Vegas, 1992, pp. 435-440.
- ¹² Friedli, P., and Anderson, D. G., "Behavior of Woven Fabrics Under Simulated Railway Loading", *Second International Conference on Geotextiles*, Las Vegas, 1992, pp. 473-478.
- ¹³ Lafleur, J., Rollin, A. L., and Mlynarek, J., "Clogging of Geotextiles under pumping loads", *Geotextiles, Geomembranes and Related Products*, Balkema, Rotterdam, 1990, pp. 189-192.
- ¹⁴ Faure, Y. H., and A. El Amir "Separation function of geotextiles laid on a soft clay" *Geotextiles, Geomembranes and Related products*, 1990 Rotterdam, pp. 253.

-
- ¹⁵ Glynn, D. T., and Cochrane, S.R., "The Behavior of Geotextiles as Separating Membranes on Glacial Till Subgrades", Geosynthetics '87 Conference, New Orleans, USA pp. 26-37
- ¹⁶ Bell, A.L., McCullough, L. M. and Gregory, B. J., "Clay Contamination in Crushed Rock Highway Sub-bases", Proceedings of Conference on Engineering Materials, New South Wales, Australia, 1981, Session II, pp. 355-365.
- ¹⁷ Hillig, J. and Lieberenz, K. "Long-term behavior of geotextile systems in railway track formation" Geotextiles, Geomembranes and Related products, 1990 Rotterdam , pp. 252.
- ¹⁸ Raymond, Gerald P. and Bathurst, Richard J. "Test results on exhumed railway track geotextiles" Geotextiles, Geomembranes and Related products, 1990 Rotterdam, pp. 197-202.
- ¹⁹ Tsai, Wen-Sen, and Holtz, Robert D. "Laboratory Model Tests to Evaluate Geotextile Separators in-Service", Geosynthetics, 1997 Long Beach Ca, USA pp. 633-646.
- ²⁰ Dempsey, B. J., and Thompson, M. R. "Interim Report - Durability Testing of Stabilized Materials", Illinois Cooperative Highway Research Program, Series No. 132, 1972.
- ²¹ Thompson, M. R., "Factors Influencing the Plasticity and Strength of Lime Soil Mixtures", Bulletin 492, Engineering Experiment Station, UI, 1967
- ²² Thompson, M. R., "Final Summary Report - Lime Stabilization of Soils for Highway Purposes", Illinois Cooperative Highway Research Program, Series No. 93, 1968.
- ²³ Van Wijk, A. J., "Rigid Pavement Pumping", Joint Highway Research Project, JHRP-85-10, Purdue University, 1985.
- ²⁴ Kawamura, M., and Diamond, S., "Stabilization of clay soils against erosion loss", Joint highway research project with Indiana DOT and USDOT, 1975.
- ²⁵ Eades, J. L., and Grim, R. E., "A quick test to determine lime requirements for lime stabilization", Highway Research Record, No. 3, pp. 66-71, 1966.
- ²⁶ Thompson, M. R., and Eades, J. L., "Evaluation of quick test for lime stabilization", J. Soil Mechanics, Foundation Division, ASCE No. 96, pp. 795-800, 1970.
- ²⁷ Litton, L.L., and Lohnes, R. A., "Attrition rates of soil-cement subjected to water jets", Transportation Research Record, No. 941, pp. 18-23, 1983.

-
- ²⁸ Dempsey, B. J., "Laboratory and Field Studies of Channeling and Pumping", Transportation Research Record, No. 849, pp. 1-12, 1982.
- ²⁹ Hansen, E. C., et. al., "Field Effects of Water Pumping Beneath Concrete Pavement Slabs", Journal of Transportation Engineering, ASCE, Vol. 117, No. 6, Nov/Dec, 1991.
- ³⁰ Dempsey, B. J., Carpenter, S. H., and Darter, M. I., "Improving Subdrainage and Shoulders of Existing Pavements", FHWA, Final Report, 1980
- ³¹ Raad, L., "Pumping Mechanisms of Foundation Soils Under Rigid Pavements", Transportation Research Record, No. 849, pp. 29-37, 1982
- ³² Crovetti, J. -A., and Dempsey, B. J., "Pavement Subbases - Final Report", Illinois Cooperative Highway Research Program, IHR-525, May 1991.
- ³³ Jackson, T. J., and Ragan, R. M., "Hydrology of Porous Pavement Parking Lots", Journal of the Hydraulics Division, ASCE, Vol. 100, No. HY12, Dec. 1974.
- ³⁴ Kazmierowski, T. J., "Field Evaluation of Various Types of Open-Graded Drainage Layers", Transportation Research Record, No. 1434, pp. 29-36., 1994.
- ³⁵ Barenberg, E. J., and Tayabji, S. D., "Evaluation of Typical Pavement Drainage Systems Using Open Graded Bituminuous Aggregated Mixture Drainage Layers", Illinois Cooperative Highway Research Program, Series No. 151, 1974.
- ³⁶ Bathurst, R. J., and Raymond, G. P., "Dynamic Response of Open-Graded Highway Aggregates", Transportation Research Record, No. 1278, pp. 35-42, 1990.
- ³⁷ Raymond, G. P., "Ballast Properties That Affect Ballast Performance", American Railway Engineering Association Bulletin, # 673, June-July, 1979.
- ³⁸ Hall, M., "Cement-Stabilized Open-Graded Base Strength Testing and Field Performance Versus Cement Content", Transportation Research Record, No. 1440, pp. 22-31, 1994.
- ³⁹ Hoffman, G. L., "Subbase Permeability and Pavement Performance", Transportation Research Record, No. 849, pp. 12-17, 1982.
- ⁴⁰ Copeland, J. A., "Fabrics in Subdrains: Mechanisms of Filtration and the Measurement of Permeability", Dept. of Civil Engineering, Oregon State University, Corvallis, Transportation Research Report 80-2, Jan. 1980.

⁴¹ Janssen, D. J., "Dynamic Test to Predict Field Behavior of Filter Fabrics Used in Pavement Subdrains", Transportation Research Record, No. 916, pp. 32-37, 1983.

⁴² Carroll Jr., R. G., "Geotextile Filter Criteria", Transportation Research Record, No. 916, pp. 46-53, 1983.

⁴³ Weimar Jr., R. D., "Mechanism of Geotextile Performance in Soil-Fabric Systems for Drainage and Erosion Control", Transportation Research Record, No. 916, pp. 37-40, 1983.

⁴⁴ Lawson, C. R., "Filter Criteria for Geotextiles: Relevance and Use", Journal of Geotechnical Engineering, ASCE, Vol. 108, No. GT10, pp. 300-317, October, 1982.

⁴⁵ Seitz, E., and Kany, M., "Filter Behavior of Non-Woven Fabrics Under Dynamic Loading", Third International Conference on Geotextiles, Vienna, 1986, pp. 1241 - 1245.

⁴⁶ Floss, R., Laier, H., and Brau, G., "Dynamic loading of geotextile-soil-systems", Geotextiles, Geomembranes and Related Products, Balkema, Rotterdam, 1990 pp. 183 - 188.

⁴⁷ Lime Stabilization, State of the Art Report 5, Transportation Research Board, 1987, pp. 13.

⁴⁸ Norgren, Engineering Information Guide, 1982, pp. 14.